**DISSERTATION**

Zur Erlangung des Grades

„Doktor der Naturwissenschaften“

im Promotionsfach Chemie

# Anionic Polymerization of Non-Conventional 1,3-Dienes


vorgelegt von

**Moritz Alexander Rauschenbach**

geboren am 07.03.1996 in Bad Homburg vor der Höhe




am Fachbereich

Chemie, Pharmazie, Geographie und Geowissenschaften der

**Johannes Gutenberg-Universität Mainz**


Mainz, 2024

Die als Dissertation vorgelegte Arbeit wurde in dem Zeitraum von Mai 2021 bis September 2024 im Department Chemie der Johannes Gutenberg-Universität Mainz angefertigt.

**Dekanin**:

**1. Berichterstatter**:

**2. Berichterstatter**:

Tag der mündlichen Prüfung: 20. November 2024

Hiermit versichere ich gemäß § 10 Abs. 3d der Promotionsordnung 24.07.2007:

Ich habe die jetzt als Dissertation vorgelegte Arbeit selbst angefertigt und alle benutzten Hilfsmittel (Literatur, Apparaturen, Material) in der Arbeit angegeben, ich habe die jetzt als Dissertation vorgelegte Arbeit nicht als Prüfungsarbeit für eine andere staatliche oder andere wissenschaftliche Prüfung eingereicht. Ich hatte weder die jetzt als Dissertation vorgelegte Arbeit noch Teile davon bei einer anderen Fakultät bzw. einem anderen Fachbereich als Dissertation eingereicht.

_____

Moritz A. Rauschenbach

## Eigenständigkeitserklärung

Hiermit erkläre ich, **Moritz Alexander Rauschenbach**, dass ich die vorliegende Arbeit mit dem Titel: ***Anionic Polymerization of Non-Conventional 1,3-Dienes*** selbstständig verfasst und keine anderen als die angegebenen Quellen und Hilfsmittel benutzt habe. Sämtliche wörtlichen oder sinngemäßen Übernahmen und Zitate sind kenntlich gemacht und nachgewiesen. Ich versichere, dass ich keine Hilfsmittel verwendet habe, deren Nutzung die Prüferin oder der Prüfer explizit ausgeschlossen hat. Folgende KI-Tools habe ich wie entsprechend beschrieben verwendet:

| **KI-Tool** | **Genutzt für...** | **Warum** | **Wann** |
|---|---|---|---|
| *DeepL Translate* | Übersetzung Begriffe von deutsch auf englisch und umgekehrt | Verständnis wissenschaftlicher Arbeiten und Hilfe Formulierung englischer Sätze | über die gesamte Arbeit hinweg |
| *DeepL Write* | Neuformulierung meiner Textentwürfe | Bessere Lesbarkeit und Verständlichkeit | über die gesamte Arbeit hinweg |
| *ChatGPT* | Neuformulierung meiner Textentwürfe | Bessere Lesbarkeit und Verständlichkeit | über die gesamte Arbeit hinweg |

Mit Abgabe der vorliegenden Leistung übernehme ich die Verantwortung für das eingereichte Gesamtprodukt. Ich verantworte damit auch jegliche KI-generierten Inhalte, die ich in meine Arbeit übernommen habe. Die Richtigkeit übernommener (KI-generierter) Aussagen und Inhalte habe ich nach bestem Wissen und Gewissen geprüft.

Mir ist bekannt, dass ein Verstoß gegen die genannten Punkte prüfungsrechtliche Konsequenzen hat und insbesondere dazu führen kann, dass die Promotionsleistung als mit „nicht bestanden“ bewertet wird. Die Einschreibung kann für bis zu zwei Jahre widerrufen werden, wenn Studierende zweimal oder häufiger bei Prüfungsleistungen täuschen (§ 69 Abs. 4 und 5 HochSchG).

_____

Ort, Datum und Unterschrift

# Für meine Großeltern

*„I can’t believe it!*

*Reading and writing actually paid of.”*

Homer Simpson

# DANKSAGUNG

# AUTHOR CONTRIBUTION

Each chapter has been enhanced by individual contributions of additional authors. The following section outlines these contributions to specify and acknowledge in accordance with the **CRediT** (Contributor Role Taxonomy) format.

**Chapter 1** was conceptualized by [redacted] and [redacted] and [redacted] contributed equally to the writing of the original draft. [redacted] contributed by supervising this work and by reviewing and editing the original draft during the writing process.

In **Chapter 2**, the concept was developed by [redacted] and [redacted]. Credit is given to [redacted] for initial ideas that eventually evolved into the concept. [redacted] further contributed to this study by investigating homopolymerization and hydrogenation experiments. He also contributed with data curation, visualization, and writing of the original draft. [redacted] investigated the influence of the polar modifier and analyzed the copolymerization kinetics. He contributed to this work with data curation, visualization, validation and writing. [redacted] while supervising this investigation, also contributed by providing the resources. He reviewed and edited the first draft of the manuscript. Finally, [redacted] is thanked for the valuable discussions and to [redacted] for performing the online NMR kinetics measurements.

**Chapter 3** [redacted] and [redacted] developed the concept of this study [redacted] continued the investigation of the monomer and polymer synthesis. He validated and curated the data prior to visualization. He wrote the first draft of the manuscript. [redacted] and [redacted] all contributed with investigations to different parts of the manuscript. All validated the analyses they contributed and reviewed the original draft of the manuscript. [redacted] provided unique resources and validated data obtained. She revised the final manuscript. [redacted] supervised the work, provided resources, and reviewed the manuscript up to the final stage. [redacted] is also acknowledged for the valuable discussions regarding kinetic experiments.

The concept of **Chapter 4**, based on unpublished results by [redacted], was conceptualized by [redacted] and [redacted] contributed

by investigating and elaborating the synthetic strategy together with [redacted]. Furthermore, [redacted] was responsible for the data curation, validation, and visualization. He prepared the original draft of the manuscript, while [redacted] reviewed and edited the manuscript. [redacted] and [redacted] are acknowledged for their contributions to the monomer synthesis.

**Chapter 5** was originally conceptualized by [redacted] and [redacted]. [redacted] proceeded to research and develop the methodology of monomer and polymer synthesis. He curated the data and managed the cooperative parts of this project. Finally, he visualized the data and wrote the original draft of the manuscript. [redacted] performed the antimicrobial assays and curated the obtained data for the original draft of the manuscript [redacted] and [redacted] were responsible for the conception of the supporting analysis for the lithium-organyl aggregation [redacted] supervised this project, provided the resources, and reviewed and edited the original draft of the manuscript. [redacted] is acknowledged for her support in evaluating the monomer synthesis and [redacted] for performing the MALDI ToF measurement. Finally, [redacted] are thanked for the constructive discussions and proofreading the manuscript.

# Table of Contents

# TABLE OF CONTENTS

# Motivation and Objectives

# MOTIVATION AND OBJECTIVES

Decades before Staudinger described the first polymer with the term "macromolecule" in 1922 (**Figure 1**) polymeric materials were already processed and used in daily life.[1,2] The success story of rubbery materials dates back to 1839 with Charles Goodyear's finding leading to the first vulcanization of natural rubber (NR).[3,4] This biopolymer is the macromolecule Staudinger referred to in his groundbreaking work. It consists of highly stereoregular *cis* – 1,4-polyisoprene (PI). Today, synthetic rubbers either prepared from butadiene (B) or isoprene (I), still compete with NR.

However, the majority of synthetic rubbers are produced *via* catalytic processes.[5] The living anionic polymerization of 1,3-dienes in apolar solvents, represents a pivotal step in the synthesis of thermoplastic elastomers, with styrene serving as an established comonomer. The living character is beneficial for obtaining diverse architectures and for the tailoring of properties through adjusting the reaction parameters. Consequently, high elasticity comparable to that of NR can be achieved through the attainment of high selectivity over the microstructure while covalently connecting polydienes to rigid polymers.

**Über Isopren und Kautschuk.**

5. Mitteilung.[1])

**Über die Hydrierung des Kautschuks und über seine Konstitution**

von

**H. Staudinger und J. Fritschi.**

(2. IX. 22.)

**Figure 1:** Title of publication from Staudinger from 1922 giving the first description over the molar composition of natural rubber using the term "macromolecule" for the first time.

The living anionic polymerization has been applied to polymerize various monomer structures for decades and has therefore reached a certain degree of maturity.[6,7] Yet, the variety of 1,3-dienes amenable to the anionic polymerization is increasing steadily with monomers either obtained from crude oil or from natural compounds. Undoubtedly, anionic polymerization is still the method of choice to obtain highly defined polymers. By adjusting the reaction parameters, the incorporation can be tailored and subsequently the material properties as well.[8] However, not all empirical

findings have been discussed fundamentally. In some cases, novel monomers were synthesized merely to support hypotheses. Occasionally, fundamental investigations of non-conventional diene monomers are pursued due to the curiosity of a scientist looking for high-potential monomers. Hence, the number of reported diene monomers is still increasing aiming for new insights in the mechanism or to induce certain materials properties.[9,10]

The first objectives of this thesis are based on a previously reported concept. Takegami *et al*. investigated two phenyl-substituted 1,3-butadiene derivatives resembling structural elements of the two highly established monomers styrene and butadiene.[11,12] Despite these in-depth investigations, the fusion of these two monomers can be further exploited. In addition, the application of current analytical methods is expected to provide new insights.

For instance, merging styrene and isoprene has not been considered to date. Chapters 2 and 3 pursue the question whether it is possible to design 1,3-dienes combining styrene and isoprene, amenable to the living anionic polymerization. It will be of great interest whether the microstructure of the resulting polydienes can be tailored like isoprene or better be described as the structurally related styrene. Lastly, the material properties of the resulting polymers will be correlated to the initial diene framework leading with the first question for both chapters:

*"Can we design 1,3-dienes exhibiting characteristics of styrene suitable for the living anionic polymerization and assess their reactivity in comparison to isoprene and styrene?"*

The synthesis of polydienes intrinsically produces one double bond per repeating unit. These have been targeted in a variety of post-polymerization modifications drastically influencing the polymer properties.[13–16] In industry, synthetic rubbers are often hydrogenated to improve their long-term stability. Alternatively, the post-polymerization cyclization represents a versatile tool to increase rigidity of the polydiene. In addition, we further raise the following question in Chapter 2 and 3:

*"To what extend are literature-known post-polymerization modification reactions applicable to the investigated systems and how do they influence the material properties?"*

*The Goodyear Tire and Rubber Company* considered cyclization of polyisoprene of triblock copolymer PI-*b*-PB-*b*-PI as a potential tool to overcome a feared styrene shortage.[17] Furthermore, this cyclization reaction has been proven to produce materials with exceptional high glass temperature ($T_g$) when starting from phenyl-substituted 1,3-butadiene.[18] However, to apply these structures in TPE-like polymer architectures and avoid the use of the hazardous butadiene alternative polymer classes are required. Therefore, acid-stable polycaprolactones are attractive as they are obtained in a straightforward manner. Their semi-crystallinity can be suppressed by an additional methyl group in the backbone.[19] Inspired by polypeptide-conjugate synthesis, Chapter 4 has the objective of combining the low-$T_g$ polymethylcaprolactone with phenyl-substituted polydienes in a triblock copolymer to ultimately target the cyclization reaction. Summarizing, we formulate the following question for Chapter 4:

*"Can we synthesize ABA triblock copolymer consisting of a non-crystalline polycaprolactone as the middle block B and polydienes for subsequent cyclization reaction as outer blocks A through a coupling strategy?"*

In principle, the living anionic polymerization of dienes is not compatible with functional groups bearing acidic protons. However, steady progress in tire development has generated new generations of polar fillers for the targeted increase in performance.[20] These fillers would require increased hydrophilicity of the so far apolar synthetic rubbers to prevent separation. To overcome this incompatibility, additional filler materials are utilized. Apart from the tire industry, the lack of functionalities limits the scope of potential applications for polydiene-based materials. To tackle this limitation, the double bonds of the polydiene backbone have been addressed *via* post-polymerization modification.[16,21,22] However, this approach provides merely limited control over the degree of functionalization.[23] Alternatively, by utilizing suitable protecting groups functional moieties can be introduce *via* newly designed dienes.[15,24,25] Those protective groups are necessary to overcome the beforementioned incompatibility of acidic protons with the anionic polymerization.[7] Nevertheless, this comes with undesired additional processing steps to cleave the protective groups from the polymer giving the polymer with functional moieties.

Aprotic functional groups, i.e. thioethers, could circumvent these steps and still be installed in a facile manner. For several polymerization methods, monomers containing thioether groups have been utilized successfully. At the same time, sulfur proves to be sufficiently nucleophilic to attach functionalities by reacting it to the respective sulfonium salt after polymerization.[26,27] The versatility of thioether-containing polymers is emphasized by examples of tertiary sulfonium species inducing antimicrobial behavior and enabling the use as a polymer electrolyte.[28,29] The incorporation of thioethers in an industrially relevant structure by using suitable 1,3-diene monomers would endow the resulting polymer with the possibility of tailoring the polydiene properties. Chapter 5 aims at the successful incorporation of thioether functional 1,3-dienes suitable for anionic polymerization. The literature-known antimicrobial effect in a polydiene represent a highly interesting material for surface coatings. In conclusion, the ensuing question arises for chapter 5:

*"Are thioether groups applicable to the living anionic polymerization of dienes and can we induce antimicrobial properties by post-polymerization reactions?"*

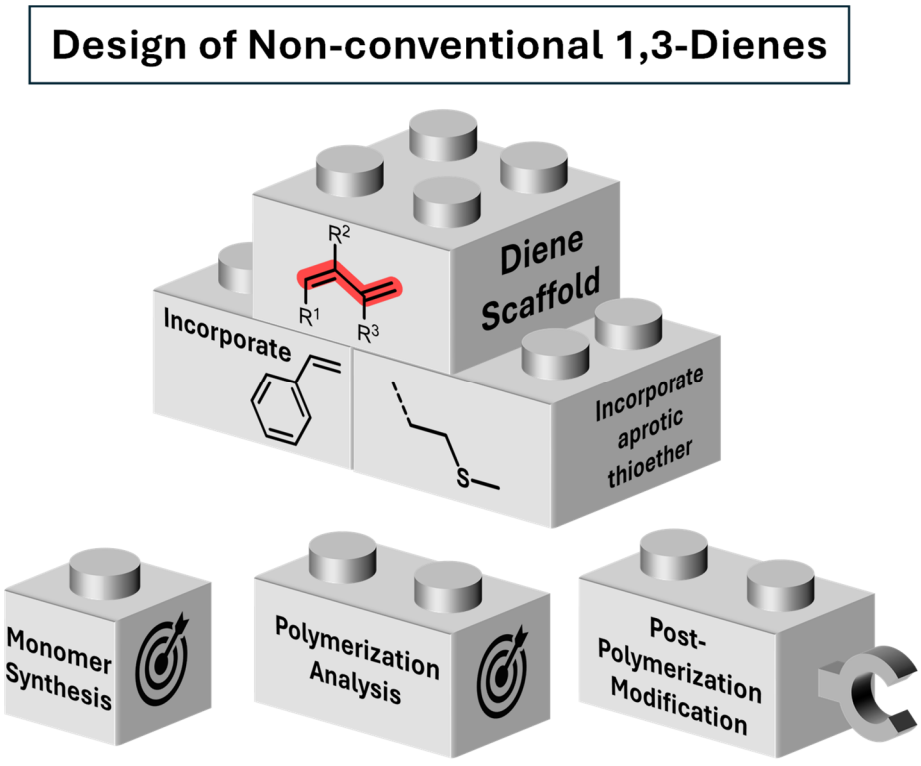


**Figure 2**: Illustration of the central parts of the dissertation and the additional components found in every chapter.

## References


1 H. Frey and T. Johann, *Polym Chem*, 2020, **11**, 8–14.

2 H. Staudinger and J. Fritschi, *Helv Chim Acta*, 1922, **5**, 785–806.

3 C. Goodyear, US 3633, 1844.

4 J. A. Calzonetti and C. J. Laursen, *Rubber Chemistry and Technology*, 2010, **83**, 303–321.

5 G. Ricci, G. Pampaloni, A. Sommazzi and F. Masi, *Macromolecules*, 2021, **54**, 5879–5914.

6 K. Ntetsikas, V. Ladelta, S. Bhaumik and N. Hadjichristidis, *ACS Polymer Au*, 2022, **3**, 158–181.

7 N. Hadjichristidis and A. Hirao, *Anionic Polymerization*, Springer, Tokio, 2015.

8 H. Hsieh and R. Quirk, *Anionic polymerization: principles and practical applications*, Dekker, New York, 1996.

9 R. D. Barent, M. Wagner and H. Frey, *Polym Chem*, 2022, **13**, 5478–5485.

10 S. Uchida, K. Togii, S. Miyai, R. Goseki and T. Ishizone, *Macromolecules*, 2020, **53**, 10107–10116.

11 T. Suzuki, Y. Tsuji and Y. Takegami, *Macromolecules*, 1978, **11**, 639–644.

12 T. Suzuki, Y. Tsuji, Y. Takegami and H. J. Harwood, *Macromolecules*, 1979, **12**, 234–239.

13 B. N. Gacal, V. Filiz, S. Shishatskiy, S. Rangou, S. Neumann and V. Abetz, *J Polym Sci B Polym Phys*, 2013, **51**, 1252–1261.

14 A. Matic and H. Schlaad, *Polym Int*, 2018, **67**, 500–505.

15 A. Matic, A. Hess, D. Schanzenbach and H. Schlaad, *Polym Chem*, 2020, **11**, 1364–1368.

16 N. Politakos, I. Moutsios, G. M. Manesi, K. Artopoiadis, K. Tsitoni, D. Moschovas, A. A. Piryazev, D. S. Kotlyarskiy, G. Kortaberria, D. A. Ivanov and A. Avgeropoulos, *Polymers (Basel)*, 2021, **13**, 4167.

17 J. Lal, *Polymer (Guildf)*, 1998, **39**, 6183–6186.

18 Y. Cai, J. Lu, G. Jing, W. Yang and B. Han, *Macromolecules*, 2017, **50**, 7498–7508.

19 A. Watts, N. Kurokawa and M. A. Hillmyer, *Biomacromolecules*, 2017, **18**, 1845–1854.

20 C. Hayichelaeh, L. A. E. M. Reuvekamp, W. K. Dierkes, A. Blume, J. W. M. Noordermeer and K. Sahakaro, *Rubber Chemistry and Technology*, 2018, **91**, 433–452.

21 C. C. Peng and V. Abetz, *Macromolecules*, 2005, **38**, 5575–5580.

22 J. P. Dilcher, H. Jürgens and G. A. Luinstra, *Advances in Polymer Science*, 2015, **269**, 163–202.

23 D. Leibig, A. H. E. Müller and H. Frey, *Macromolecules*, 2016, **49**, 4792–4801.

24 C. Wahlen, M. Rauschenbach, J. Blankenburg, E. Kersten, C. P. Ender and H. Frey, *Macromolecules*, 2020, **53**, 9008–9017.

25 C. Hahn, M. Wagner, A. H. E. Müller and H. Frey, *Macromolecules*, 2022, **55**, 4046–4055.

26 J. Herzberger, K. Fischer, D. Leibig, M. Bros, R. Thiermann and H. Frey, *J Am Chem Soc*, 2016, **138**, 9212–9223.

27 T. J. Deming, *Bioconjug Chem*, 2017, **28**, 691–700.

28 S. T. Hemp, M. H. Allen, A. E. Smith and T. E. Long, *ACS Macro Lett*, 2013, **2**, 731–735.

29 B. Zhang, M. Li, M. Lin, X. Yang and J. Sun, *Cite this: Biomater. Sci*, 2020, **8**, 6969.

# Abstract

# ABSTRACT

This thesis explores the synthesis of non-conventional 1,3-dienes and their behavior in the living carbanionic polymerization. A variety of approaches for the synthesis of isoprene derivatives. albeit with structural similarities to styrene are examined. Furthermore, this dissertation examines the impact of thioether groups on the living anionic polymerization of a bio-inspired diene structure.

**Chapter 1** provides an introduction to the anionic polymerization of 1,3-dienes, placing recent achievements within a general context. The insertion mechanism that determines the final microstructure has been a topic of scientific debate for decades. This chapter aims at integrating the latest findings with existing theories, thereby providing a comprehensive overview of the current understanding of the mechanism. This includes the intentional manipulation of the insertion process using polar modifiers or alterations in the substitution pattern, accompanied by a summary of the resulting glass temperatures. Given the growing interest in bio-derived monomers, this chapter also explores a variety of new and biobased diene monomers. This approach is particularly focused on the utilization of terpene-based dienes as a substitute for isoprene. It will be demonstrated that this methodology can be employed to target the rigid properties of polystyrene as well. Moreover, the utilization of solvents derived from natural feedstocks is examined with the objective of a more sustainable synthesis of polydienes. The following section will address the statistical copolymerization of dienes with styrene that is known from literature. This includes a discussion of the reactivity ratios obtained through *in situ* analysis. Additionally, the impact of polar modifiers on the copolymerization of dienes with styrene is reviewed in a detailed manner, as is the copolymerization of two diene monomers. In conclusion, this chapter provides a comprehensive overview of the recently reported approaches and current challenges associated with the synthesis of functional polydienes.

**Chapter 2** approaches the idea of a partially hydrogenated styrene derivative, which possesses a conjugated diene unit. The targeted monomer, vinyl cyclohexene (VCH), exhibits structural similarities to both styrene and isoprene. Consequently, a non-conventional 1,3-diene is obtained, anticipated to yield a high $T_g$ polydiene. Beginning with the monomer synthesis relying on a straight-forward hydrogenation of

1-ethynyl-1-cyclohexene, the living anionic polymerization of VCH was examined. Narrowly distributed polymers with molar masses up to 120 kg mol$^{-1}$ were obtained. Subsequently, the impact of increasing concentration of the polar additive THF on the microstructure is discussed. Both the influence of molar mass and the determined microstructure were correlated with the glass temperatures measured by thermal analysis. Furthermore, copolymerizations of VCH with styrene and isoprene, respectively, were investigated separately *via in situ* $^{1}$H NMR kinetics. From the obtained values the reactivity ratios were determined. Lastly, hydrogenation of two polymer samples exhibiting the highest and the lowest content of 1,4-stereoisomers was conducted. The thermal properties were compared in accordance with the precursors revealing the high impact of the initial monomer incorporation.

**Chapter 3** provides a comprehensive study of the anionic polymerization of two monomers, 1-phenyl isoprene (1PhI) and 4-phenyl isoprene (4PhI). Both monomers can be regarded as phenyl-substituted isoprenes or *β*-substituted styrene derivatives. The Wittig reaction was utilized to synthesize 1PhI and 4PhI, respectively, in good yields and high purity. In this instance, an elaborate purification strategy was employed. The monomers were characterized based on the previously identified correlation between *β*-carbon shift and reactivity. The $^{13}$C NMR spectra demonstrated that the chemical shifts of the respective methylene groups of the two monomers differed. In addition, the electron densities obtained from DFT calculations ultimately led to the assumption of different reactivities of both dienes. The anionic polymerization of 1PhI and 4PhI yielded well-defined polymers with low dispersity. In general, the molar mass was found to be highly controllable; however, the SEC-determined values exhibited a significant dependence on the calibration standard. The relatively broad range of $T_g$ from 47 °C – 69 °C for polydienes indicates that the introduced phenyl rings and the microstructures of the respective polydiene exert a notable influence. The addition of the polar additive THF did not alter the microstructure as would be expected from literature regarding established dienes, which illustrates the significant influence of the pendant phenyl ring. The initial postulated reactivities were found to correspond with the trend determined by *in situ* $^{1}$H NMR kinetics with styrene as a comonomer. However, copolymerization with isoprene yielded outcomes disparate to the initial hypothesis. Lastly, the homopolymers were subjected to a cyclization reaction under

acidic conditions. The cyclized materials show increasing $T_g$s while maintaining solubility in common solvents. This modification reaction induced an unusual fluorescence, which was investigated both in solution and solid state.

**Chapter 4** employs monomers 1PhI and 4PhI, introduced in Chapter 3, to synthesize ABA triblock copolymers. The objective was to achieve exceptional rigidity in the outer blocks based on the targeted cyclization reaction. Accordingly, an appropriate, elastic mid-block had to be prepared with the capacity to withstand the strong acidic conditions of the cyclization reaction while simultaneously allowing for the synthesis of high molar masses. The selected monomer *γ*-methyl-*ε*-caprolactone (MCL) was synthesized and polymerized yielding polyesters with molar masses up to 38 kg mol$^{-1}$. A coupling strategy analogous to peptide synthesis was developed for the purpose of combining thermoplastic poly(phenyl isoprene) with the elastic poly(*γ*-methyl-*ε*-caprolactone). In accordance with the proposed methodology,, the end groups were modified in advance of the coupling reaction to comprise a carboxy and an amine functionality, respectively. However, the results of the different analyses were not uniform, and thus did not provide consistent support for the successful coupling. Nevertheless, the cyclization for non-conventional thermoplastic elastomers was performed without degradation of the polyester midblock.

In **Chapter 5**, the first anionic polymerization of a thioether-containing 1,3-diene and its synthesis is described. In the preliminary assessment of the monomer synthesis, particular attention was paid to the isomeric mixture of the diene, which is a result of the synthesis. Therefore, the anionic polymerization of 6-methylthiohexa-1,3-diene (MTHD) led to rather high dispersity values *Đ*, exceeding 1.24. *In situ* $^1$H NMR kinetics demonstrated that the polymer chains propagate rapidly, while the homopolymerization is correctly described as a stereocopolymerization of both isomers. Anionic polymerization of MTHD with isoprene yielded well-defined copolymers ($Đ < 1.19$) with precise control over the molar ratio of MTHD and isoprene and molar mass (10 – 50 kg mol$^{-1}$). A large variety of post-polymerization modifications, including alkoxylation, alkylation, and oxidation, are effective methods for targeting the sulfur in thioether-containing polymers. The oxidation process selectively targeted the sulfur atoms over the double bond, thereby emphasizing its potential as an internal antioxidant moiety for polydienes. Alkylation and alkoxylation enable the insertion of

various functionalities in quantitative manner. A selection of the modified polydienes, dispersible in water, were tested regarding their antimicrobial behavior. The sulfonium species induced by methyl iodide had no inhibiting effect. In contrast, the alkoxylation, which employs the commercially established PO, revealed remarkable efficacy in inhibiting bacterial growth of both *E. coli* and *S. aureus*, comparable to the antibiotics ampicillin and kanamycin. This inhibition of bacterial growth demonstrates the considerable potential of thioether-dienes for novel materials.

The article presented in Chapter 2 has also been published in the German edition of the journal. In Appendix A1 the German translation of Chapter 2 is presented.

# ZUSAMMENFASSUNG

Im Rahmen dieser Thesis wird die Synthese von unkonventionellen 1,3-Dienen und deren Verhalten in der lebenden anionischen Polymerisation untersucht. Es wurden unterschiedliche Ansätze zur Darstellung von Isoprenderivaten durchgeführt, welche zudem strukturelle Motive des Styrols aufweisen. Außerdem behandelt diese Dissertation den Einfluss von Thioethergruppen auf die lebende anionische Polymerisation anhand eines bioinspirierten 1,3-Diens.

**Kapitel 1** beginnt mit der Einführung der anionischen Polymerisation von 1,3-Dienen und ordnet sie in einen allgemeinen Hintergrund ein. Bereits vor Jahrzehnten wurde über den Einbaumechanismus der Monomere debattiert, welcher die letztendliche Mikrostruktur bestimmt. In diesem Kapitel werden neue Erkenntnisse mit den bestehenden Theorien verknüpft, woraufhin der Mechanismus nach aktuellem Verständnis beschrieben wird. Dies beinhaltet die vorsätzliche Manipulation des Einbauprozesses durch (i) polare Additive oder (ii) Variation des Substitutionsmusters sowie deren Einfluss auf die resultierende Glastemperatur. Aufgrund der steigenden Nachfrage nach bioverfügbaren Monomeren, werden in diesem Kapitel eine Vielfalt neuer und biobasierter Diene vorgestellt. Ein besonderer Fokus wird hierbei auf Terpen-basierte Diene als Ersatz zum Isopren gelegt. Zusätzlich werden Monomere beschrieben, welche die starren Eigenschaften des Polystyrols erschließen. Lösungsmittel aus nachwachsenden Rohstoffen werden für eine nachhaltigere Synthese von Polydienen diskutiert und deren Einflüsse zusammengefasst. In der Folge wird die statistische Copolymerisation von in der Literatur bekannten Dienen mit Styrol auf Basis von Copolymerisationsparametern erörtert, welche durch *in situ* Analysen bestimmt wurden. Dabei wird ferner auf den Einfluss von polaren Additiven eingegangen, sowie die Copolymerisation von zwei Dien-Monomeren diskutiert. Abschließend werden verschiedene Ansätze für die Synthese von funktionellen Polydienen sowie aktuelle Herausforderungen erörtert.

**Kapitel 2** befasst sich mit dem Konzept eines partiell hydrierten Styrolderivats, welches eine konjugierte Dien-Einheit aufweist. Das angestrebte Monomer 1-Vinylcyclohexen (VCH) weist strukturelle Ähnlichkeiten sowohl zu Styrol als auch zu Isopren auf. Durch die anionische Polymerisation dieses unkonventionelle Diens wird

ein rigides Polydien mit einem hohen $T_g$ erwartet. Ausgehend von der Monomer-Synthese über eine simple Hydrierung von 1-Ethinylcyclohexen wurde anschließend die lebende anionische Polymerisation von VCH durchgeführt. Es wurden Polymere mit engen Verteilungen und molaren Massen bis zu 120 kg mol$^{-1}$ erhalten. Der Einfluss des polaren Additivs THF auf die Mikrostruktur wurde durch systematische Steigerung der Konzentration analysiert. Neben dem Einfluss der molaren Masse wurde die Mikrostruktur mit den Glastemperaturen korreliert, welche durch thermische Analysen ermittelt wurden. Die Copolymerisationen mit den Comonomeren Isopren und Styrol wurden separat mittels *in situ* $^1$H-NMR-spektroskopischen Kinetikmessungen untersucht. Die resultierenden Werte wurden zur Bestimmung der Copolymerisationsparameter verwendet. Schließlich wurden die beiden Homopolymere, mit dem höchsten und dem niedrigsten Anteil an 1,4-Einheiten, katalytisch hydriert. Die thermischen Eigenschaften wurden analog zu den Ausgangspolymeren verglichen, wobei der hohe Einfluss des ursprünglichen Monomer-Einbaus verdeutlicht wurde.

In **Kapitel 3** wird die anionische Polymerisation der beiden Monomere 1-Phenylisopren (1PhI) und 4-Phenylisopren (4PhI) im Detail untersucht. Beide Monomere können als Phenyl-substituierte Isopren- oder als *β*-substituierte Styrol-Derivate beschrieben werden. Mittels der verwendeten Wittig-Reaktion wurden 1PhI und 4PhI in guten Ausbeuten und hoher Reinheit gewonnen. Dabei wurde eine ausgereifte Aufreinigungsmethode erarbeitet. Die beiden Monomere wurden basierend auf einer zuvor beschriebenen Korrelation zwischen der Reaktivität und der *β*-Kohlenstoffverschiebung charakterisiert. Die $^{13}$C-NMR-Spektren wiesen für die jeweiligen Methylen-Gruppen eindeutige Abweichungen der chemischen Verschiebungen auf. Darüber hinaus ergaben DFT-Berechnungen Elektronendichten, die zusammenfassend zur Hypothese von unterschiedlichen Reaktivitäten der beiden Monomere führte. Die anionische Polymerisation von 1PhI und 4PhI führte zu hochdefinierten Polymeren mit niedrigen Dispersitäten. Insgesamt wurde eine hohe Kontrolle über die molare Masse festgestellt. Allerdings wiesen die mittels GPC-bestimmten Werte eine starke Abhängigkeit von dem Kalibrationsstandard auf. Es wurden erhöhte Glastemperaturen im Bereich von 47 °C – 69 °C ermittelt, welche vor allem auf die eingebauten Phenylringe und die Isomerie der eingebauten

Monomereinheit zurückgeführt wurden. Die Zugabe des polaren Additivs THF zeigte nicht den Einfluss auf die Mikrostruktur, wie sie für etablierte Diene beschrieben ist. Dies offenbarte die Auswirkung der benachbarten Phenylringe. Die Auswertung von *in situ* $^{1}$H-NMR-Kinetiken mit Styrol als Comonomer bestätigte die Tendenz der eingangs postulierten Reaktivitäten beider Monomere. Im Gegensatz dazu wichen die Ergebnisse aus den Copolymerisationen mit Isopren zu den gemachten Hypothesen ab. Abschließend erfolgte eine Zyklisierungsreaktion der Homopolymere unter Zugabe von Trifluormethansulfonsäure. Die zyklisierten Materialien wiesen hohe Glastemperaturen (> 130 °C) auf und waren weiterhin in gängigen Lösemitteln löslich. Diese Modifizierungsreaktion rief eine ungewöhnliche Fluoreszenz in den Polymeren hervor, welche in Lösung und als Feststoff untersucht wurde.

**Kapitel 4** beschreibt die Verwendung der in Kapitel 3 vorgestellten Monomere 1PhI und 4PhI zur Synthese von ABA-Triblockcopolymeren. Mit dem Ziel einer Zyklisierungsreaktion sollen außergewöhnlich starre, äußere Blöcke erhalten werden. Dafür benötigt es ein geeignetes Polymer als elastischen, mittleren Block, der kompatibel mit den stark sauren Bedingungen der Zyklisierungsreaktion und mit hohen molaren Massen darstellbar ist. Das ausgewählte Monomer *γ*-Methyl-*ε*-caprolacton (MCL) wurde zunächst synthetisiert und anschließend polymerisiert. Hierbei wurden Polyester mit molaren Massen bis zu 38 kg mol$^{-1}$ erhalten. Zur Kombination des Thermoplasten Poly(Phenylisopren) mit denen des Elastomers Poly(*γ*-Methyl-*ε*-caprolacton) wurde eine Strategie zur Kupplung entwickelt. Dabei wurden Reagenzien verwendet, die aus der Peptidsynthese bekannt sind. Hierfür wurden die Endgruppen beider Polymerspezies synthetisch in eine Carboxyl- respektive Amin-Funktionalität überführt, wodurch die Voraussetzung der Kupplungsreaktion geschaffen wurden. Die Ergebnisse verschiedener Analysemethoden ergaben diesbezüglich keine einheitliche Bestätigung der erfolgreichen Kupplung. Die Zyklisierung hinzu unkonventionellen thermoplastischen Elastomeren wurde ohne Anzeichen eines Abbaus des Polyestermittelblocks durchgeführt.

**Kapitel 5** beschreibt die erste anionische Polymerisation eines 1,3-Diens mit einer Thioether-Funktion ausgehend von dessen Synthese. Im Zuge der Monomersynthese wurde die Bildung eines isomeren Gemischs beobachtet. Die anionische Polymerisation von 6-Methylthiohexa-1,3-dien (MTHD) resultierte in Polydienen mit

erhöhten Dispersitäten von Đ > 1.24. Dieses Ergebnis wurde zu Teilen auf das vorgefundene Isomerengemisch zurückgeführt. Eine *in situ* $^{1}$H-NMR-spektroskopische Kinetik offenbarte die rasante Bildung der Polymerketten, wobei sich die Homopolymerisation als Stereocopolymerisation der beiden Isomere herausstellte. Die anionische Polymerisation von MTHD mit Isopren resultierte in hochdefinierten Copolymeren (Đ < 1.19) mit guter Kontrolle über den molaren Anteil des MTHD und Isopren sowie über die molare Masse (10 – 50 kg mol$^{-1}$). Die Alkylierung, Alkoxylierung und Oxidation veranschaulichen die mannigfaltigen Möglichkeiten zur effektiven Modifikation des Schwefels von Polymeren mit Thioether-Gruppen. Die Oxidation erfolgte ausschließlich am Schwefel und nicht an den Doppelbindungen des Polymerrückgrats, wodurch das Potential des Thioethers als intramolekulare Antioxidans-Einheit verdeutlich wurde. Die Alkylierung ermöglichte ebenso wie die Alkoxylierung den Einbau verschiedener Funktionalitäten in quantitativer Weise. Eine Auswahl der modifizierten Polydiene, welche in Wasser dispergierbar waren, wurde hinsichtlich ihrer antimikrobiellen Wirkung evaluiert. Die Sulfonium-Spezies, welche durch Alkylierung mit Methyliodid erhalten wurde, wies keinen inhibierenden Einfluss auf. Im Gegensatz dazu wurde nach der Alkoxylierung mit dem industriell etablierten PO eine ähnliche Wirksamkeit festgestellt, wie bei den Antibiotika Ampicillin und Kanamycin. Dies betrifft die hemmende Wirkung auf den bakteriellen Wachstum von *E.coli* und *S. aureus*. Die Hemmung des bakteriellen Wachstums ist ein Beleg für das große Potential von Thioether-Dienen als Baustein für neuartige Materialien.

Der Artikel aus Kapitel 3 wurde außerdem in der deutschen Ausgabe des Journals publiziert. Im **Anhang A1** wird die deutsche Fassung des Kapitel 2 gezeigt.

# Graphical Abstract

# GRAPHICAL ABSTRACT

**Chapter 1: Green Perspective Drives the Renaissance of Carbanionic Polymerization of Dienes**

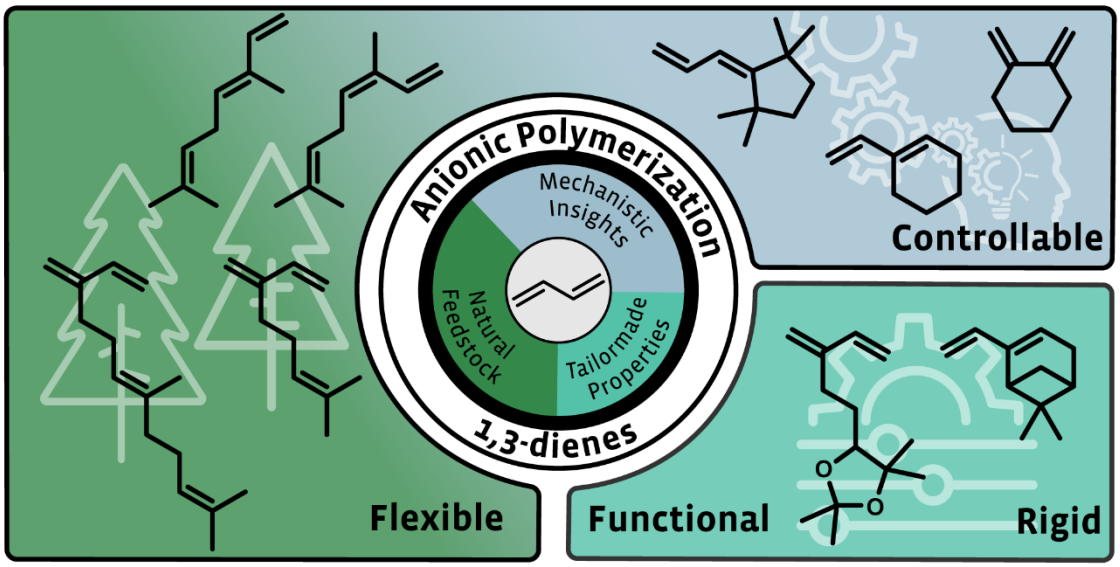


**Chapter 2: Merging Styrene and Diene Structures to a Cyclic Diene: Anionic Polymerization of 1-Vinylcyclohexene (VCH)**

**Chapter 3: Anionic Polymerization of Phenyl-Substituted Isoprene Derivatives: Polymerization Behaviour and Cyclization-Enabled Fluorescence**


**Chapter 4: Polydiene-Derived High Glass Temperature Polymers in Thermoplastic Elastomers: Coupling with Non-Crystalline Polycaprolactone as the Mid-Block**

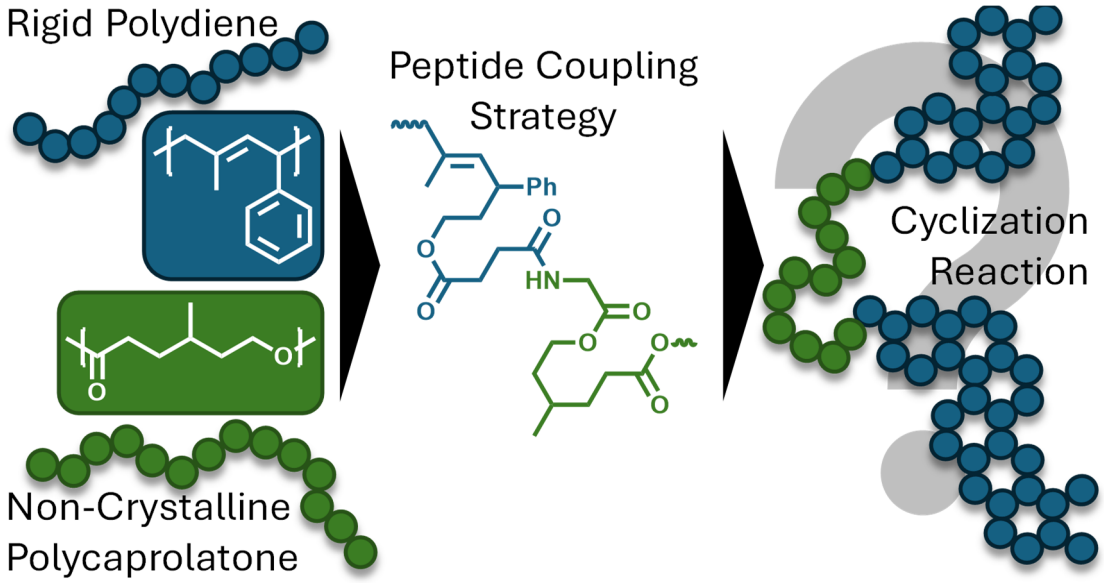

**Chapter 5: The Impact of Thioether Groups in the Anionic Polymerization of Diene Monomers for Post-Polymerization Modification.**

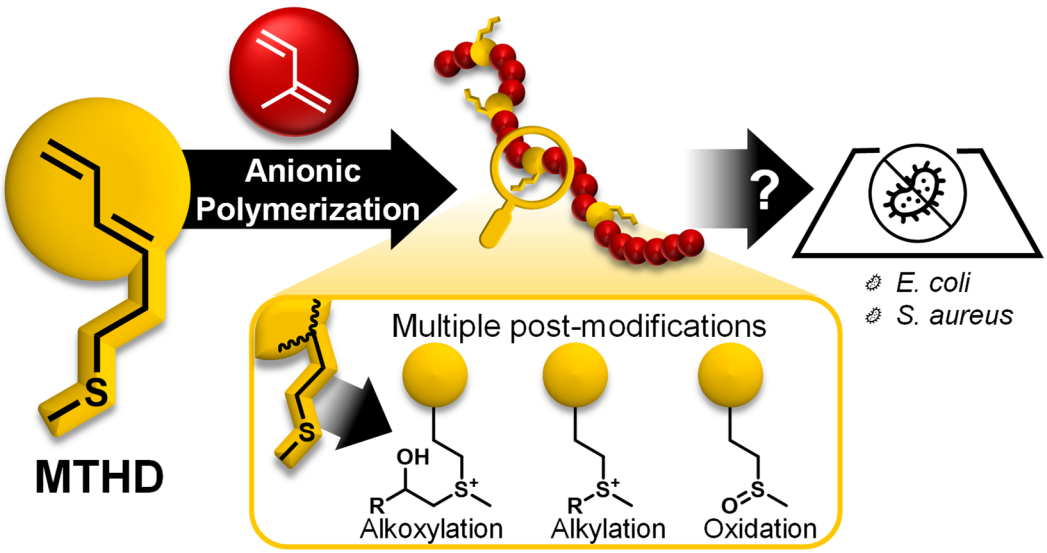

# CHAPTER 1

## Green Perspective Drives the Renaissance of Carbanionic Polymerization of Dienes

# CHAPTER 1

Published in *Polymer Chemistry,* 2024, **15**, 4291-4368.
*DOI: 10.1039/D4PY00805G*

# Green Perspective Drives the Renaissance of Anionic Diene Polymerization

Moritz Rauschenbach,[a,†] Moritz Meier-Merziger,[a,†] and Holger Frey [a,†,*]

[a] Department of Chemistry, Johannes Gutenberg University Mainz, Duesbergweg 10 – 14, D-55128 Mainz, Germany.

[†] All authors have contributed equally

The following chapter was written in equal parts by the first two authors and is adapted with permission from M. Rauschenbach, M. Meier-Merziger and H. Frey; Green Perspective Drives the Renaissance of Anionic Diene Polymerization, *Polymer Chemistry*, 2024, **15**, 4291-4368. DOI: 10.1039/D4PY00805G. 

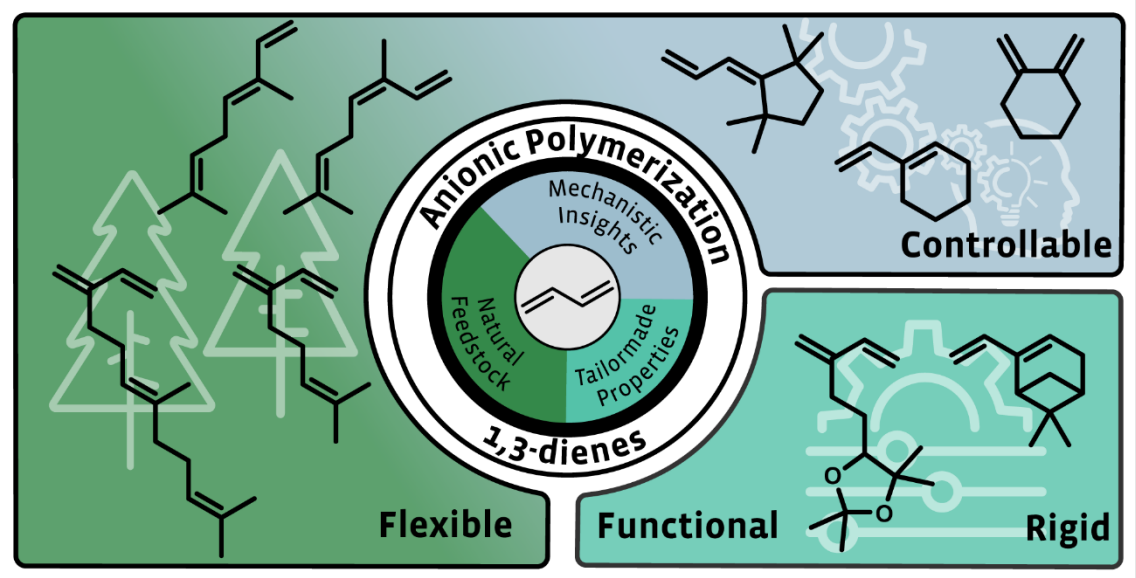


**Abstract:** Polymers based on 1,3-diene monomers play a pivotal role in many commercial elastomers and thermoplastic elastomers. This perspective summarizes the state of the art and recent developments in the living anionic polymerization of dienes, permitting to finely tune the properties of the resulting polymers. An emphasis is placed on novel biobased diene monomers (myrcene, farnesene, etc.) and polymerization solvents, which bear promise for more sustainable elastomers in the future. Furthermore, statistical copolymerization of dienes with vinyl monomers and the *in situ* monitoring of monomer gradients and formation of tapered di- and triblock copolymers due to disparate reactivity ratios is also reviewed. Thermoplastic elastomers based on tri- and multiblock architectures as well as recently reported diene-based polymer architectures are discussed as well. A summary of current challenges and future options for the carbanionic diene polymerization concludes this short review article.

## 1. Introduction

Polymers based on 1,3-diene monomers played a pivotal role in the early days of macromolecular science, when Staudinger introduced the term “macromolecule” in 1920, specifically referring to polyisoprene (PI).[1,2] Although the first anionic diene polymerization was observed already a decade earlier by Matthews,[3] who stored isoprene in the presence of sodium, it was *IG Farben* that later commercialized the alkali metal-initiated polybutadiene (PB) based elastomers as “Buna”. This development was prompted by a substantial increase in demand for natural rubber.[4,5] From a molecular perspective, natural rubber derived from *hevea brasiliensis* consists of 1,4-*cis* (>98%) polyisoprene.[6] Nowadays, synthetic rubber based on diene polymerization is produced on megaton scale and is often combined or blended with natural rubber.[7] Both synthetic polydienes and natural rubber possess a double bond per repeating unit, rendering them suitable for crosslinking *via* vulcanization. The resulting elastomers are used for applications as diverse as tires and medical gloves. The anionic polymerization of dienes continues to garner significant attention in today’s industrial and scientific research.[8] This leads to continuous new insights also for the established dienes such as butadiene (B) and isoprene (I). Synthetic rubber offers advantages over natural rubber due to its versatile and adjustable properties, since the exact chemical nature of the polymer can be influenced during the polymerization process.[9] The commercial importance also arises from the option to produce homo- and copolymers with controlled molar masses and the capability to precisely regulate the microstructure by so called “modifiers” that coordinate the counterion to tailor a variety of material specifications.[10] Moreover, 1,3-dienes are used in copolymers such as acrylonitrile-butadiene-styrene (ABS) and styrene-butadiene-styrene triblocks (SBS), which are frequently utilized materials. The thermoplastic elastomers SBS and the analogue SIS using isoprene instead of butadiene have been investigated in-depth and were commercialized under various trade names (i.e. *Kraton™* or *Styroflex™*).[11] S/I-copolymers have remained a key research topic of our group, elucidating how different polymerization conditions affect the statistical copolymerization and the resulting monomer gradients and mechanical properties.[5,12–17] Consecutive monomer addition steps can be used to generate precisely defined, high molar mass tapered multiblock copolymers (MBCP) that are

not accessible by other techniques.[5,13–15] Precise knowledge regarding the incorporation statistics of two monomers within a polymer chain, expressed by their reactivity ratios, can be used to reduce the number of monomer addition steps to increase synthetic efficiency. Therefore, *in situ* kinetics measurements relying on online $^{1}$H NMR or near infrared (NIR) kinetics have become the methods of choice to determine the reactivity ratios of a large variety of copolymerizations in recent years.[16–23] Furthermore, in the last decade a variety of new diene monomers has been introduced that extend the range of materials for elastomers and thermoplastic elastomers far beyond PB and PI.

Polydienes are commonly synthesized by anionic or catalytic polymerization techniques. Catalytic polymerization strategies are employed on large commercial scale. Recently the long-time challenge of incorporation of polar monomers was achieved by the groups of Cui and Mecking, who also introduced the catalytic polymerization of functional dienes.[24,25] We emphasize that a detailed overview of the catalytic polymerization of 1,3-dienes will not be covered in in this short review. Readers are referred to recently published excellent summaries in this area.[26,27] Characteristic polymer properties found and discussed for polydiene materials naturally apply regardless of the polymerization technique used. The main advantage of the catalytic polymerization is the precise control of stereoselectivity.[26] The development of a Gd-based catalyst enabled similarly high 99.9% *cis*-1,4-polyisoprene stereocontrol, as known from natural rubber.[28]

Due to the high basicity of the carbanion, the highest extent of control in anionic polymerization is achieved by the challenging break-seal method.[29] This requires not only a synthetic skillset, but also glassblowing skills. The more accessible high vacuum technique, that has long been established, still enables exceptional control over the polymerization. This allows to synthesize new polydienes and to investigate the impact of polymerization conditions. Besides the established production of polydienes *via* batch synthesis, also continuous flow reactors for the carbanionic polymerization can be employed for the polymerization of dienes.[30–33] Recently, Haddleton and coworkers reported on the anionic diene polymerization without monomer/solvent purification steps, making it more widely applicable, albeit for lower molar mass polymers, e.g. for polymer additives and surfactants.[34,35] With respect to precision, anionic

polymerization surpasses the catalytic approach, thanks to its distinctive living character, which enables to synthesize of a wide range of polymer architectures and also tailormade gradient and tapered chain compositions in copolymers.[8]

In recent years, there has been a notable shift in academic research as well as in industry towards bio-derived monomers. Efforts to tailor material properties for enhanced performance accompany this research direction, with the aim of matching or surpassing the properties of established fossil fuel-based materials. In this review we will cover 1,3-dienes beyond the classical representatives, butadiene and isoprene. A selection of the discussed mono- and disubstituted 1,3-dienes is shown in **Figure 1**. While some can be found in nature, additional synthetic modification steps are required for others. The number of synthetically accessible 1,3-dienes for the anionic polymerization is steadily increasing.

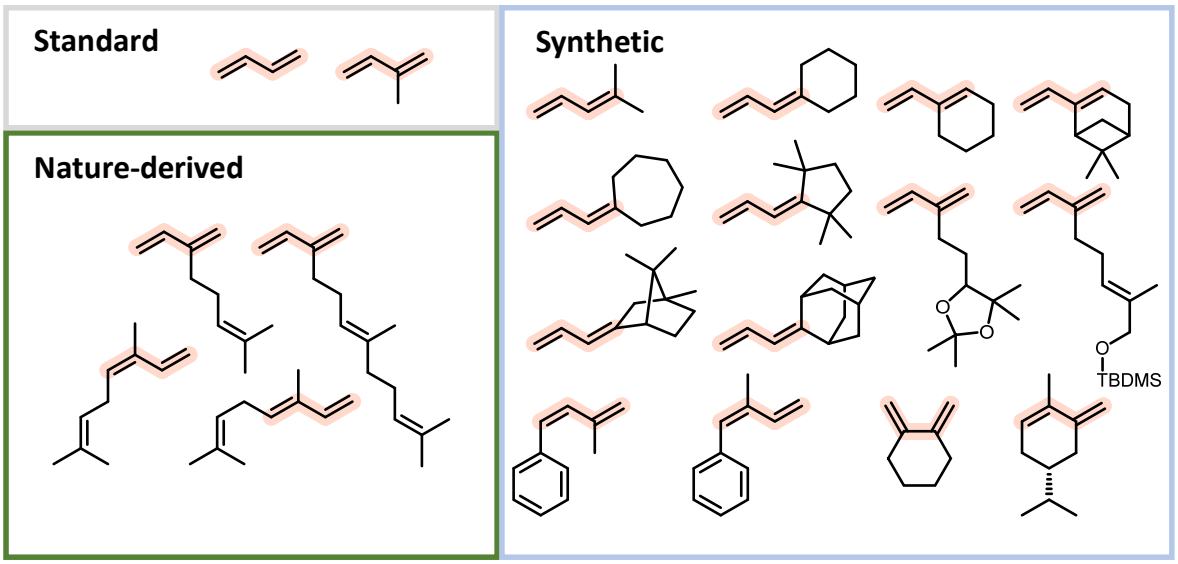


**Figure 1.** Overview of a selection of 1,3-dienes discussed in this perspective, including recently introduced diene monomers. Reactive diene moieties are marked for each monomer.

## 2. Is the Anionic Polymerization of Dienes Genuinely a Coordinative Process?

Butadiene and isoprene have been the most investigated and industrially used diene monomers to date. They both can lead to different isomeric units along the chain, with respect to regio- and stereo structure (**Scheme 1**b). As detailed by Carlotti *et al.*,[9] varying the microstructure is a powerful handle to adjust the materials properties, for instance for tire applications, where high degrees of elasticity over a broad

temperature range are desired, which are usually correlated with a high 1,4-content. This involves minimizing the glass temperature ($T_g$) as much as possible to achieve the widest possible application temperature range. The overall regio- and stereochemistry of the anionic polymerization of 1,3-dienes has been widely discussed in the last decade with respect to their dependency on the counter ion,[10,36,37] solvent,[10,38] and the presence of a polar modifier.[17,19] The formation of aggregates during the polymerization in nonpolar solvents and their suppression by the use of polar solvents or modifiers was found to be one of the key aspects of the propagation mechanism. The number of the aggregating chains evolves from the kinetic order, expressed by the following **Equation 1**:

$$\log(k_{app}) \sim \frac{1}{n}\log[\mathrm{Ini}]_0 \qquad \textbf{(1)}$$

$k_{app}$ gives the apparent rate constant of the propagation, $[\mathrm{Ini}]_0$ the initial concentration of the initiator and $n$ the number of aggregating chains. Importantly, the aggregates are in an equilibration with the unimers which are considered to be the active species capable of sustaining the propagation mechanism, see **Scheme 1**. M. Szwarc already reported that the relative rates of propagation for isoprene and butadiene are ordered as isoprene > butadiene, while both exhibit a number of aggregating chains of $n = 4$.[10,39] However, it was found that polyisoprenyl lithium aggregation also depends on the concentration of active chain ends. An overall equilibration between tetramers and dimers was observed, with $n$ approaching ~2 with decreasing concentration.[10,38] $\beta$-Myrcene and $\beta$-farnesene, although kinetically investigated under the assumption of tetramer formation, have not been explored with respect to their aggregation behavior.[19,22] The observation that their propagation rate surpasses that of isoprene suggests the presence of an equilibrium solely between dimers and unimers. It should be noted that this assumption has not yet been empirically confirmed.

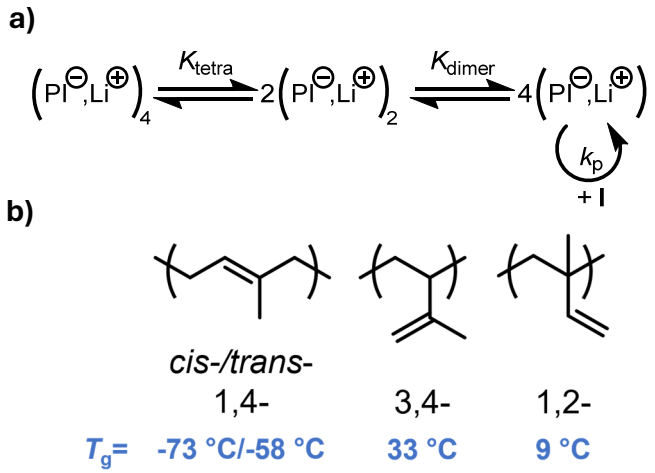


**Scheme 1.** a) Aggregation equilibrium of polyisoprenyl lithium in nonpolar solvents in analogy to Müller and Matyjaszewski; b) possible microstructures of PI and their respective glass temperatures.[38,40]

The coordination of the counterion to the incoming monomer and its spatial orientation mainly dictate the regioselectivity, see **Scheme 2**. In nonpolar media, it has been reported to undergo a six-membered transition state, where the diene is added in a *cis*-form, explaining overall high amount of 1,4-addition. The final *cis/trans* ratios have been extensively elucidated by Gebert *et al*. who suggested an isomerization of the *cis*-oriented chain end to a *trans*-form before the next monomer addition.[38,41,42] Worsfold and Bywater further proposed that the isomerization occurs in competition with the monomer addition.[10,43] Based on these fundamental studies, the final ratio of *cis* and *trans* 1,4-units can be explained.

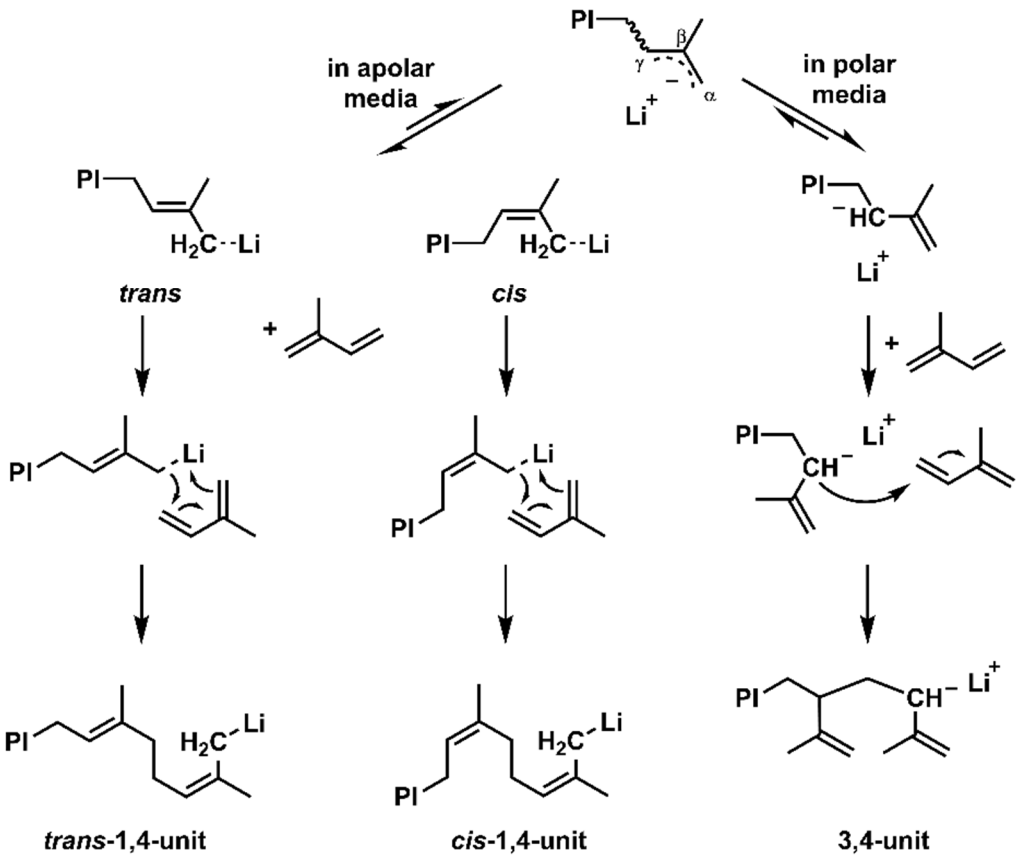


**Scheme 2.** Proposed mechanism of the polymerization of isoprene with lithium as a counter ion in apolar or polar media, respectively; image is reproduced from Frey *et al*.[41] with permission of Royal society of Chemistry, 2022.

By changing the counterion from $Li^+$ to $Na^+$ or $K^+$, for instance, the interionic distance increases, which reduces the 1,4-content of polydienes.[10,44] Based on the industrially most popular diene representative 1,3-butadiene, Carlotti and coworkers have investigated the impact of bimetallic initiator systems with lithium and potassium or calcium, respectively. They studied the influence of the additional coordinative center on the microstructure. While the addition of potassium led to an expected increase of 1,2-units, the designed calcium-lithium initiators enabled high control towards *trans*-1,4-units.[45,46] Reviewing the accessible microstructures of polybutadiene, Carlotti *et al*. also reported on the combined effect of both variation of the counterions as well as changing to polar solvents.[9] The polymerization in polar solvents, e.g. THF, or the addition of polar modifiers are both associated with a suppression of the coordination between the chain end, the counterion and the diene. In consequence, the resulting increased vinyl content enhances the backbone rigidity of the polydiene, which is reflected by an increase of the glass temperature (**Scheme 1**b).[38,41] The influence of solvents on the anionic polymerization will be discussed below in greater detail.

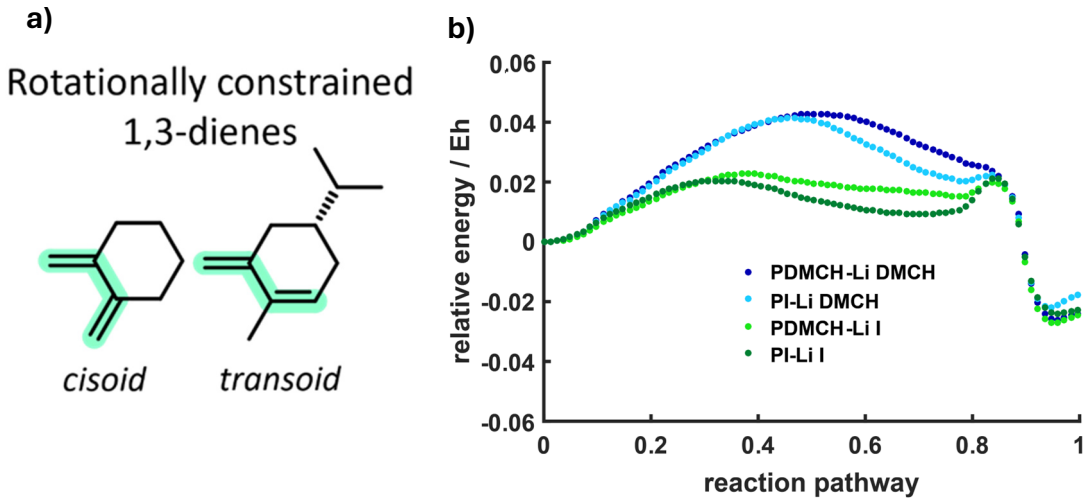


**Figure 2.** a) Rotationally constrained dienes with a *cisoid* (DMCH) and a *transoid* (IMMCH) geometry; b) Reaction pathways for the four possible propagation steps of the copolymerization of isoprene and DMCH (Addition of DMCH, blue; Addition of isoprene, green), image is reproduced from Frey *et al.*[41] with permission of Royal society of Chemistry, 2022.

A rather new aspect in this field is the examination of the orientation of the double bonds with respect to each other in the 1,3-diene scaffold. In this regard, DFT calculations can give mechanistic insights beyond the mere conversion in a copolymerization. In a recent publication we investigated rotationally constrained dienes.[41] Two model compounds were synthesized to obtain a *cisoid* and a *transoid* monomer as shown in **Figure 2**a. DFT calculations identified deviations of the torsion angle in both monomers and allow for an assumption regarding the reactivity given by the electron densities. A crucial finding from the simulation is that if a fixed *transoid* geometry is present, only one of the double bonds can coordinate with the lithium counterion. This crucial step should prevent the polymerization. In contrast, the *cisoid* model compound coordinates with both double bonds, albeit a distortion of the ring is required. Consequently, only homopolymers with the *cisoid* 1,2-dimethylene-cyclohexane (DMCH) were obtained and copolymerization with isoprene was achieved. DFT calculations show that the energy required for the polymerization of DMCH is significantly increased compared to isoprene due to a required distortion of the ring, see **Figure 2**b. Empirically, this was observed *via in situ* $^{1}$H NMR kinetics. In the copolymerization with isoprene, isoprene is consumed predominantly, resulting in a gradient structure along the chain. The homopolymerization of DMCH itself required unusual conditions to keep the growing chain in solution: high temperatures of 140 °C

were applied in the high-boiling solvent tetralin. Noteworthy, the analysis of PDMCH confirmed the exclusive formation of 1,4-units and a $T_g$ of 53 °C. In contrast, no polymers were obtained with the *transoid* monomer IMMCH. In 2015, Ishizone and coworkers described the anionic polymerization of the *transoid*-fixed benzofulvene in both polar and apolar media.[47–49] This can be attributed to the conjugation with the aromatic ring that leads to a planar cross-conjugated π-system resulting in a higher reactivity. The removal of the aromatic ring, e.g., in methylene cyclopentane resulted in the expected reduction of the reactivity. For this monomer 70 °C and a reaction time of 4 days were required to achieve full conversion.[50] Consequently, it can be concluded that *transoid* dienes are not suitable for the living anionic polymerization in nonpolar solvents at mild conditions.

Moreover, already a methyl group can interfere with the coordinative process and prevent the formation of a narrow molar mass distribution. This was shown for the two isomers *trans*- and *cis*-pentadiene. They exhibit rate constants in the order *cis* > *trans* while only the *trans*-isomer gives well-defined polymers ($Đ \leq 1.09$).[51] Surprisingly, the polymerization is gradually decelerated, if both isomers are mixed, leading to the order of the rate constants as follow: *cis* > *trans* > *cis*/*trans*.[52]

Taking these recent results of geometrically constrained dienes together, one can tentatively answer the initially raised question: the classic anionic polymerization shows indeed many features of a coordinative process in apolar media. Various parameters can be changed to influence the coordination, either by relying on a solvent that coordinates the counter ion or by changing the substitution pattern of the diene, which was found to influence the mechanism drastically as in the diastereomers isoprene and *cis*-pentadiene. These strategies are being further pursued by various groups present.

## 3. Controlling the Microstructure of Polydienes

The resulting microstructure is directly dependent on the propagation mechanism, as introduced previously. Primarily for rubber applications, 1,4-repeating units are favored because of the known low $T_g$ of the polymers and lower entanglement molar mass.[5,44] On the other hand, for specific post-polymerization modification

reactions[53,54] or to suppress crystallization as for hydrogenated polybutadiene,[55] an increased vinyl content is targeted. Polydienes, such as polyisoprene, were widely investigated to understand their microstructural changes with respect to solvent polarity. It is well-known that polymerization in polar solvents like THF results in significantly higher content of 3,4- (62%) and 1,2-units (24%).[56] However, the monomer incorporation mode can also be tailored by using small amounts of polar modifiers in nonpolar solvents. Morton and Fetters reported that for isoprene the addition of aliquots of THF initially increases the propagation rate.[57] Surprisingly, further addition leads to a subsequent decrease, as Bywater had previously demonstrated for styrene.[58] Recently, we have been able to give a detailed view of the impact of THF on the statistical copolymerization of styrene and isoprene, relying on online NIR monitoring of the anionic copolymerization. When increasing the THF concentration the vinyl content of the isoprene-units increases.[17] In other works based on online kinetics, polymerization of the analogous $\beta$-myrcene was investigated to compare the influence of ditetrahydrofuryl propane (DTHFP) and tetramethyl ethylene diamine (TMEDA) as polar modifiers with the established THF. As shown in **Table 4**, both DTHFP and TMEDA show a stronger impact on the microstructure than THF.[19,59] The addition of 2 equivalents with respect to the lithium-ion concentration leads to predominant 3,4-units (> 57%). Undesirably, this leads to an increase of the low glass temperature. Polydiene based elastomer chains usually exhibit a $T_g$ below − 60 °C. When gradually increasing the ratio of vinylic units, the $T_g$ of polyisoprene can reach 0 °C.[60] Although the $T_g$ of polydienes shows this correlation with the proportion of the different microstructures, polyfarnesene (PFar), discussed later in this perspective, shows a different behavior. Due to its long side chain in every repeating unit, the $T_g$ remains nearly unaffected by increasing the vinyl content, as illustrated in **Figure 3**.

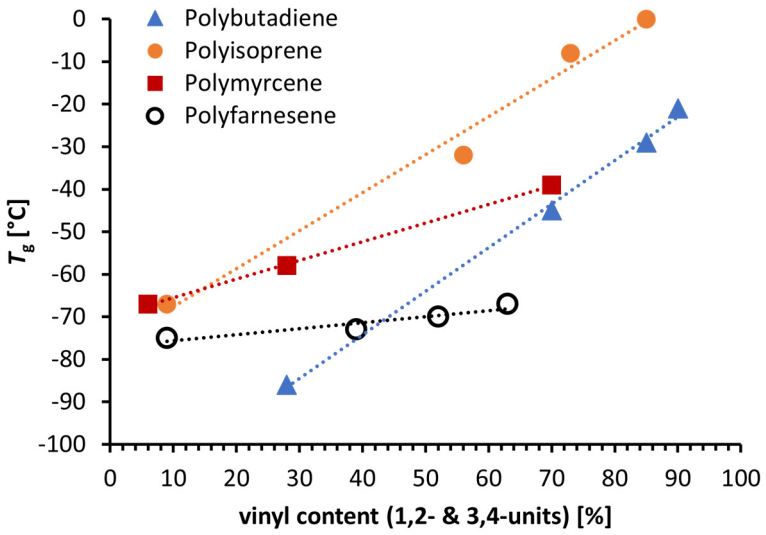


**Figure 3.** Correlation of glass temperature of polydienes with the vinyl content. The values are combined from several original works.[60–63]

In addition to altering the system's polarity, it is well-known that increasing bulkiness of the substituent results in an almost exclusive formation of *cis*-1,4-units. This was demonstrated for the anionic polymerization of 2-substituted 1,3-butadiene derivatives with a methyl, ethyl, *n*-propyl or isopropyl group.[64–66] Pendant phenyl groups, as seen in 1-phenyl butadiene (PhB), 1-phenyl isoprene (1PhI) and 4-phenyl isoprene (4PhI), have demonstrated a predominant occurrence of 1,4-addition (>80%), even in the polar solvent THF.[67–69] Furthermore, Ishizone and coworkers achieved control over the incorporation by designing rather unusual allylidene monomers.[70,71] The reported butadiene-derivatives were 1,1-disubstituted with increasing bulkiness of the pendant group. Various substituents, ranging from two methyl groups to a bornane ring and even the bulky adamantyl group, were attached to the dienyl-unit. Hence, the sterically hindered 1,4-addition could be further prohibited with increasing bulkiness, which is underlined by the absence of 1,2-units. The structures shown in **Figure 4a** were sufficiently effective to increase 3,4-units to more than 20% in apolar media. The bulky substituents of the structures in **Figure 4b** result almost exclusively in 3,4-incorporation. As a result, these polymers turned out to be very rigid materials with high glass temperatures of nearly 200°C in case of the pendant bornane-ring. In theory, this might allow for application in high temperature resistant thermoplastic elastomers (TPEs) as a hard segment, but on the other hand this will also necessitate extremely high processing temperatures.

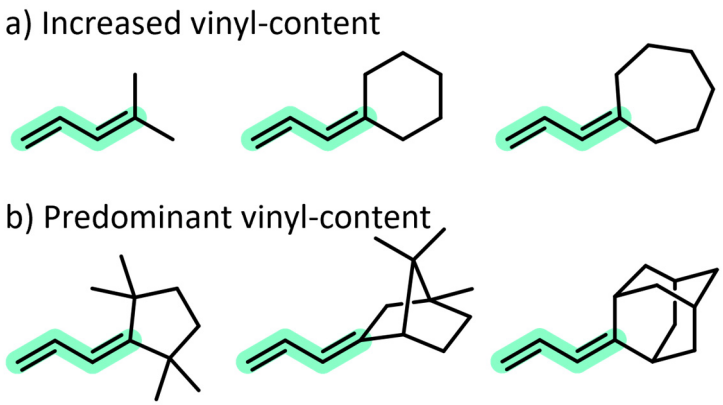


**Figure 4.** 1,1-Disubstituted 1,3-dienes studied with respect to their behavior in the anionic polymerization, reported by Ishizone *et al*.[70,71]

The monomer 1-vinyl cyclohexene (VCH) serves as a model compound with one double bond that is sterically constrained within a cyclic structure. The key question is whether VCH behaves as a 1,3-diene or as a styrenic vinyl monomer in the anionic polymerization in nonpolar media. In analogy to other diene structures, the homopolymerization in cyclohexane (CHx) lead to a predominant formation of 64% 1,4-units.[72] The extent of 1,4-incorporation is comparable to the allylidene cyclohexane with a reported 66% 1,4-units when polymerized in benzene.[71] However, the added rigidity from the ring in the backbone increased the $T_g$ to 78 °C. The microstructure of PVCH was adjusted to enhance the vinyl content, reaching up to 78% of 3,4-PVCH upon addition of the polar modifier THF. The resulting material properties, with a $T_g$ of up to 89 °C, are much closer to those of PS ($T_g$ = 100 °C).[73] Likewise, hydrogenation leads to a high amount of polyvinylcyclohexane (PVCH) segments, as obtained by hydrogenation of PS.

## 4. Bio-Derived Diene Alternatives

The dwindling fossil resources evolved to be a major motivation in finding new substitutes for established systems such as polydiene-based (co)polymers. Wahlen and Frey presented a wide scope of terpene monomers that are amenable to the anionic polymerization.[74] Predominantly, *β*-myrcene (Myr) and *β*-farnesene (Far) have gained significant attention owing to their structural similarity to the 2-substituted isoprene framework and their biobased origin from turpentine oil and sugar cane, respectively. Both monomers show similar dependencies of the polymer structures on

the polymerization conditions and result in comparable polymer properties. A highly 1,4-dominated microstructure is obtained when polymerizing in apolar solvents, which results in a similarly low $T_g$ as polyisoprene, with $T_g$ < – 60 °C (**Figure 3**).[60,62] This renders PFar and PMyr suitable for the application as soft phase in thermoplastic elastomers. Combinations with polystyrene or polylactide (PLA) as the vitrified plastic domains have also been reported. When polystyrene is used for the rigid phase, classical linear ABA-triblock copolymers can be synthesized. Sequential addition yields block architectures, whereas tapered structures are obtained by one-step statistical copolymerization.[19,23,62] This will be discussed in greater detail in one of the following sections. By the combination with polylactide as the rigid phase even more complex architectures were realized, e.g., graft polymers and *H*-shaped triblock structures, see **Figure 5**.[75–77]

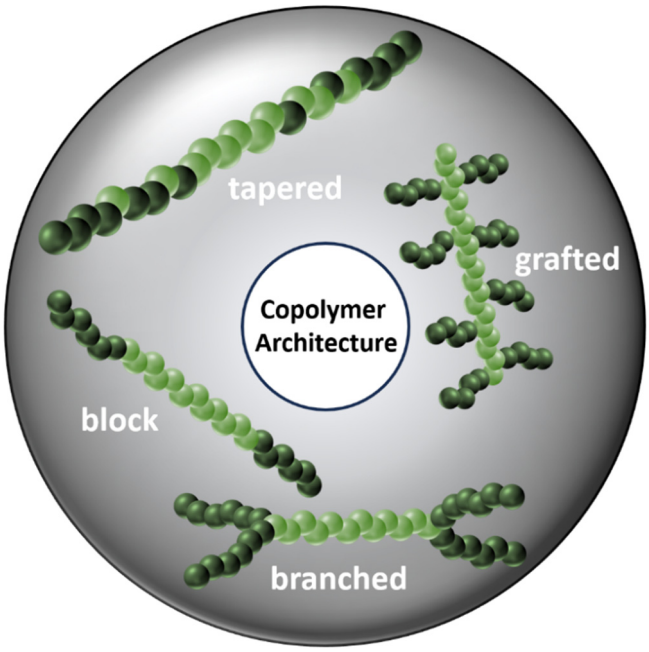


**Figure 5.** Different copolymer architectures for TPEs based on block, tapered and branched triblock structures as well as graft-copolymers.[22,75–78]

Due to the increasing length of the side chains in PMyr and PFar that do not contribute to the polymer backbone length, the entanglement molar mass strongly increases from 7 kg mol$^{-1}$ for PI, 18 kg mol$^{-1}$ for PMyr to 50 kg mol$^{-1}$ for PFar.[79–81] This effect has considerable consequences for elastic mechanical properties that are strongly dependent on the entanglements of the polymer chains. Therefore, higher molar masses compared to PI are required for PFar to obtain similar mechanical properties.

The first report on the anionic polymerization of *β*-myrcene by our group focused on the behavior in statistical copolymerization with isoprene, styrene and 4-methyl styrene (4MS), respectively.[23] *In situ* $^1$H NMR kinetics was performed revealing *β*-myrcene to be a suitable substitute for isoprene with similar behavior in the copolymerization with styrene. Both systems show a steep gradient, as discussed later in this perspective. This was further investigated using the *in situ* NIR method.[19] A series of S/Myr-copolymers were synthesized to investigate the impact of an increasing amount of THF on the nature of the gradient structure of the copolymers. It was shown that the gradient structure can be tuned by a variety of modifiers, even to complete inversion of the reactivity ratios, similar to the behavior observed earlier for isoprene.[17] Furthermore, we showed that Far forms a gradient structure in the statistical copolymerization with styrene and that the polymerization in cyclohexane became significant faster when moving up the homologous series of terpenes: $k_{p,I} < k_{p,Myr} < k_{p,Far}$.[16,19,21]

Although renewable feedstocks are one of the most important current research fields, their impact on nature and, above all, the possible competition with food sources should always be considered as well. *β*-Farnesene, relatively price competitive, as shown by its use as sustainable jet fuel besides its application in materials, is mainly derived from sugar cane.[82] PFar products are already widely available in industry, e.g., PFar-diol is used for the preparation of polyurethanes.[60,83] Therefore, additional feedstocks are being sought. It was already shown that heterotrophic as well as lithoautotrophic bacteria are capable of producing Far from cultivation on a variety of substrates.[84]

Furthermore, the additional double bonds in the side chain allow for further post-modification with respect to thiol-ene click chemistry and epoxidation, respectively.[85,86] Thereby, these monomers offer the possibility of introducing functionalities along the polydienes chains, which would require suitable protecting groups if introduced prior polymerization. This will be addressed in a later section of this overview. In addition to these aforementioned examples, there are also less known representatives in the field of terpenes. For instance, our group reported on the anionic polymerization of *β*-ocimene (Oc).[87] As Oc resembles a 1,2-disubstitued diene it naturally occurs as a mixture of the *cis* and *trans*-isomer, similar to 1,3-pentadiene.

The anionic polymerization in cyclohexane resulted in an unusually high dispersity up to 2. *In situ* $^1$H NMR kinetics revealed a preferred consumption of the *trans*-isomer over the *cis*-form ($r_{trans}$ = 3.16 and $r_{cis}$ = 0.316) turning the apparent Oc homopolymerization into a copolymerization of the two stereoisomers. Surprisingly, the addition of styrene inverted the trend to an accelerated consumption of the *cis*-isomer. Taking advantage of these findings, both isomers were isolated by polymerization of the respective other isomer. Consequently, the NMR kinetics with styrene could be elucidated separately. The values given in **Table 2** reveal the presumed consumption of styrene over the *trans*-isomer ($r_{trans}$ = 0.628 and $r_S$ = 1.59), while unexpectedly the *cis*-isomer showed an almost random incorporation of both monomers ($r_{cis}$ = 1.01 and $r_S$ = 0.98). This phenomenon is quite uncommon in the field of carbanionic polymerization, as mostly gradient structures are obtained. An overview of a broad range of diene copolymerizations and their respective reactivity ratios is given in **Table 2**. For reference, the established S/I-copolymerization in cyclohexane shows a steep gradient, characterized by $r_I$ = 10 and $r_S$ = 0.015.[17]

1,3-Diene structures offer potential beyond low $T_g$ and high elasticity, as their structures can be highly diverse. Ishizone *et al*. presented a variety of 1,1-disubstituted dienes that possess cyclic structural elements and were already discussed in more detail earlier in this perspective.[70,71] Their unusually high $T_g$s are attributed to the rigidity of the ring structure and the resulting high content of 3,4-units. Cyclic elements can also be incorporated by 1,2-substitution as mentioned for the monomer VCH.[72] With the monomer nopadiene (Nopa), 1*R*,5*S*-2-ethenyl-6,6-dimethylbicyclo [3.1.1] hept-2-ene, our group recently presented a sterically even more demanding structure, due to its bicyclic structure. Thereby, a strikingly high $T_g$ of 160 °C for PNopa can be achieved. Nopadiene was therefore presented as a potential biobased substitute of styrene in TPE materials. Nopa can be derived from myrtenal or nopol, again originating from *β*-pinene. An exclusive diene structured and fully biobased TPE can be obtained using the monomers Myr and Nopa.[88] Furthermore, we also developed a one-step synthesis for TPEs. By precisely controlling the reaction conditions, we achieved reactivity ratios that favor the incorporation of low $T_g$ PFar, followed by high $T_g$ PNopa. Since a bifunctional initiator was employed for this reaction, a telechelic polymerization was realized and thus, two-sided tapered ABA-triblock structures are accessible in a single

polymerization step, enabling an extremely rapid strategy for the synthesis of biobased thermoplastic elastomers.[78]

The diversity of natural sourced compounds, e.g. terpenes, offers vast potential to customize material properties. However, many parameters must be considered. As many biobased monomers have expanded the portfolio of polymers accessible *via* carbanionic polymerization, a compilation of a variety of the resulting diene polymers in terms of their glass temperature is listed in **Table 1**. The data show the enormous diversity of diene structures and their potential in the field of materials science, as they can be tailored to a wide range of thermal properties. Among those listed, 4,8-dimethylnona-1,3,7-triene (DMNT) has not yet been presented in an original work yet.

**Table 1.** Summary of a variety of polydienes accessible *via* carbanionic polymerization, listed with increasing glass temperatures.

| Polymer | 1,4 [%] | $T_g$ [°C] | Ref. | Polymer | 1,4 [%] | $T_g$ [°C] | Ref. |
|---|---|---|---|---|---|---|---|
| PB | 72 | − 86 | [60] | PDMNT | 74 | − 30 | - |
| PFar | 91 | − 75 | [60] | POc | 15 | − 26 | [87] |
| PFar | 61 | − 73 | [60] | PB | 10 | − 21 | [60] |
| PFar | 48 | − 70 | [60] | PI | 15 | 0 | [60] |
| PMyr | 94 | − 67 | [61] | PMyrDOL | 67 | 11 | [89] |
| PI | 91 | − 67 | [60] | P4PhI | 94 | 48 | [69] |
| PFar | 37 | − 66 | [75] | PDMCH | 100 | 53 | [41] |
| PMyr | 72 | − 58 | [63] | P1PhI | 35 | 65 | [69] |
| PMyrOSi | 69 | − 53 | [61] | PVCH | 22 | 89 | [72] |
| PB | 30 | − 45 | [60] | PNopa | 51 | 158 | [88] |
| PMyr | 30 | − 39 | [62] | PAad* | 0.0 | 178 | [70] |
| PI | 44 | − 32 | [60] | PATMC5** | 0.0 | 194 | [71] |

* 2-allylidene-adamantane (Aad) ** 2-allylidene-1,1,3,3-tetramethylcyclopentane (ATMC5)

## 5. New Solvents for the Anionic Polymerization of 1,3-Dienes

Usually, the requirements for solvents used in the carbanionic polymerization are (i) their aprotic nature and (ii) high base-stability. Often non-polar solvents like cyclohexane or benzene are used, as is mostly the case for butadiene and isoprene systems. The reason for this is the previously discussed solvent effect on the microstructure and the associated changes in material properties. Accordingly, cyclohexane, hexane mixtures, benzene, and toluene are established solvents. Toluene is less favored due to reported transfer reactions.[90] Cyclohexane is used for the industrial synthesis of thermoplastic elastomers by anionic polymerization.[11] For specific demands, e.g., solubility of bifunctional initiators, functional initiators and monomers, tetrahydrofuran (THF) is primarily used to increase the polarity and to suppress aggregation. Proton abstraction at ambient temperatures restricts its use to low temperatures, usually − 78 °C.[91,92] However, the polymerization of dienes is thermodynamically hindered at these low temperatures. Gallei *et al*. took advantage of this to prepare block copolymers by using a one-pot synthesis of styrene/myrcene mixtures, applying a temperature change to polymerize the diene monomer. Only styrene polymerizes at low temperatures, whereas myrcene requires temperatures above − 30 °C in THF to polymerize.[93]

Further, the awareness of sustainability and a shift towards more biobased systems has led to a reconsideration of solvents, as they make up for a large proportion of a synthesis. Consequently, biobased, more sustainable solvents are currently under investigation, see **Figure 6**.

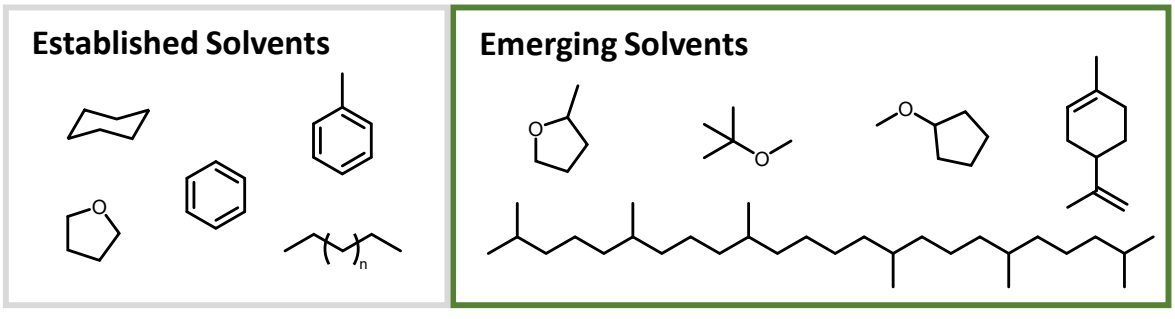


**Figure 6.** Established and emerging solvents for the anionic polymerization.

Looking beyond butadiene and isoprene, other new and often biobased monomers may require the use of more polar solvents. As introduced above, PFar maintains a low

$T_g$ when polymerized in a polar medium, whereas the syntheses of other polydienes require an apolar solvent to achieve similar material properties. Schlaad and coworkers investigated the polymerization of isoprene and *β*-myrcene in a variety of "green" solvents, i.e. limonene, 2-methyl tetrahydrofuran (2-MeTHF) and cyclopentyl methyl ether (CPME).[56,94] On the one hand, 2-MeTHF appeared to have almost the same impact on the microstructure as THF, affording a majority of 3,4-incoorporation (54%). On the other hand, CPME yielded a major fraction of 1,4-units of 64%. The apolar solvent limonene strikingly resulted in 90% 1,4-incorporation. In all solvents, moderate to low dispersities below 1.15 were obtained. Recently, CPME has also been employed for the copolymerization of styrene with isoprene or 1,3-pentadiene, as well as for the copolymerization of isoprene and 1,3-pentadiene. Kinetic studies were conducted to assess its suitability for use in anionic polymerization.[95] Additionally, 2-MeTHF and CPME were both evaluated as additives in the anionic polymerization of 1,3-cyclohexadiene. Notably, CPME in a toluene system demonstrated promising results, with quantitative yields and successful achievement of targeted molar masses, while maintaining low dispersities of $Đ < 1.12$.[96] In addition, Haddleton *et al*. investigated the use of squalane, bearing a $C_{30}$ framework, in its unpurified form as a polymerization medium. Despite the high dispersity ($Đ = 1.84$), attributed to the avoidance of purification steps, the low polarity yielded 94% of 1,4-incorporation.[35] In one of our recent works we showed that the moderately polar solvent methyl *tert*-butyl ether (MTBE) is ideally suited to solvate the bifunctional initiator 1,3-diisopropenyl benzene (DIB). A synergy can be found, as MTBE enables a reliable bifunctional initiation, as it prevents aggregation, while the associated increase in vinyl content does not affect the properties of PFar.[75,78] MTBE, besides being cheap due to industrial scale production for petrol-additives, can also potentially be obtained from renewable feedstocks, i.e. bio-methanol and bio-isobutylene.[97] It is therefore somewhat surprising that it has not received more attention in carbanionic polymerization to date. This can certainly be attributed to the prevalence of the "classical" solvents established over decades. Recently, we investigated MTBE in-depth as moderately polar solvent and additive in homo- and copolymerizations.[98]

## 6. Functional Polydienes *via* Functional Monomers or Post-Polymerization Modification

So far, all presented polydienes discussed solely consist of carbon and hydrogen. In many elastomer applications inorganic fillers are used to enhance mechanical performance (i.e. modulus, and strength etc.). A common filler material used is silica, which is poorly dispersed in a fully non-polar diene material. Silica is known to enhance the performance of tires, one of the main applications of rubber, e.g., by increasing the wet grip for higher safety standards and by reducing the rolling resistance to lower fuel consumption.[99] In this context, the incompatibility of hydrophilic fillers and hydrophobic polydienes has led to an increased interest in modifying polydienes. Early works showed that functionalities have to be separated from the propagating diene unit to prevent the so-called "*back side collapse*" as an undesired side-reaction (**Scheme 3**).[44,100,101]

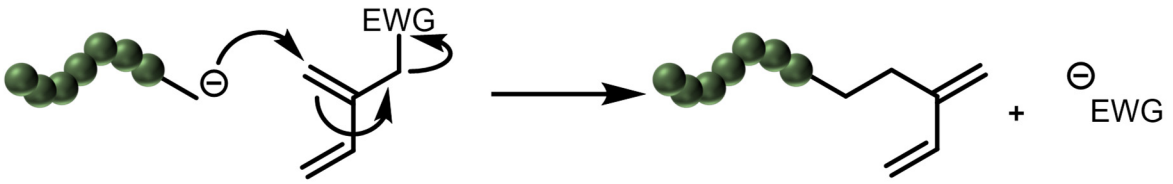


**Scheme 3:** Proposed mechanism of the backside-collapse, as described in the works of Takenaka *et al*.[100,101]

Our group reported on two approaches for functional diene-monomers. Both are based on *β*-myrcene as a precursor that was converted to a hydroxyl-functionalized structure. As free hydroxyl groups are incompatible with the carbanionic polymerization, suitable protecting groups must be employed. A single hydroxyl group was protected using a siloxy functionality (MyrOSi), and a dioxolane-based structure (MyrDOL) was used to incorporate two protected hydroxyl groups. Both functional monomers had a modifier effect on the polymerization, as the masked polar functionalities can interact with the counterion and thereby influence the polymerization mechanism. In this case, the diene acts both as a monomer as well as a modifier. The functionalized *β*-myrcene derivatives, MyrOSi and MyrDOL, showed 31% 3,4-units when polymerized in cyclohexane.[61,89]

Copolymers offer vast possibilities to tune, combine or design materials properties. A variety of copolymers exclusively synthesized *via* anionic polymerization were discussed before. Beyond this, there is a broad field of copolymers that are composed of monomers that require different polymerization techniques. This can be accomplished by preparing a macroinitiator from monomer A. Subsequently, Poly(A) serves as macroinitiator for monomer B to form Poly(A)-*b*-Poly(B) block copolymers in a second reaction using a different polymerization technique. For this purpose, functional groups, e.g. hydroxyl groups, have to be incorporated at the polydiene framework. Controlled end-functionalization of carbanionic living chains is a suitable pathway. For this purpose, lithium, commonly present as a counterion in carbanionic polymerization has the advantage of forming highly stable ion pairs with oxygen. Hence, by using an epoxide for the termination step of a carbanionic synthesis, lithium alkoxides are formed that are not capable of polymerizing any further. As a result, a single epoxide monomer reacts with each chain end, leading to a degree of functionalization of up to 99%.[102,103] Based on the large variety of epoxides available, this method offers vast potential for complex polymer architectures. We recently applied this method to a bifunctional system to simultaneously introduce hydroxyl groups at both chain ends. Whereas ethylene oxide is known to introduce one hydroxyl group, ethoxy ethyl glycidyl ether (EEGE) and isopropylidene glyceryl glycidyl ether (IGG) can be used to introduce two and three hydroxyl groups, respectively. Ultimately, this yields telechelic $OH_2$-polydiene-$OH_2$ and $OH_3$-polydiene-$OH_3$ macroinitiators. *Via* subsequent organocatalyzed chain extension relying on the ring-opening polymerization of L-lactide, elaborate architectures, e.g., *H-super-H*-shaped triblock copolymers rapidly are accessible.[75,104]

Another example for the subsequent formation of a second polymer is grafting from a macroinitiator bearing suitable functional groups at the chains. The high abundance of unsaturated groups present in polydienes was used to introduce functionalities in a post-polymerization pathway. This was demonstrated by the group of Li *et al*. using epoxidation of PMyr.[77,105] Another efficient pathway is based on the use of polymers derived from functional monomers, e.g. PMyrOSi, that can be exploited as a macroinitiator after the cleavage of the protecting group. Again, by L-lactide grafting so-called bottlebrush structures are accessible.[61]

The coupling of polymers offers a third option for producing block copolymers, and particularly for complex polymer architectures. Coupling in the carbanionic polymerization can be achieved directly by introducing multifunctional coupling reagents, e.g. chlorosilanes, at the living polymer chains.[106] In this manner, complex branched structures can be prepared, enhancing the material properties in terms of lowering viscosity in melt and solution. Coupling strategies are also employed for commercial products like Styrolux.[11] Our group introduced a distillable *tetra*-functional chlorosilyl compound to produce well-defined multiblock star polymers.[107,108] In the past, this has been pushed to the limit, with reports of up to 128-arm star polymers.[109] The versatile chemistry of polydienes has recently been exploited by Hirschberg *et al*. in elegant work, who used epoxidized PI to couple with living polystyrenyl chains to obtain *pom-pom* architectures.[110]

## 7. Behavior of 1,3-Dienes in the Statistical Copolymerization

The statistical copolymerization of styrene and butadiene in apolar solvents, leading to so-called "*tapered*" block copolymers was patented as early as 1958 by *Phillips Petroleum Company*.[111,112] Further development by *Shell Co*. resulted in gradient copolymers for commercial application.[113] The statistical copolymerization is an efficient tool to form block-like, tapered structures that still retain microphase segregation like sequential block copolymers. Therefore, the investigation of the gradient formed in a statistical anionic copolymerization is of significant interest. In recent works, we compared tapered multiblock copolymers composed of isoprene and styrene with their respective analogues obtained *via* sequential monomer addition. SAXS patterns revealed weaker segregation, clearly attributed to a reduced effective Flory-Huggins parameter, $\chi_{eff}$.[14] Consequently, the order-disorder transition (ODT) temperature, $T_{ODT}$, decreases, which is desirable for industrial applications targeting high-speed processing *via* melt extrusion.[11] The synthesis of tapered block copolymers relies on significantly different reactivity ratios.[114,115] In 2013, we reported on *in situ* $^{1}$H NMR spectroscopy to track the individual comonomer consumption throughout the living carbanionic copolymerization. The decreasing integrals of the respective monomer signals can be used to determine the reactivity ratios of each system. By this means, one can directly monitor the copolymerization of isoprene and

styrene in apolar media up to full monomer conversion, demonstrating the formation of a steep gradient. The associated reactivity ratios were determined to be $r_I$ = 11 and $r_S$ = 0.053. This can be attributed to a faster cross-propagation rate of S to I, compared to *vice versa* ($k_{SI} >> k_{IS}$).[16,116] Consequently, by initiation of a monomer mixture, two blocks, PI-*grad*-PS, linked by a short gradient structure are obtained. This can be repeated multiple times to generate multiblock copolymers with exceptional material properties, while minimizing the number of reaction steps required.[5,13–15,117] Driven by the interest for biobased monomers we also investigated the terpenes *β*-myrcene and *β*-farnesene in the copolymerization with styrene. Interestingly, both show an even steeper gradient when combined with styrene. **Table 2** summarizes 1,3-dienes that have been investigated regarding their statistical copolymerization with styrene. First, butadiene and monosubstituted 1,3-dienes form very pronounced gradients. Secondly, the homopolymerization becomes less preferred when additional substituents are introduced to the monomer scaffold. For instance, VCH with a double bond captured in the ring is consumed slower than styrene, indicating that the cross-over reaction is highly dependent on the sterics of the respective 1,3-diene. Furthermore, the aforementioned ocimene and its two isomers reveal an impact of the configuration of the double bonds. While the *trans*-isomer is consumed first when both isomers are polymerized together, the reactivity order inverts when both are copolymerized with styrene. This observation was supported by $^1$H NMR chemical titration, which revealed a surprising interaction between styrene solely with the *cis*-isomer.

**Table 2.** Summary of reported reactivity ratios for the copolymerizations of 1,3-dienes with styrene in cyclohexane, together with the resulting monomer gradients.

| Diene | Solvent | *T* [°C] | $r_{diene}$ | $r_S$ | Molar gradient | Ref. |
|---|---|---|---|---|---|---|
| Myr | CHx | 20 | 40 | 0.024 | 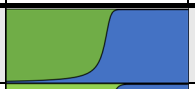 | 19 |
| *β*-farnesene | CHx | 23 | 27 | 0.037 |  | 22 |
| butadiene | CHx | 25 | 15.5 | 0.04 | 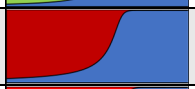 | 10 |
| isoprene | CHx | 20 | 10.1 | 0.013 | 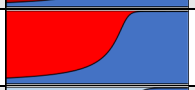 | 16 |
| 4PhI | CHx | 25 | 9.2 | 0.109 | 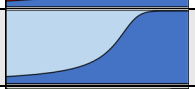 | 69 |
| MyrDOL | CHx | 25 | 5.2 | 0.19 | 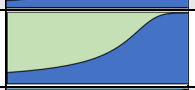 | 89 |
| 1PhI | CHx | 25 | 3.38 | 0.3 | 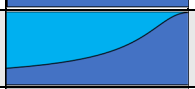 | 69 |
| nopadiene | CHx | 25 | 3.26 | 0.31 | 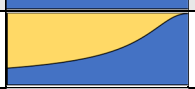 | 88 |
| *cis*-ocimene | CHx | 23 | 1.015 | 0.985 | 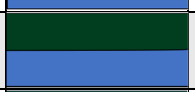 | 87 |
| *trans*-ocimene | CHx | 23 | 0.62 | 1.59 | 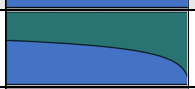 | 87 |
| VCH | CHx | 25 | 0.39 | 2.56 | 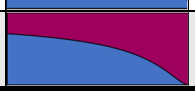 | 72 |

The copolymerization of two 1,3-dienes, mostly with isoprene as a comonomer, has also been investigated, see **Table 3**. Generally, rather weak gradients in comparison to diene/S-systems are observed. The *β*-myrcene derivative MyrDOL has been found to form the steepest gradients when copolymerized with either isoprene or *β*-myrcene, respectively. However, this monomer can hardly be compared with other systems due to its increased polarity resulting from the functional side chain, which is expected to reduce the formation of aggregates, similar to a polar modifier. Noteworthy, the copolymerization of isoprene with the DMCH and VCH, which are both rotationally constrained, results in a favored consumption of isoprene.

**Table 3.** Reported reactivity ratios for the copolymerization of two 1,3-dienes in apolar media, together with the resulting monomer gradients.

| Diene 1 | Diene 2 | Solvent | *T* [°C] | $r_1$ | $r_2$ | Molar gradient | Ref. |
|---|---|---|---|---|---|---|---|
| MyrDOL | isoprene | CHx | 25 | 9.22 | 0.11 | 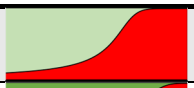 | 89 |
| *β*-myrcene | | CHx | 23 | 4.4 | 0.23 | 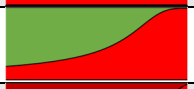 | 23 |
| butadiene | | *n*-hexane | 20 | 2.82 | 0.42 |  | 118 |
| 1PhI | | CHx | 25 | 0.865 | 1.155 |  | 69 |
| VCH | | CHx | 25 | <<1 | >>1 | | 72 |
| DMCH | | CHx | 25 | 0.087 | 11.51 |  | 41 |
| MyrDOL | *β*-myrcene | CHx | 25 | 6.22 | 0.16 |  | 89 |
| nopadiene | | CHx | 25 | 0.13 | 7.49 | 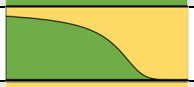 | 88 |
| nopadiene | *β*-farnesene | CHx | 25 | 0.155 | 6.50 |  | 78 |

More recently, we also implemented NIR-spectroscopy to track monomer consumption.[16] The reactions can be monitored directly in the stirred polymerization solution in the reactor, which means that the product formed is directly characterized with respect to its monomer gradient in the chains. Using *in situ* NIR spectroscopy, we studied the influence of polar modifiers, i.e. THF and DTHFP, in the copolymerizations of I/S and Myr/S. Gradually increasing the ratio of [THF]/[Li] can be used as a tool to control the molar composition of the copolymer chains, as indicated by the profiles shown in **Table 4**. Both isoprene and *β*-myrcene are incorporated to a reduced extent, when the polarity of the system increases, resulting in the preferred consumption of styrene.[17,19] In case of the copolymerization of *β*-myrcene and styrene, the chelating DTHFP and TMEDA were shown to have a much stronger impact compared to THF. Already 0.5 eq of [DTHFP]/[Li] influences the copolymerization stronger than 20 eq of THF. Only 2 eq of either DTHFP or TMEDA already lead to an enhanced incorporation of styrene, as indicated by reactivity ratios of $r_S \geq 17.5$ and $r_{Myr} \leq 0.15$, respectively.[19,59]

**Table 4.** Reported reactivity ratios for the copolymerization of dienes with styrene in the presence of polar modifier, together with resulting molar gradients of the chains.

| Diene | Polar Modifier | eq | *T* [°C] | $r_{Diene}$ | $r_S$ | Molar gradient | Ref. |
|---|---|---|---|---|---|---|---|
| isoprene | THF | 0.5 | 20 | 2.856 | 0.093 | 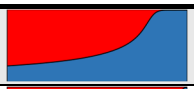 | 17 |
| isoprene | THF | 2 | 20 | 1.06 | 0.262 |  | |
| isoprene | THF | 20 | 20 | 0.374 | 0.925 |  | |
| isoprene | THF | 240 | 20 | 0.148 | 4.196 | 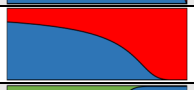 | |
| *β*-myrcene | THF | 0.5 | 20 | 12.3 | 0.082 | 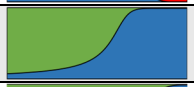 | 19 |
| *β*-myrcene | THF | 2 | 20 | 4.38 | 0.23 | 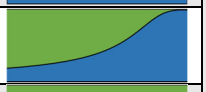 | |
| *β*-myrcene | THF | 20 | 20 | 0.87 | 1.15 |  | |
| *β*-myrcene | THF | 240 | 20 | 0.17 | 5.77 | 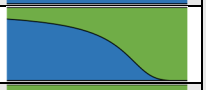 | |
| *β*-myrcene | DTHFP | 0.5 | 20 | 0.41 | 2.42 | 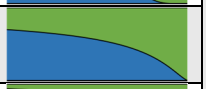 | |
| *β*-myrcene | DTHFP | 2 | 20 | 0.056 | 18.0 | 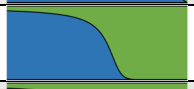 | |
| *β*-myrcene | TMEDA | 2 | - | 0.15 | 17.52 | 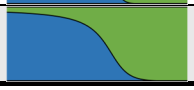 | 59 |

## 8. Current Challenges and Perspective

Anionic polymerization is still the benchmark when it comes to high precision polymer synthesis. Since the polymer chains can be obtained with high uniformity, details of structure-property correlations can be determined and consequently tailored with great accuracy. The current shift towards more sustainable feedstocks comes has led to an increased diversity of diene structures and transforms the deemed “old-fashioned” and fossil fuel-based status of carbanionic diene polymerization. This also motivates fundamental works regarding carbanionic polymerization to further investigate the mechanisms and eventually to develop high performance materials. As most products based on dienes are used as high-volume materials, the economy of scale is a key factor in this area.

An aspect not to be neglected is the responsibility of the industrialized countries to regulate the usage of the available farmland between the production of renewable raw

materials and agriculture for food production. For this reason, many different feedstocks are under investigation to obtain dienes *via* truly sustainable pathways. One approach relies on utilizing bacteria in fermentation processes that are capable of turning waste streams into valuable resources.[84] Another approach addresses turpentine oil as a feedstock, which does not compete with food production. This shows that the future holds many challenges when fossil fuel-based isoprene and butadiene are to be replaced as standard diene-building blocks. New routes are therefore mandatory to adapt the new monomers to specific material properties. Other aspects such as more sustainable solvents or more efficient processes are also driving current research.

A major challenge for the polymerization of novel dienes is the transfer of innovations from academia to industry as this sets the starting point for economic considerations of more sustainable solutions. This involves a shift from only three primarily used monomers, i.e., styrene, butadiene, and isoprene at present towards a variety of biobased diene structures.

## 9. Conclusion

In this short review, we have briefly described the significance of polydienes in the past and also highlighted recent developments. Capitalizing on the high precision of the anionic polymerization technique, a variety of 1,3-dienes have been successfully polymerized in a living manner. Besides matching the properties of fossil fuel-based PB or PI with biobased candidates, the synthesis of unprecedented rigid polydienes like PNopa was recently achieved. Nopadiene shows promising performance as a biobased substitute for PS. This monomer permitted the first synthesis of fully diene-based TPEs. The flexibility of polydienes can be either tuned by the addition of different polar modifiers or by changing the substitution pattern of the monomer. This has great impact on the reactivity ratios when copolymerized with styrene. While monosubstituted 1,3-dienes showed a block-like polymer composition, disubstituted 1,3-dienes reacted almost randomly with styrene in apolar media. The increase in steric demand is directly correlated to the resulting microstructure of the polydiene. Further, if the degrees of freedom are reduced to a minimum *via* constrained

1,3-dienes of a *cisoid* or *transoid* structure, respectively, the requirement of a *cisoid*-state was revealed. A large variety of copolymerizations and their respective reactivity ratios within the field of dienes in the carbanionic polymerization was presented, alongside with insights into new emerging fields including new and often biobased monomers, solvents and modifiers. We emphasize that the findings of the past years, summarized in this overview, are crucial for creating new innovations in the future and are of general relevance for the field of carbanionic polymerization and polydienes.

## 10. References


1 H. Frey and T. Johann, *Polym Chem*, 2020, **11**, 8–14.

2 H. Staudinger and J. Fritschi, *Helv Chim Acta*, 1922, **5**, 785–806.

3 F. Mollwo Perkin, *J R Soc Arts*, 1912, **61**, 85–102.

4 A. Holt, *Angew. Chem.*, 1914, **27**, 153.

5 M. Steube, T. Johann, R. D. Barent, A. H. E. Müller and H. Frey, *Prog Polym Sci*, 2022, **124**, 101488.

6 S. Thomas, C. Han Chan, L. A. Pothen and H. J. Maria, *RSC Polymer Chemistry Series Natural Rubber Materials Volume 1: Blends and IPNs*, Royal Society of Chemistry, Cambridge, 2014, vol. 1

7 Official Website of Malaysian Rubber Council, Rubber Industry: Industry Overview, https://www.myrubbercouncil.com/industry/world_production.php, (accessed 2 February 2024).

8 K. Ntetsikas, V. Ladelta, S. Bhaumik and N. Hadjichristidis, *ACS Polymer Au*, 2022, **3**, 158–181.

9 A. Forens, K. Roos, C. Dire, B. Gadenne and S. Carlotti, *Polymer (Guildf)*, 2018, **153**, 103–122.

10 H. Hsieh and R. Quirk, *Anionic polymerization: principles and practical applications*, Dekker, New York, 1996.

11 K. Knoll and N. Nießner, *Macromol Symp*, 1998, **132**, 231–243.

12 E. Galanos, C. Wahlen, H. J. Butt, H. Frey and G. Floudas, *Macromol Chem Phys*, 2022, **223**, 2200033.

13 E. Grune, M. Appold, A. H. E. Müller, M. Gallei and H. Frey, *ACS Macro Lett*, 2018, **7**, 807–810.

14 R. D. Barent, I. Perevyazko, N. Mikusheva, G. Floudas and H. Frey, *Macromolecules*, 2023, **56**, 5792–5802.

15 M. Steube, T. Johann, E. Galanos, M. Appold, C. Rüttiger, M. Mezger, M. Gallei, A. H. E. Müller, G. Floudas and H. Frey, *Macromolecules*, 2018, **51**, 10246–10258.

16 M. Steube, T. Johann, M. Plank, S. Tjaberings, A. H. Gröschel, M. Gallei, H. Frey and A. H. E. Müller, *Macromolecules*, 2019, **52**, 9299–9310.

17 M. Steube, T. Johann, H. Hübner, M. Koch, T. Dinh, M. Gallei, G. Floudas, H. Frey and A. H. E. Müller, *Macromolecules*, 2020, **53**, 5512–5527.

18 S. P. Wadgaonkar, S. Schüttner, E. Berger-Nicoletti, A. H. E. Müller and H. Frey, *Macromolecules*, 2022, **55**, 4721–4732.

19 D. A. H. Fuchs, H. Hübner, T. Kraus, B. J. Niebuur, M. Gallei, H. Frey and A. H. E. Müller, *Polym Chem*, 2021, **12**, 4632–4642.

20 P. Von Tiedemann, J. Blankenburg, K. Maciol, T. Johann, A. H. E. Müller and H. Frey, *Macromolecules*, 2019, **52**, 796–806.

21 A. Natalello, M. Werre, A. Alkan and H. Frey, *Macromolecules*, 2013, **46**, 8467–8471.

22 C. Wahlen, J. Blankenburg, P. Von Tiedemann, J. Ewald, P. Sajkiewicz, A. H. E. Müller, G. Floudas and H. Frey, *Macromolecules*, 2020, **53**, 10397–10408.

23 E. Grune, J. Bareuther, J. Blankenburg, M. Appold, L. Shaw, A. H. E. Müller, G. Floudas, L. R. Hutchings, M. Gallei and H. Frey, *Polym Chem*, 2019, **10**, 1213–1220.

24 C. Yao, N. Liu, S. Long, C. Wu and D. Cui, *Polym Chem*, 2016, **7**, 1264–1270.

25 H. Leicht, I. Göttker-Schnetmann and S. Mecking, *ACS Macro Lett*, 2016, **5**, 777–780.

26 G. Ricci, G. Pampaloni, A. Sommazzi and F. Masi, *Macromolecules*, 2021, **54**, 5879–5914.

27 L. Friebe, O. Nuyken and W. Obrecht, *Advances in Polymer Science*, 2006, **204**, 1–154.

28 S. Kaita, Y. Doi, K. Kaneko, A. C. Horiuchi and Y. Wakatsuki, *Macromolecules*, 2004, **37**, 5860–5862.

29 N. Hadjichristidis, H. Iatrou, S. Pispas and M. Pitsikalis, *J Polym Sci A Polym Chem*, 2000, **38**, 3211–3234.

30 F. Wurm, D. Wilms, J. Klos, H. Löwe and H. Frey, *Macromol Chem Phys*, 2008, **209**, 1106–1114.

31 K. Iida, T. Q. Chastek, K. L. Beers, K. A. Cavicchi, J. Chun and M. J. Fasolka, *Lab Chip*, 2009, **9**, 339–345.

32 K. Pérez, S. Leveneur, F. Burel, J. Legros and D. Vuluga, *React Chem Eng*, 2023, **8**, 432–441.

33 C. Tonhauser, D. Wilms, F. Wurm, E. Berger-Nicoletti, M. Maskos, H. Löwe and H. Frey, *Macromolecules*, 2010, **43**, 5582–5588.

34 J. Zhang, W. Pointer, G. Patias, L. Al-Shok, R. A. Hand, T. Smith and D. M. Haddleton, *Eur Polym J*, 2023, **183**, 111755.

35 J. Zhang, C. Aydogan, G. Patias, T. Smith, L. Al-Shok, H. Liu, A. M. Eissa and D. M. Haddleton, *ACS Sustainable Chem. Eng.*, 2022, **10**, 9654–9664.

36 A. V. Tobolsky and C. E. Rogers, *Journal of Polymer Science*, 1959, **40**, 73–89.

37 A. V. Tobolsky and C. E. Rogers, *Journal of Polymer Science*, 1959, **38**, 205–207.

38 A. H. E. Müller and K. Matyjaszewski, *Controlled and Living Polymerizations: From Mechanisms to Applications*, Wiley-VCH Verlag, Weinheim, 2010.

39 M. Szwarc, *Nature*, 1956, **178**, 1168–1169.

40 J. E. Mark, *Physical properties of polymers*, Springer, New York, 2007.

41 R. D. Barent, M. Wagner and H. Frey, *Polym Chem*, 2022, **13**, 5478–5485.

42 W. Gebert, J. Hinz and H. Sinn, *Makromol. Chem.*, 1971, **144**, 97–115.

43 D. J. Worsfold and S. Bywater, *Macromolecules*, 1978, **11**, 582–586.

44 N. Hadjichristidis and A. Hirao, *Anionic Polymerization*, Springer, Tokio, 2015.

45 S. Carlotti, S. Ménoret, A. Barabanova, P. Desbois and A. Deffieux, *Macromol Chem Phys*, 2004, **205**, 656–663.

46 A. Forens, K. Roos, C. Dire, B. Gadenne and S. Carlotti, *Chinese Journal of Polymer Science (English Edition)*, 2020, **38**, 357–362.

47 Y. Kosaka, R. Goseki, S. Kawauchi and T. Ishizone, *Macromol Symp*, 2015, **350**, 55–66.

48 Y. Kosaka, K. Kitazawa, S. Inomata and T. Ishizone, *ACS Macro Lett*, 2013, **2**, 164–167.

49 Y. Kosaka, S. Kawauchi, R. Goseki and T. Ishizone, *Macromolecules*, 2015, **48**, 4421–4430.

50 S. Kobayashi, C. Lu, T. R. Hoye and M. A. Hillmyer, *J Am Chem Soc*, 2009, **131**, 7960–7961.

51 K. Liu, Q. He, L. Ren, F. Xu and W. J. Xu, *J Polym Sci A Polym Chem*, 2016, **54**, 2291–2301.

52 L. Ren, K. Liu, Q. He, E. Ou, Y. Lu and W. Xu, *RSC Adv*, 2016, **6**, 51533–51543.

53 C. Rüttiger, M. Appold, H. Didzoleit, A. Eils, C. Dietz, R. W. Stark, B. Stühn and M. Gallei, *Macromolecules*, 2016, **49**, 3415–3426.

54 A. H. Gabor, E. A. Lehner, G. Mao, L. A. Schneggenburger and C. K. Ober, *Chemistry of Materials*, 1994, **6**, 927–934.

55 B. Rodgers, *Rubber Compounding: Chemistry and Applications*, CRC Press, Boca Raton, 2016.

56 J. Glatzel, S. Noack, D. Schanzenbach and H. Schlaad, *Polym Int*, 2021, **70**, 181–184.

57 M. Morton and L. J. Fetters, *J Polym Sci A*, 1964, **2**, 3311–3326.

58 S. Bywater and D. J. Worsfold, *Can J Chem*, 1962, **40**, 1564–1570.

59 L. Shaw and L. R. Hutchings, *Polym Chem*, 2020, **11**, 7020–7025.

60 T. Yoo and S. K. Henning, *Rubber Chemistry and Technology*, 2017, **90**, 308–324.

61 C. Wahlen, M. Rauschenbach, J. Blankenburg, E. Kersten, C. P. Ender and H. Frey, *Macromolecules*, 2020, **53**, 9008–9017.

62 J. M. Bolton, M. A. Hillmyer and T. R. Hoye, *ACS Macro Lett*, 2014, **3**, 717–720.

63 J. Zhang, J. Lu, K. Su, D. Wang and B. Han, *J Appl Polym Sci*, 2019, **136**, 1–10.

64 R. Ohno, Y. Tanaka and M. Kawakami, *Polymer Journal 1973 4:1*, 1973, **4**, 56–60.

65 T. Suzuki, Y. Tsuji, Y. Takegami and H. J. Harwood, *Macromolecules*, 1979, **12**, 234–239.

66 Y. X. Ding and W. P. Weber, *Macromolecules*, 1988, **21**, 530–532.

67 T. Suzuki, Y. Tsuji and Y. Takegami, *Macromolecules*, 1978, **11**, 639–644.

68 T. Suzuki, Y. Tsuji, Y. Watanabe and Y. Takegami, *Polym J*, 1979, **11**, 651–660.

69 M. Rauschenbach, L. Stein, G. M. Linden, R. Barent, K. Heinze and H. Frey, *Polym Chem*, 2024, **15**, 3204–3213.

70 R. Goseki, S. Miyai, S. Uchida and T. Ishizone, *Polym Chem*, 2021, **12**, 3602–3611.

71 S. Uchida, K. Togii, S. Miyai, R. Goseki and T. Ishizone, *Macromolecules*, 2020, **53**, 10107–10116.

72 C. Hahn, M. Rauschenbach and H. Frey, *Angew. Chem. Int. Ed.*, 2023, **62**, e202302907.

73 W. M. Haynes, D. R. Lide and T. J. Bruno, *CRC handbook of chemistry and physics: a ready-reference book of chemical and physical data*, CRC Press, Hoboken, 95th edn., 2015.

74 C. Wahlen and H. Frey, *Macromolecules*, 2021, **54**, 7323–7336.

75 M. Meier-Merziger, J. Imschweiler, F. Hartmann, B.-J. Niebuur, T. Kraus, M. Gallei and H. Frey, *Angewandte Chemie*, 2023, **62**, e202310519.

76 C. Zhou, Z. Wei, X. Lei and Y. Li, *RSC Adv.*, 2016, **6**, 63508–63514.

77 C. Zhou, Z. Wei, C. Jin, Y. Wang, Y. Yu, X. Leng and Y. Li, *Polymer (Guildf)*, 2018, **138**, 57–64.

78 M. Meier-Merziger, N. Fotaras, I. Tzourtzouklis, C. Allouch, M. Wagner, A. H. E. Müller, G. Floudas and H. Frey, *ACS Sustain Chem Eng*, 2024, **12**, 9922–9933.

79 C. Iacob, T. Yoo and J. Runt, *Macromolecules*, 2018, **51**, 4917–4922.

80 L. J. Fetters, D. J. Lohse, D. Richter, T. A. Witten and A. Zirkel, *Macromolecules*, 1994, **27**, 4639–4647.

81 L. J. Fetters, *Journal of Research of the National Bureau of Standards-A. Physics and Chemistry*, 1964, **69**, 33–37.

82 P. Oßwald, R. Whitside, J. Schäffer and M. Köhler, *Fuel*, 2017, **187**, 43–50.

83 J. Zhang, J. Chen, M. Yao, Z. Jiang and Y. Ma, *J Appl Polym Sci*, 2019, **136**, 47673.

84 S. Milker and D. Holtmann, *Microb Cell Fact*, 2021, **20**, 1–7.

85 A. Matic and H. Schlaad, *Polym Int*, 2018, **67**, 500–505.

86 A. Matic, A. Hess, D. Schanzenbach and H. Schlaad, *Polym Chem*, 2020, **11**, 1364–1368.

87 S. P. Wadgaonkar, M. Wagner, L. A. Baptista, R. Cortes-Huerto, H. Frey and A. H. E. Müller, *Macromolecules*, 2023, **56**, 664–677.

88 C. Hahn, I. Göttker-Schnetmann, I. Tzourtzouklis, M. Wagner, A. H. E. Müller, G. Floudas, S. Mecking and H. Frey, *J Am Chem Soc*, 2023, **145**, 26688–26698.

89 C. Hahn, M. Wagner, A. H. E. Müller and H. Frey, *Macromolecules*, 2022, **55**, 4046–4055.

90 A. L. Gatzke and E. D. Vanzo, *Chemical Communications*, 1967, **22**, 1180–1181.

91 R. B. Bates, L. M. Kroposki and D. E. Potter, *Journal of Organic Chemistry*, 1972, **37**, 560–562.

92 C. A. Ogle, F. H. Strickler and B. Gordon, *Macromolecules*, 1993, **26**, 5803–5805.

93 J. Bareuther, M. Plank, B. Kuttich, T. Kraus, H. Frey, M. Gallei, J. Bareuther, M. Plank, B. Kuttich, T. Kraus, H. Frey and M. Gallei, *Macromol Rapid Commun*, 2021, **42**, 2000513.

94 A. Dev, A. Rösler and H. Schlaad, *Polym Chem*, 2021, **12**, 3084–3087.

95 Y. Fu, S. Yang, Q. Xiong, Z. Gu, Q. Dai, H. Tan, L. Zhou, M. Geng, F. Xie, W. jun Yi, L. Li and K. Liu, *Polym Int*, 2024, **73**, 326–336.

96 I. Natori, S. Natori, J. Taehee and K. Ogino, *Polymer (Guildf)*, 2022, **250**, 124821.

97 J. Wilson, S. Gering, J. Pinard, R. Lucas and B. R. Briggs, *Biotechnol Biofuels*, 2018, **11**, 1–11.

98 M. Meier-Merziger, D. A. H. Fuchs, H. Frey and A. H. E. Müller, *Macromolecules*, 2024, **57**, 8154–8161.

99 C. Hayichelaeh, L. A. E. M. Reuvekamp, W. K. Dierkes, A. Blume, J. W. M. Noordermeer and K. Sahakaro, *Rubber Chemistry and Technology*, 2018, **91**, 433–452.

100 K. Takenaka, Y. Akagawa, H. Takeshita, M. Miya and T. Shiomi, *Polym J*, 2009, **41**, 106–107.

101 K. Takenaka, D. Nakashima, M. Miya, H. Takeshita and T. Shiomi, *Journal of Soft Materials*, 2013, **9**, 14–19.

102 C. Tonhauser and H. Frey, *Macromol Rapid Commun*, 2010, **31**, 1938–1947.

103 P. Dreier, J. Ahn, T. Chang and H. Frey, *Macromol Rapid Commun*, 2022, **43**, 2200560.

104 M. Meier-Merziger, M. Fickenscher, F. Hartmann, B. Kuttich, T. Kraus, M. Gallei and H. Frey, *Polym Chem*, 2023, **14**, 2820–2828.

105 C. Zhou, Z. Wei, Y. Wang, Y. Yu, X. Leng and Y. Li, *Eur Polym J*, 2018, **99**, 477–484.

106 N. Hadjichristidis, M. Pitsikalis, S. Pispas and H. Iatrou, *Chem Rev*, 2001, **101**, 3747–3792.

107 P. Von Tiedemann, K. Maciol, J. Preis, P. Sajkiewicz and H. Frey, *Polym Chem*, 2019, **10**, 1762–1768.

108 P. Von Tiedemann, J. Yan, R. D. Barent, R. J. Spontak, G. Floudas, H. Frey and R. A. Register, *Macromolecules*, 2020, **53**, 4422–4434.

109 J. Roovers, L.-L. Zhou, P. M. Toporowski, M. van der Zwan, H. Iatrou and N. Hadjichristidis, *Macromolecules*, 1993, **26**, 4324–4331.

110 V. Hirschberg, M. G. Schußmann, M. C. Röpert, N. Dingenouts, S. Buchheiser, H. Nirschl, J. Berson and M. Wilhelm, *Macromolecules*, 2024, **57**, 3387–3396.

111 N. R. Legge, *Rubber Chemistry and Technology*, 1987, **60**, 83–117.

112 L.Porter, GB 888624A, 1962.

113 G. Holden and R. Milkovich, US 3265765, 1966.

114 D. J. Worsfold, *J Polym Sci A1*, 1967, **5**, 2783–2789.

115 G. Kraus and K. W. Rollmann, *Die Angewandte Makromolekulare Chemie*, 1971, **16**, 271–296.

116 E. Grune, T. Johann, M. Appold, C. Wahlen, J. Blankenburg, D. Leibig, A. H. E. Müller, M. Gallei and H. Frey, *Macromolecules*, 2018, **51**, 3527–3537.

117 W. Wang, W. Lu, A. Goodwin, H. Wang, P. Yin, N. G. Kang, K. Hong and J. W. Mays, *Prog Polym Sci*, 2019, **95**, 1–31.

118 D. J. T. Hill, J. H. O□Donnell, P. W. O□Sullivan, J. E. McGrath, I. C. Wang and T. C. Ward, *Polymer Bulletin*, 1983, **9**, 292–298.

# CHAPTER 2

## Merging Styrene and Diene Structures to a Cyclic Diene: Anionic Polymerization of 1-Vinylcyclohexene (VCH)

# CHAPTER 2

Published in *Angewandte Chemie International Edition,* 2023, **62**, e202302907.
DOI: 10.1002/anie.202302907

# Merging Styrene and Diene Structures to a Cyclic Diene: Anionic Polymerization of 1-Vinylcyclohexene (VCH)

Christoph Hahn,[a,b,†] Moritz Rauschenbach,[a,†] and Holger Frey [a,†,*]

[a] Department of Chemistry, Johannes Gutenberg University, Duesbergweg 10 – 14, D-55128 Mainz (Germany)
[b] Max-Planck Graduate Center, MPGC, Staudingerweg 9, D-55128, Mainz (Germany)

[†] All authors have contributed equally

The following chapter was written in equal parts by the first two authors and is adapted with permission from C. Hahn, M. Rauschenbach, and H. Frey; Merging Styrene and Diene Structures to a Cyclic Diene: Anionic Polymerization of 1-Vinylcyclohexene (VCH), *Angewandte Chemie International Edition*, 2023, **62**, e202302907. 

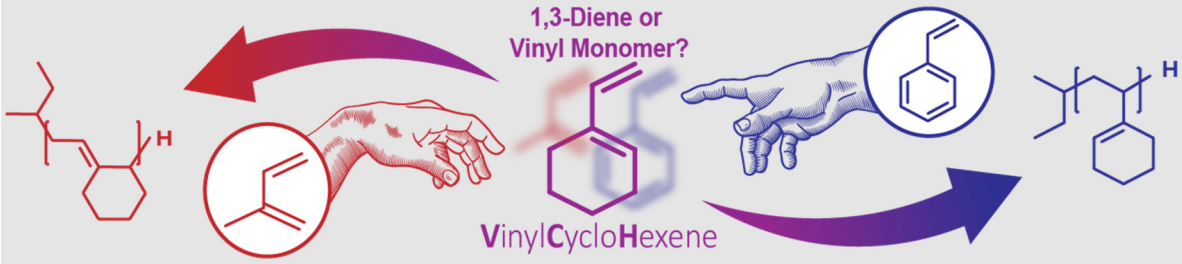


**Abstract**: We report the first anionic polymerization of 1 vinylcyclohexene (VCH). This structure may be considered as an intermediate between dienes and styrene. The polymerization of this cyclic 1,2-disubstituted 1,3-diene proceeded quantitatively in cyclohexane at 25 °C with *sec*-butyl lithium as an initiator. The obtained polymers have well-controlled molecular weights in the range of 5 to 142 kg/mol, controlled by the molar ratio of monomer and initiator, with narrow molecular weight distributions (Đ < 1.07 – 1.20). *In situ* $^{1}$H NMR kinetic characterization revealed a weak gradient structure for the copolymers of styrene and VCH, ($r_{Sty}$ = 2.55, $r_{VCH}$ = 0.39). P(VCH) obtained in cyclohexane with *sec*-BuLi as an initiator showed both 1,4- and 3,4-incorporation mode (ratio: 64:36). It was demonstrated that the microstructure of the resulting P(VCH) can be altered by the addition of a modifier (THF), resulting in increasing 3,4-microstructure (up to 78%) and elevated glass-transition temperature up to 89 °C. Thus, the monomer VCH polymerizes carbanionically like a diene, however leading to rigid polymers with high glass transition temperature, which provides interesting options for combination with other dienes to well-defined polymer architectures and materials.

Linear 1,3-dienes can be polymerized by various polymerization techniques such as emulsion polymerization, controlled and free radical polymerization, living anionic polymerization and catalytic or insertion polymerization.[1,2] Linear dienes play a key role for highly flexible polymers for manifold elastomer applications. However, cyclic 1,3-dienes with one vinyl double bond have been explored only to a limited extent. The first report on the polymerization of 1-vinylcyclohexene (VCH) was published in 1971 by Hara *et. al*.[3] They polymerized VCH by cationic initiators and reported both 3,4- and 1,4-propagation mode, albeit no SEC measurements were conducted. Bonnans-Plaisance investigated the polymerization of VCH by cationic or radical initiators.[4] In 1997 Longo *et al*. reported that VCH polymerized exclusively in 3,4-addition mode in the presence of methylaluminoxane (MAO) and *rac*-[ethylene-bis(1-indenyl)]-$ZrCl_2$.[5] However, the poor catalytic activity resulted in extremely low monomer conversion (0.1%). On the contrary, the (Flu)(Cp)$^i$Pr$ZrCl_2$-MAO system afforded polymers with 1,4-*trans* microstructure.

In general, it was demonstrated that cyclic 1,3-dienes with different substitution pattern can undergo living anionic polymerization. Following the definition of Szwarc, no transfer and termination reactions occur during polymerization.[6,7] Ishizone *et al*. reported anionic polymerization of a series of extremely sterically hindered allylidene monomers. 1,1-disubstiuted 1,3-butadiene derivatives were polymerized in a living manner, using *sec*-BuLi either in cyclohexane at 40 °C or in THF at 0 – 30 °C.[8] The substituents in 1,1-position studied were dimethyl, cyclohexyl, cycloheptyl, 2,2,5,5-tetramethylcyclopentyl, and bornyl. It is noteworthy that less bulky substituents resulted in polymers, wherein the 1,4-*trans* microstructure was predominant, whereas bulkier substituents resulted in an exclusive 3,4-microstructure under the very same conditions.[8] Selective hydrogenation of PI in PS-*b*-PI-*b*-PS triblock copolymers is employed to enhance thermal stability and induces altered mechanical properties, such as pronounced strain hardening.[9–11] Furthermore, the hydrogenation of polymers can increase the Flory–Huggins parameter ($\chi$) and the order-disorder-transition temperature ($T_{ODT}$). The key challenge lies in the selective hydrogenation of the PI block, retaining PS without saturation and without chain scission under the harsh conditions of the procedure.[12] For full saturation of all double bonds in PI-PS copolymers (olefinic and aromatic), heterogeneous palladium catalyst supported on calcium carbonate

can be utilized. The hydrogenated 3,4-microstructure of VCH is identical with a fully hydrogenated PS, i.e. formally polyvinylcyclohexane.[5,13]

In this work, we report on the polymerization of VCH by anionic polymerization in order to evaluate the behavior of a conjugated cyclic 1,3-diene, possessing one cyclic and one vinyl double bond. We aim at understanding, whether the polymerization behavior is comparable to a conjugated diene (as isoprene) or to styrene due to the related molecular structure. In terms of the resulting polymer materials, the cyclic 1,3-diene structure should provide sufficient rigidity to result in a high glass-transition temperature polymer comparable to PS. Additionally, the cyclic 1,3-diene may be viewed as a less delocalized styrene analog with a partially hydrogenated aromatic ring. In contrast to the catalytic polymerization mentioned above, we aimed at quantitative monomer conversion and a living polymerization mechanism.

The monomer 1-vinylcyclohexene (VCH) was synthesized according to literature, starting from 1-ethynylcyclohexene by partial hydrogenation of the terminal alkyne with $Pd/CaCO_3$, deliberately contaminated with $Pb(OAc)_2$.[14]

To the best of our knowledge, the living anionic polymerization of VCH in apolar media with organo-lithium initiators as shown in **Scheme 1** has not been reported to date. The onset of the living polymerization was proven by kinetical studies and was accompanied by an intense yellow color (**Figure S21**) upon initiation with *sec*-butyl lithium, demonstrating the delocalization of the living carbanion.

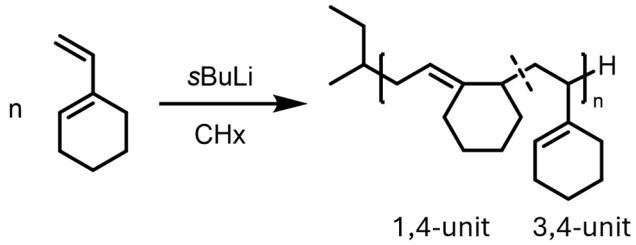


**Scheme 1**: Anionic polymerization of VCH in cyclohexane. For reasons of clarity, we exclude the *cis*-1,4 microstructure in the scheme. (For details regarding characterization of the microstructures see Supporting Information).

We synthesized a series of homopolymers with targeted molecular weights in the range of 5 to 148 kg/mol (SEC, THF, PS calibration). A summary of the results can be found in **Table 1**. The resulting dispersities were in the range of $Đ$ = 1.07 - 1.20. In addition, the absolute molecular weight of low molecular weight polymer was determined *via*

MALDI-ToF MS, confirming the narrow distribution and incorporation of 1-vinylcyclohexene (108.18 g/mol). The MALDI-ToF spectrum (**Figures S6, S7**) shows the different species assigned to the respective distributions with different cations. The relative molecular weight (GPC, 5130 g/mol) and absolute molecular weight according to MALDI-ToF MS (4800 g/mol) are in good agreement.

DSC measurements reveal that the $T_g$ values of the PVCH homopolymers are in the range of 62 to 78 °C, reaching a plateau value with constant $T_g$ at 18.000 g/mol, i.e. somewhat lower than for polystyrene. The polymerization of VCH was investigated regarding the addition of modifiers with respect to their influence on the microstructure. The microstructure was determined by integration of the allylic protons (5.1 ppm and 5.3 ppm) in the $^1$H NMR spectra of the resulting polymer (**Figure 1**).

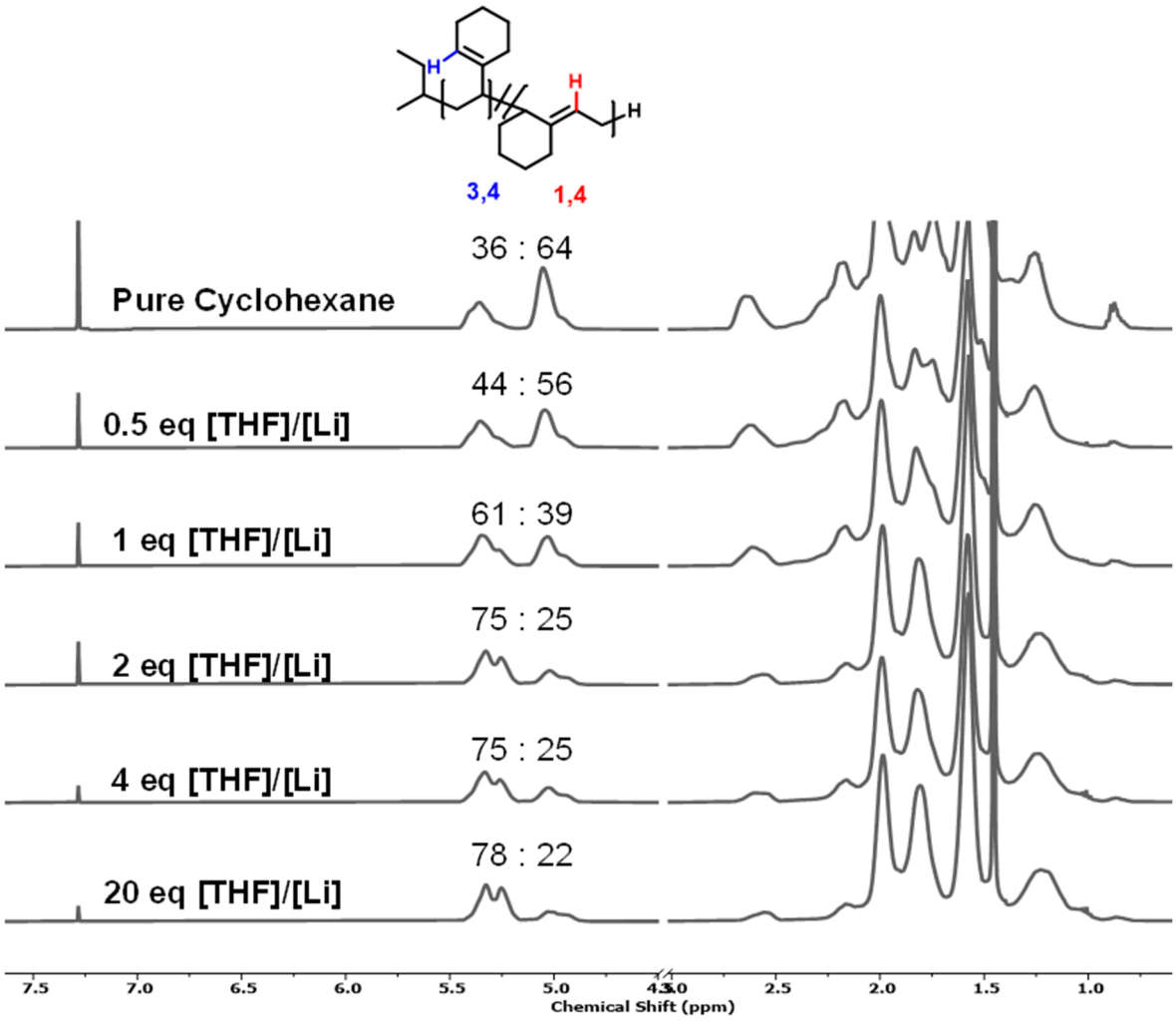


**Figure 1**: Stacked NMR spectra ($CDCl_3$, 25°C, 400 MHz) of P(VCH) with different equivalents (from top to bottom: pure cyclohexane, 0.5 eq, 1 eq, 2 eq, 4 eq, 20 eq) of THF as a modifier.

Poly(vinylcyclohexene) (P(VCH)) obtained in cyclohexane by anionic polymerization with *sec*-BuLi as an initiator resulted in 64% 1,4-microstructure (36 % 3,4-microstructure, respectively). The determination of the 1,4- and 3,4-units by NMR spectroscopy was carried out in agreement with literature.[5] **Figure 1** shows the change of the structure of P(VCH) as a consequence of an increasing amount of the modifier THF towards 3,4-incorporation in $^{1}$H NMR spectroscopy. Further investigation of the polymer structure by NMR spectroscopy is illustrated in the Supporting Information (**Figure S9-S12**).

As seen in other studies based on catalytic polymerization, no 1,2-microstructure of VCH was observed (see Supporting Information **Figure S11**). Polar additives such as THF are known to alter the microstructure of 1,3-dienes towards higher 3,4-microstructure (and 1,2-microstructure) content.[15] We utilized small quantities of polar modifiers to obtain a high content of 3,4-microstructure PVCH. This microstructure is comparable to a (semi)-hydrogenated polystyrene. *Via* NMR spectroscopy it was observed that the polymers possess an increasing amount of 3,4-units with increasing ratio of THF/Li. Upon the addition of more than 20 eq. of THF, no further increase of 3,4-units was observed. As a result of the modified microstructures, we determined significantly higher glass-transitions temperatures upon addition of THF, compared to polymers obtained in cyclohexane ($T_g$ = 74 to 89 °C).

We further investigated VCH with respect to statistical copolymerization with styrene and isoprene, since it is structurally related to both monomers. We were interested in understanding the behavior of the VCH monomer, particularly whether it is comparable to a 1,3-diene or rather to a vinyl monomer, such as styrene.

**Table 1**: Characterization data of the synthesized homopolymers of VCH in cyclohexene and with the addition of THF, microstructure and glass-transition temperatures are summarized.

| No. | $M_{theo}$ kg/mol | $M_n$[a] kg/mol | Đ | [THF]/[Li] | 1,4/3,4 % | $T_g$ °C |
|---|---|---|---|---|---|---|
| P1 | 5 | 5.1 | 1.07 | 0 | 64/36 | 62 |
| P2 | 7.5 | 6.5 | 1.15 | 0 | 64/36 | 65 |
| P3 | 15 | 15.4 | 1.17 | 0 | 64/36 | 77 |
| P4 | 20 | 18.7 | 1.20 | 0 | 64/36 | 76 |
| P5 | 40 | 36.2 | 1.09 | 0 | 64/36 | 78 |
| P6 | 50 | 48.7 | 1.07 | 0 | 64/36 | 77 |
| P7 | 140 | 142.6 | 1.19 | 0 | 64/36 | n.d. |
| P8 | 15 | 15.3 | 1.05 | 0.5 | 56/44 | 74 |
| P9 | 15 | 15.2 | 1.07 | 1 | 39/61 | 75 |
| P10 | 15 | 16.2 | 1.11 | 2 | 25/75 | 83 |
| P11 | 15 | 18.1 | 1.08 | 4 | 25/75 | 83 |
| P12 | 15 | 19.8 | 1.09 | 20 | 22/78 | 89 |

[a] SEC, eluent THF, PS calibration

The results of the online kinetics of VCH with styrene and isoprene as well as a description of the method are shown in the Supporting Information. The reactivity ratios of styrene and VCH were determined to be $r_{Sty}$ = 2.55 and $r_{VCH}$ = 0.39. The cross-over of PS-Li to P(VCH)-Li is indicated by a significant color chance in the block-copolymerization of P(S-*b*-VCH) (see Supporting Information **Figure S21**).

To our surprise, we observed inverse reactivity ratios of VCH and styrene in comparison to those known from conventional diene/styrene copolymers.[16,17] In general, copolymerization of styrene and 1,3-dienes (e.g. isoprene and butadiene) results in pronounced gradient or tapered structures due to the slow cross-over of PI-Li to styrene. The online NMR data show that styrene is consumed preferentially in the statistical copolymerization of styrene/VCH. This finding suggests fast cross-over from P(VCH)-Li to styrene, in contrast to linear dienes, such as isoprene or myrcene.[18] Generally, the reactivity of styrene derivatives can be estimated from their *β*-carbon

shift in $^{13}C$ NMR spectroscopy. The reactivity of the monomer is mainly based on the electron charge density of the reactive vinyl bond, which correlates with the chemical shift of the *β*-carbon. VCH shows a significantly decreased *β*-carbon shift (109.72 ppm) compared to styrene (113.36 ppm).[19] Based on these observations, we conclude a lower reactivity of VCH compared to styrene. This is tentatively explained by the vinyl bond in the 1,3-diene being considerably less delocalized than the vinyl group at an aromatic ring in case of styrene. In other words, reduced stabilization is assumed compared to styrene.

Sequential block copolymerization of VCH with isoprene resulted in bimodal distributions with rather high dispersity of >1.35. We attribute this to the high reactivity difference between isoprene and VCH, resulting in a very low crossover rate to the less favored monomer. To further elucidate the slow cross-over rate, we initiated VCH with living poly(isoprenyl)-lithium and *vice versa*. The results reveal that irrespective of the first monomer, the SEC traces show bimodal distributions (**Figure S23**). Consequently, the condition of fast initiation for a controlled polymerization is not fulfilled, leading to the observed bimodal molecular weight distribution. Surprisingly, the living chain ends of isoprene and VCH both showed incomplete initiation of the respective other monomer, leading to bimodal distributions in both cases. Moreover, increasing polymerization temperature to 40 °C did not improve the resulting molecular weight distributions (**Figure S23**). The online kinetics study of the statistical copolymerization showed full consumption of isoprene. However, the integrals of the respective signals of VCH remained nearly unchanged, and propagation of VCH only started when no $r_I \gg 1$ and $r_{VCH} \ll 1$ confirming the unfavorable crossover reaction (**Figures S24-27**) and a very steep gradient, as known from the system isoprene/4-methyl-styrene.[20]

P(VCH) generated by polymerization in cyclohexane (P3, 36% 3,4-additon) and P(VCH) obtained with 20 eq of THF modifier (P11, 78% 3,4-addition) were hydrogenated, using palladium on carbon (10w%) as a catalyst under 30 bar $H_2$ pressure at 130°C in a Parr reactor. The hydrogenation led to full saturation of the polymer, confirmed by $^{1}H$ NMR spectroscopy (**Figures S28, S29**). Poly(vinylcyclohexane) P(CHE) has been prepared previously by coordination polymerization of vinylcyclohexane or by complete catalytic hydrogenation of PS. In comparison to literature, we found identical shifts in $^{1}H$ and $^{13}C$ NMR signals to P(CHE) for hydrogenated P(VCH).[5]

For Sample P11, we observed an increase in $T_g$ from 89 to 114 °C after hydrogenation. The hydrogenated polymer consists of 78% poly(vinylcyclohexane) moieties with a $T_g$ of 140 °C.[9] No evidence of any chain scission or degradation of the polymer backbone after hydrogenation (see SEC traces, **Figure S30**) was found. A $T_g$ of 70 °C was observed after hydrogenation of Sample P3 (**Figure S31**), which is tentatively explained by the increased freedom of rotation of the saturated polymer backbone.

The living anionic polymerization of VCH, which has not been reported to date, affords polymers with good control over molecular weights and moderate to narrow molecular weight distributions. Compared to the catalytic approach[5] full conversion was always obtained due to the living character of the anionic polymerization. The results show that the microstructure of P(VCH) can be altered by the addition of THF, leading to a higher extent of 3,4 incorporation.[21] In this case, a rigid polydiene with a tunable $T_g$ in the range of 77 – 89 °C is obtained.

Initially, the question whether the monomer acts as a 1,3-diene or as a styrenic monomer was raised. Based on this study, VCH acts comparable to established dienes in the anionic polymerization, however, the final material properties are similar to polystyrene, with similar rigidity. The hydrogenation of P(VCH) resulted in polymers containing poly(vinylcyclohexane) segments, causing an increase in $T_g$ to 114 °C with a monomodal molecular weight distribution without any evidence of chain degradation.

This work demonstrates the significant effect of one double bond in a 1,3-diene being sterically constrained on the anionic polymerization behavior. It is important to emphasize that VCH represents a model system for a variety of biobased 1,3-dienes, derived from natural terpenes. VCH itself shows intriguing potential to produce fully hydrogenated high $T_g$ materials, with improved phase separation behavior and access to complex macromolecular architectures *via* living anionic copolymerization.

**References**

1 W. Cooper and G. Vaughan, *Prog Polym Sci*, 1967, **1**, 91–160.

2 S. Bywater, Y. Firat and P. E. Black, *Journal of Polymer Science: Polymer Chemistry Edition*, 1984, **22**, 669–672.

3 K. Hara, Y. Imanishi, T. Higashimura and M. Kamachi, *J Polym Sci A1*, 1971, **9**, 2933–2948.

4 C. Bonnans-Plaisance, *Eur Polym J*, 1979, **15**, 581–585.

5 P. Longo, A. Grassi, F. Grisi and S. Milione, *Macromol Rapid Commun*, 1998, **19**, 229–233.

6 I. Natori and S. Inoue, *Macromolecules*, 1998, **31**, 4687–4694.

7 R. D. Barent, M. Wagner and H. Frey, *Polym Chem*, 2022, **13**, 5478–5485.

8 S. Uchida, K. Togii, S. Miyai, R. Goseki and T. Ishizone, *Macromolecules*, 2020, **53**, 10107–10116.

9 B. S. Beckingham and R. A. Register, *Macromolecules*, 2013, **46**, 3084–3091.

10 F. S. Bates, G. H. Fredrickson, D. Hucul and S. F. Hahn, *AIChE Journal*, 2001, **47**, 762–765.

11 A. Laramée, P. Goursot and J. Prud□homme, *Colloid and Polymer Science 1977 255:11*, 1977, **255**, 1141–1141.

12 P. Von Tiedemann, J. Yan, R. D. Barent, R. J. Spontak, G. Floudas, H. Frey and R. A. Register, *Macromolecules*, 2020, **53**, 4422–4434.

13 D. A. Hucul and S. F. Hahn, *Advanced Materials*, 2000, **12**, 1855–1858.

14 E. N. Marvell and J. Tashiro, *Journal of Organic Chemistry*, 1965, **30**, 3991–3993.

15 D. A. H. Fuchs, H. Hübner, T. Kraus, B. J. Niebuur, M. Gallei, H. Frey and A. H. E. Müller, *Polym Chem*, 2021, **12**, 4632–4642.

16 D. J. Worsfold and S. Bywater, *Can J Chem*, 1964, **42**, 2884–2892.

17 S. Quinebèche, C. Navarro, Y. Gnanou and M. Fontanille, *Polymer (Guildf)*, 2009, **50**, 1351–1357.

18 E. Grune, J. Bareuther, J. Blankenburg, M. Appold, L. Shaw, A. H. E. Müller, G. Floudas, L. R. Hutchings, M. Gallei and H. Frey, *Polym Chem*, 2019, **10**, 1213–1220.

19 P. Von Tiedemann, J. Blankenburg, K. Maciol, T. Johann, A. H. E. Müller and H. Frey, *Macromolecules*, 2019, **52**, 796–806.

20 E. Grune, T. Johann, M. Appold, C. Wahlen, J. Blankenburg, D. Leibig, A. H. E. Müller, M. Gallei and H. Frey, *Macromolecules*, 2018, **51**, 3527–3537.

21 A. Forens, K. Roos, C. Dire, B. Gadenne and S. Carlotti, *Polymer (Guildf)*, 2018, **153**, 103–122.

# Supporting Information

## General Information:

**Reagents.** Chemicals and solvents were purchased from commercial suppliers (*Acros*, *Sigma-Aldrich*, *Fisher Scientific*, *Alfa Aesar*, *TCI*). Deuterated solvents were obtained from *Deutero GmbH*. Isopropyl alcohol and methanol were used as received without further purification. Cyclohexane was purified by stirring over diphenylhexyllithium (adduct of *sec*-butyl lithium and 1,1-diphenylethylene), vacuum-transferred and degassed by four freeze-pump-thaw cycles prior to use. The monomers VCH, styrene and isoprene were purified by stirring over $CaH_2$ overnight, followed by distillation. All monomers for the anionic polymerization were degassed by four freeze-pump-thaw cycles prior to use.

**Instrumentation.** All NMR spectra ($^1H$; $^{13}C$; ed. HSQC; HMBC; $^1H$-$^1H$-COSY and DOSY) were recorded on a *Bruker Avance II 400* spectrometer equipped with a 5 mm BBFO-SmartProbe with z gradient and ATM, as well as a SampleXPress 60 sample changer. All spectra are referenced internally to residual proton signals of the deuterated solvent.

Size exclusion chromatography (SEC) measurements were performed using an Agilent 1100 Series, equipped with a SDV column set from *PSS* (SDV 103, SDV 105, SDV 106). Tetrahydrofuran (THF) was used as the mobile phase (flow rate 1 mL $min^{-1}$) and as the solvent. Poly(styrene) standards were provided by PSS for calibration. The measurements were carried out at 30 °C with an RI and UV (275 nm) detector. For analysis the *PSS WinGPC® UniChrom* (V 8.31, Build 8417) software provided by *PSS Polymer Standards Service GmbH* was used.

Glass transitions temperatures ($T_g$) were determined by evaluating differential scanning calorimetry (DSC) curves recorded on a *Perkin Elmer 8500* differential scanning calorimeter. A temperature range from 0 °C to 150 °C was used. For the first cycle a heating rate of 10 °C $min^{-1}$ and a cooling rate of 20 °C $min^{-1}$ were employed. A second heating cycle (20 °C $min^{-1}$) was used to evaluate the thermal properties of the (co)polymers. For the hydrogenated polymers a temperature range between 0°C and 200 °C was used.

MALDI-ToF MS measurements were performed on a *Bruker Rapiflex*. 2-(4-hydroxyphenylazo)benzoic acid (HABA) was used as a matrix (1:1 in water) for P(VCH) The spectrum was measured in a linear positive mode with a laser wavelength of 337 nm. The mass spectrum was recorded in a reflector positive mode with a 337 nm laser. For all polymers 1 mg analyte was dissolved in 1 mL dichloromethane.

**General polymerization procedure in apolar media (cyclohexane)**

All polymerizations were carried out in cyclohexane at room temperature, or as indicated, in an argon-filled glovebox (MBraun UNILAB, <0.1 ppm of $O_2$ and <0.1 ppm of $H_2O$) in 40 mL glass vials equipped with a magnetic stir bar, screw caps and septa. Dry and degassed cyclohexane was distilled into a Schlenk flask equipped with a Teflon stopper. Dry and degassed THF was used as a modifier. Inside the glove box the monomer(s) and cyclohexane were added into glass vessel with septum. For the synthesis of a homopolymer and copolymer the monomer/solvent (10 wt%) mixture was initiated with 0.1 mL or 0.05 mL *sec*-butyl lithium (1.3 M in cyclohexane/ hexane 92/8) *via* 0.1 mL syringe. The polymerization was terminated after full conversion by adding 0.5 mL of isopropanol (degassed with argon for 1 h prior to use) by a syringe. The polymers were precipitated in 30 mL of a cold methanol/isopropanol mixture and dried under reduced pressure.

**Monomer synthesis**

*1-Vinylcyclohexene*. – For the synthesis of this compound, 25 mL of 1-ethynylcyclohexene (Sigma-Aldrich) was hydrogenated selectively with $Pd/CaCO_3$ contaminated with $Pb(OAc)_2$ in pentane and 1 bar of hydrogen atmosphere at room temperature.[1] The catalyst was removed by filtration and the solvent was distilled under reduced pressure. VCH was distilled over $CaH_2$, followed by trioctylaluminum for 24 h and was freshly distilled under reduced pressure prior to use.

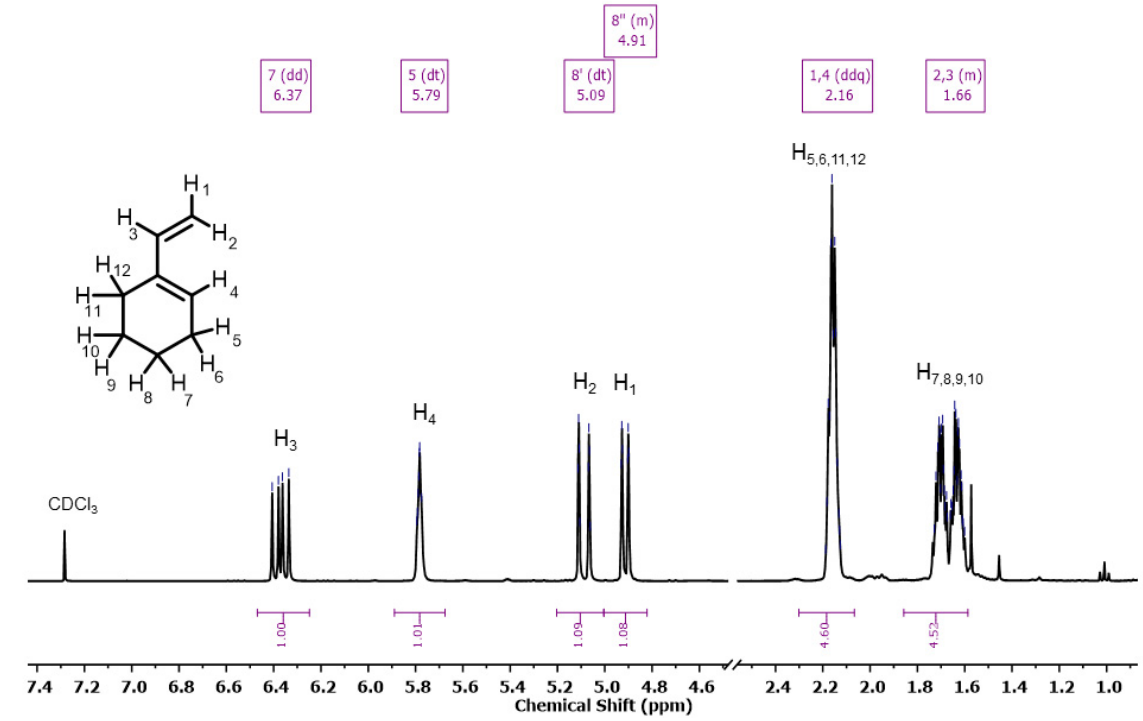


**Figure S1:** $^{1}$H NMR spectrum (400 MHz, C*D*Cl$_3$, 25 °C) of VCH.

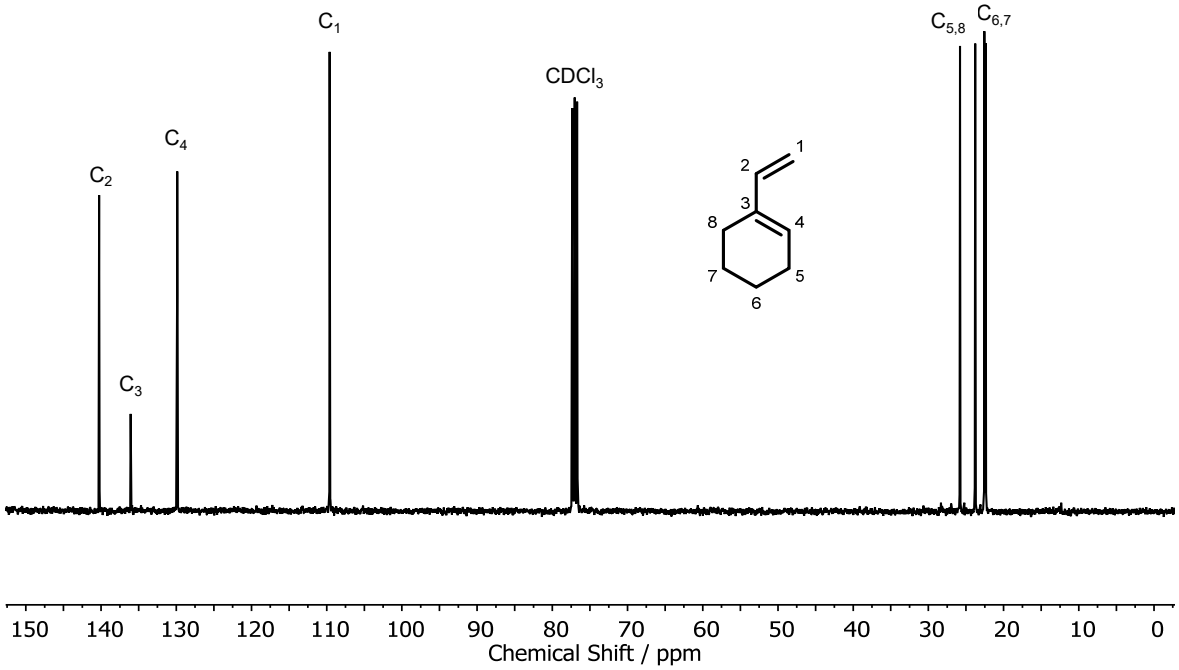


**Figure S2**: $^{13}$C NMR spectrum (100 MHz, C*D*Cl$_3$, 25 °C) of VCH.

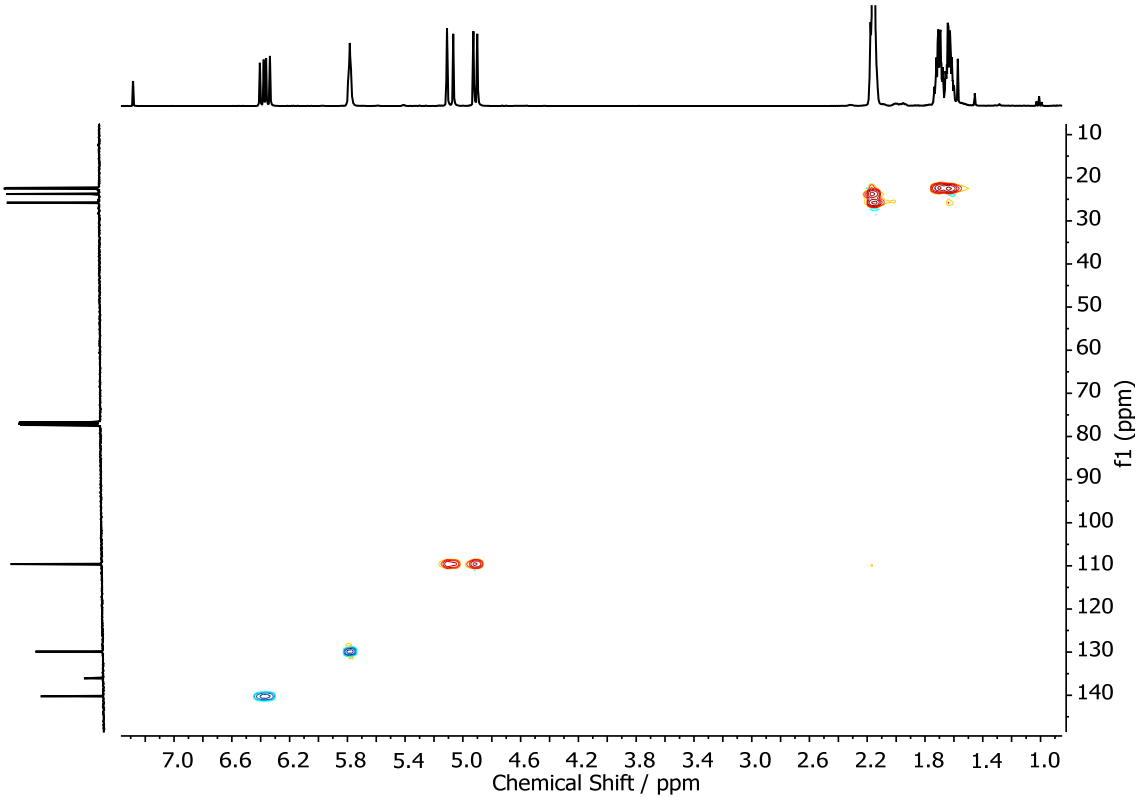


**Figure S3**: HSQC NMR spectrum (400 MHz/100 MHz, C*D*Cl$_3$, 25 °C) of VCH.

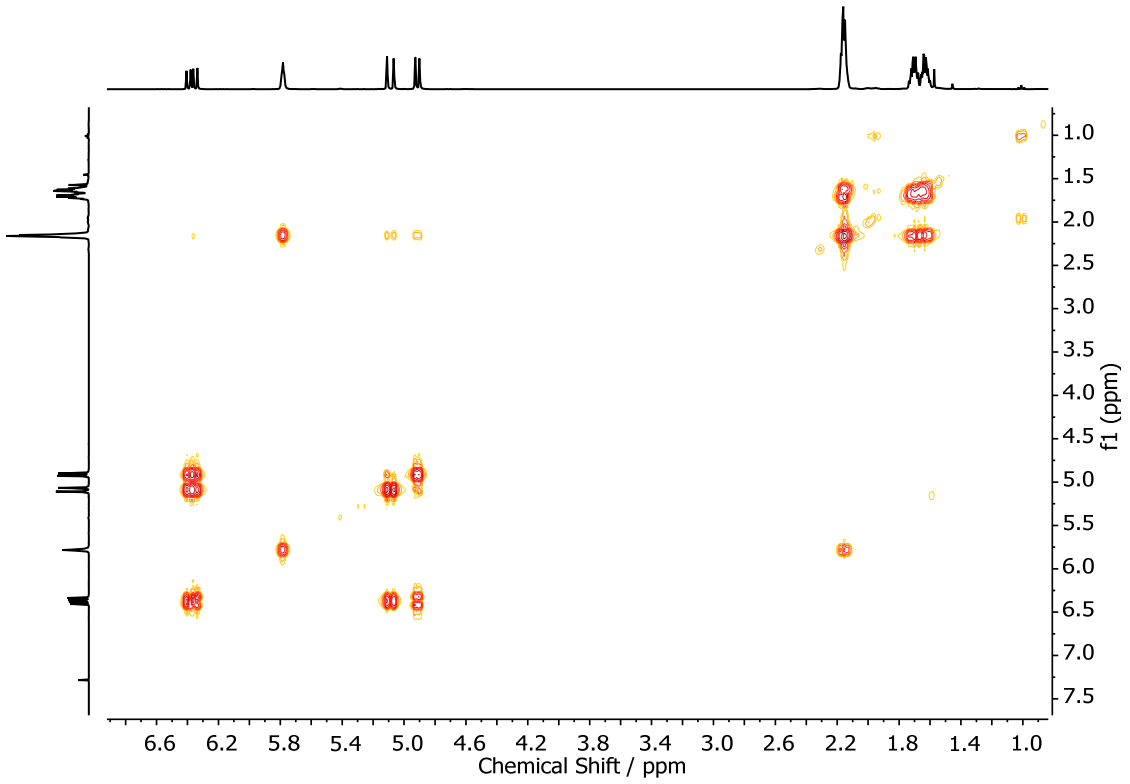


**Figure S4**: COSY NMR spectrum of VCH (400 MHz, C*D*Cl$_3$, 25 °C).

## Homopolymers of VCH

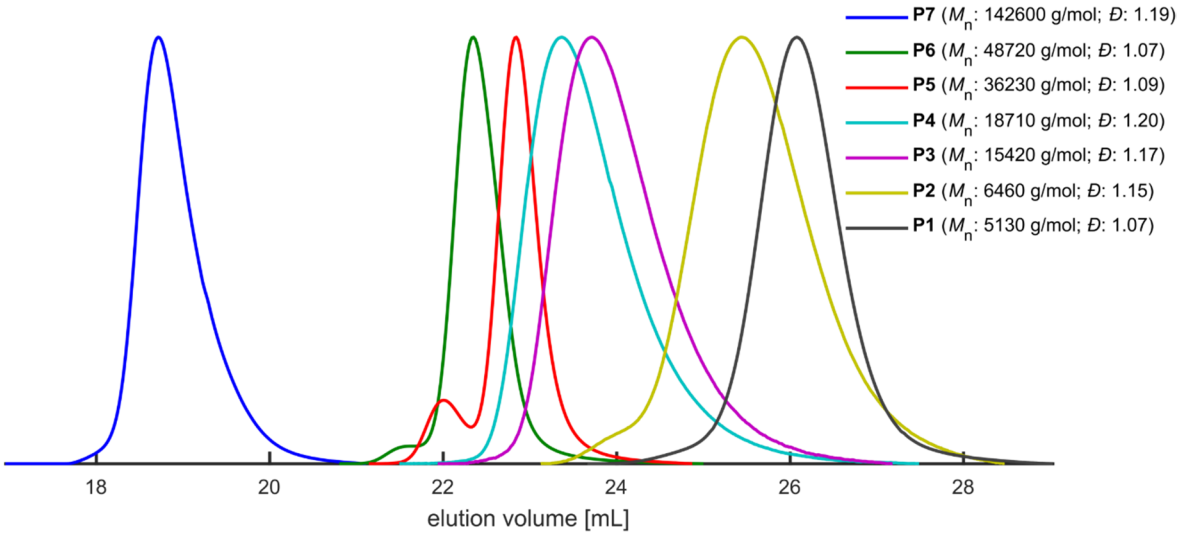


**Figure S5**. SEC traces of homopolymers of VCH (**Table 1**); eluent THF, PS calibration.

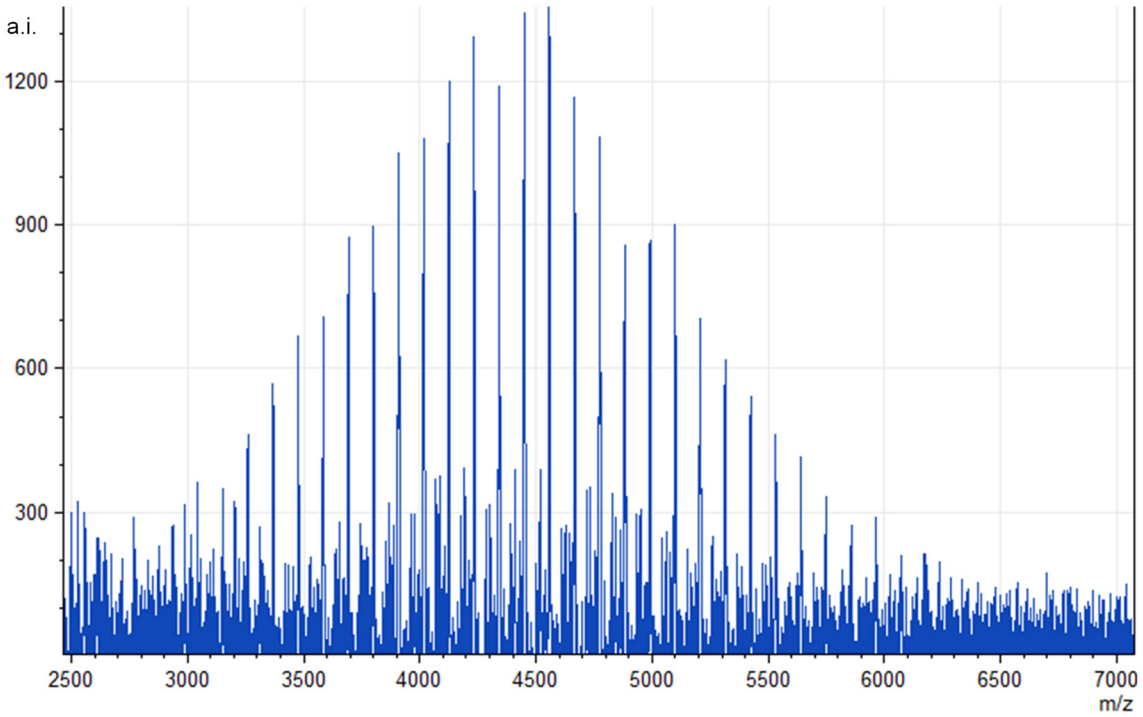


**Figure S6**: MALDI ToF-MS of P1 (DCTB matrix).

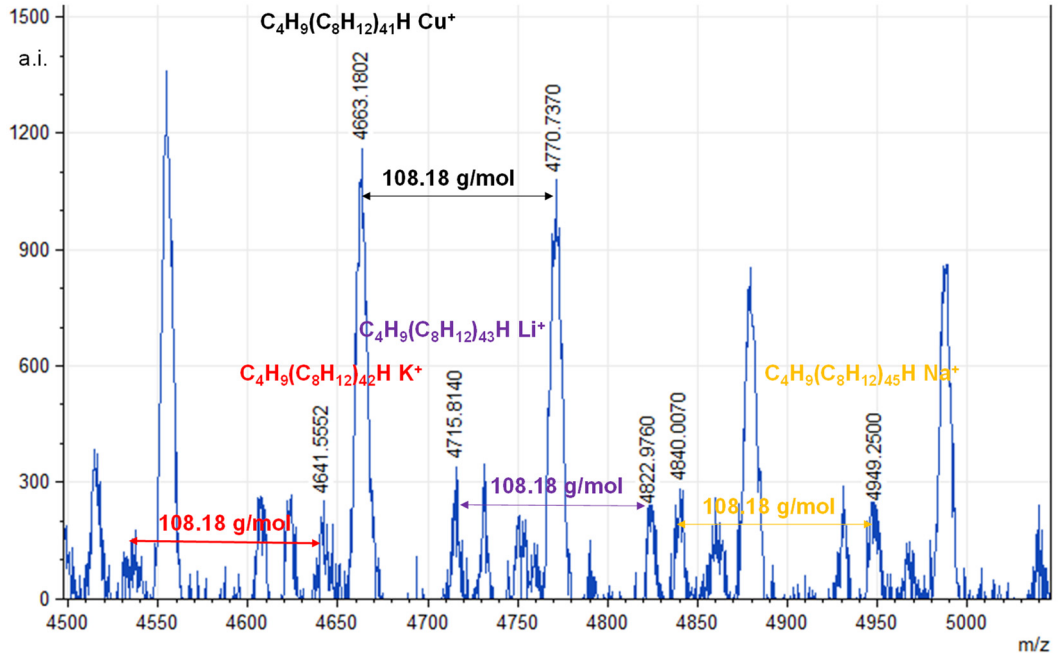


**Figure S7**: MALDI ToF-MS of P1, zoom in of Figure 6.

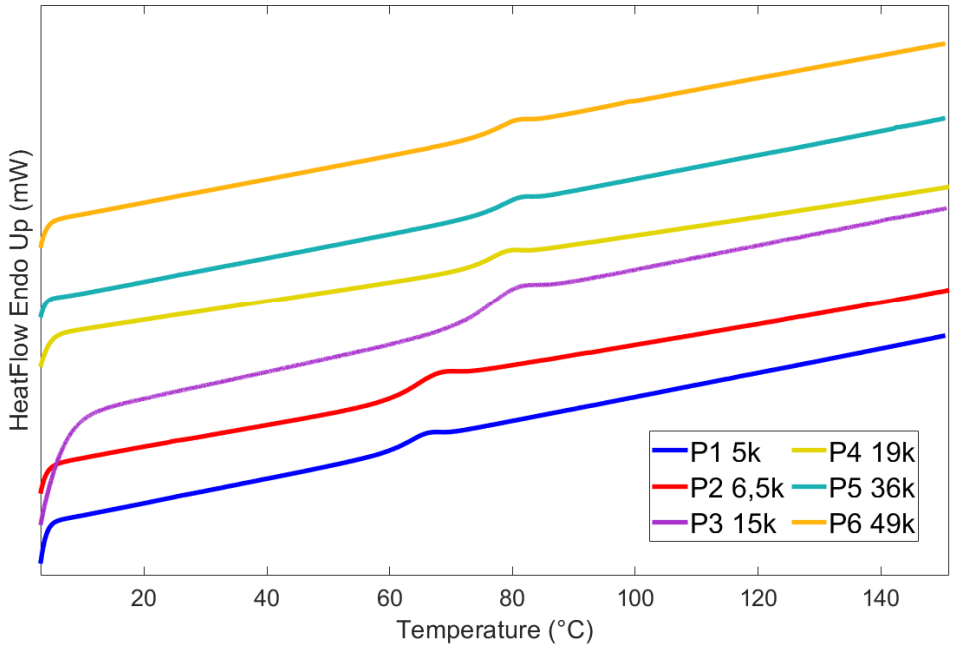


**Figure S8**: DSC data of homopolymers P1 – 6 (**Table1**).

## Investigation of the microstructure

Here is an exemplary description of the microstructure of sample P12. The results agree with data from literature of poly(vinylcyclohexene), polymerized by Ziegler-Natta type catalysts, albeit resulting in high dispersity polymers due to the heterogeneous method.

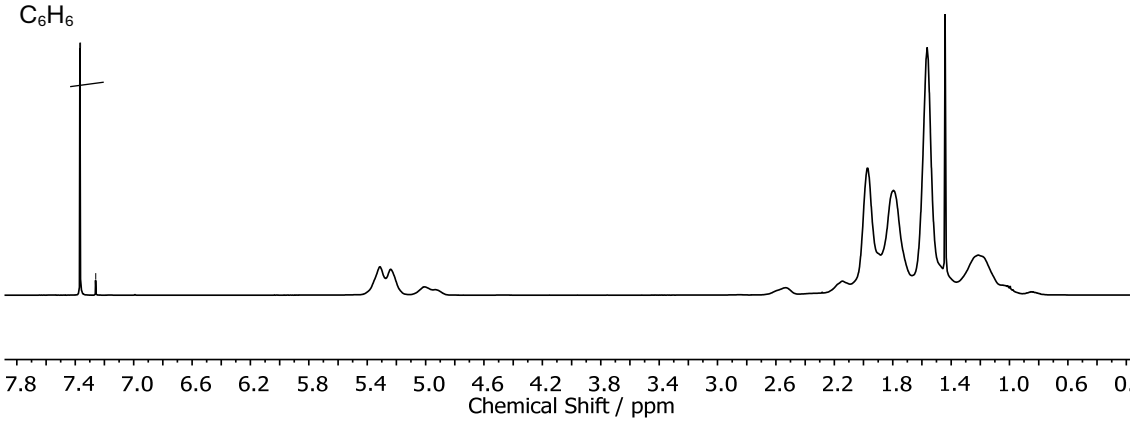


**Figure S9**: $^{1}$H NMR spectrum (400 MHz, C*D*Cl$_3$, 25 °C) of PVCH sample (P12).

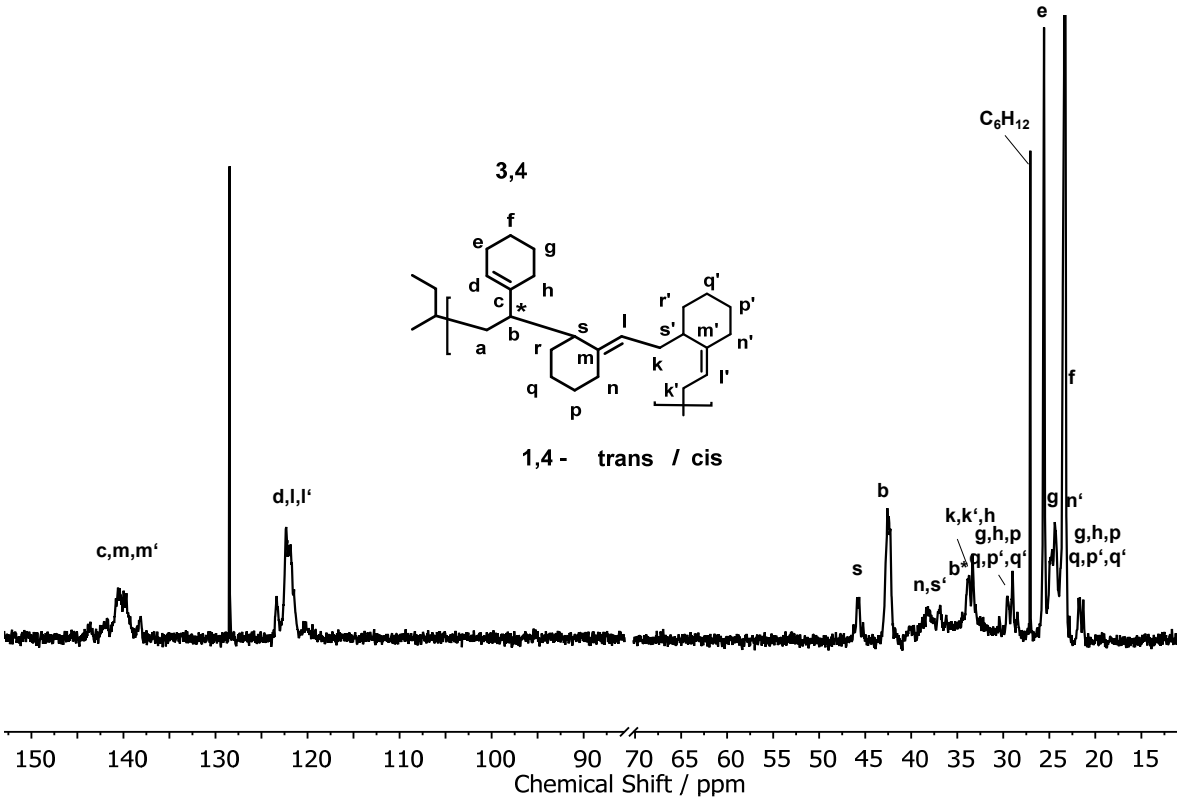


**Figure S10**: $^{13}$C NMR spectrum (101 MHz, C*D*Cl$_3$, 25°C) of PVCH (P12).

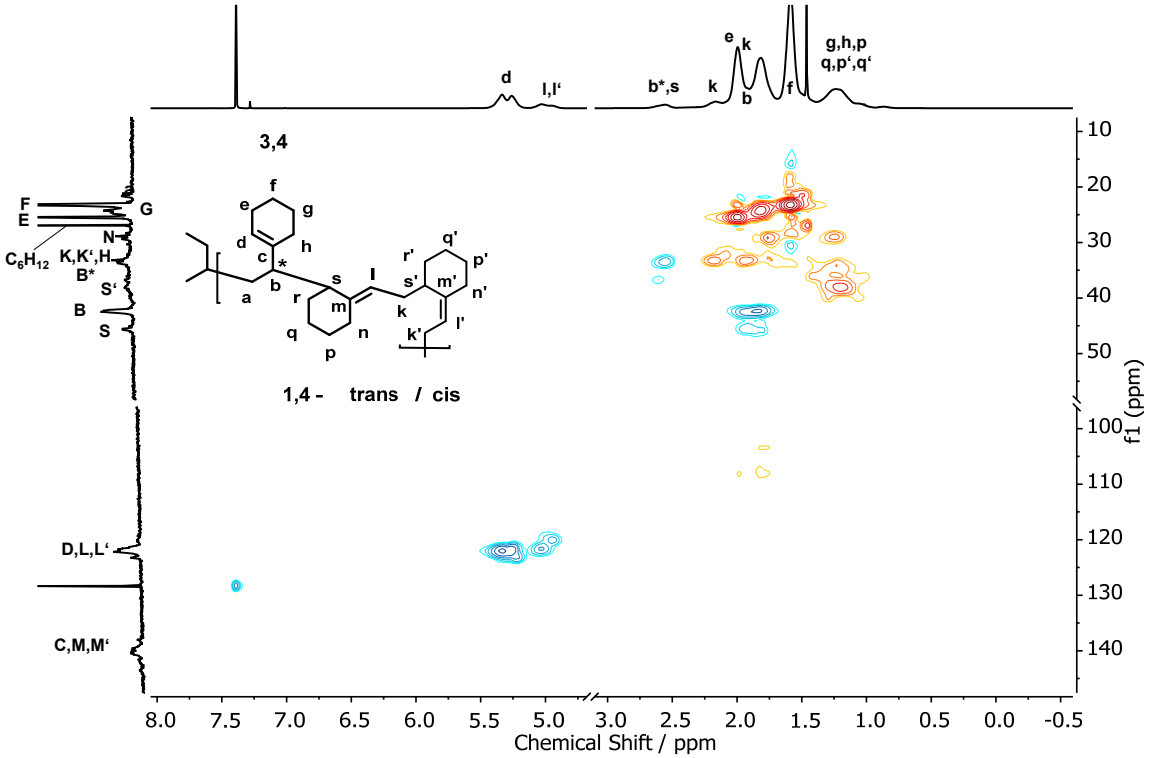


**Figure S11**: HSQC NMR spectrum (400 MHz/100 MHz, C*D*Cl$_3$, 25°C) of PVCH (P12).

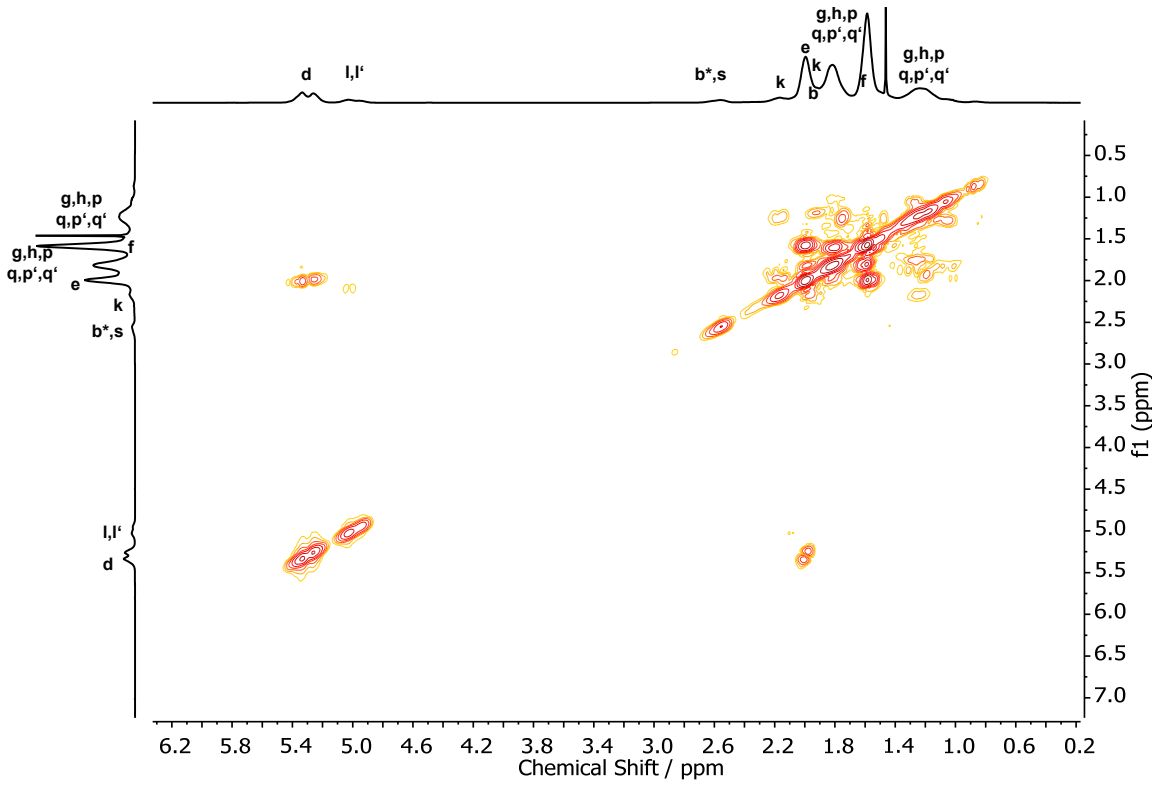


**Figure S12**: $^1$H/$^1$H COSY NMR spectrum (400 MHz, C*D*Cl$_3$, 25°C) of PVCH (P12).

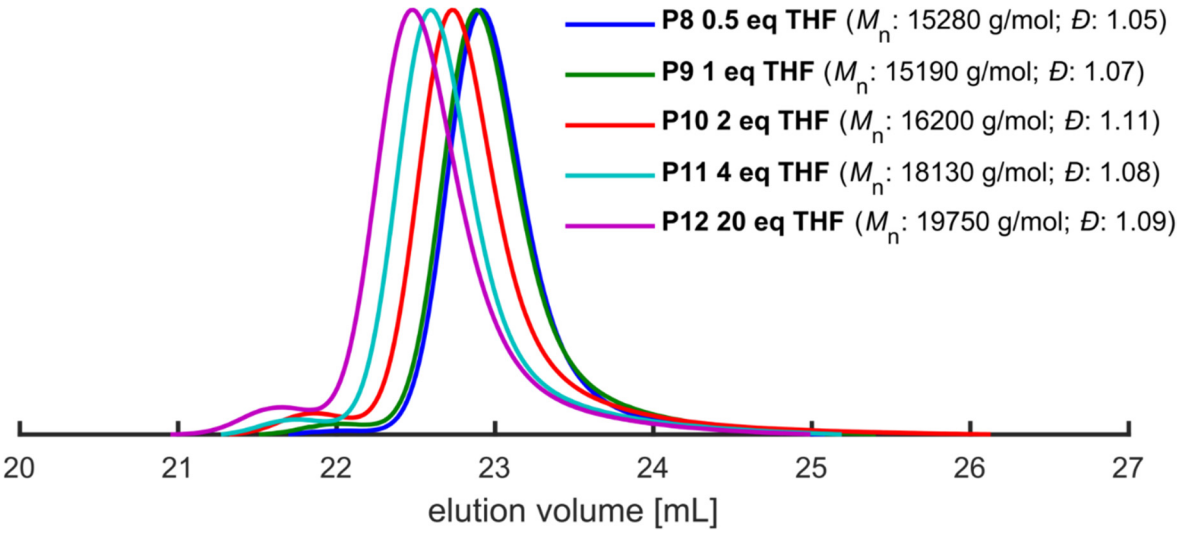


**Figure S13**: SEC traces of the homopolymers of VCH obtained with different equivalents of THF as a modifier (eluent: THF, PS calibration).

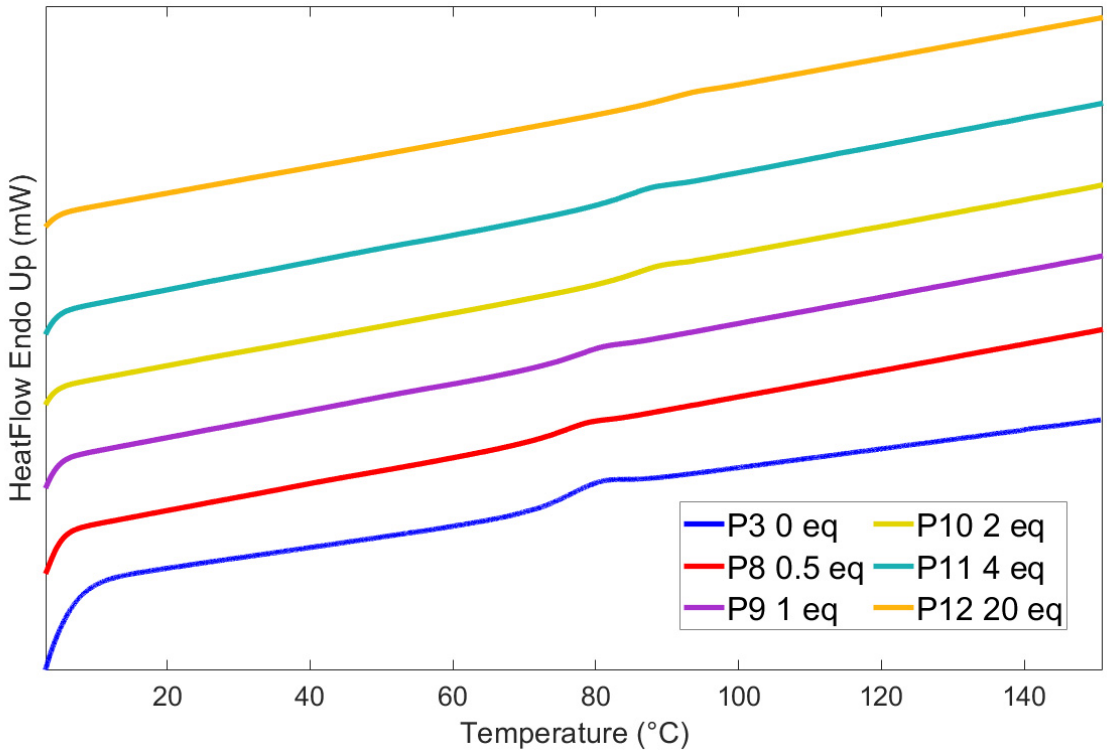


**Figure S14**: DSC data of homopolymers P3+7 – 12 with different equivalents of THF.

## Copolymerization kinetics

The copolymerization of VCH and styrene was investigated *via* online $^{1}$H NMR kinetic studies. The integrated signals used for VCH and styrene are shown in Scheme S1 and The diminishing signals of VCH are in the region of 6.32 – 6.41 ppm, whereas the decreasing signals for styrene are at 5.23 ppm.

For comparison reasons, we employed different models for the evaluation of the reactivity ratios. We utilized Jaacks, Meyer-Lowry, and the integrated version of the Meyer-Lowry model to fit the data.[2] The summary of the fit results is demonstrated in **Table S2**.

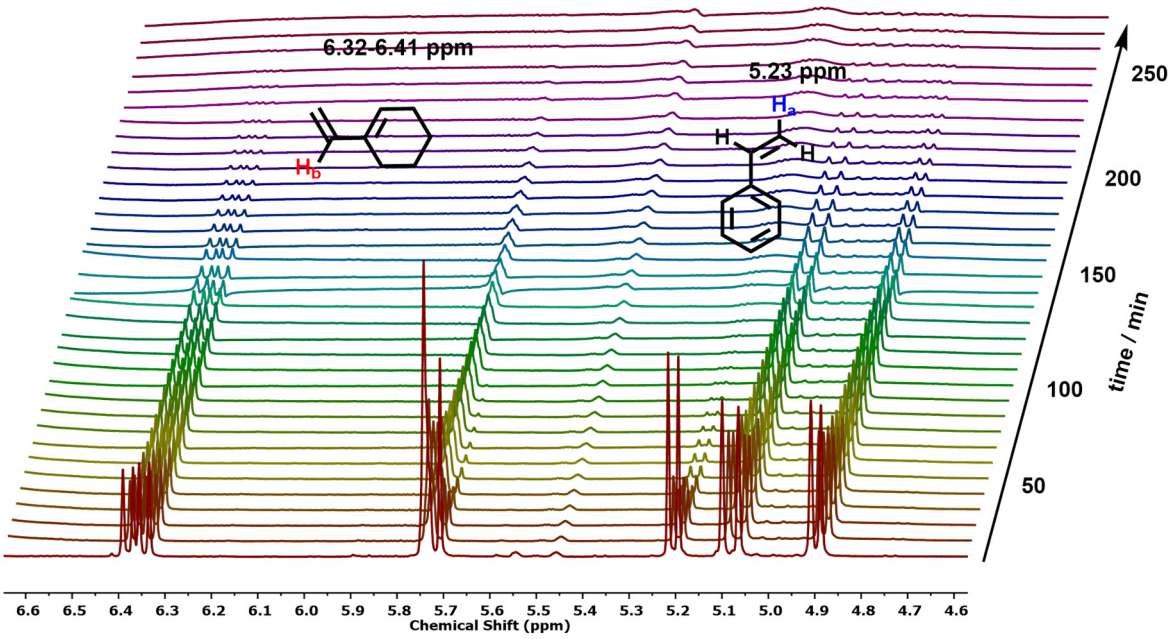


**Scheme S1**: Chemical shifts of decreasing signal of VCH (6.32 – 6.41 ppm, $H_b$) and styrene in the statistical copolymerization of both monomers (5.23 ppm, $H_a$).

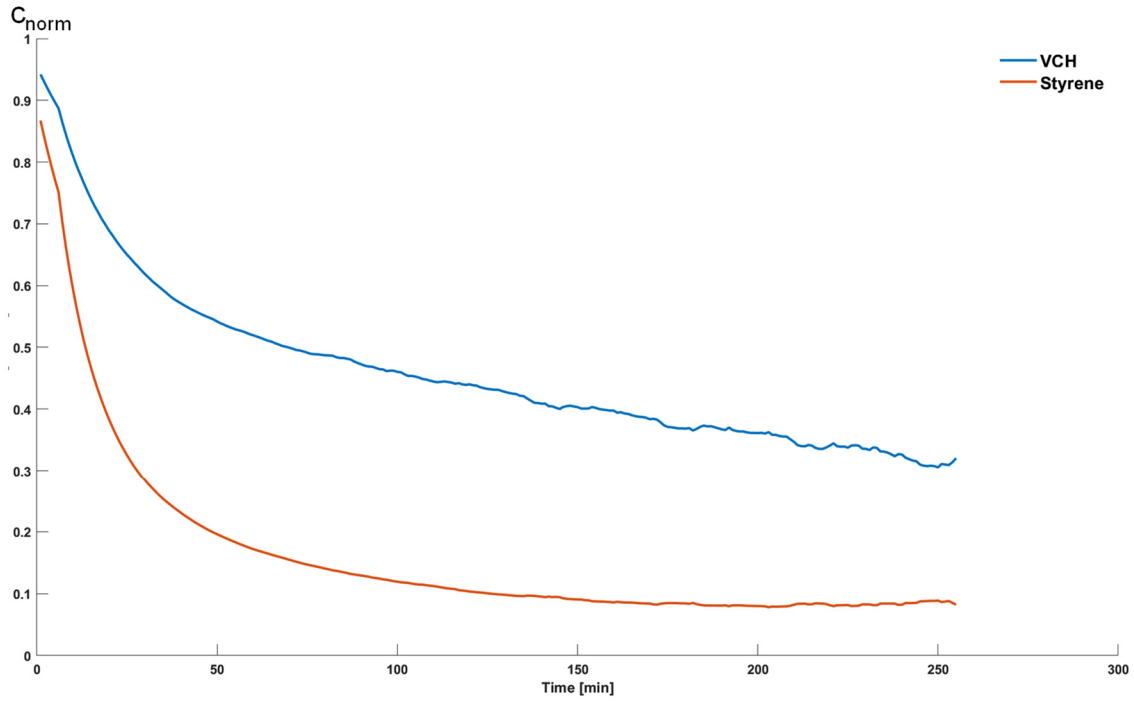


**Figure S15**: Normalized comonomer concentrations $c_{norm}$ vs. time in the statistical copolymerization of VCH and styrene in cyclohexane at 25 °C.

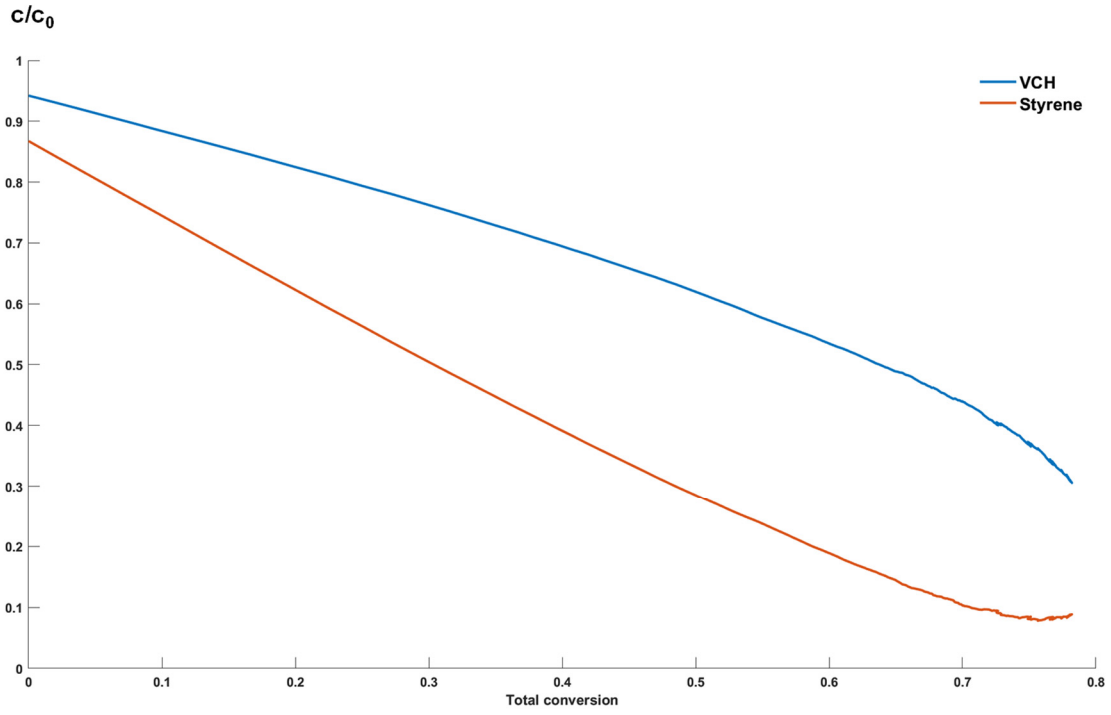


**Figure S16**: Individual monomer concentrations as a function of the total monomer conversion in the statistical copolymerization of VCH and styrene.

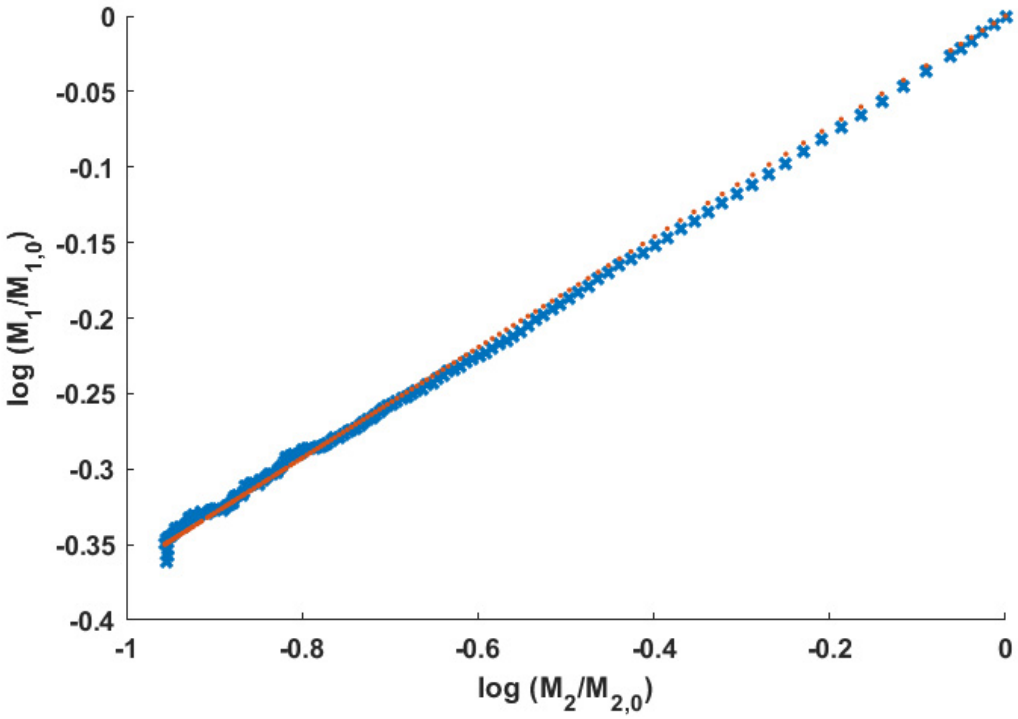


**Figure S17**: Jaacks fit (red dots) of the copolymerization of VCH and styrene, showing excellent agreement with experimental data obtained from online NMR.

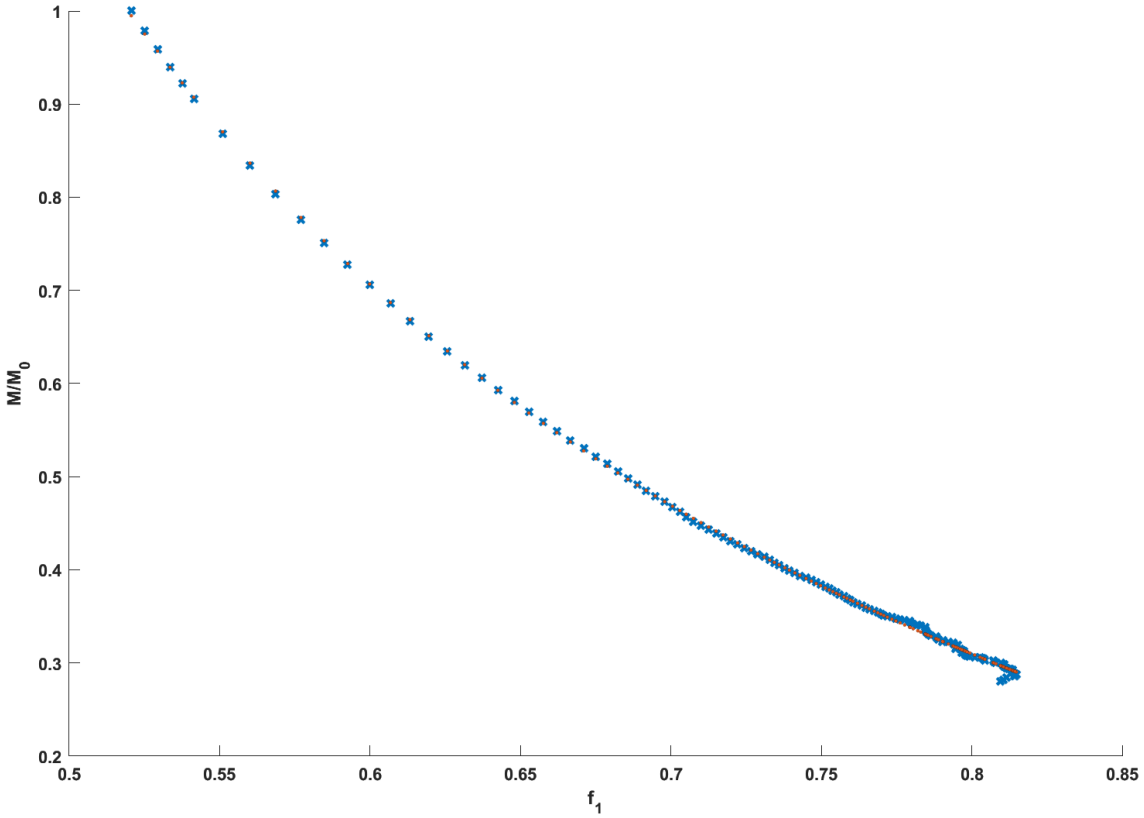


**Figure S18**: Ideal integrated fit[2] (red dots) of the copolymerization of VCH and styrene ($f_1$).

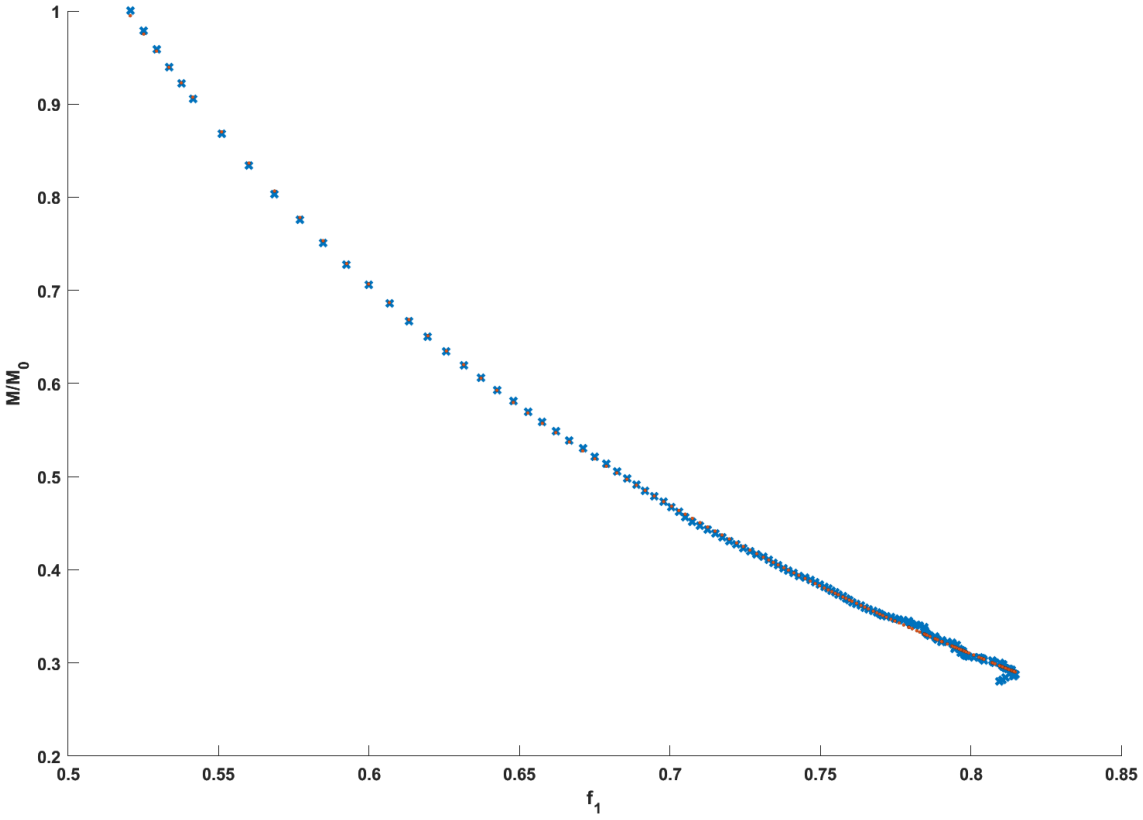


**Figure S19**: Meyer-Lowry fits (red dots) (1-X (total conversion)) versus actual fraction of styrene in the feed, $f_1$ for the copolymerization of VCH and styrene in CH

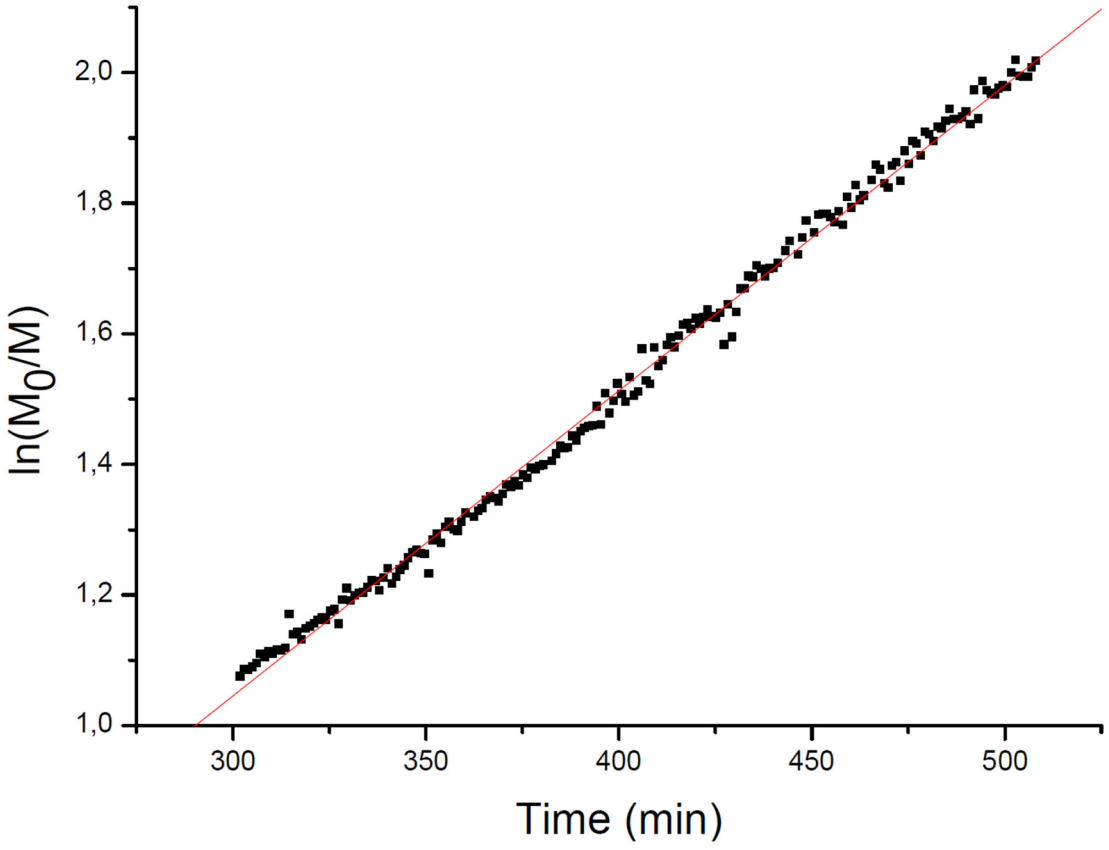


**Figure S20**: Ln($M_0$/M) vs. time plot of the copolymerization of VCH and styrene after the complete consumption of styrene.

**Table S1**. Summary of fit results copolymerization of VCH ($r_2$) and styrene ($r_1$).

| Method | $r_1$ | $r_{1error}$ | $r_2$ | $r_{2error}$ | $r_1 . r_2$ | $r_1 . r_{2\,error}$ | $R^2$ |
|---|---|---|---|---|---|---|---|
| Jaacks | 2.552 | 0.008 | 0.392 | 0.001 | 1 | 0.0043 | 0.9978 |
| Meyer-Lowry ideal | 2.770 | 0.014 | 0.361 | 0.002 | 1 | 0.007 | 0.9968 |
| Meyer-Lowry | 2.144 | 0.047 | 0.249 | 0.008 | 0.535 | 0.002 | 0.9995 |

**Table S2**: $\beta$-carbon shift of styrene, 4-isopropylstyrene and VCH ($^{13}C$ NMR)

| Monomer | styrene | 4-isopropyl-styrene | VCH |
|---|---|---|---|
| $\beta$-C shift (ppm) | 113.36 | 113.00 | 109.72 |

*400MHz, $CDCl_3$

**Figure S21**. Typical colors of the living chains of P(VCH)-Li (left) and P(VCH-*b*-S)-Li (right).

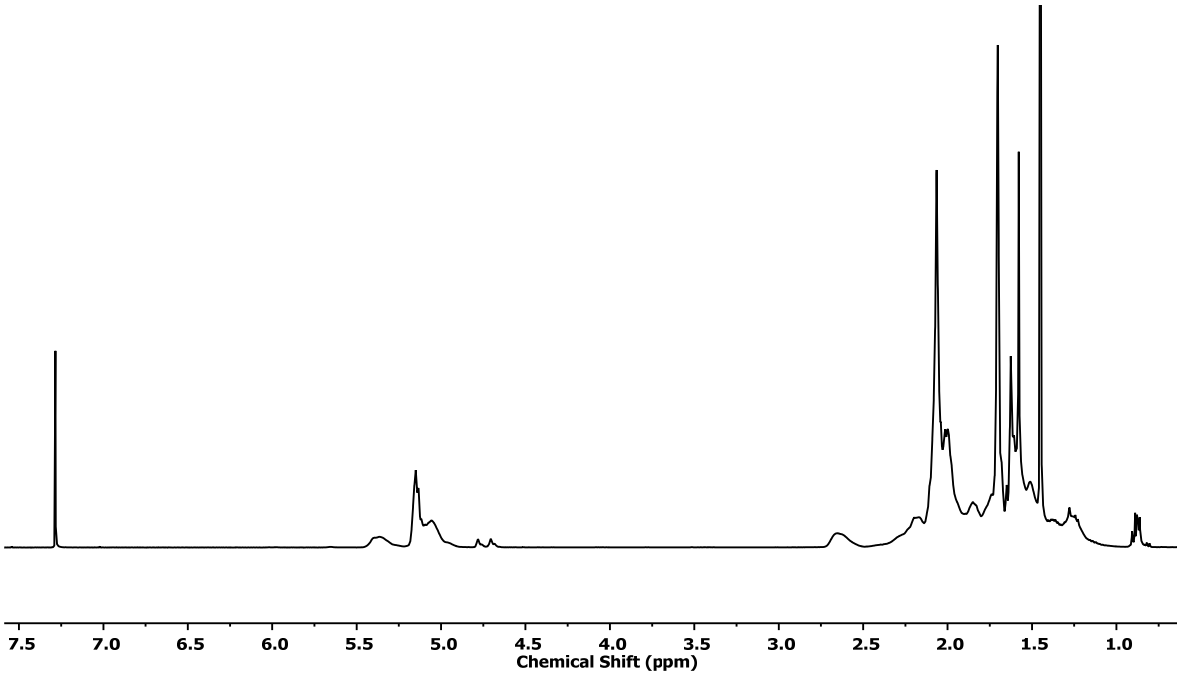


**Figure S22**: $^{1}$H NMR spectrum (400 MHz, C*D*Cl$_3$, 25 °C) of statistical copolymer P(VCH-*co*-I).

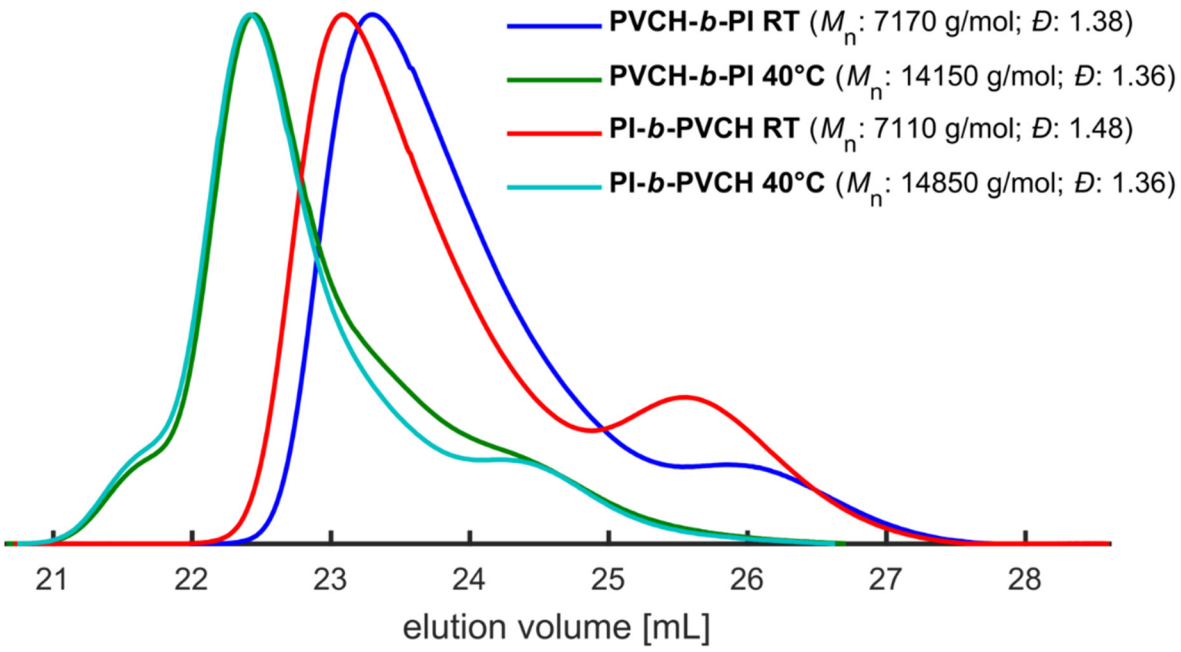


**Figure S23**: SEC traces of the copolymers of VCH and isoprene.

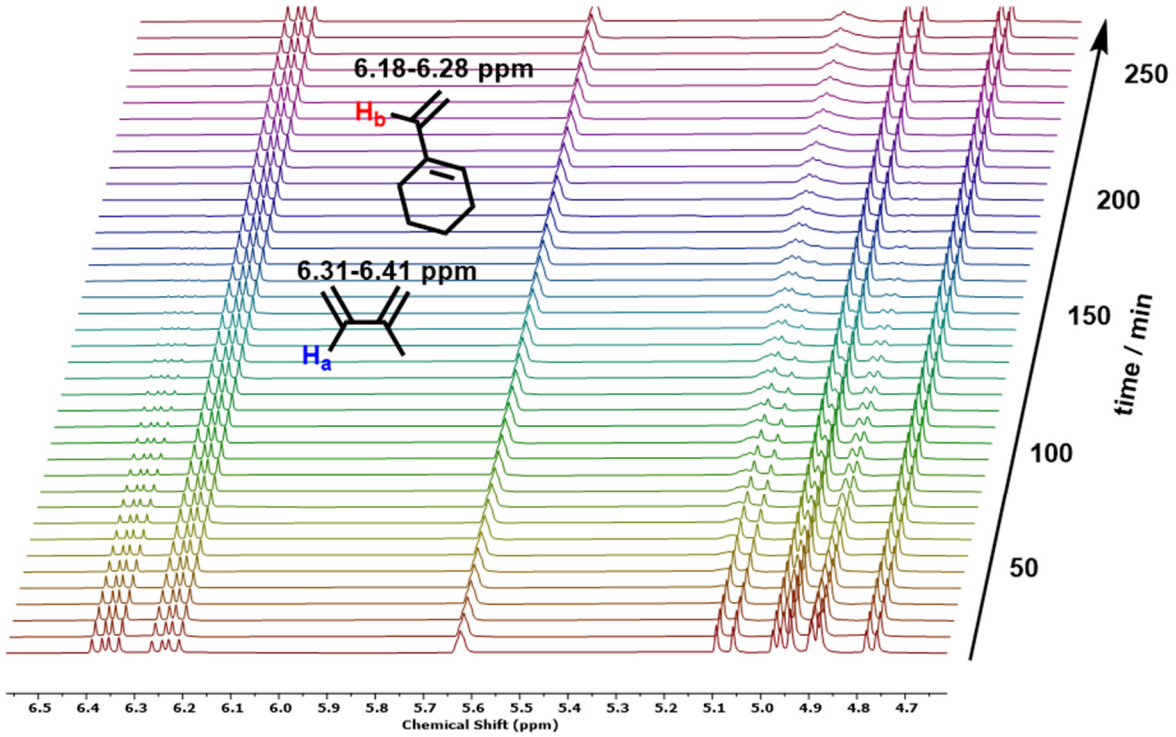


**Figure S24**: Chemical shifts of decreasing signal of Isoprene (6.31 – 6.41ppm, $H_a$) and VCH in the statistical copolymerization of both monomers (6.18 – 6.28 ppm, $H_b$).

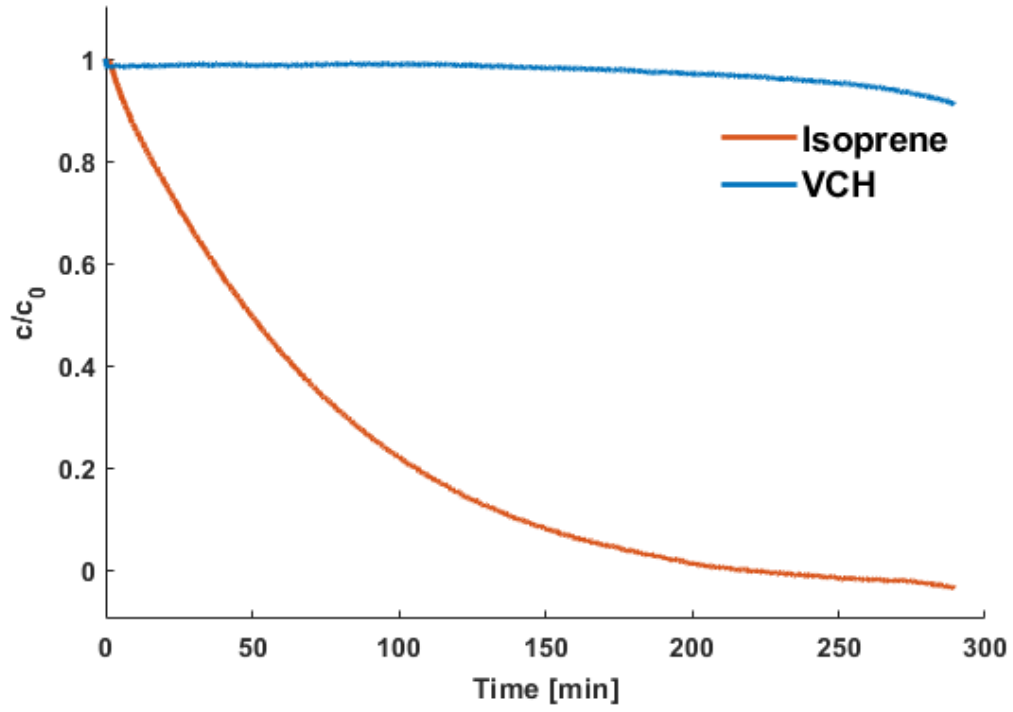


**Figure S25**: Normalized comonomer concentrations vs. time in the statistical copolymerization of VCH and isoprene in cyclohexane at 25 °C.

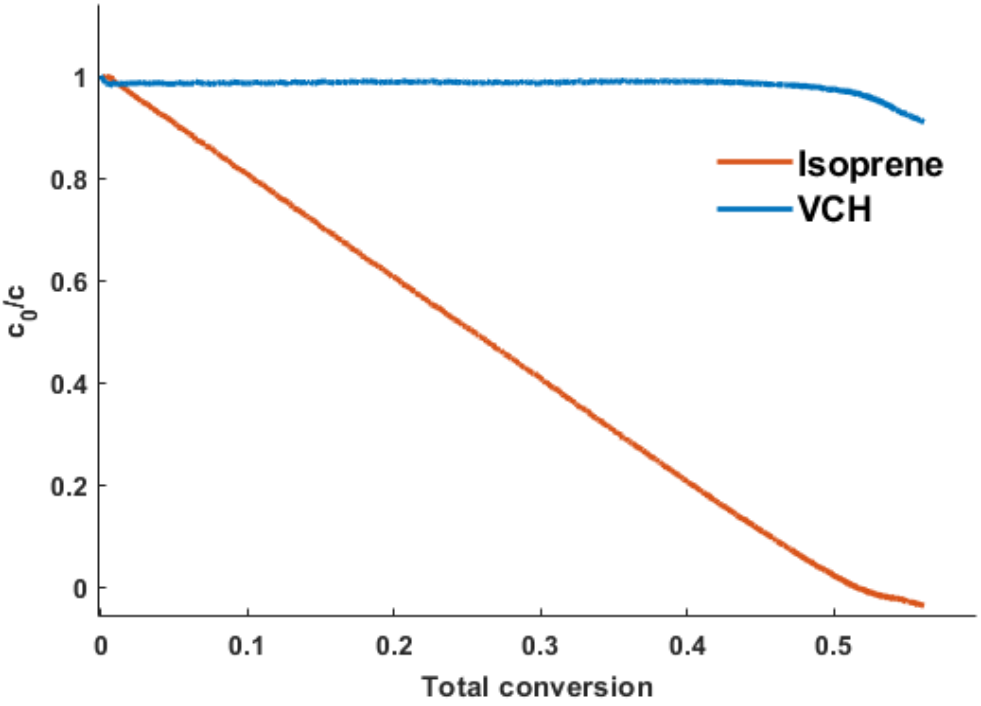


**Figure S26**:Individual monomer concentrations as a function of the total monomer conversion in the statistical copolymerization of VCH and isoprene.

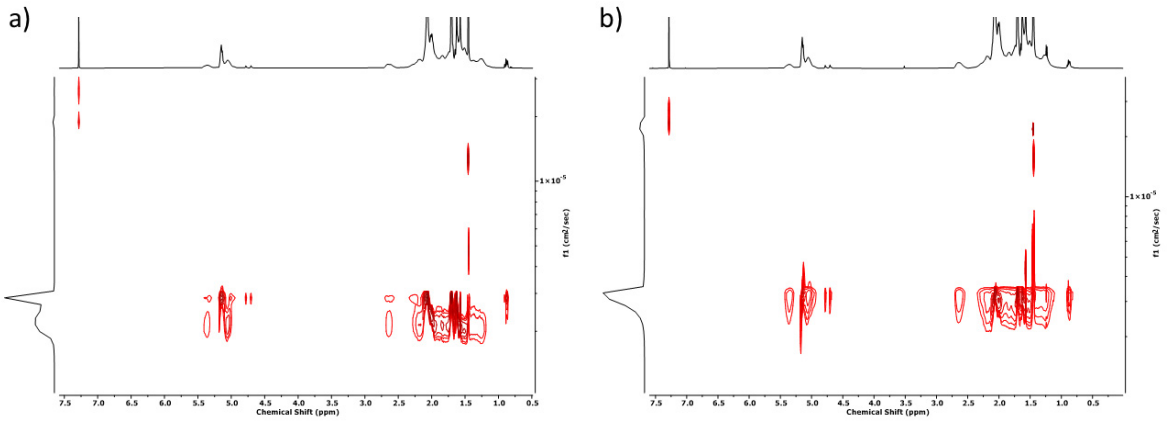


**Figure S27**: DOSY NMR spectra (400 MHz, C*D*Cl$_3$, 25 °C) of the two block copolymers a) PI-*b*-PVCH and b) PVCH-*b*-PI.

## Hydrogenation

The hydrogenation of P(VCH) was catalyzed with palladium on carbon (10 w%) under 30 bar $H_2$ at 130 °C in a 300 mL Parr reactor. Typically, 100 mg polymer and 80 mg Pd/C were dissolved in 25 mL of *n*-decane, and the hydrogenation reaction was conducted for 48 h. The hydrogenation led to full saturation of the polymer, confirmed by $^1$H NMR.

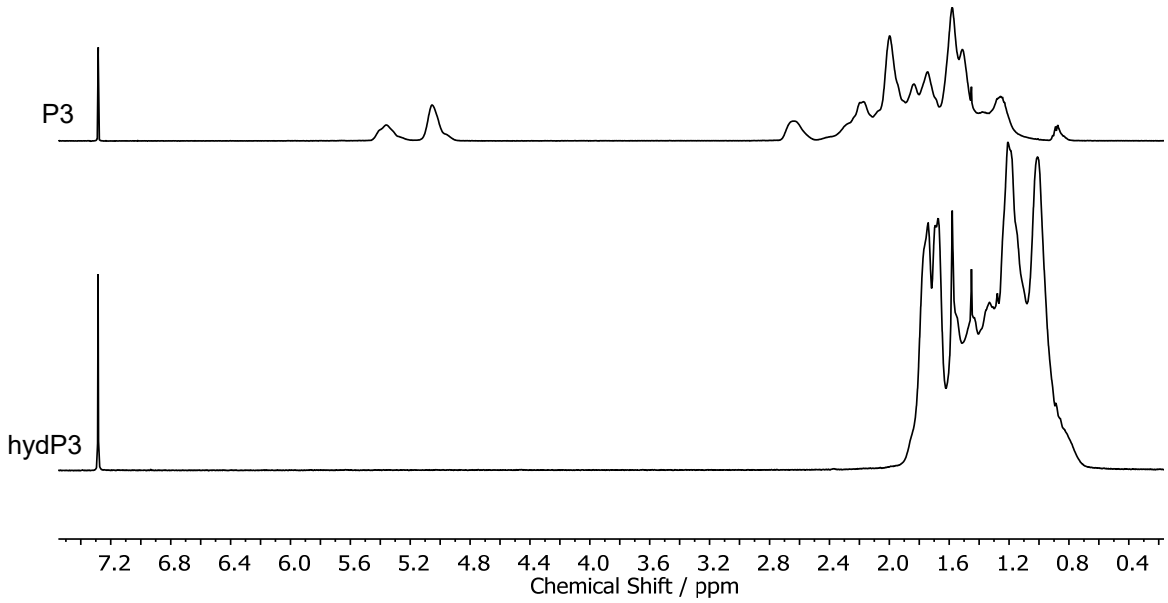


**Figure S28**: Stacked $^{1}$H NMR spectra (400 MHz, C*D*Cl$_3$, 25 °C) of PVCH (P3) before and after hydrogenation, sample hydP3.

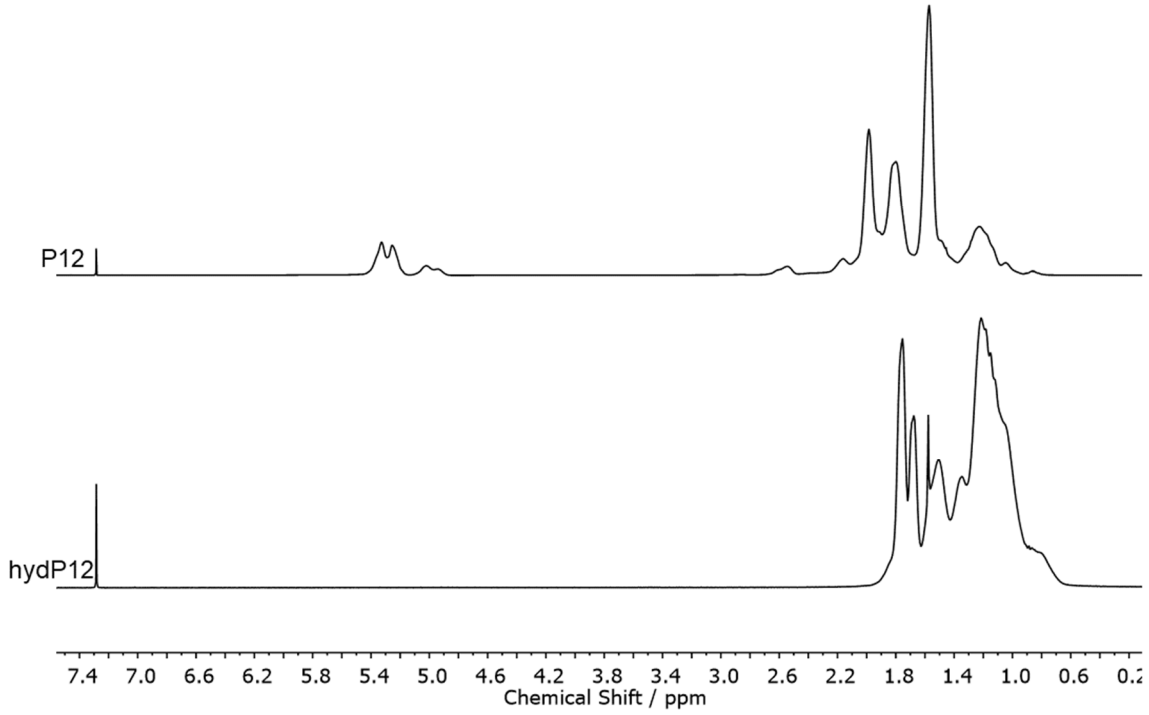


**Figure S29**: Stacked $^{1}$H NMR spectra (400 MHz, C*D*Cl$_3$, 25 °C) of PVCH (P12) and its hydrogenated form hydP12.

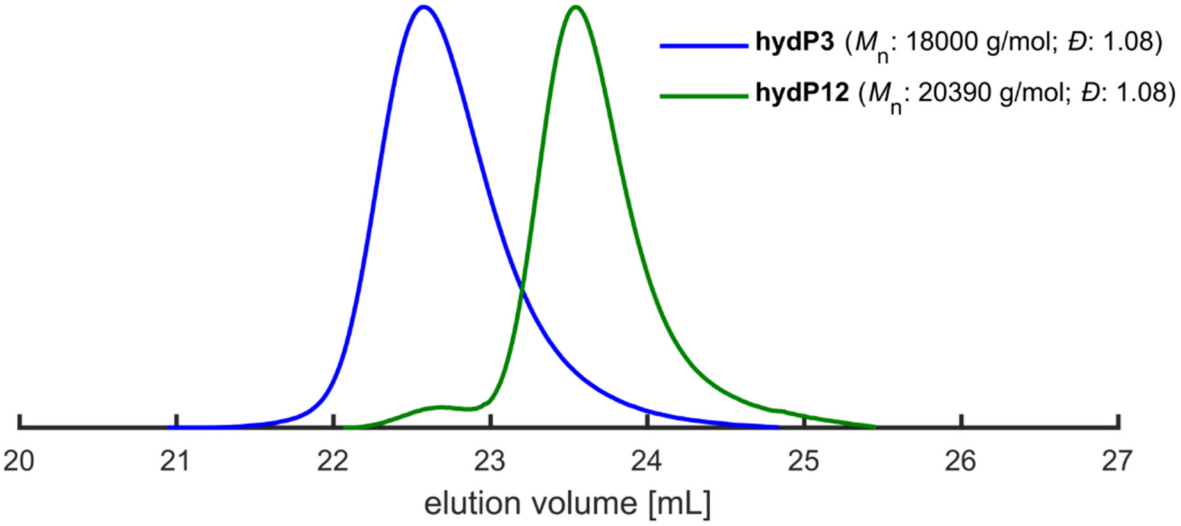


**Figure S30**: SEC traces of the hydrogenated polymers hydP3 and hydP12 (Eluent: THF, PS calibration), showing that no chain degradation occurred.

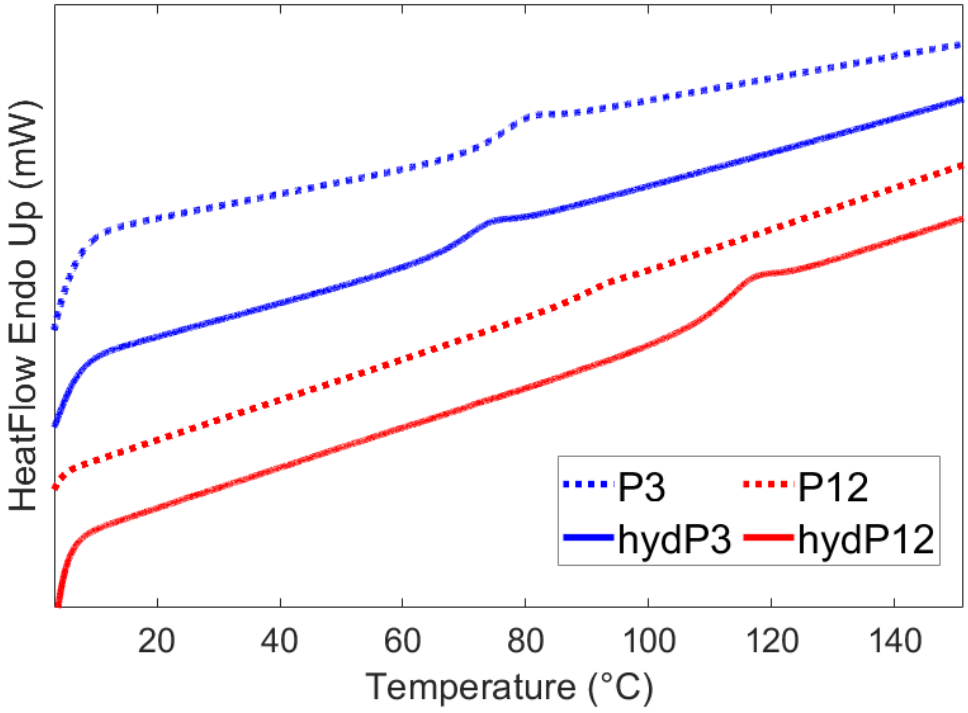


**Figure S31**: DSC data of the hydrogenated polymers hydP3 and hydP12.

## References

1 E. N. Marvell and J. Tashiro, Journal of Organic Chemistry, 1965, 30, 3991–3993.

2 J. Blankenburg, E. Kersten, K. Maciol, M. Wagner, S. Zarbakhsh and H. Frey, Polym Chem, 2019, 10, 2863–2871.

# CHAPTER 3

## Anionic Polymerization of Phenyl-Substituted Isoprene Derivatives: Polymerization Behaviour and Cyclization-Enabled Fluorescence

# CHAPTER 3

Published in *Polymer Chemistry,* 2024, **15**, 3204–3213.
DOI: 10.1039/D4PY00601A

# Anionic Polymerization of Phenyl-Substituted Isoprene Derivatives: Polymerization Behaviour and Cyclization-Enabled Fluorescence

Moritz Rauschenbach,[a] Laura Stein,[a] Gregor M. Linden,[a] Ramona Barent,[a,b] Katja Heinze,[a] and Holger Frey [a,*]

[a] Department of Chemistry, Johannes Gutenberg University, Duesbergweg 10 – 14, D-55128 Mainz (Germany)

[b] Max Planck Graduate Center, Forum Universitatis 2, D-55122 Mainz, Germany

The following chapter is adapted with permission from M. Rauschenbach, L. Stein, G. M. Linden, R. Barent, K. Heinze, and H. Frey; Anionic Polymerization of Phenyl-Substituted Isoprene Derivatives: Polymerization Behaviour and Cyclization-Enabled Fluorescence, *Polymer Chemistry*, 2024, **15**, 3204 – 3213. 


**Abstract:** 1,3-dienes are important monomers for the living anionic polymerization. However, phenyl-substituted diene monomer structures have been hardly investigated. Based on DFT-calculations and $^{13}C$ NMR spectroscopy, a discrepancy in the reactivity of the two monomers 1-phenyl isoprene (1PhI) and 4-phenyl isoprene (4PhI) in the anionic polymerization is expected. Starting from a Wittig reaction including an optimized extraction procedure, the disubstituted 1,3-dienes were obtained that resulted in polymers with different prevalence of 1,3-incorporation. The polymers have been characterized by $^{1}H$ NMR spectroscopy and using different SEC conditions. Molecular weights up to 48.8 kg mol$^{-1}$ with narrow dispersities ($Đ \leq 1.13$) were achieved. The addition of the modifier THF led to an initial increase of vinyl-units as well as a loss of control for the polymerization of 4PhI. Increasing the THF concentration further resulted in a rather unusual decrease of the vinyl units and climaxed in more than 80% 1,4-units in pure THF. Copolymerizations with styrene (S) and isoprene (I), respectively, were tracked *via in situ* $^{1}H$ NMR kinetics. The observed ideally random copolymerization of I and 1PhI as well as the gradient copolymers with S were further investigated by the synthesis of copolymers with a targeted $M_n$ of 40 kg mol$^{-1}$. In a subsequent reaction step, the homopolymers were cyclized using trifluoromethyl sulfonic acid inducing fluorescent properties. The different microstructure and substitution pattern of the original polymers differ in both emission maximum and the quantum yield.

## Introduction

The living anionic polymerization introduced by Michael Szwarc in 1956 offers excellent control over molecular weights and the dispersity *Đ* of polymers.[1,2] It has been widely used for the polymerization of 1,3-dienes such as 1,3-butadiene and isoprene to generate polydiene materials for synthetic rubber. The elastic properties of these polydienes after crosslinking notably depend on their microstructure. Therefore, the main target of early works of anionic polymerization of 1,3-dienes was the optimization of reaction parameters (e.g., initiator, solvent, further additives, and temperature) to obtain a high *cis*-1,4-content.[3]

The copolymerization of 1,3-dienes such as 1,3-butadiene (B) and isoprene (I) with styrene (S) affords a variety of possible polymer architectures.[4,5] ABA triblock copolymers have attracted attention as thermoplastic elastomers (TPEs). This architecture relies on a flexible, low $T_g$ polydiene midblock B (e.g. polyisoprene) and two outer polystyrene A blocks that act as crosslinks after cooling and vitrification.[6] In 1966, Holden and Milkovich reported that the statistical copolymerization of isoprene and styrene in apolar solvents like cyclohexane results in block-like gradient copolymers that were later designated "tapered".[7] The addition of a small quantity of THF with respect to the lithium-ion concentration leads to a change of the reactivity ratios and the respective monomer gradient. By variation of the THF concentration, the incorporation of both monomers can be tuned to an ideally random incorporation, and even complete reversal of the molar composition is possible, as shown by detailed online NIR kinetics recently.[8] However, the addition of THF as a "modifier" at the same time also influences the incorporation mode of isoprene (increasing extent of 3,4-addition) and therefore has an undesired impact on the elastic properties. As described in manifold studies, an increase of the amount of 1,2- and 3,4-units in polydienes is observed when increasing the polarity of the system.[8–11]

Only few studies have been reported for phenyl-substituted butadiene derivatives.[12,13] As an example, the 1-phenyl-1,3-butadiene (PhB) monomer has been polymerized *via* either anionic or catalytic approaches.[14–17] It can be considered as a *β*-substituted styrene or as a 1-phenyl-substituted 1,3-butadiene.[18] This combination of two very established monomers provides an intriguing perspective. Suzuki *et al*. systematically

investigated the anionic polymerization of PhB regarding its copolymerization with butadiene and styrene as well as the microstructure with respect to various parameters.[12,19–22] $^{1}$H NMR studies of the resulting microstructure of PhB in different solvents revealed different behaviour compared to established dienes. The addition of aliquots of THF enhanced the formation of the vinylic microstructure. However, a 1,4-dominated microstructure was obtained when polymerization was performed in THF, confirmed by NMR analysis based on the chemical shifts of the aromatic protons of oligomeric structures in deuterated THF. The authors concluded that the negative charge is localized in *α*-position of the phenyl ring to form the most stable anion as the active chain end. This explains why poly(1-phenyl butadiene) (PPhB) polymerized in THF shows predominantly 1,4-units.[21]

The phenyl-substituted polybutadienes showed a glass transition temperature ($T_g$) of around 30 °C.[17] Worth mentioning, the $T_g$ is in between the structurally similar polyisoprene ($T_g \leq -65$°C)[23] and polystyrene ($T_g = 100$°C)[11]. Han *et al*. reported the catalytic polymerization with a 3,4-content of 94%, resulting in a $T_g$ of 82 °C indicating a high dependency on the respective microstructure.[24] In a cationic polymerization approach phenyl butadiene underwent cyclization as a side-reaction. Fundamental works report on the targeted cationic cyclization post-polymerization of polydienes to obtain an unsaturated polycyclic species.[25–28] More recently, the cyclization reaction was adapted to P(PhB) to maximize the $T_g$. Depending on the microstructure the $T_g$ of the cyclized material can reach nearly 200 °C, ranging the material among the highest reported $T_g$s for aliphatic hydrocarbon polymers.[29] Additionally, cyclized poly (phenylbutadiene) (*cyc*P(PhB)) showed fluorescence.

Herein, we report the combination of styrene and isoprene to “phenylisoprenes”. For isoprene, attachment of the phenyl-ring can take place either at the 1- or the 4-position, resulting in a 1,2- or a 1,3-disubstituted 1,3-diene structure. While the 4-phenyl isoprene (4PhI) has been briefly described with respect to its anionic polymerization[30], to the best of our knowledge the 1-phenyl isoprene (1PhI) has not been employed for the anionic polymerization to date. In this work, we contrast 1PhI and 4PhI on a theoretical basis using density functional theory (DFT) as well as $^{13}$C NMR spectroscopy to predict its reactivity in anionic polymerization. We use styrene and isoprene, respectively, as a comparison. Both phenylisoprene monomers are

investigated in-depth regarding their behaviour in the anionic polymerization and are copolymerized with either isoprene or styrene. For the determination of reactivity ratios online $^{1}$H NMR spectroscopy was employed. We monitored the anionic copolymerization with the structurally related monomers styrene and isoprene in cyclohexane, respectively. Finally, polymer cyclization is explored according to literature procedures, aiming at fluorescent, high $T_g$ materials based on the reported monomers.[17,24,29,31]

## Results and discussion

### Synthesis of phenyl-substituted isoprene derivatives

1PhI and 4PhI were synthesized *via* a one-step Wittig reaction starting from commercially available aldehyde and ketone structures, respectively. For the synthesis of 1PhI, using potassium *tert*-butoxide monomer yields exceeding 75% were achieved. However, the stronger base sodium hexamethyldisilyl amine (NaHMDS) is required to achieve similar yields for the ketone benzylidene acetone. A straightforward method was established for the separation of the triphenylphosphine oxide including precipitation, centrifugation and subsequential distillation. Details are given in the ESI.

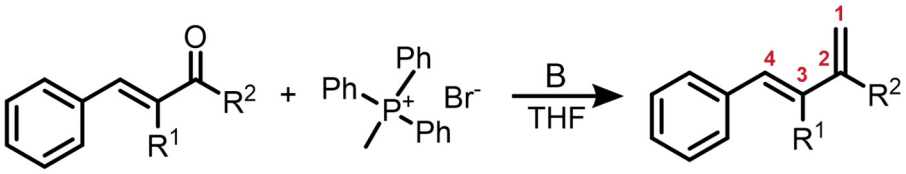


1PhI: $R^1 = CH_3$; $R^2 = H$; B = KO*t*Bu
4PhI: $R^1 = H$; $R^2 = CH_3$; B = NaHDMS

**Scheme 1**: Synthesis route to the phenyl-substituted isoprene derivatives

Since 1PhI and 4PhI can be viewed as *β*-substituted styrene derivatives we estimate the reactivity of both monomers in analogy to previously described methods. $^{13}$C NMR spectroscopy was utilized to estimate the reactivity of *para*-substituted styrene derivatives by Hirao *et al*..[32] The *β*-carbon shift identifies the electron charge density of the reactive vinyl bond. Increasing the polarization of the reacting carbon-carbon bond leads to increased reactivity. Therefore, it is in good agreement with the monomer reactivity in anionic polymerization. If 1PhI and 4PhI are viewed as styrene derivatives the chemical shift of C1 as assigned in **Scheme 1** was identified. Thus, 4PhI

(δ = 117.45 ppm, $CDCl_3$) is expected to be much more reactive compared to styrene (δ = 113.36 ppm, $CDCl_3$) while 1PhI (δ = 113.02 ppm, $CDCl_3$) should be slightly less reactive in anionic copolymerization in apolar media.

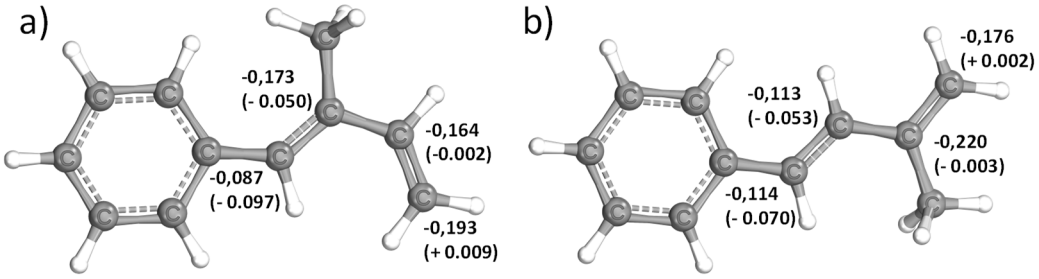


**Figure 1**: 3D visualization of (a) 1PhI and (b) 4PhI, respectively, with the corresponding partial charges of the dienic carbon atoms calculated using DFT. In brackets, the deviations from the calculated electron densities of isoprene are given. [33,34]

Furthermore, DFT calculations of both monomers were conducted to obtain further theoretical insights. **Figure 1** shows the relative electron densities of both 1PhI and 4PhI in comparison to the values calculated for isoprene (differences shown in brackets). Focusing on the free methylene groups, which are most likely to be attacked by nucleophilic reagents, 4PhI (− 0.176e) exhibits a lower charge at this position compared to 1PhI (− 0.193e). Hence, the nucleophilic attack as part of the propagation is prone to occur, supporting expectation based on $^{13}C$ NMR spectroscopy. Nevertheless, the electron densities of the reactive double bond show just minor deviation from the 3,4-double bond in isoprene, which is assumed to be the one reacting in the anionic polymerization. This could be interpreted in terms of a fast crossover reaction in both directions.

## Homopolymerization of PhIs with *sec*-BuLi in Cyclohexane

Both monomers 1PhI and 4PhI can be interpreted as a structural combination of styrene and isoprene. To investigate whether their behaviour in the anionic polymerization resembles rather S or I, a series of homopolymers with increasing $M_n$ has been synthesized. All polymerizations were carried out in cyclohexane, using *sec*-butyl lithium as an initiator at room temperature. Subsequently, the homopolymers were characterized *via* SEC, $^1H$ NMR spectroscopy and DSC. **Table 1** summarizes all characterization data of the obtained polymers, which possessed molecular weights in good agreement with the targeted values in a range of 4.6 – 48.8 kg $mol^{-1}$ (SEC, eluent

THF, and PS calibration) with low dispersities (Đ ≤ 1.13). The SEC-determined molecular weights are strongly dependent on the calibration standard employed.

**Table 1**: Overview of the homopolymers synthesized *via sec*-butyl lithium-initiated polymerization in cyclohexane.

| Entry | M | $M_n^{targ}$ [kg mol$^{-1}$] | $M_n^{a}$ [kg mol$^{-1}$] | $M_n^{b}$ [kg mol$^{-1}$] | Đ | 1,4-PhI [%]$^{c}$ | 1,2-PhI [%]$^{c}$ | $T_g$ [°C] |
|---|---|---|---|---|---|---|---|---|
| 1 | 1PhI | 5 | 3.6 | 4.6 | 1.06 | 42 | 58 | 62 |
| 2 | | 10 | 6.5 | 8.5 | 1.05 | 34 | 66 | 69 |
| 3 | | 20 | 13.6 | 18.4 | 1.04 | 35 | 65 | 65 |
| 4 | | 40 | 24.0 | 32.4 | 1.02 | 37 | 63 | 69 |
| 5 | 4PhI | 5 | 3.8 | 4.7 | 1.13 | 85 | 15 | 47 |
| 6 | | 10 | 10.7 | 13.6 | 1.07 | 94 | 6 | 47 |
| 7 | | 20 | 22.6 | 30.0 | 1.09 | 94 | 6 | 48 |
| 8 | | 40 | 48.8 | 64.8 | 1.11 | 94 | 6 | 48 |

[a] Determined by SEC (THF, PI-calibration, RI-detector) [b] Determined by SEC (THF, PS-calibration, RI-detector) c Determined from the olefinic region of the $^1$H NMR spectra (400 MHz, $CDCl_3$)

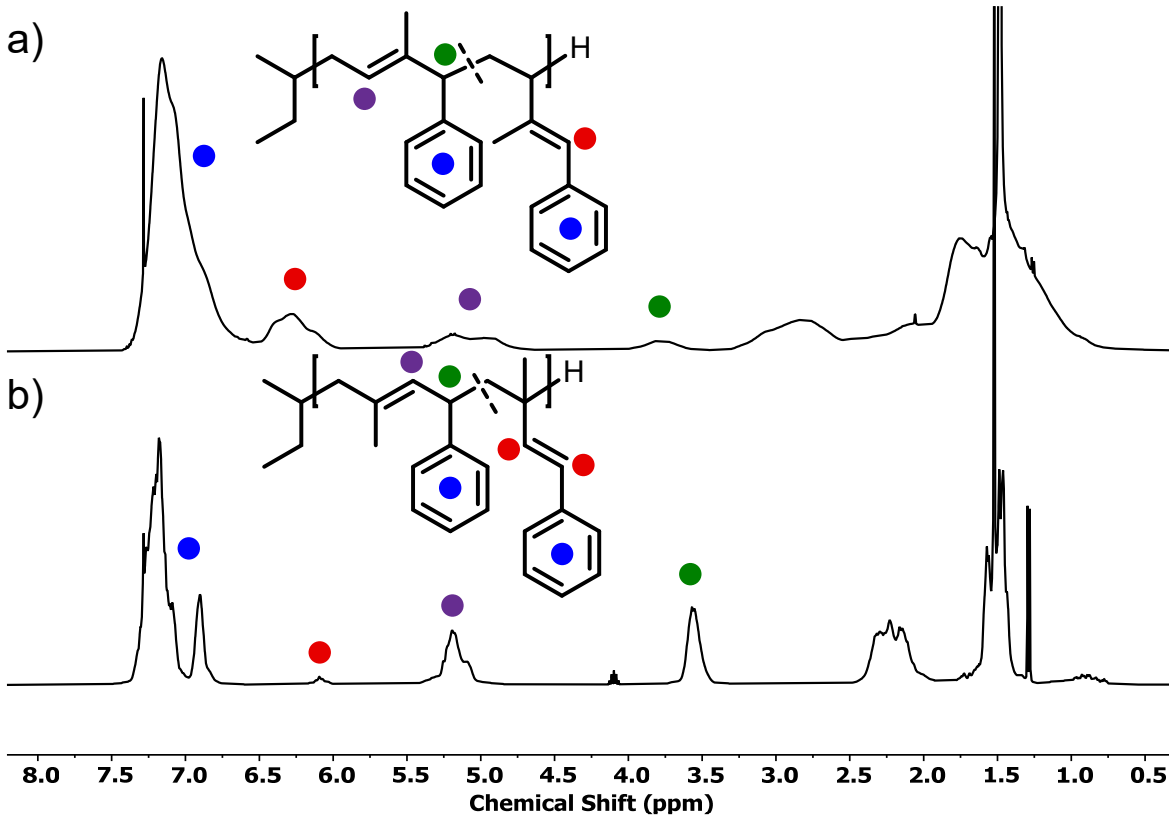


**Figure 2**: $^1$H NMR spectra ($CDCl_3$, 400 MHz) of a) P(1PhI) and b) P(P4PhI).

The microstructures of both P(1PhI) and P(4PhI) were investigated by $^{1}$H NMR spectroscopy in analogy to previously reported works.[12,17] The spectra (**Figure 2**) show the olefinic signals used for the determination of the microstructures. The signals were assigned according to the reported microstructure of P(1-phenyl butadiene).[12] The sharp signals of P(4PhI) indicate a highly defined composition, which is supported by the integration, showing 94% of 1,4-units. This is consistent with the microstructure of polyisoprene obtained under these conditions.[35] In comparison, the $^{1}$H NMR spectrum of P(1PhI) displays broad signals with a microstructure consisting of 66% 1,2-units. This result can be explained by a sterically hindered 1,4-addition reaction, as previously suggested for 1,1-disubstituted 1,3-dienes.[36]

The SEC-traces shown in **Figure 3** confirm good control of the polymerization for both monomers, resulting in narrow, monomodal distributions. A high degree of agreement was observed between the targeted molecular weights and the results based on PI calibration, which can be taken as indirect confirmation of the predominant 1,4-microstructure. On the contrary, the prevalence of the 1,2-microstructure in P(1PhI) samples underlines why PS calibration yields values that exhibit closer proximity to theoretical predictions.

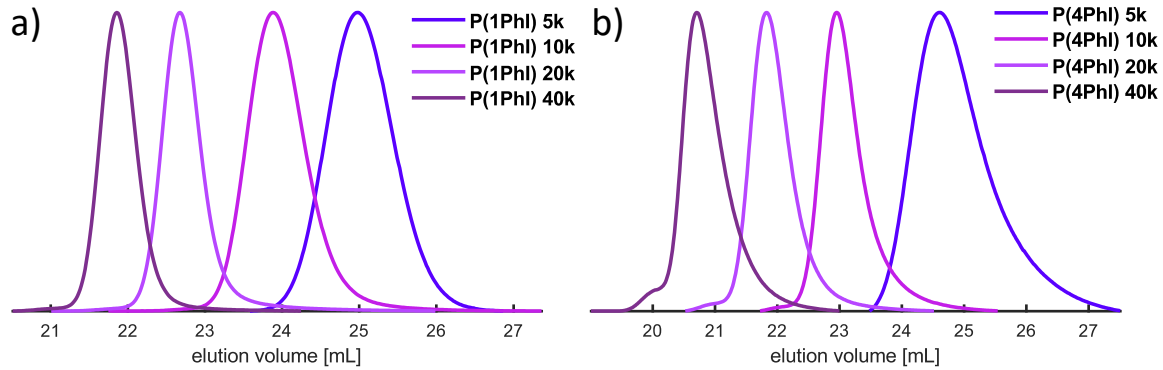


**Figure 3**. SEC traces of synthesized homopolymers with increasing targeted $M_n$ from a) 1-phenyl isoprene and b) 4-phenyl isoprene.

## Addition of polar additives

The polymerization of 1,3-dienes is known to depend on several parameters (e.g. chain end and monomer concentration, temperature, solvent, etc.) in terms of the regio-isomeric composition of the resulting polymers.[8,37–40] The polarity of the solvent is a key parameter, since it determines the coordination of the chain end to the lithium ion.[41] In

numerous studies it was shown that the addition of aliquots of THF in the polymerization of 1,3-dienes increase the content of vinylic units.[8,9,42] Furthermore, the addition of THF accelerates propagation kinetics. This effect has been observed in both isoprene and styrene, where propagation reaches a maximum before further addition of THF decelerates propagation.[43,44]

For 1-phenyl butadiene it was reported that upon addition of a few aliquots of THF the ratio of 1,2-units increases.[12] Further increasing the content of THF and polymerization in pure THF led to a maximum of 90% 1,4-content. In similar fashion, we conducted the polymerization of 1PhI and 4PhI in cyclohexane with 2 and 20 equivalents of THF with respect to the lithium-ion concentration. Furthermore, we carried out the polymerization reaction in pure THF at -78°C. It should be noted that common dienes such as myrcene and isoprene are not capable of polymerizing under these conditions.[45,46] As listed in **Table 2** the addition of THF has an impact on the resulting microstructure as the ratio of vinyl units increases. In line with previous observations for PhB, in pure THF more than 80% 1,4-units were formed. A tentative explanation might be given by the reactivity of the chain end and the resulting propagation rates. Strohmann *et al* reported experiments of *tert*-butyl lithium and THF in a ratio of 1:2 revealing a remarkable aggregation leading to an increase in reactivity compared the ratios 1:1 and 1:2.5.[47] Consequently, the polymerization rate is enhanced by small amounts of THF, promoting the formation of vinylic units. The faster kinetics may also explain the broad distribution observed for entry 12. Carrying out the polymerization of 4PhI with 2 equivalents THF with respect to BuLi concentration did not result in dispersities lower than 1.4, as illustrated in **Figure S16**. Further increasing the polarity supports the formation of the most stable anion. For both 1PhI and 4PhI the charge will be delocalized in the aromatic ring as demonstrated for PhB.[21,22] Therefore, one observes predominant formation of 1,4-units with increasing polarity of the system by comparison of the respective $^{1}$H NMR spectra (**Figure 4**).

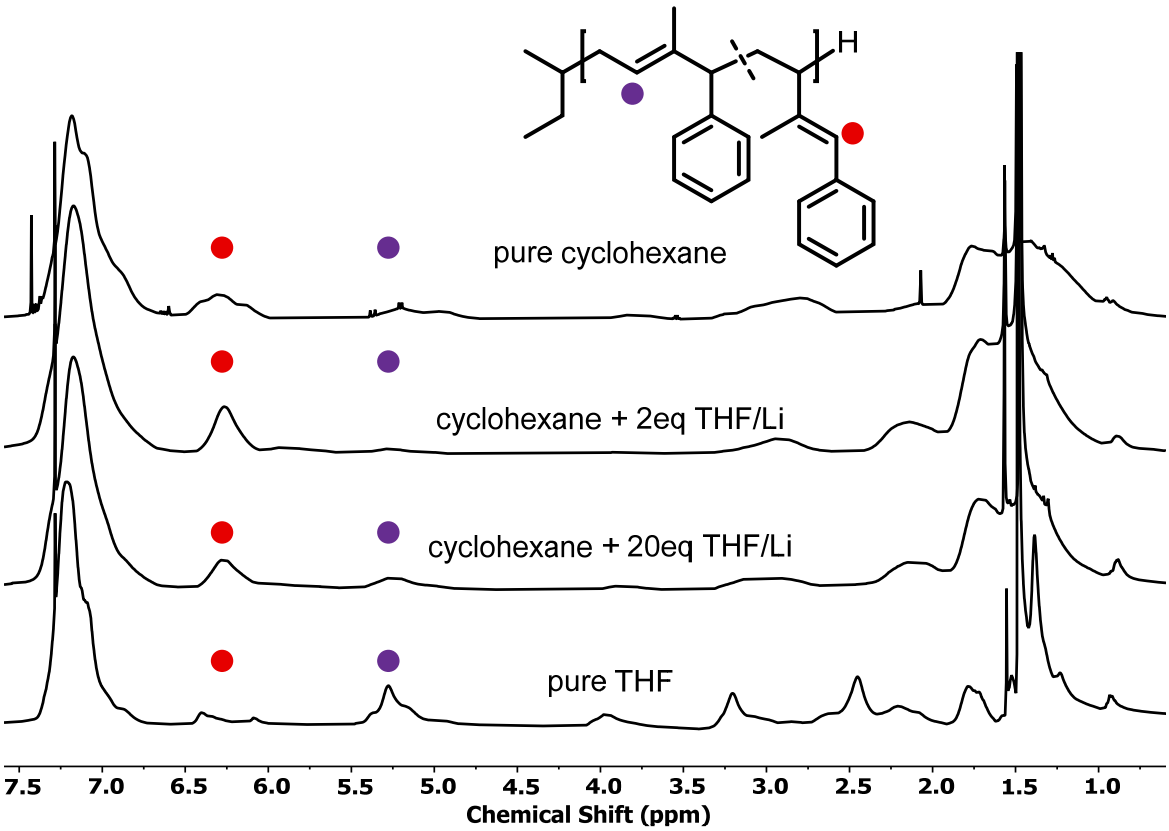


**Figure 4**: Stacked $^{1}$H NMR spectra of P(1PhI) polymerized with increasing concentration of THF resulting in microstructures with shifting ratios.

As expected, DSC measurements of the resulting polymers show a clear correlation between the glass transition and the respective microstructure. For example, 1PhI polymerized in THF with a high 1,4-content exhibited a lower $T_g$ of 50°C compared to 67°C when polymerized in cyclohexane due to its more flexible backbone compared to P1PhI synthesized in cyclohexane, which is dominated by a 1,2-microstructure (**Figure S14**). As shown by the values in **Table 2** the $T_g$s for the P1PhI samples prepared in different systems are shifted to higher temperature with increasing solvent polarity. P4PhI polymerized in either cyclohexane or THF always resulted in a high 1,4-content. Therefore, as shown in **Figure S15** the $T_g$s of both samples are in the same range of 50 – 56°C. Tailoring the microstructure to obtain higher 1,2-content can increase the $T_g$ up to 73°C.

**Table 2**: Data of the obtained polymers investigating the impact of THF on the polymerization of PhI monomers in cyclohexane.

| Entry | M | $M_n^{targ}$ [kg mol$^{-1}$] | $M_n^{b}$ [kg mol$^{-1}$] | [THF]/[Li] | $Đ$ | 1,4-PhI [%][c] | 1,2-PhI [%][c] | $T_g$ [°C] |
|---|---|---|---|---|---|---|---|---|
| 1 | 1PhI | 10 | 7.8 | 0 | 1.05 | 34 | 66 | 67 |
| 9 | | 10 | 10.3 | 2 | 1.07 | 12 | 88 | 62 |
| 10 | | 10 | 11.1 | 20 | 1.08 | 33 | 67 | 53 |
| 11[a] | | 10 | 9.6 | pure | 1.06 | 85 | 15 | 50 |
| 5 | 4PhI | 10 | 13.9 | 0 | 1.09 | 94 | 6 | 56 |
| 12 | | 10 | 7.1 | 2 | 1.44 | n.d. | n.d. | 73 |
| 13 | | 10 | 8.7 | 20 | 1.15 | 56 | 44 | 63 |
| 14[a] | | 10 | 9.9 | pure | 1.08 | 82 | 18 | 50 |

[a] Polymerization in −78 °C. [b] Determined by SEC (THF, PS-calibration, RI-detector) [c] Calculation using the respective olefinic signals of the $^1$H NMR spectra.

## *In Situ* $^1$H NMR kinetics with styrene as a comonomer

Living poly(1PhB) chain ends were not sufficiently reactive to initiate butadiene or styrene in THF. Reaching a maximum of 35% block efficiency, only bimodal distributions were reported. However, reverse monomer addition resulted in monomodal SEC traces, confirming that all living chain ends initiated 1PhB.[20]

To investigate the statistical copolymerization behaviour of both monomers with styrene and isoprene, respectively, we conducted real-time $^1$H NMR spectroscopy to evaluate the reactivity ratios. First, copolymerization reactions of styrene with 1PhI and 4PhI, respectively, were conducted. During the statistical copolymerization individual monomer peaks were traced to determine monomer conversion. Due to the absence of termination and transfer reactions in a classical anionic polymerization, monitoring of the integrals can be also used to determine the relative position along the growing chains.[48,49] The stacked $^1$H NMR spectra for the copolymerization of styrene and 1PhI are shown in **Figure 5** and in **Figure S18** for 4PhI. The monomer concentrations plotted as a function of time and total conversion, respectively, show preferential consumption of the phenyl isoprenes over styrene in both cases.

The collected data were used to calculate the reactivity ratios $r_{PhI}$ and $r_S$, listed in **Table 3**. They define the ratio of the rate of the homopolymerization and the crossover reaction. Using the non-terminal model of Jaacks the values were determined.[50] Based on these evaluated parameters, plots of the relative comonomer position along the chain were generated. As illustrated in **Figure 6** b) and c) for both systems a pronounced gradient is observed. The steeper gradient for the 4PhI system confirms 4PhI to be more reactive, the hypothesis derived from the *β*-C-shift. However, in contrast to the abovementioned assumption, 1PhI is consumed faster, although the carbon shift indicated the opposite. This demonstrates that these simple considerations cannot be applied to diene systems. Reactivity ratios calculated by the terminal model of the Meyer-Lowry fit are given in the Supporting Information.

In comparison to the reactivity ratios observed for the copolymerization of styrene with isoprene (substituted in 2-position) and myrcene (**Table 3**), the di-substituted 1PhI and 4PhI display a less pronounced gradient. Nevertheless, it is worth noting that the 1,2-disubstituted 1PhI demonstrates higher reactivity ratios compared to previously reported 1,2-disubstuted dienes (i.e. *trans*- and *cis*-ocimene and 1-vinyl cyclohexene)[51,52]. To the best of our knowledge 4PhI is the first 1,3-disubstituted 1,3-diene that has been investigated regarding its copolymerization kinetics with styrene.

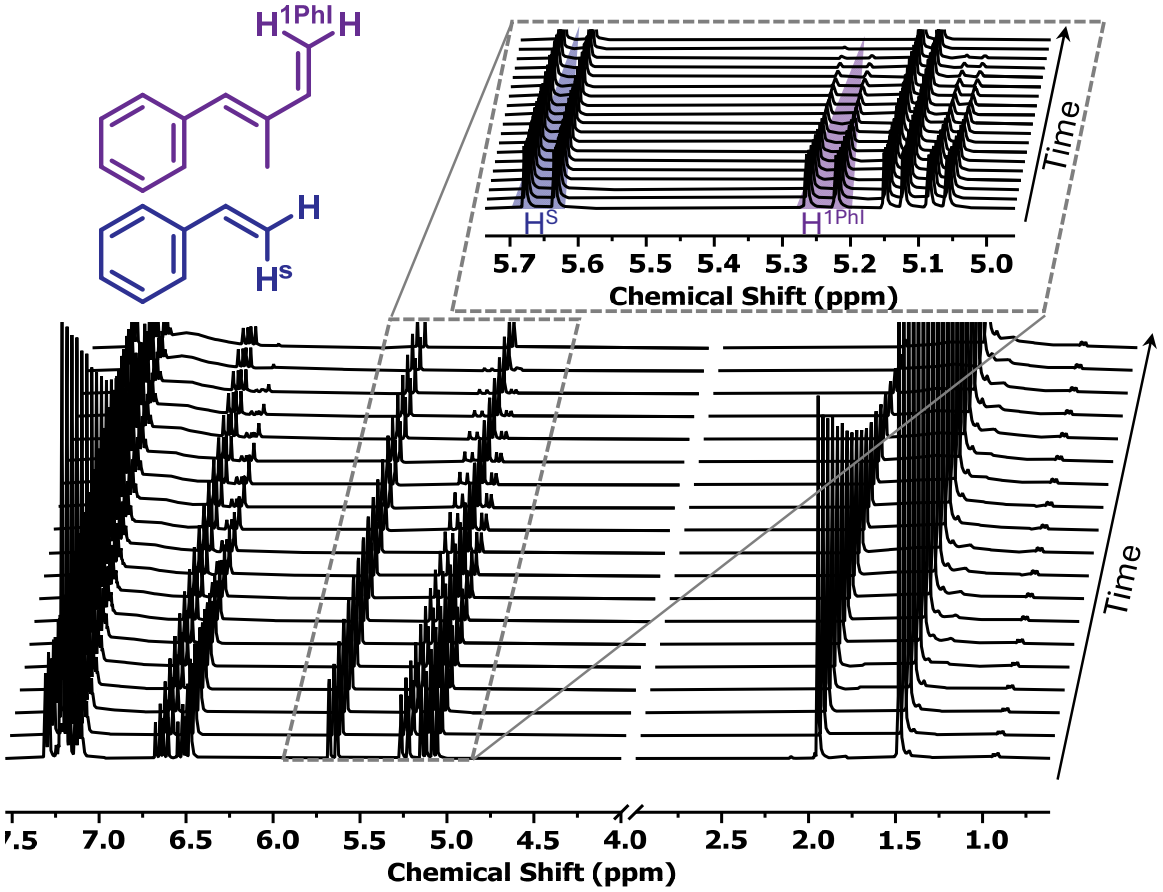


**Figure 5**: Stacked $^{1}$H NMR spectra (400 MHz, $C_6D_{12}$) of the copolymerization of styrene/1PhI as a function of time. The zoomed-in region shows the peaks tracked for the evaluation of the respective comonomer consumption.

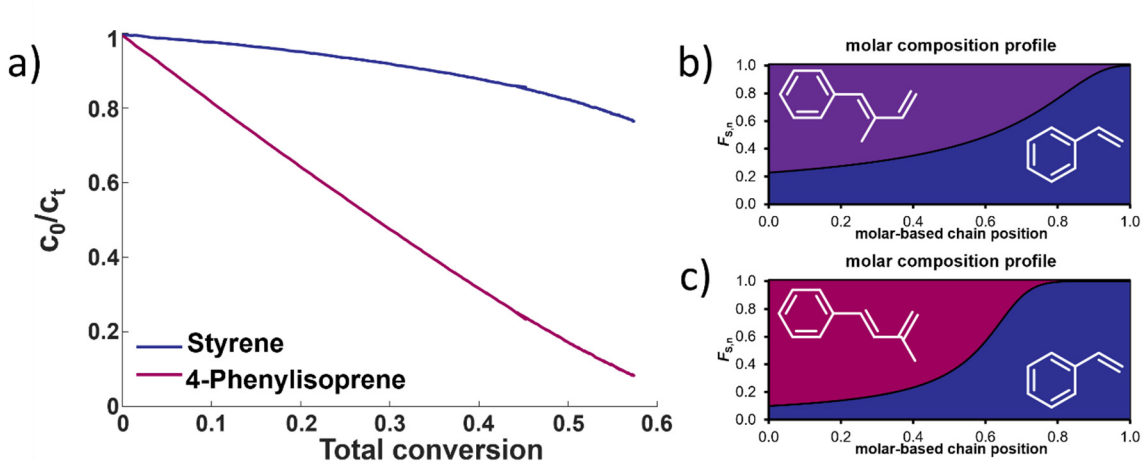


**Figure 6**: a) Obtained monomer conversion for the copolymerization of S and 4PhI. Calculated molar composition profiles of S and b) 1PhI and c) 4PhI, respectively.

**Table 3**: Evaluated reactivity ratios of the copolymerization of Styrene and 1PhI and 4PhI, respectively, evaluated with the Jaacks model. For comparison the reactivity ratios of dienes and styrene are given as well.

| Diene | $r_{diene}$ | $r_S$ |
|---|---|---|
| 1-Phenyl isoprene | 3.38 | 0.30 |
| 4-Phenyl isoprene | 9.20 | 0.109 |
| Isoprene[53] | 11 | 0.049 |
| *β*-Myrcene[54] | 36 | 0.028 |
| *β*-Farnesene[55] | 27 | 0.037 |
| *cis*-Ocimene[51] | 1.015 | 0.985 |
| *trans*-Ocimene[51] | 0.62 | 1.52 |
| Vinylcyclohexene[52] | 0.39 | 2.56 |

## *In Situ* $^1$H NMR kinetics with isoprene as a comonomer

In analogy to the investigation of the copolymerization with styrene we conducted *in situ* $^1$H NMR kinetics also for the copolymerization with isoprene (I). Due to the diene nature of both monomers the respective peaks overlapped, as shown in the stacked spectra as a function of time in **Figures S21** and **S22**. From the obtained data the plots of the comonomer concentrations *vs*. the total conversion and against time are given **Figure 7** and in the Supporting Information. To our surprise the copolymerization of 4PhI with I did not result in plausible results neither for the Jaacks nor the Meyer-Lowry fit, when carried-out in equimolar ratio. Repeating the copolymerization under the same conditions or with a ratio of 70:30 did not improve the given results which are illustrated in the SI. Using the Meyer-Lowry fit, in all cases the reactivity ratios were calculated to exceed 1 as summarized in **Table S3**. In comparison, the obtained data do not reflect the theoretical Jaacks-fit. Nevertheless, the stacked NMR spectra in **Figure S22** indicates a faster consumption of isoprene over 4PhI.

The Jaacks-fit was successfully used for 1PhI and isoprene, confirming the almost ideally random copolymerization with reactivity ratios of $r_I$ = 1.155 and $r_{1PhI}$ = 0.865. The cross-over reaction seems to be independent of the monomer. This might be explained

by the similar electron densities calculated by DFT. A comparison with the known reactivity ratios using myrcene as another diene is given in **Table 4**.

**Table 4**: Reactivity ratios of the copolymerization of isoprene and reported 1,3-dienes.

| Monomer A | $r_A$ | $r_I$ |
|---|---|---|
| 1PhI | 0.865 | 1.155 |
| 4PhI | n.d. | n.d. |
| $\beta$-Myrcene[50] | 4.4 | 0.23 |

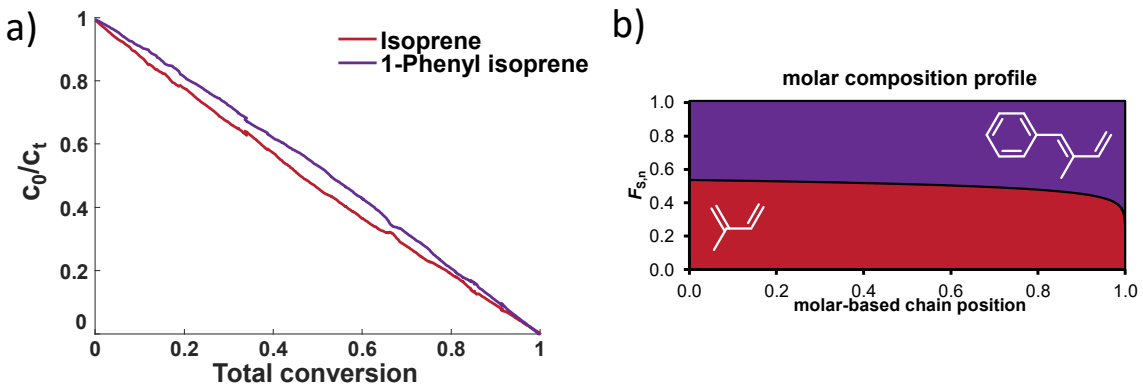


**Figure 7**: Obtained monomer conversion of the copolymerization of I and 1PhI and b) the molar composition profile of the copolymer of I and 1PhI.

## Copolymerization with Isoprene and Styrene

The determined reactivity ratios may lead to unique material properties. Therefore, the copolymerizations were conducted on a larger scale. A rather high molecular weight of 40 kg mol$^{-1}$ was targeted to induce phase separation despite the gradient structure (**Table 5**). In all cases monomodal distributions with low dispersity ($Đ < 1.11$) were obtained. The stacked $^1$H NMR spectra in **Figure S28** show characteristic signals of the monomers. The gradient structure in anionic copolymerization of I and S can be visually tracked by the gradual colour change with monomer conversion. This results in a decreasing concentration of the colorless polydienyl chain ends and gradually increasing concentration of orange polystyryl chain ends. For both copolymerizations with isoprene an immediate coloration of the solution was observed after initiation. Throughout the polymerization no colour change was observed. Therefore, as shown before, a significant number of polyphenylisoprenyl chain ends were present from the beginning. To lend further support to the completely random distribution of 1PhI

throughout the chain when copolymerized with isoprene we observed only one glass transition at 3°C. The copolymer P(I-*co*-4PhI) exhibits a broad softening regime rather than a defined glass transition. Further drying in high-vacuum and the change of the heating rate did not clarify the inflection point. The soft gradients of the styrenic copolymers prevented a phase segregation resulting in merely one $T_g$ >60°C.

**Table 5**: Summarized data of the copolymerization of the phenyl isoprenes with isoprene or styrene as a comonomer.

| Entry | Monomer A | Monomer B | $M_n^{targ}$ [kg mol$^{-1}$] | $M_{n,SEC}$[a] [kg mol$^{-1}$] | $Đ$ | $T_g$ [°C] |
|---|---|---|---|---|---|---|
| 15 | 1PhI | I | 40 | 33.8 | 1.04 | 3 |
| 16 | 1PhI | S | 40 | 35.6 | 1.05 | 67 |
| 17 | 4PhI | I | 40 | 37.9 | 1.09 | − 10 |
| 18 | 4PhI | S | 40 | 29.7 | 1.11 | 61 |

[a] Determined by SEC (THF, PS-calibration, RI-detector)

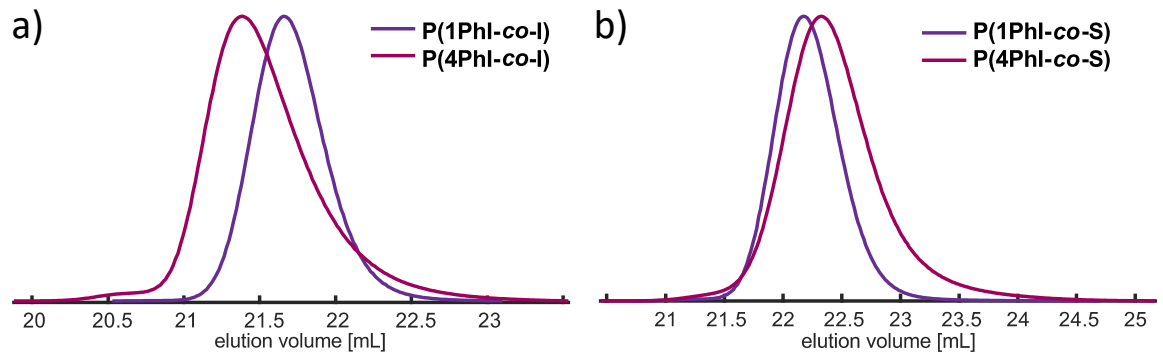


**Figure 8**: SEC-traces of the copolymerization of 1PhI and 4PhI with a) isoprene and b) styrene.

## Cyclization to enhance thermal properties and prepare fluorescence materials

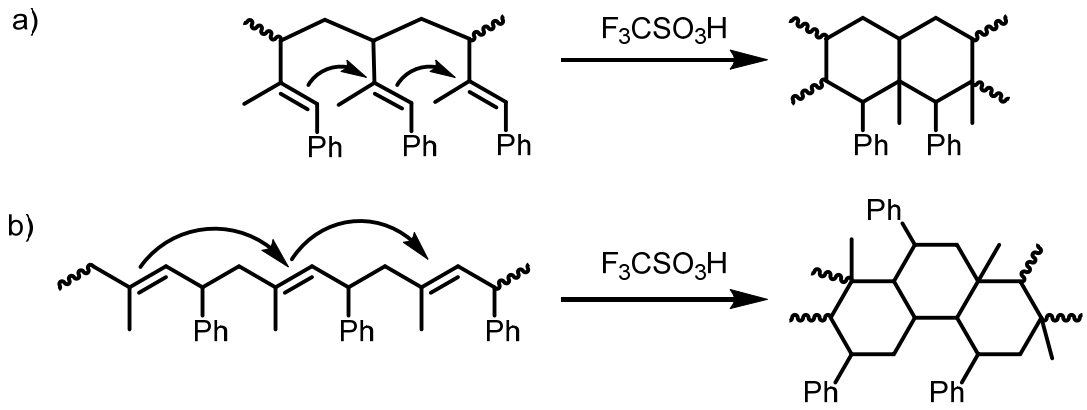


**Scheme 2**: Proposed mechanism for the cyclization of the predominant microstructures of (a) P1PhI and (b) P4PhI in analogy to the literature.[24]

The synthesized homopolymers show lower $T_g$s compared to polystyrene ($T_g$ = 100 °C)[11]. However, since the phenyl rings are all adjacent to double bonds, a cationic cyclization can be performed to alter the thermal properties. As already presented for butadiene-derived structures, the trifluoromethane sulfonic acid-initiated modification influences the thermal properties of these polymers drastically.[16,17,24,29,31,56–58] Consequently, the cyclized P(PhI) structures are expected to exhibit strongly increased rigidity and thus high $T_g$ values. The selected polymers (entries 4 and 8 of **Table 1**) with a targeted molecular weight of 40 kg mol$^{-1}$ were cyclized using $CF_3SO_3H$ in cyclohexane at room temperature (**Scheme 2**). After drying, amber-coloured powders were obtained. Since the samples remained soluble in a variety of solvents after the intramolecular cyclization, they were investigated by SEC and NMR analysis. The SEC traces shown in **Figure 9** and **S33** present the expected shift to higher elution volume.

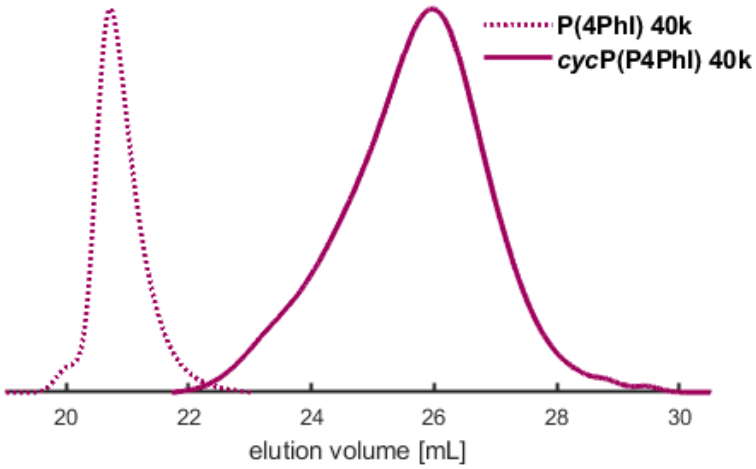


**Figure 9**: SEC-trace of the cyclized P4PhI in comparison to the initial polymer (entry 8, **Table1).**

The SEC traces in **Figure S33** contain retention of the flow rate marker toluene, indicating the presence of a polymer rather than degradation to small molecules. This discovery was described by Han *et al*. and attributed to the compression of the polymer chain and an increase in hydrodynamic radii.[29] DSC measurements verified the expected increase of the $T_g$ values. The cyclization effect on the $T_g$s is stronger for *cyc*P(1PhI), with $T_g$ reaching 180°C after cyclization. The $T_g$ of *cyc*P(4PhI) was determined to 131°C.

**Table 6**: Summarized data of the changed material properties after the cyclization reaction.

| Entry | Entry of Precursor | Polymer | $M_n$[a] [kg mol$^{-1}$] | $Đ$ | $T_g$ [°C] |
|---|---|---|---|---|---|
| 19 | 4 | P1PhI | 3.2 | 1.63 | 187 |
| 20 | 8 | P4PhI | 2.9 | 1.45 | 131 |

[a]Determined by SEC (THF, PS-calibration, RI-detector)

In agreement with the reported *cyc*P(PhB) of Ma and coworkers we observed that the cyclized P(PhI) samples show fluorescence when irradiated with UV light (**Figure 9**).[17] This observation is most likely explained by a clusterization-triggered emission.[59] To quantify the photochemical properties dependent on the presumed clusterization, absorption and emission properties were determined using four different concentrations (2, 0.2, 0.02, 0.002 mg mL$^{-1}$). The main questions raised were, (i)

whether the introduction of the methyl-group leads to a shift of the emission maximum compared to the *cyc*P(PhB) polymer due to different ordering and (ii) whether the differing initial microstructures of P1PhI and P4PhI might result in distinct emission properties. In **Figure 10a)** the emission spectra of the solutions of *cyc*P(P4PhI) with decreasing dilution are shown ($\lambda_{exc}$ = 330 nm). Due to the high optical density and therefore self-absorption, the sample with the highest concentration shows a significantly reduced emission intensity compared to the other concentrations with the same setting. At the same time, the emission maximum shifts from 375 nm to 395 nm (**Table S4**). Contrary to previously reported interpretation clusterization-triggered emission[59], we propose that the emission maximum shifts apparently and its intensity decreases due to inner filter effects with increasing concentration. Going from *cyc*P1PhI to *cyc*P4PhI, a presumed impact of the initial microstructure is observable with the emission maximum shifting from 360 nm to 377 nm (**Figure 10b**). The absolute quantum yields of both samples in the solid state were determined using an integrating sphere. In both cases, the observed self-absorption decreases the overall quantum yield. As it is higher for *cyc*P4PhI (4.1%) than for *cyc*P1PhI (2.9%), *cyc*P4PhI is a more efficient candidate for utilization in organic light-emitting diodes (OLEDs).

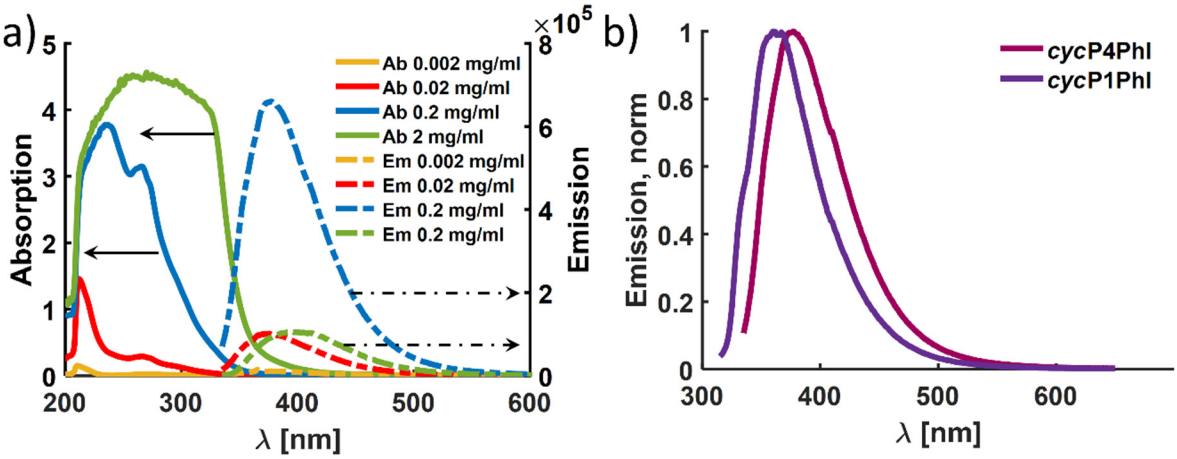


**Figure 10**: a) Absorption (solid) and emission (dashed) spectra of cyclized P4PhI at different concentrations in toluene ($\lambda_{exc}$ = 330 nm) and b) normalized emission spectra of *cyc*P1PhI and *cyc*P4PhI in toluene (c = 0.2 mg mL$^{-1}$, $\lambda_{exc,cycP1PhI}$ = 310 nm and $\lambda_{exc,cycP4PhI}$ = 330 nm).

## Experimental

**Terminology**. (E)-(2-methylbuta-1,3-dien-1-yl)benzene and (E)-(3-methylbuta-1,3-dien-1-yl)benzene are abbreviated as 1PhI and 4PhI respectively.

**Instrumentation.** SEC measurements were performed using an *Agilent 1100 Series* system equipped with a SDV column set from *PSS GmbH* (SDV 103, SDV 105, SDV 106). Tetrahydrofuran (THF) was used as the mobile phase (flow rate 1 mL $min^{-1}$) and as the solvent. Standards of polystyrene and polyisoprene, respectively, were provided by *PSS GmbH* for calibration. Measurements were performed at 30 °C with both RI and UV (275 nm) detector and used toluene as a reference. The data analysis was carried out using *PSS WinGPC UniChrom* (V 8.31, Build 8417) software provided by *PSS Polymer Standards Service GmbH*. NMR spectra were recorded on a *Bruker Advance 400* spectrometer at 400 MHz for $^{1}$H NMR and 103 MHz for $^{13}$C NMR. Determination of glass transition temperatures ($T_g$) was performed on a DSC 250 (TA Instruments) differential scanning calorimeter. Two heating cycles and one cooling cycle were conducted at a rate of 10°C/min. A detailed description of the DSC measurements as well as the description over the photochemical measurements are given in the SI.

**Monomer and Polymer Synthesis**. Both novel monomers 1PhI and 4PhI were synthesized in a one-step Wittig reaction. Alterations of published procedures are given in the SI together with a detailed description of the polymerization conditions.

**Real-Time $^{1}$H NMR.** The measurements were conducted on a 400 MHz *Bruker Advance* spectrometer. All spectra are referencing internally to the residual proton signal of deuterated cyclohexane-$d_{12}$. The polymerization mixtures were prepared in an argon-filled glove box. The monomers and the solvents were purified over calcium hydride and trioctyl aluminum in case of the monomers. The measurements were performed in a conventional NMR tube sealed with a rubber septum.

Prior to initiation, a first spectrum was recorded and equilibrated to a temperature of 25°C. Following the initiation using 30 µL of *sec*-butyl lithium (0.65 M in cyclohexane) the NMR experiment was started in which every 30 s a scan was performed over a period of 6 to 7 hours. By tracking the decrease of the respective monomer signals, determination of the reactivity ratios was achieved, using the NIREVAL software designed in our group.[60]

**Cyclization**. The cyclization reaction was performed according to literature. In a solution of 200 mg P(4PhI) dissolved in 25 mL cyclohexane trifluoro sulfonic acid (0.2 mL, 2 eq regarding the double bonds in every repeating unit) was added. The dark solution was quenched after 1 hour using a 1%w aqueous sodium carbonate solution.

After washing with water, the polymer was precipitated in methanol and dried under vacuum.

## Conclusion

In this work the anionic polymerization of two isoprene derivatives 1-phenyl isoprene and 4-phenyl isoprene was conducted. 4PhI was investigated in more detail than in earlier reports, and 1PhI has not been described to date. The difference in the substitution pattern of the 1,3-dienes was expected to result in different reactivities, as already indicated by their ß-C-shifts and by DFT-calculations. The butyl lithium-initiated polymerizations allowed for the synthesis of polymers with narrow molar mass distributions and good control over the molecular weights in a range of 4.6 to 48.8 kg mol$^{-1}$. $^{1}$H NMR spectroscopy revealed the expected differences in the microstructures. This was further modified using THF, leading to unusual behaviour caused by the attached phenyl ring. Online NMR kinetics uncovered a preference for the phenyl-substituted isoprene over styrene, despite initial theoretical results predicting reduced reactivity of 1PhI. Nevertheless, these predictions are in line with the data obtained from kinetics with isoprene, which showed random incorporation for 1PhI/I. DSC measurements of the respective composition further revealed merely one glass transition. In a post-polymerization cyclization, soluble materials with differing photophysical properties were obtained. The characterization revealed an apparent dependency of the fluorescence maximum on the different microstructures of the starting materials due to self-absorption. As those materials also present an increase in rigidity indicated by the drastic increase of the glass transition, they could be considered as intriguing building block for block copolymers with an intramolecular crosslinked high $T_g$ block.

## References

1 M. Szwarc, *Nature*, 1956, **178**, 1168–1169.

2 A. Hirao, R. Goseki and T. Ishizone, *Macromolecules*, 2014, **47**, 1883–1905.

3 N. Hadjichristidis and A. Hirao, *Anionic Polymerization*, Springer, Tokio, 2015.

4 F. S. Bates, M. A. Hillmyer, T. P. Lodge, C. M. Bates, K. T. Delaney and G. H. Fredrickson, *Science (1979)*, 2012, **336**, 434–440.

5 K. Ntetsikas, V. Ladelta, S. Bhaumik and N. Hadjichristidis, *ACS Polymer Au*, 2022, **3**, 158–181.

6 W. Wang, W. Lu, A. Goodwin, H. Wang, P. Yin, N. G. Kang, K. Hong and J. W. Mays, *Prog Polym Sci*, 2019, **95**, 1–31.

7 US 3265765, 1966.

8 M. Steube, T. Johann, H. Hübner, M. Koch, T. Dinh, M. Gallei, G. Floudas, H. Frey and A. H. E. Müller, *Macromolecules*, 2020, **53**, 5512–5527.

9 D. A. H. Fuchs, H. Hübner, T. Kraus, B. J. Niebuur, M. Gallei, H. Frey and A. H. E. Müller, *Polym Chem*, 2021, **12**, 4632–4642.

10 L. Shaw and L. R. Hutchings, *Polym Chem*, 2020, **11**, 7020–7025.

11 A. H. E. Müller and K. Matyjaszewski, *Controlled and Living Polymerizations: From Mechanisms to Applications*, Wiley-VCH Verlag, Weinheim, 2010.

12 T. Suzuki, Y. Tsuji and Y. Takegami, *Macromolecules*, 1978, **11**, 639–644.

13 T. Suzuki, Y. Tsuji, Y. Takegami and H. J. Harwood, *Macromolecules*, 1979, **12**, 234–239.

14 S. Pragliola, M. Cipriano, A. C. Boccia and P. Longo, *Macromol Rapid Commun*, 2002, **23**, 356–361.

15 J. Lin, F. Wang, C. Zhang, H. Liu, D. Li and X. Zhang, *RSC Adv*, 2021, **11**, 23184–23191.

16 Y. Jiang, X. Kang, Z. Zhang, S. Li and D. Cui, *ACS Catal*, 2020, **10**, 5223–5229.

17 H. Bai, L. Han, W. Li, C. Li, S. Zhang, X. Wang, Y. Yin, H. Yan and H. Ma, *Macromolecules*, 2021, **54**, 1183–1191.

18 Y. Qi, Z. Liu, S. Liu, L. Cui, Q. Dai, J. He, W. Dong and C. Bai, *Catalysts*, 2019, **9**, 97.

19 T. Suzuki, Y. Tsuji, Y. Watanabe and Y. Takegami, *Macromolecules*, 1980, **13**, 849–852.

20 Y. Tsuji, T. Suzuki, Y. Watanabe and Y. Takegami, *Macromolecules*, 1981, **14**, 1194–1196.

21 T. Suzuki, Y. Tsuji, Y. Watanabe and Y. Takegami, *Polym J*, 1979, **11**, 651–660.

22 Y. Tsuji, T. Suzuki, Y. Watanabe and Y. Takegami, *Polym J*, 1981, **13**, 1099–1110.

23 J. M. Widmaier and G. C. Meyer, *Macromolecules*, 1981, **14**, 450–452.

24 Y. Cai, J. Lu, D. Zuo, S. Li, D. Cui, B. Han and W. Yang, *Macromol Rapid Commun*, 2018, **39**, 1800298.

25 R. K. Agnihotri, D. Falcon and E. C. Fredericks, *J Polym Sci A1*, 1972, **10**, 1839–1850.

26 A. Priola, M. Bruzzone, F. Mistrali and S. Cesca, *Angew. Makromol. Chem.*, 1980, **88**, 1–19.

27 R. Y. Asami, K.-I. Hasegawa and T. Onoe, *Polym J*, 1976, **8**, 43–52.

28 J. Lal, *Polymer (Guildf)*, 1998, **39**, 6183–6186.

29 Y. Cai, J. Lu, G. Jing, W. Yang and B. Han, *Macromolecules*, 2017, **50**, 7498–7508.

30 J. Li and J. He, *ACS Macro Lett*, 2015, **4**, 372–376.

31 Q. Lv, C. K. Yu, Q. Yin, J. Lu and B. Han, *Journal of Macromolecular Science, Part A*, 2020, **57**, 388–397.

32 T. Ishizone, A. Hirao and S. Nakahama, *Macromolecules*, 1993, **26**, 6964–6975.

33 A. E. Reed, R. B. Weinstock and F. Weinhold, *J Chem Phys*, 1998, **83**, 735.

34 T. Y. Nikolaienko, L. A. Bulavin and D. M. Hovorun, *Comput Theor Chem*, 2014, **1050**, 15–22.

35 H. Hsieh and R. Quirk, *Anionic polymerization: principles and practical applications*, Dekker, New York, 1996.

36 S. Uchida, K. Togii, S. Miyai, R. Goseki and T. Ishizone, *Macromolecules*, 2020, **53**, 10107–10116.

37 A. Forens, K. Roos, C. Dire, B. Gadenne and S. Carlotti, *Polymer (Guildf)*, 2018, **153**, 103–122.

38 T. A. Antkowiak, A. E. Oberster, A. F. Halasa and D. P. Tate, *J Polym Sci A1*, 1972, **10**, 1319–1334.

39 W. Gebert, J. Hinz and H. Sinn, *Makromol. Chem.*, 1971, **144**, 97–115.

40 D. J. Worsfold and S. Bywater, *Macromolecules*, 1978, **11**, 582–586.

41 H. Hsieh, D. J. Kelley and A. V. Tobolsky, *J. Polym. Sci.*, 1957, **26**, 240–242.

42 C. A. Uraneck, *J Polym Sci A1*, 1971, **9**, 2273–2281.

43 S. Bywater and D. J. Worsfold, *Can J Chem*, 1962, **40**, 1564–1570.

44 M. Morton and L. J. Fetters, *J Polym Sci A*, 1964, **2**, 3311–3326.

45 J. Bareuther, M. Plank, B. Kuttich, T. Kraus, H. Frey, M. Gallei, J. Bareuther, M. Plank, B. Kuttich, T. Kraus, H. Frey and M. Gallei, *Macromol Rapid Commun*, 2021, **42**, 2000513.

46 A. Garton, R. P. Chaplint and S. Bywater, *Eur Polym J*, 1976, **12**, 697–700.

47 J. Kleinheider, T. Schrimpf, R. Scheel, T. Mairath, A. Hermann, K. Knepper and C. Strohmann, *Chemistry - A European Journal*, 2024, **30**, e202304226.

48 A. Natalello, M. Werre, A. Alkan and H. Frey, *Macromolecules*, 2013, **46**, 8467–8471.

49 T. Johann, D. Leibig, E. Grune, A. H. E. Müller and H. Frey, *Macromolecules*, 2019, **52**, 4545–4554.

50 V. Jaacks, *Makromol. Chem.*, 1972, **161**, 161–172.

51 S. P. Wadgaonkar, M. Wagner, L. A. Baptista, R. Cortes-Huerto, H. Frey and A. H. E. Müller, *Macromolecules*, 2023, **56**, 664–677.

52 C. Hahn, M. Rauschenbach and H. Frey, *Angew. Chem. Int. Ed.*, 2023, **62**, e202302907.

53 E. Grune, T. Johann, M. Appold, C. Wahlen, J. Blankenburg, D. Leibig, A. H. E. Müller, M. Gallei and H. Frey, *Macromolecules*, 2018, **51**, 3527–3537.

54 E. Grune, J. Bareuther, J. Blankenburg, M. Appold, L. Shaw, A. H. E. Müller, G. Floudas, L. R. Hutchings, M. Gallei and H. Frey, *Polym Chem*, 2019, **10**, 1213–1220.

55 C. Wahlen, J. Blankenburg, P. Von Tiedemann, J. Ewald, P. Sajkiewicz, A. H. E. Müller, G. Floudas and H. Frey, *Macromolecules*, 2020, **53**, 10397–10408.

56 K. Liu, F. Zhang, M. Sun, F. Xie, S. Ying, Z. Yang, C. Zhou, J. Xia, A. Li, K. Liu, F. Zhang, M. Sun, F. Xie, S. Ying, Z. Yang, C. Zhou, J. Xia and A. Li, *Macromol Chem Phys*, 2020, **221**, 2000161.

57 A. Nakahara, K. Satoh and M. Kamigaito, *Macromolecules*, 2009, **42**, 620–625.

58 A. Nakahara, K. Satoh, H. Saito and M. Kamigaito, *J Polym Sci A Polym Chem*, 2012, **50**, 1298–1307.

59 H. Zhang, Z. Zhao, P. R. McGonigal, R. Ye, S. Liu, J. W. Y. Lam, R. T. K. Kwok, W. Z. Yuan, J. Xie, A. L. Rogach and B. Z. Tang, *Materials Today*, 2020, **32**, 275–292.

60 M. Steube, T. Johann, M. Plank, S. Tjaberings, A. H. Gröschel, M. Gallei, H. Frey and A. H. E. Müller, *Macromolecules*, 2019, **52**, 9299–9310.

# Supporting Information

## Instrumentation

### Gel Permeation Chromatography (GPC)

GPC analysis was performed on an Agilent 1260 Infinity II instrument containing a MZ-GEL-DS plus $10^5/10^3/100$ Å column set from *MZ-Analysetechnik* (Mainz, Germany). All detections were performed by a RI detector (Agilent G1362A). THF was the eluent, and the injection volume was 100 µL. All measurements were measured at 20°C using a flow rate of 1 mL/min. The analysis was calibrated on a toluene standard. The chosen polystyrene and polyisoprene standards are purchased from *PSS Polymer Standard Service GmbH* (Mainz, Germany).

### Nuclear Magnetic Resonance (NMR) spectroscopy

All NMR spectra ($^1$H, $^{13}$C, $^1$H-$^1$H COSY, $^1$H-$^{13}$C HSQC, $^1$H-$^{13}$C HMBC, and real-time kinetics) were recorded on a *Bruker Advance 400* spectrometer equipped with a 5 mm BBFO-SmartProbe with z gradient and ATM as well as a SampleXPress 60 sample changer. Every spectrum was referenced internally to the assigned proton signal of the used deuterated solvent ($CDCl_3$ and $C_6D_{12}$). The measured spectra were evaluated using *MestReNova* 14.2.0 from *Mestrelab Research S.L.* (Santiago de Compostela, Spain).

### Differential Scanning Chromatography (DSC)

The thermal analysis was conducted using a DSC 250 from *TA Instruments* with an RCS 90 compressor calibrated with an indium and *n*-octane standard. A minimum of 5 mg polymer was weighed in a pan and subsequently sealed. Firstly, to remove any thermal history the samples were heated before the actual analysis was performed using the second heating ramp using a rate of 10 K/min. All measurements were performed under a nitrogen atmosphere. The different temperature ranges are summarized in the following **Table S1**.

**Table S1**: Temperature ranges of the DSC analysis depending on the polymer entry.

| Entries | $T_{min}$ °C | $T_{max}$ °C |
|---|---|---|
| 1 – 14 | 0 | 120 |
| 15 – 18 | − 90 | 120 |
| 19 – 20 | 0 | 250 |

**Density functional theory (DFT)** calculations were performed using the ORCA 4.2.1 software on the MOGON II supercomputer, located at the high-performance computing center of Johannes Gutenberg University Mainz. The BXLYP hybrid density functionals were selected due to the availability of the calculation of the analytical Hessian matrix. Additionally, the D3BJ atom-pairwise dispersion correction was applied to the DFT energy, with Becke-Johnson damping. The combination of the Grid6 integration grid and TightSCF convergence criteria was chosen to ensure accurate single-point energy calculations, while the def2-TZVP valence triple-zeta basis set was employed for all calculations. Geometry optimization was performed using the RIJCOSX approximation and a GridX7 integration grid, providing significant acceleration. Geometrical Counterpoise Correction (gCP) was applied to mitigate artificial overbinding effects. As the experiments involved the use of cyclohexane, with its low dielectric strength ($\varepsilon_r = 2.02$), which offers only a negligible solvent effect, solvation effects were not considered. IboView18 was utilized for the visualization of molecular geometries.

**UV/Vis absorption spectra in solution** were recorded on a Jasco V770 spectrometer using 1.0 cm quartz cells. In advance, three solutions were prepared with increasing dilution. 40 mg of the cyclized sample were dissolved in 20 mL dry toluene to obtain a concentration of 2 mg $mL^{-1}$. A dilution series yielded the solutions with concentrations of 0.2 and 0.02 mg $mL^{-1}$.

**Emission spectra (solution samples)** were recorded with an FS5 spectrometer from Edinburgh Instruments equipped with the photomultiplier detector R928P (200 – 870 nm). A xenon arc lamp (150 W) was used for excitation. The same solutions were used for the UV/Vis absorption experiments.

**Emission spectra (powder samples)** were recorded with an FLS1000 spectrometer from Edinburgh Instruments equipped with the cooled photomultiplier detector N-G11

PMT-980 (250 – 980 m). A xenon arc lamp Xe2 (450 W) was used for excitation. Absolute luminescence quantum yields $\Phi$ were determined using an integrating sphere from Edinburgh Instruments. Relative uncertainty of $\Phi$ is estimated to be ±20%. The samples were dried under vaccuo before measurements. The powder was placed on the Teflon sample holder to give an evenly distribution.

## Experimental section

**Reagents**. Chemicals and solvents were purchased from commercial suppliers (*Alfa Aesar*, *Sigma Aldrich*, *Carbolution Chemicals GmbH*, *Acros Organics*, *TCI* and *Fisher Scientific*). Both Chloroform-d and cyclohexane-$d_{12}$ were purchased from *Deutero GmbH*. Cyclohexane and THF were dried prior to use. THF was purified using *sec*-butyl lithium and 1,1-diphenylethylene (DPE) as an indicator. Cyclohexane was dried using sodium and benzophenone as an indicator.

**Monomer synthesis**:

Both monomers were synthesized *via* Wittig-reaction starting from the respective carbonyl moiety.

*Synthesis of E-(2-Methylbuta-1,3-dien-1-yl) benzene (1-Phenyl isoprene, 1PhI)*: In a flame dried 1 L-Schlenk flask methyltriphenylphosphonium bromide (128 g, 0.36 mol, 1.2 eq) was suspended in dry THF (600 mL). 40 g (0.36 mol, 1.2 eq) potassium *tert*-butoxide was added slowly to the solution to form the corresponding ylide. After 1 hour, the carbonyl reagent (44 g, 0.3 mol, 1 eq) was added and the solution was stirred for 14 hours at room temperature. After completion, the reaction mixture, first diluted with 50 mL *n*-pentane, was concentrated under reduced pressure. The precipitated byproducts were removed from the solution *via* centrifugation. Subsequently, the solvents were removed by distillation under reduced pressure. First, the crude product crude product was removed from the TPPO by distillation in high vacuum ($1.0 \times 10^{-3}$ mbar, 150 °C oil bath temperature). Subsequently, a fractionated distillation was performed to receive the pure diene under high vacuum ($1.0 \times 10^{-3}$ mbar, $T_b$ = 36 °C).

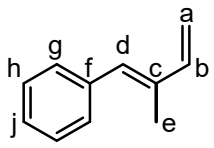


1PhI

**$^1$H NMR** (400 MHz, $CDCl_3$) δ(ppm) = 7.46 – 7.28 (m, H-**g,h**, 4H), 7.34 – 7.24 (m, H-**j**, 1H), 6.69 – 6.53 (m, H-**b,d**, 2H), 5.43 – 5.20 (m, H-**a**, 2H), 2.07 (d, H-**e**, 3H).

**$^{13}$C NMR** (101 MHz, $CDCl_3$) δ(ppm) = 141.94 (H-**D**), 137.79 (H-**F**), 136.03 (H-**C**), 131.71 (H-**B**), 129.27 (H-**H**), 128.18 (H-**G**), 126.67 (H-**J**), 113.02 (H-**A**), 13.22 (H-**E**).

$T_b$ = 104°C (40 mbar)

*Synthesis of (E)-(3-methylbuta-1,3-dien-1-yl) benzene (4-Phenyl isoprene, 4PhI)*: In a flame dried 1 L-Schlenk flask methyltriphenylphosphonium bromide (128 g, 0.36 mol, 1.2 eq) was suspended in dry THF (600 mL). 196 mL of a 2 M solution of sodium hexamethyldisiloxyamine (NaHMDS) in THF was added slowly to the solution to form the corresponding ylide. After 1 hour, the carbonyl reagent (44 g, 0.3 mol, 1 eq) was added and the solution was stirred for 14 h at 50 °C. After completion, the reaction mixture, first diluted with 50 mL *n*-pentane, was concentrated under reduced pressure. The precipitated byproducts were removed from the solution *via* centrifugation. Subsequently, the solvents were removed by distillation under reduced pressure. First, the crude product was removed from the TPPO by distillation in high vacuum ($1.0 \times 10^{-3}$ mbar, 150 °C oil bath temperature). Subsequently, a fractionated distillation was performed to receive the pure diene under high vacuum ($1.0 \times 10^{-3}$ mbar, $T_b$ = 36 °C).

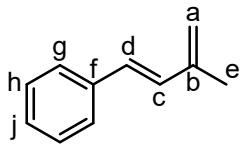


4PhI

**$^1$H NMR** (400 MHz, $CDCl_3$) δ (ppm) = 7.56 – 7.49 (m, H-**g**, 2H), 7.46 – 7.37 (m, H-**h**, 2H), 7.36 – 7.26 (m, H-**j**, 1H), 6.99 (d, J = 16.1 Hz, H-**d**, 1H), 6.64 (d, J = 16.1 Hz, H-**c**, 1H), 5.25 – 5.15 (m, H-**a**, 2H), 2.08 (dd, J = 1.5, 0.8 Hz, H-**e**, 3H).

**$^{13}$C NMR** (101 MHz, $CDCl_3$) δ(ppm) = 142.12 (H-**B**), 137.48 (H-**F**), 131.76 (H-**D**), 128.74 (H-**C,H**), 127.51 (H-**J**), 126.57 (H-**G**), 117.45 (H-**A**), 18.68 (H-**E**).

$T_m$ = 33 °C $T_b$ = 47 °C ($1 \times 10^{-3}$ mbar)

**General procedure for the carbanionic polymer synthesis:**

*Homopolymerization in CHx:* Residual protonic traces of all monomers were eliminated by drying over calcium hydride and trioctylaluminium. Subsequently, the monomers were distilled into an anionic flask. In an argon-flooded glove box the monomers and solvents were volumetrically added into the reaction vessel. Due to the crystallin nature of 4PhI this monomer was measured gravimetrically. The polymerizations were initiated by the addition of *sec*-butyl lithium into the vigorous stirred solution. After stirring overnight, the polymerizations were terminated outside of the glove box by addition of degassed methanol. Precipitation of the polymer solution was performed in a 50:50 solution of methanol and 2-propanol. After drying under reduced pressure, the samples were stored under absence of light and air at − 20 °C.

*Homopolymerization in THF:* Deviating from the procedure described above the prepared solution were dissolved in an anionic flask and later transferred outside the glove box. In a liquid $N_2$/ethanol cooling bath, the reaction flask was cooled to − 78 °C. Under argon, the polymerization was initiated *via sec*-butyl lithium using a syringe. After 4 hours, the termination was performed through addition of methanol. The polymer was precipitated into a 50:50 solution of methanol and 2-propanol. The polymers were dried under vacuo and stored under absence of light and air at − 20 °C.

# NMR Analysis

## NMR characterization of monomers 1PhI and 4PhI

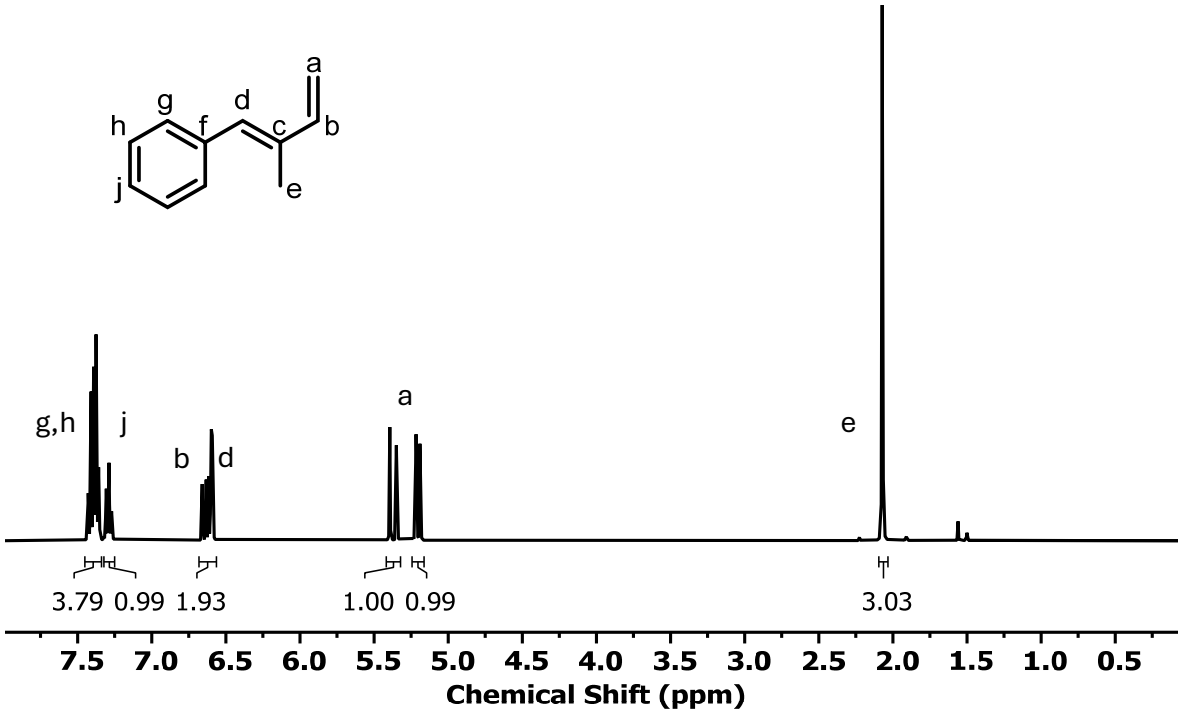


**Figure S1**: $^{1}H$ NMR spectrum (400 MHz, $CDCl_3$) of 1PhI

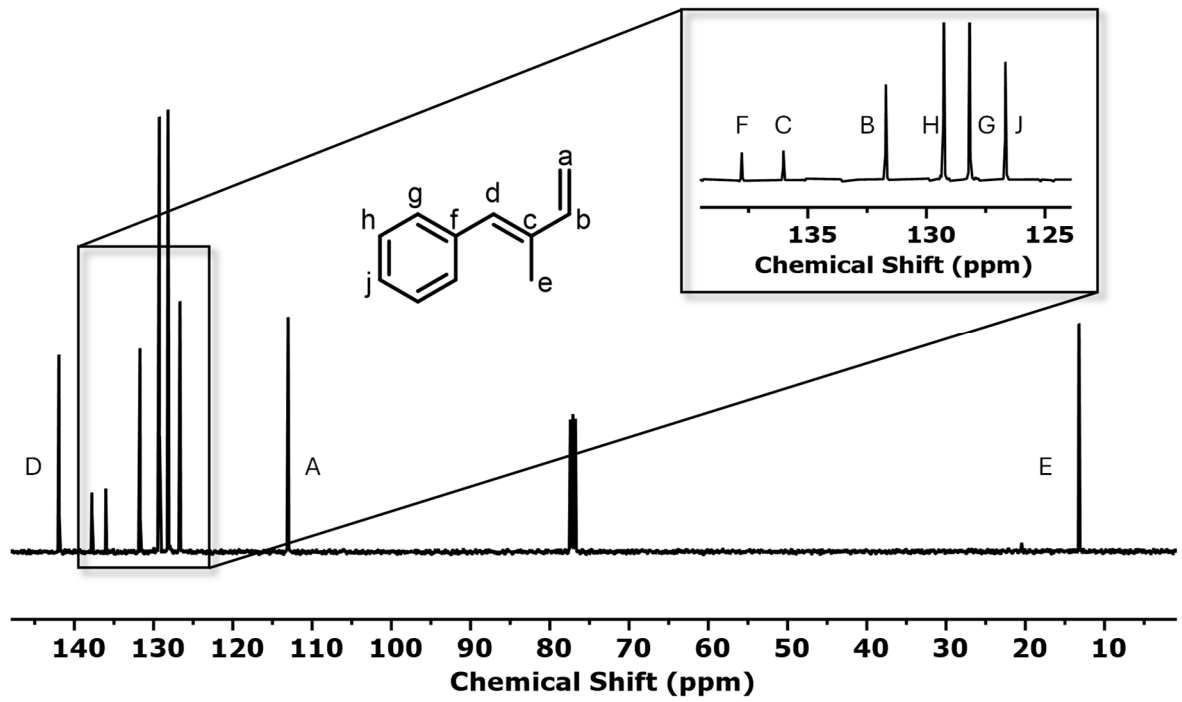


**Figure S2**: $^{13}C$ NMR spectrum (103 MHz, $CDCl_3$) of 1PhI.

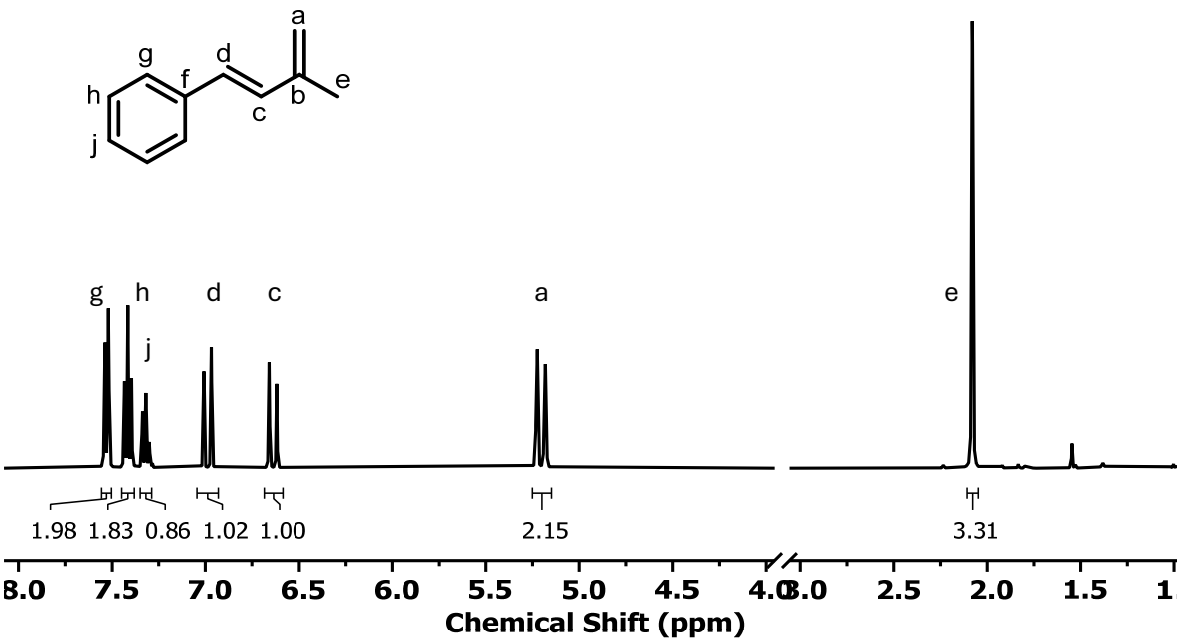


**Figure S3**: $^{1}$H NMR spectrum (400 MHz, $CDCl_3$) of 4PhI

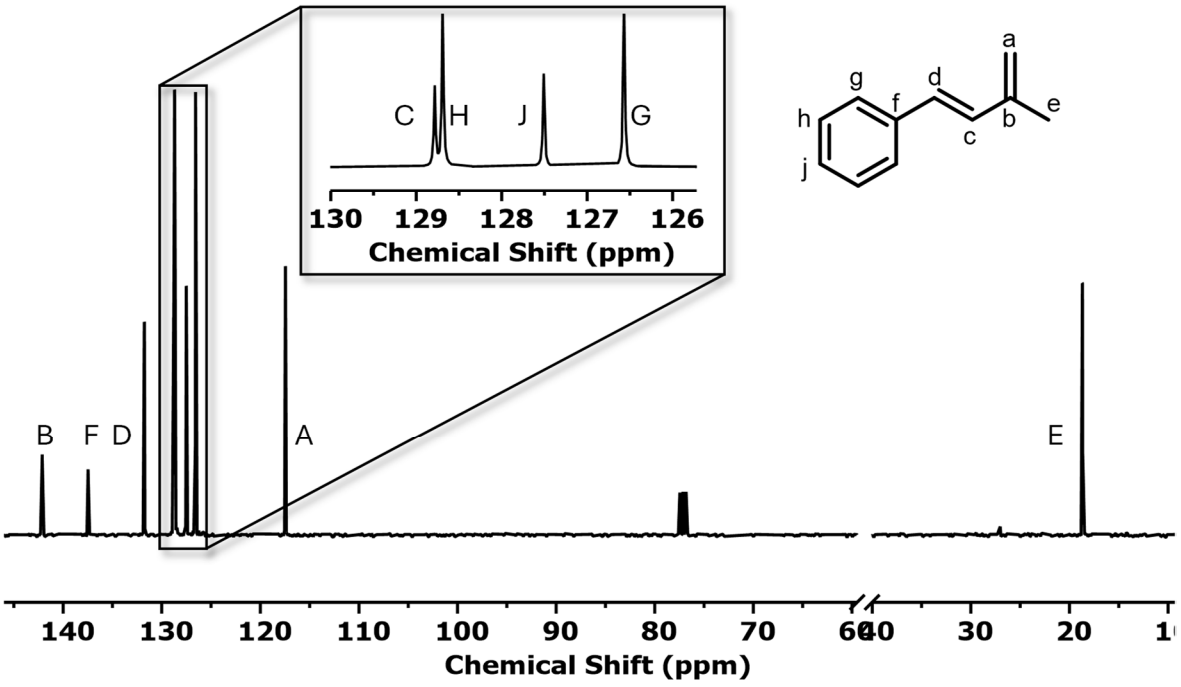


**Figure S4**: $^{13}$C NMR spectrum (103 MHz, $CDCl_3$) of 4PhI.

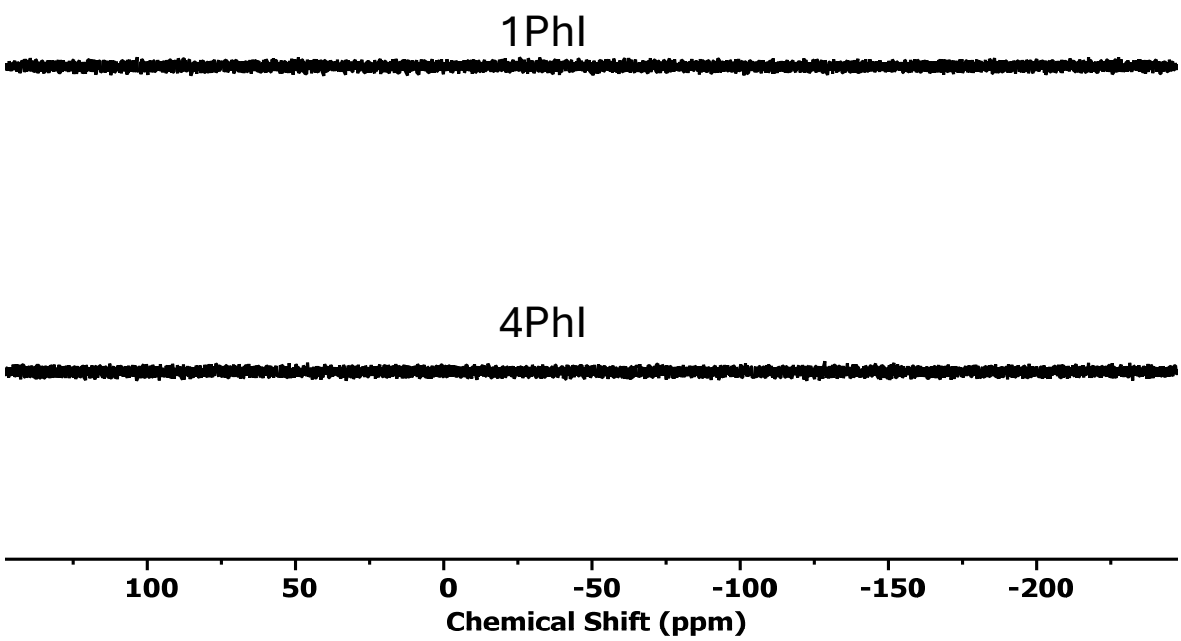


**Figure S5**: $^{31}P$ NMR spectra (162 MHz, $CDCl_3$) of 1PhI and 4PhI.

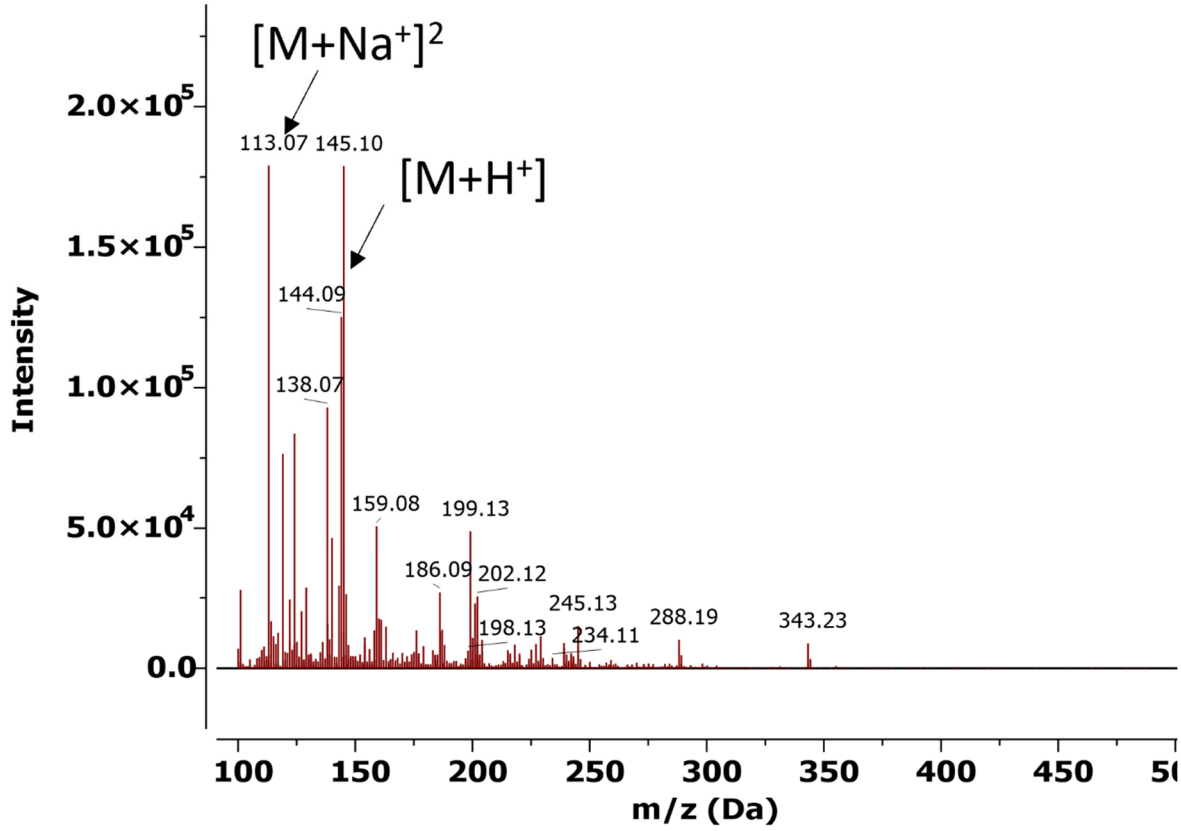


**Figure S6**: Mass spectrum of 1PhI recorded on a G6545A Q-ToF (Agilent GmbH, Waldbronn) *via* atmospheric pressure chemical ionization (APCI). This experiment was repeated twice. Lower purity was traced back to the literature known suppression of adduct ions by acetonitrile.[1]

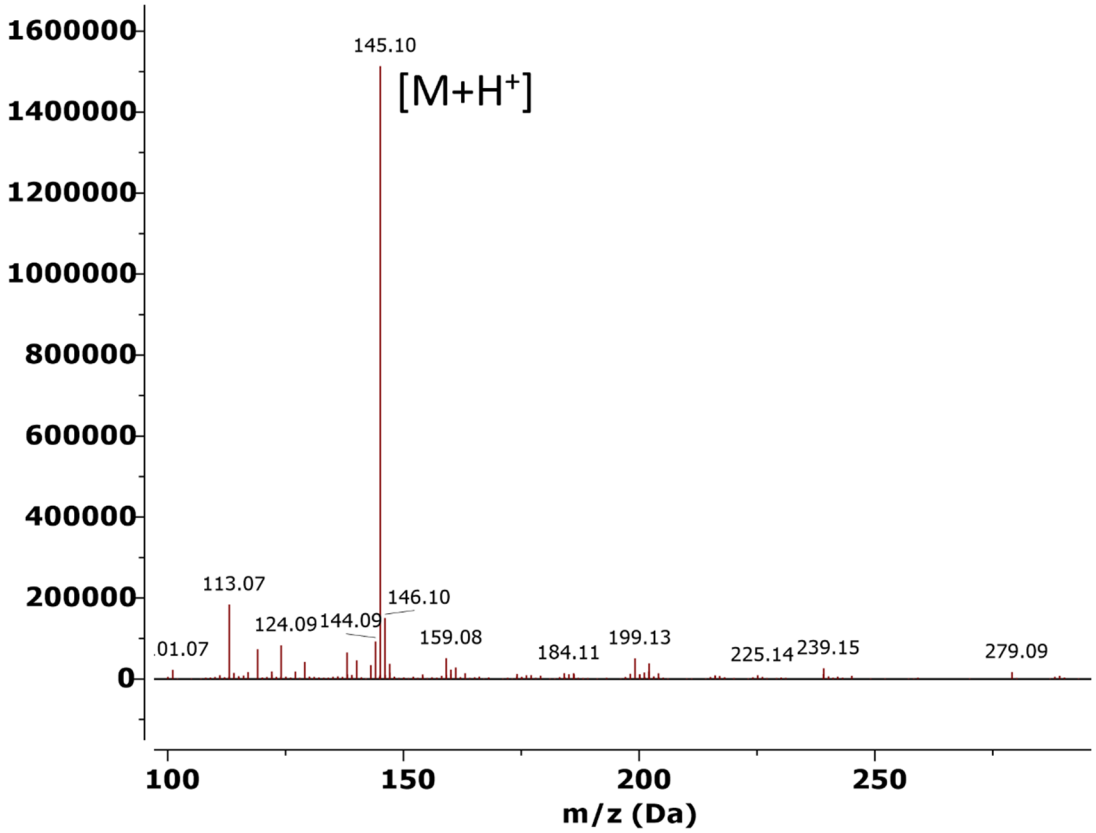


**Figure S7**: Mass spectrum of 4PhI recorded on a G6545A Q-ToF (Agilent GmbH, Waldbronn) *via* atmospheric pressure chemical ionization (APCI).

## NMR characterization of the homopolymers P(1PhI) and P(4PhI)

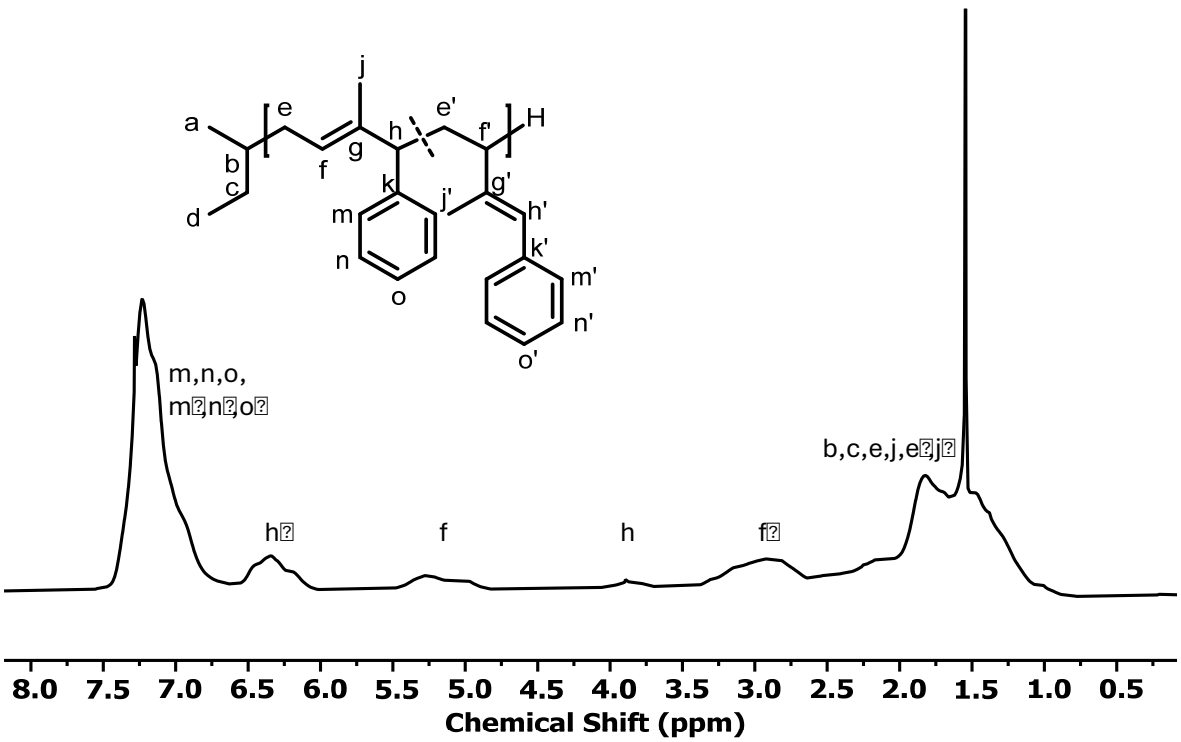


**Figure S8**: $^{1}H$ NMR spectrum (400 MHz, $CDCl_3$) of P(1PhI)

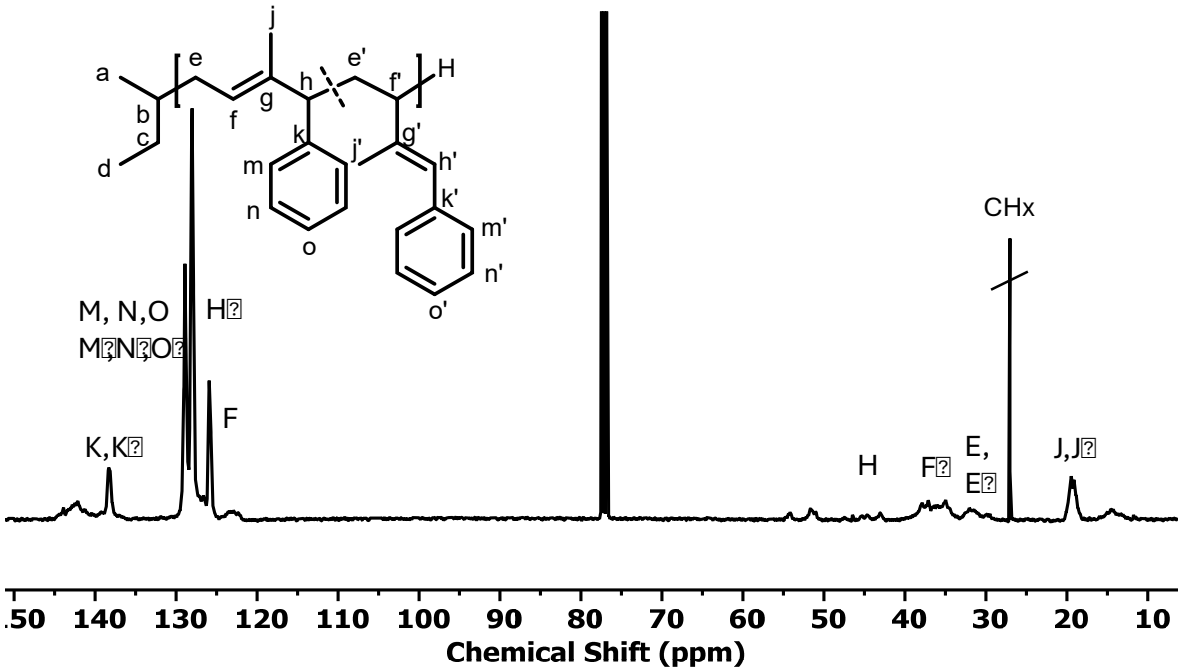


**Figure S9**: $^{13}C$ NMR spectrum (103 MHz, $CDCl_3$) of P(1PhI).

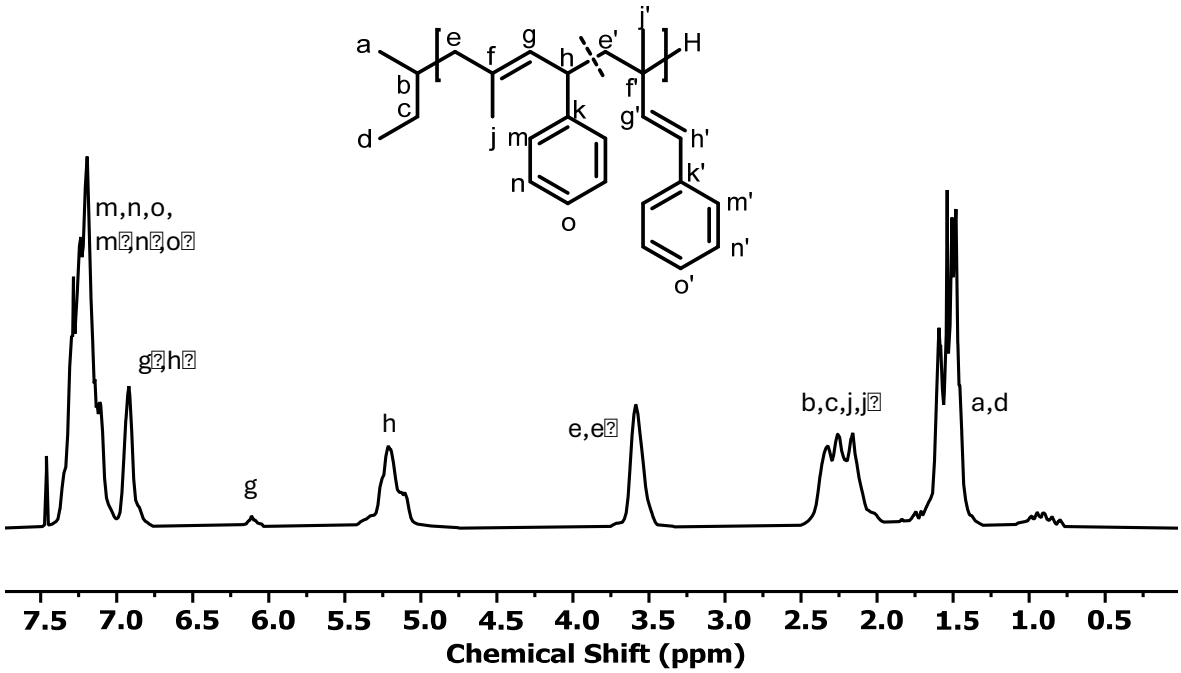


**Figure S10**: $^{1}H$ NMR spectrum (400 MHz, $CDCl_3$) of P(4PhI)

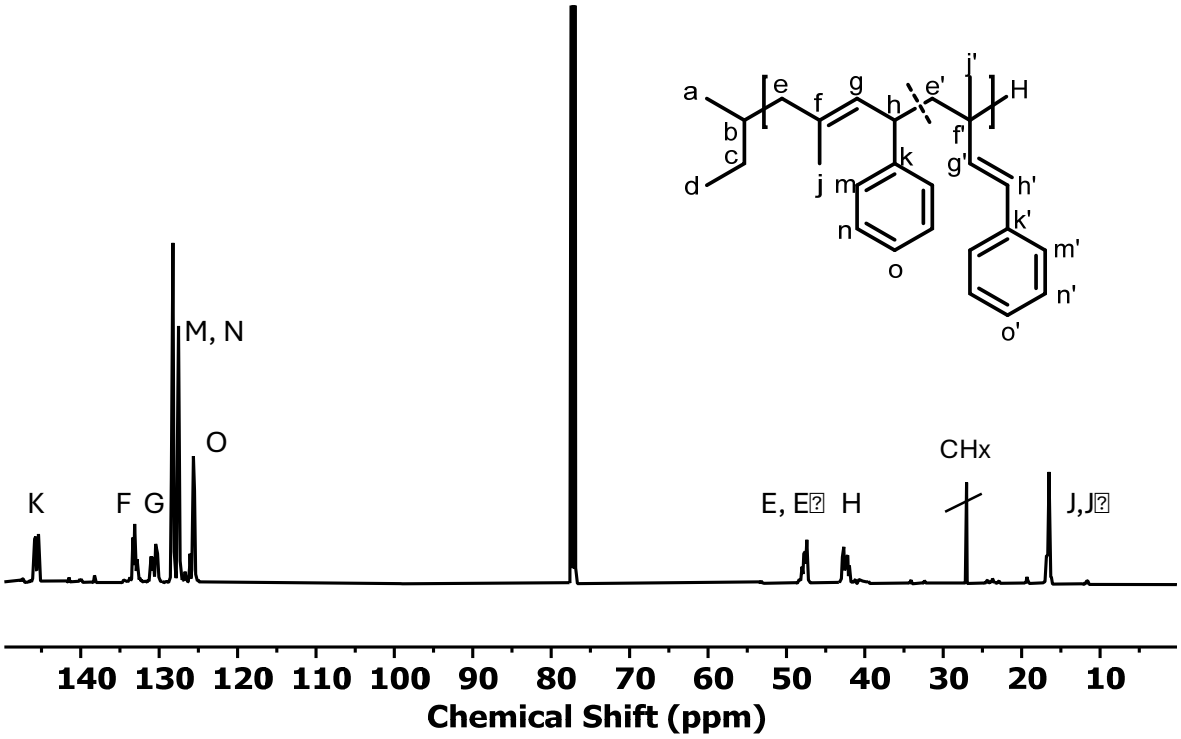


**Figure S11**: $^{13}C$ NMR spectrum (103 MHz, $CDCl_3$) of P(4PhI).

## Thermal Analysis of homopolymers

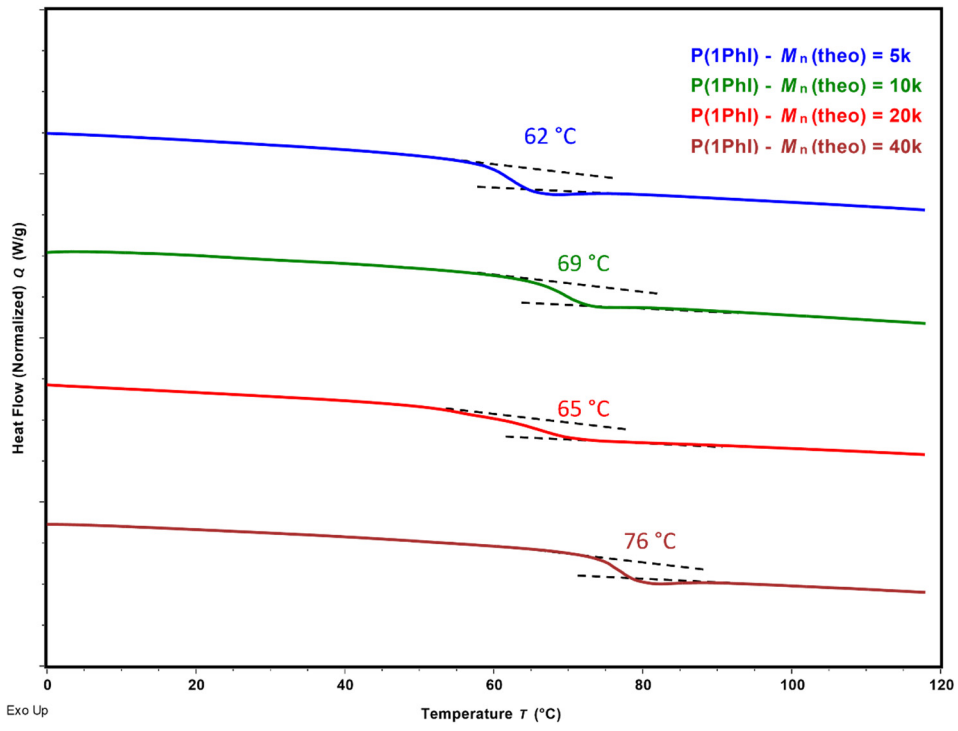


**Figure S12**:DSC curves for the homopolymers P(1PhI) with increasing $M_{n,targ}$ of 5 to 40 kg mol$^{-1}$ (**Table 1**, entries 1-4).

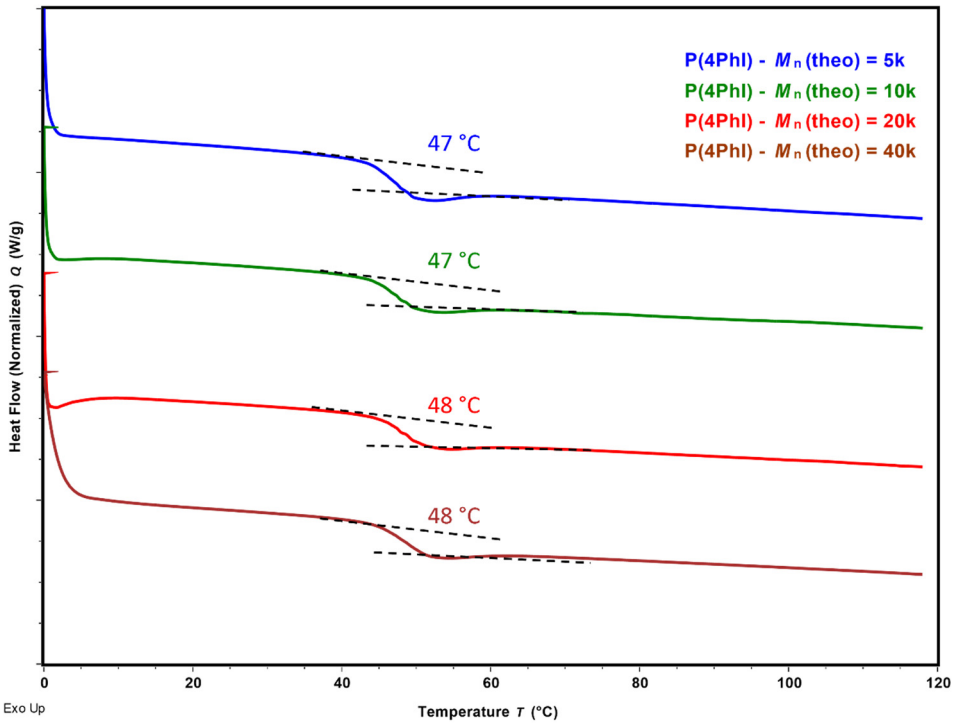


**Figure S13**: DSC curves for the homopolymers P(4PhI) with increasing $M_{n,targ}$ of 5 to 40 kg mol$^{-1}$ (**Table 1**, entries 5 – 8).

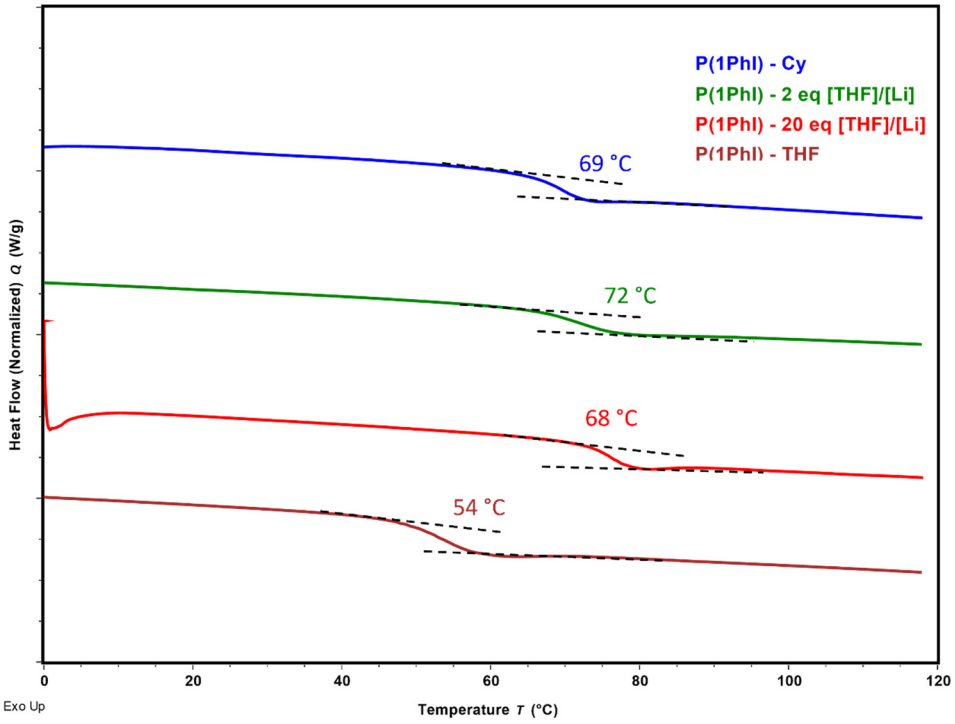


**Figure S14**: DSC curves for the homopolymers P(1PhI) polymerized in dependency of modifier concentration (**Table 2**, entries 1, 9 – 11).

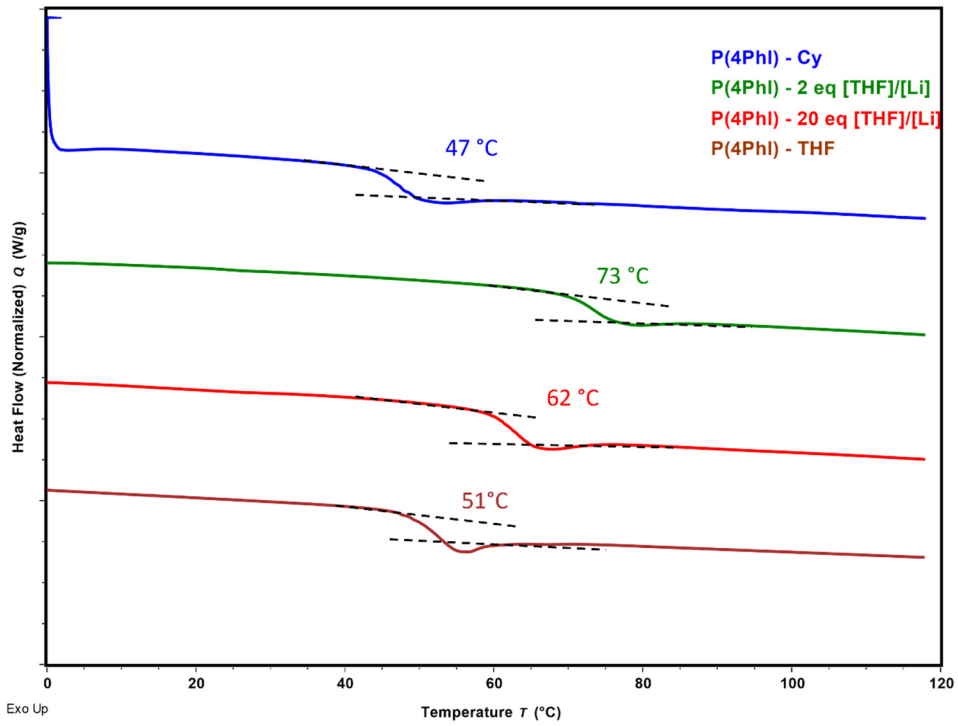


**Figure S15**: DSC curves for the homopolymers P(4PhI) polymerized in dependency of modifier concentration (**Table 2**, entries 5,12 – 14).

## GPC Analysis

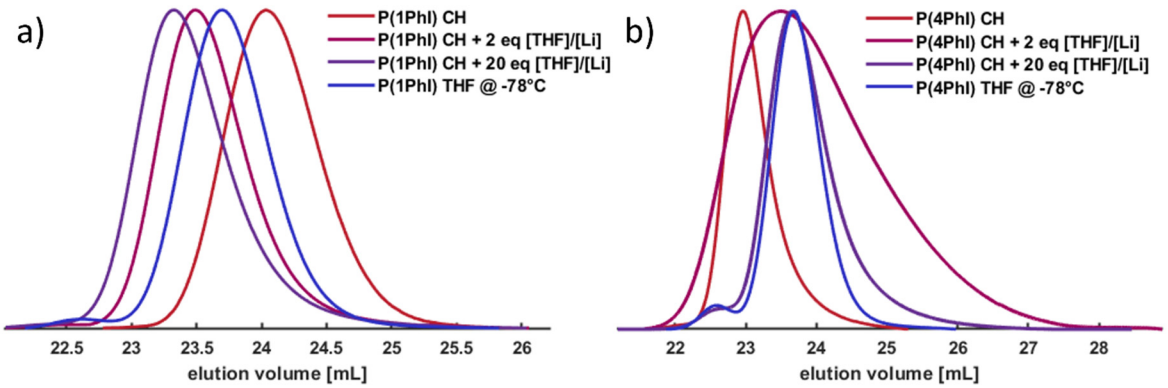


**Figure S16**: GPC traces of the polymerizations of a) 1PhI and b) 4PhI respectively containing increasing amount of THF in the polymerizations.

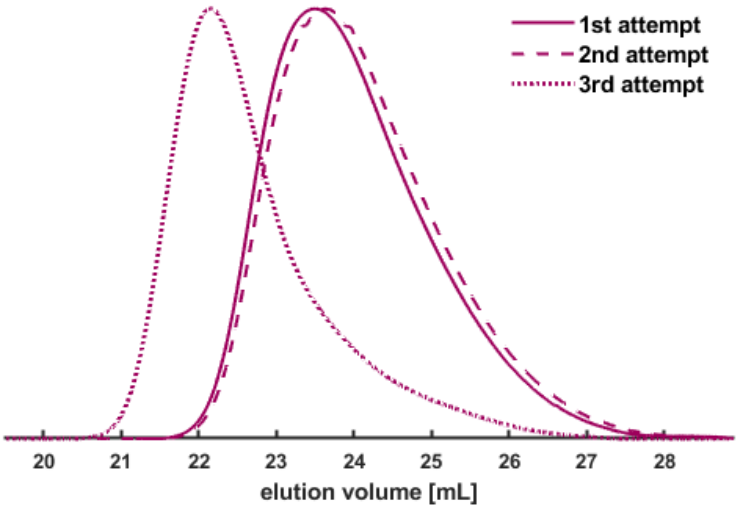


**Figure S17**: Broad GPC traces of all three attempts for the polymerization of 4PhI in the presence of 2 eq [THF]/[Li].

## *In situ* $^1$H NMR kinetics of copolymerization

**Table S2**: Evaluated reactivity ratios of the copolymerization of styrene and 1PhI and 4PhI, respectively, using the Meyer-Lowry model.

| Diene | $r_{diene}$ | $r_S$ |
|---|---|---|
| 1-Phenyl isoprene | 2.37 | 0.10 |
| 4-Phenyl isoprene | 9.1 | 0.101 |

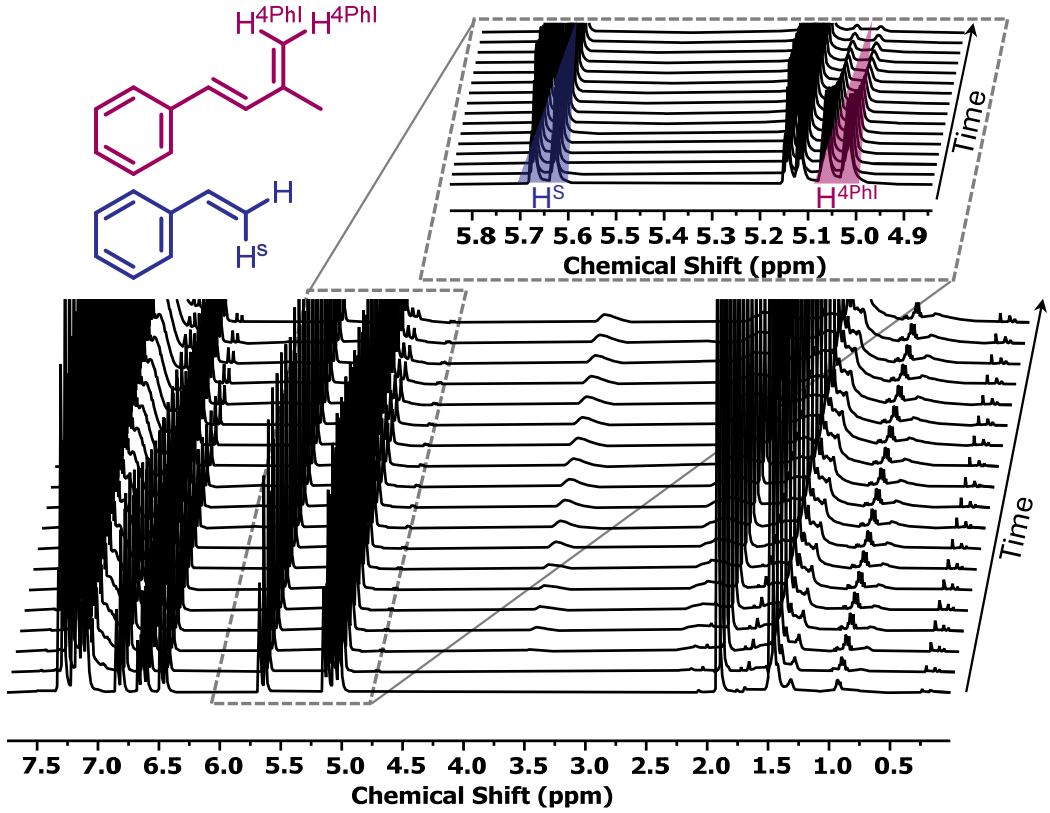


**Figure S18**: Stacked $^{1}$H NMR spectra of the *in situ* kinetics of styrene and 4PhI and an expansion of the traced monomer signals.

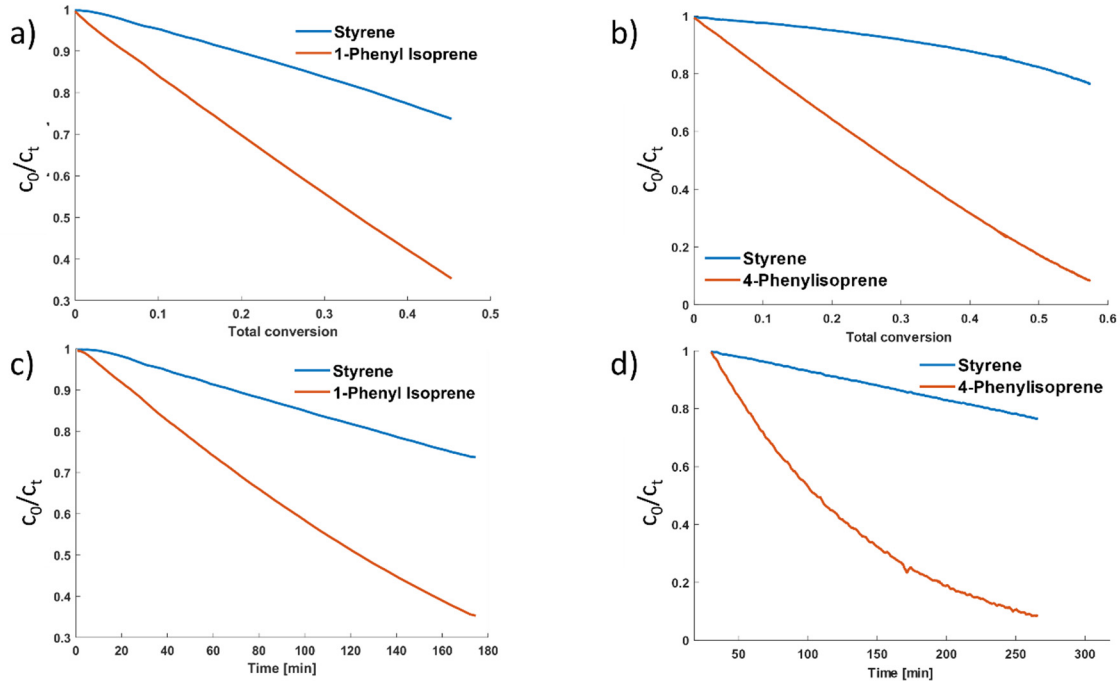


**Figure S19**: Individual monomer conversion of the copolymerization with styrene and a) 1PhI and b) 4PhI as well as the time-depended monomer conversion of the copolymerization using c) 1PhI and d) 4PhI.

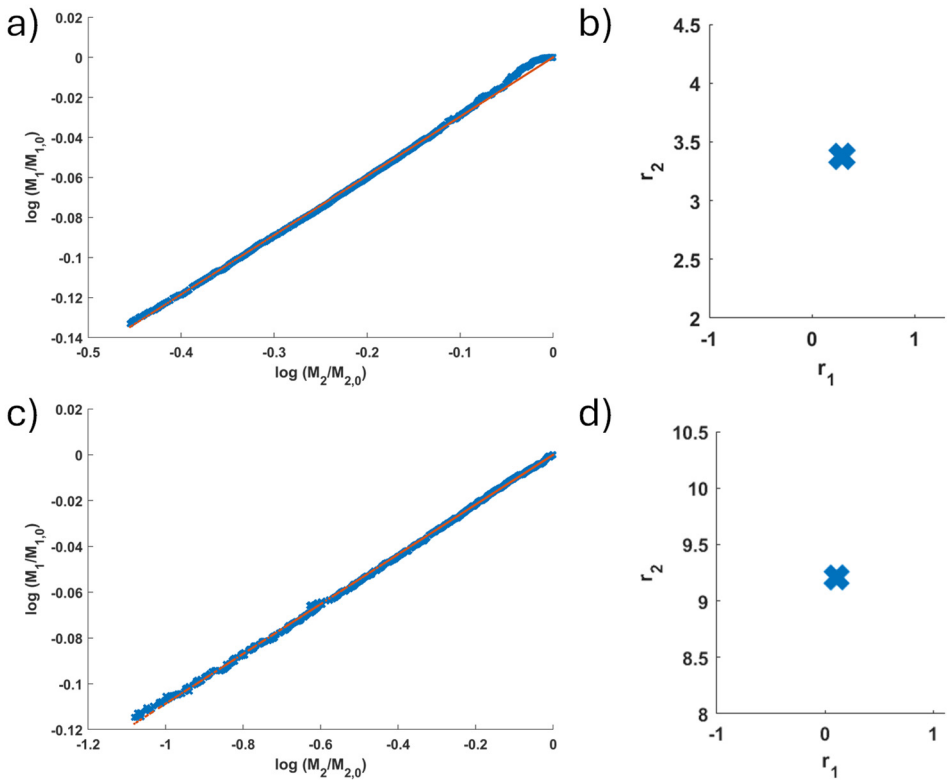


**Figure S20**: Obtained data applied on the Jaacks-Fits for the copolymerization of styrene with a) 1PhI and b) the given error values for 1PhI + S as well as the copolymerization with c) 4PhI and the d) corresponding error values.

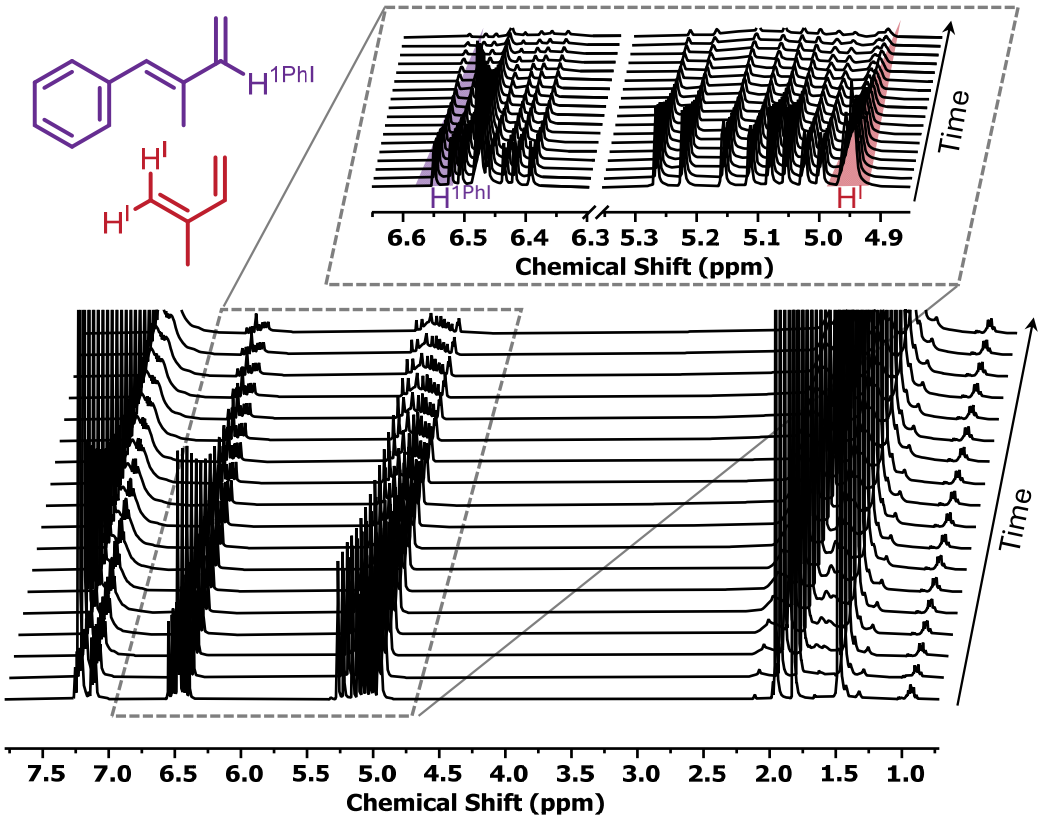


**Figure S21**: Stacked $^{1}$H NMR spectra of the *in situ* kinetics of isoprene and 1PhI and an expansion of the traced monomer signals.

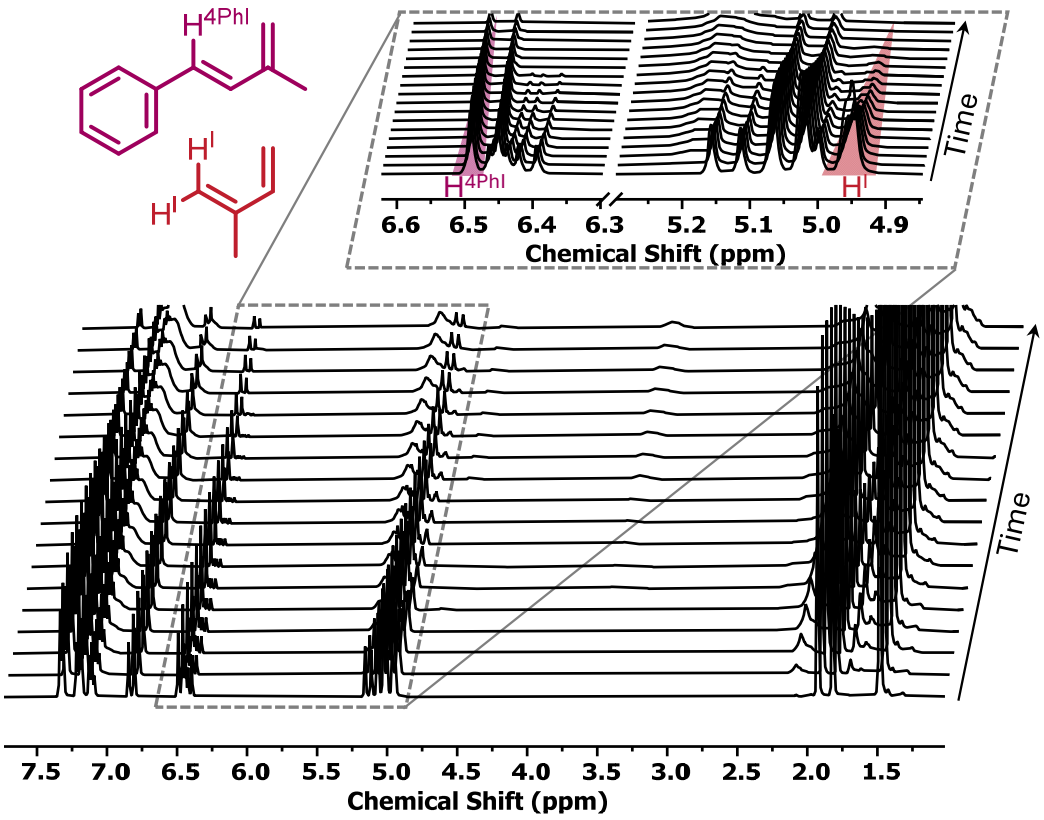


**Figure S22**: Stacked $^{1}$H NMR spectra of the real-time kinetics of isoprene and 4PhI and an expansion of the traced monomer signals.

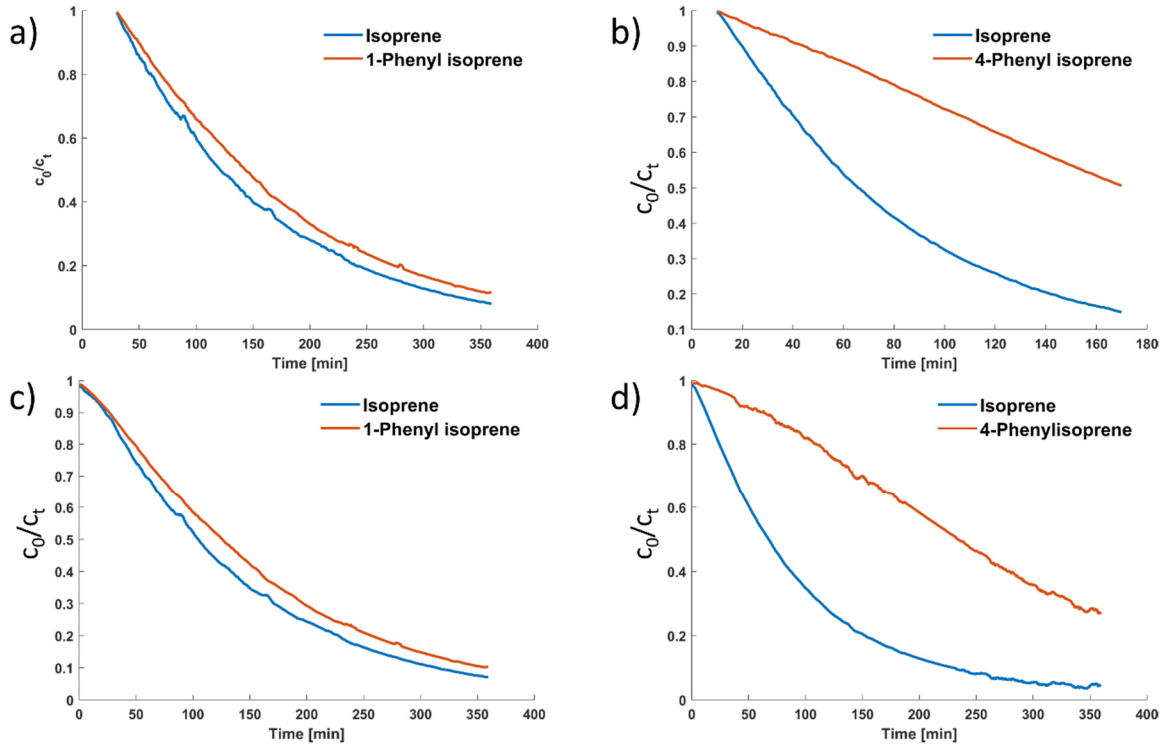


**Figure S23**: Individual monomer conversion of the copolymerization with isoprene and a) 1PhI and b) 4PhI as well as the time-depended monomer conversion of the copolymerization using c) 1PhI and d) 4PhI.

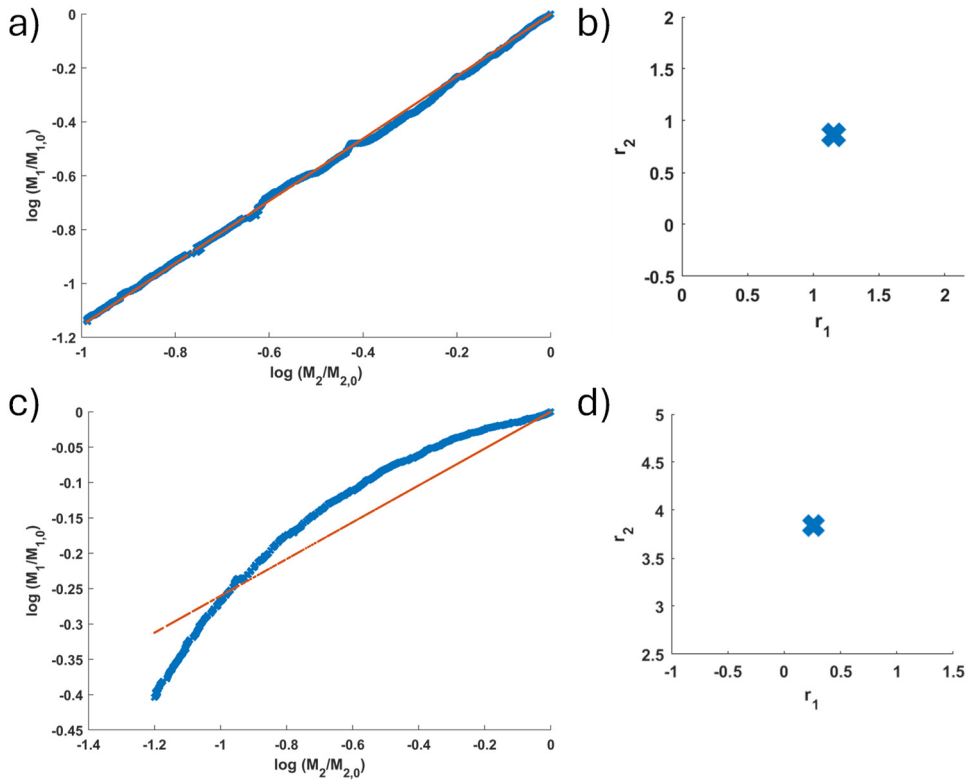


**Figure S24**: Obtained data applied on the Jaacks-Fits for the copolymerization of isoprene with a) 1PhI and b) the given error values for 1PhI + S as well as the copolymerization with c) 4PhI and the d) corresponding error values.

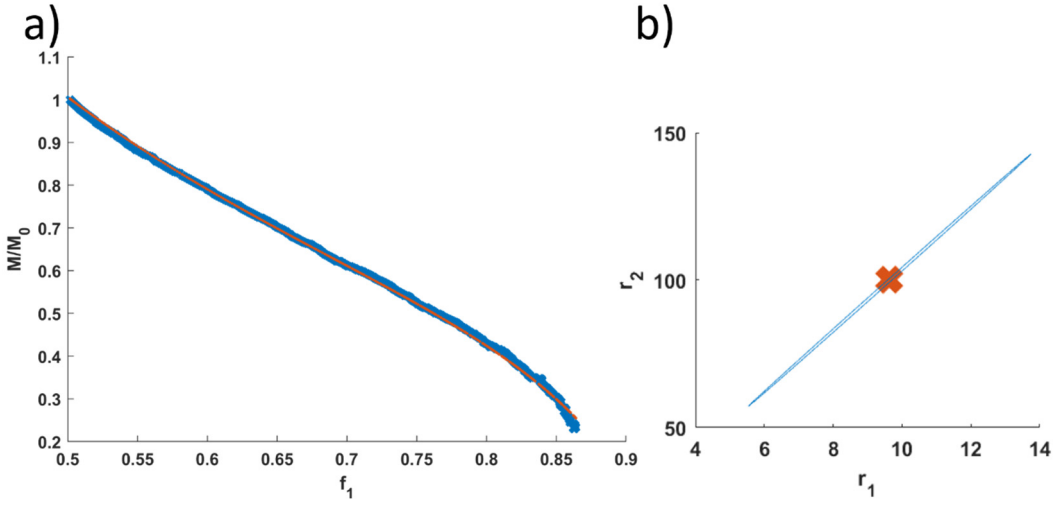


**Figure S25**: Evaluation of the kinetic experiment of 4PhI and I applying the obtained data with the Meyer-Lowry method. a) The fit of the calculation and b) the error values of the obtained reactivity ratios.

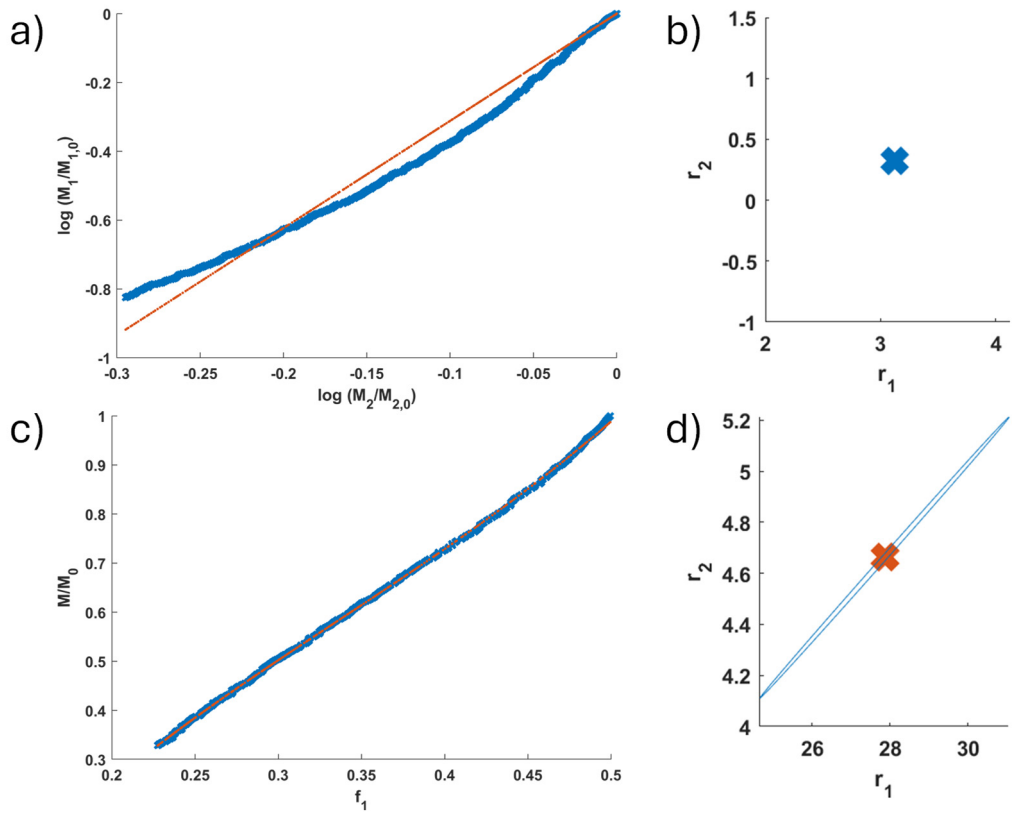


**Figure S26**: Evaluation of the repeated copolymerization of 4PhI and isoprene at an equimolar ratio using a) the Jaacks fit and b) the corresponding error values as well as c) using the Meyer-Lowry fit and d) the corresponding error values.

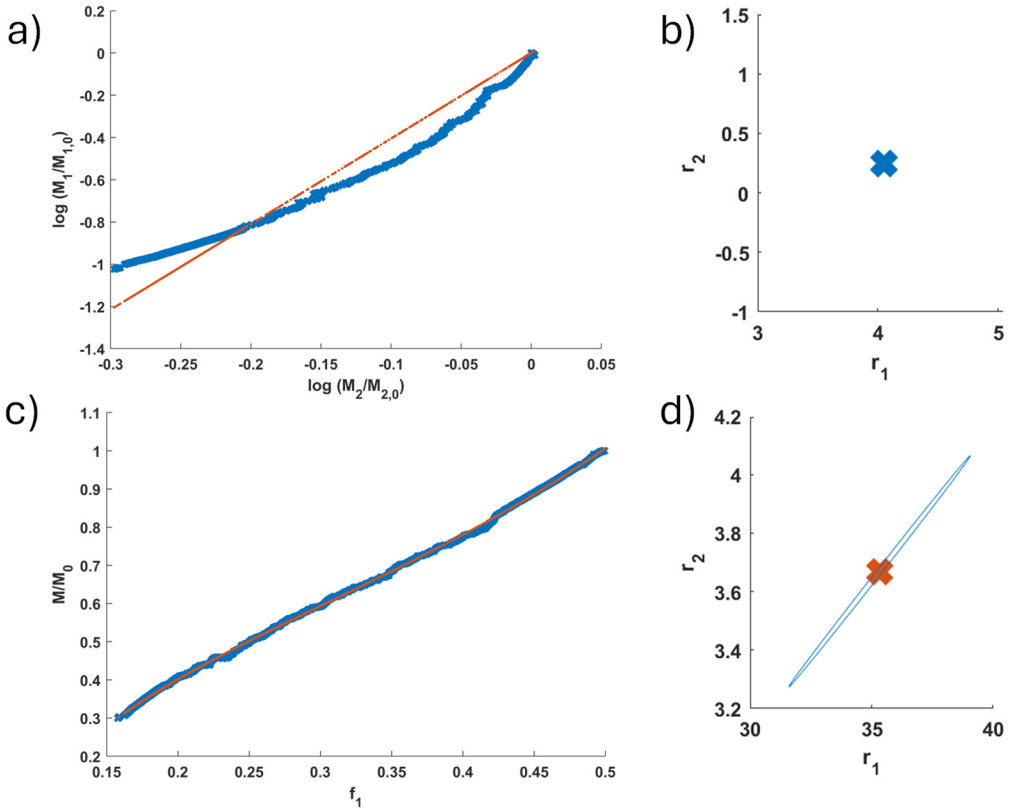


**Figure S27**: Evaluation of the repeated copolymerization of 4PhI and isoprene with a molar composition of 30 to 70 using a) the Jaacks fit and b) the corresponding error values as well as c) using the Meyer-Lowry fit and d) the corresponding error values.

**Table S3**: Summary of the performed $^{1}$H NMR kinetics of isoprene and 4PhI with different molar ratios. All three attempts were analyzed *via* the Jaacks fit and the Meyer-Lowry fit representing a non-terminal and a terminal model.

| Attempt | [4PhI]:[I] | $r_I$ [a] | $r_{4PhI}$ [a] | $r_I$ [b] | $r_{4PhI}$ [b] |
|---|---|---|---|---|---|
| 1 | 50:50 | 3.84 | 0.260 | -- | -- |
| 2 | 50:50 | 3.12 | 0.32 | 27 | 4.6 |
| 3 | 30:70 | 4.05 | 0.247 | 35 | 3.7 |

[a] Non-terminal model of the Jaacks fit used for the determination of the reactivity ratios.
[b] Terminal model of the Meyer-Lowry fit used for the determination of the reactivity ratios.

## Characterization of the copolymerizations with isoprene and styrene

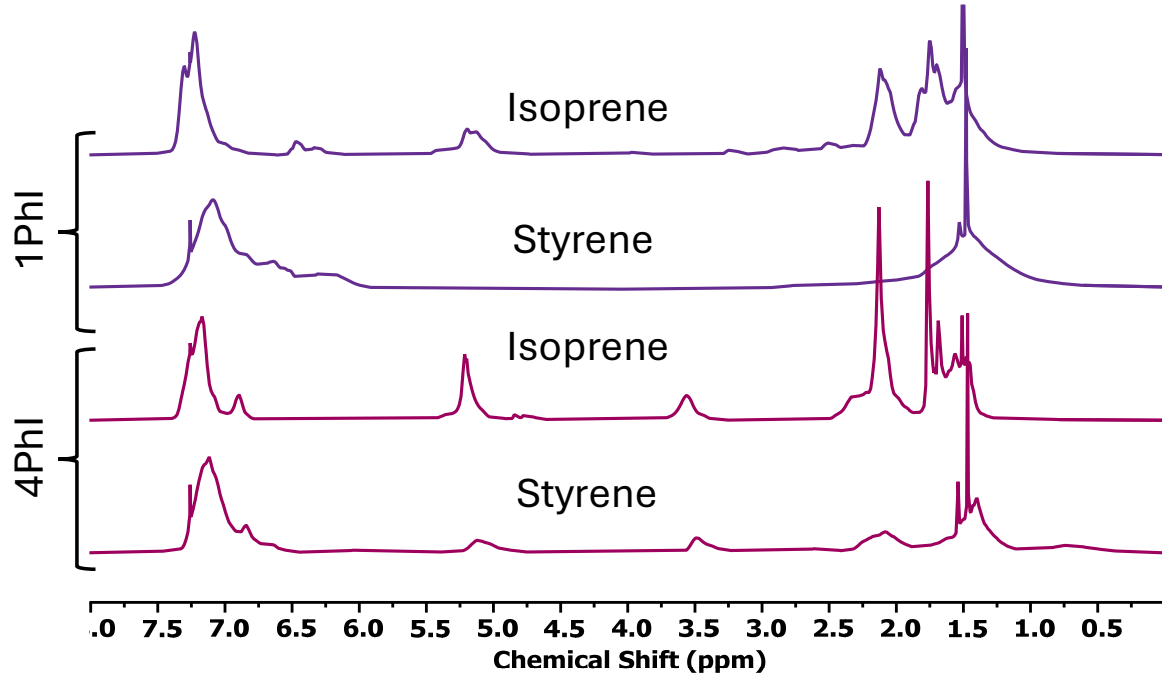


**Figure S28**: Stacked $^{1}$H NMR spectra (400 MHz, $CDCl_3$) of the copolymers containing 1PhI (dark purple) and 4PhI (light purple) with either isoprene or styrene.

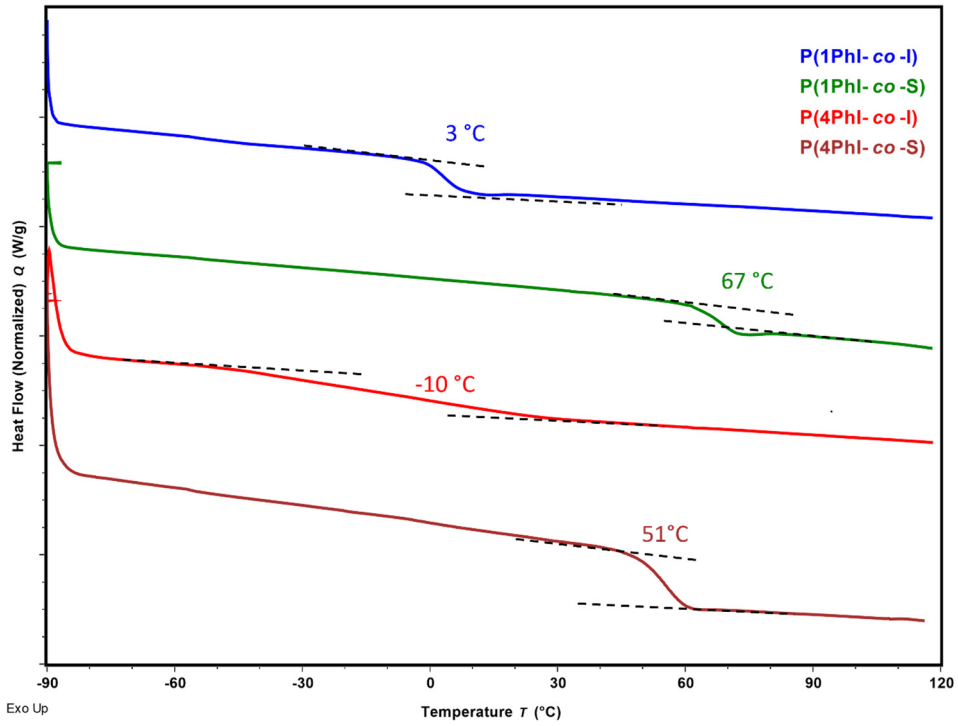


**Figure S29**: DSC curves for the copolymers of 1PhI and 4PhI, respectively, with isoprene or styrene as a comonomer (entries 15 – 18).

## Characterization of the cyclized structures

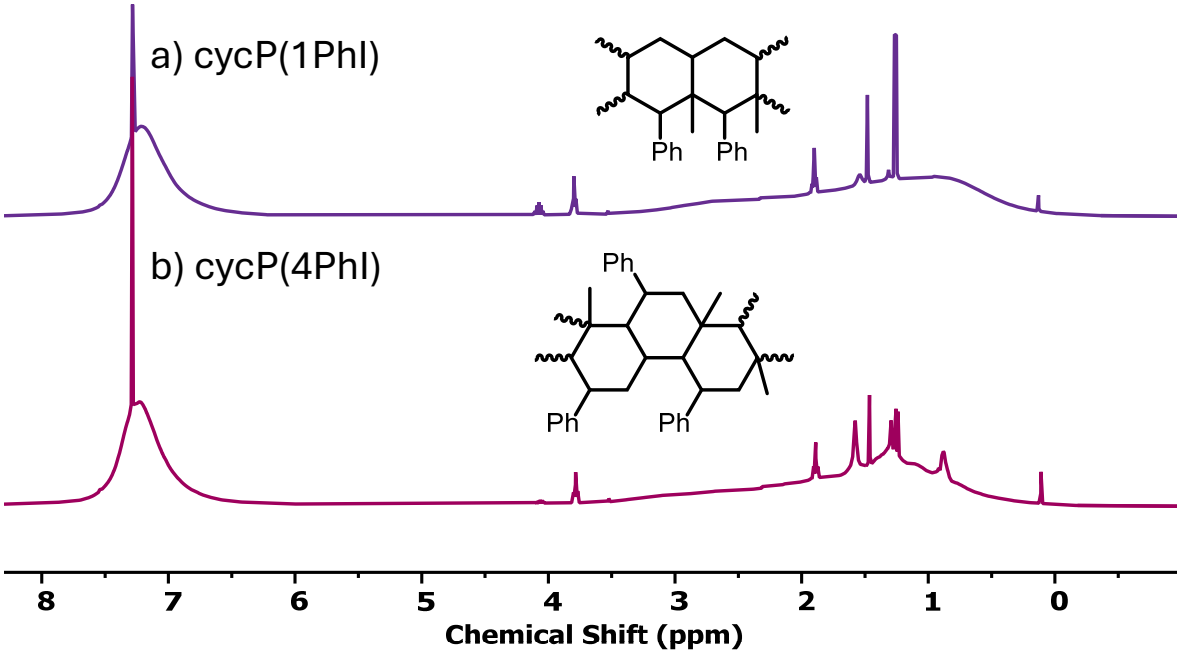


**Figure S30**: Stacked $^{1}$H NMR spectra (400 MHz, $CDCl_3$) of the cyclized polymers containing a) 1PhI (dark purple) and b) 4PhI (light purple).

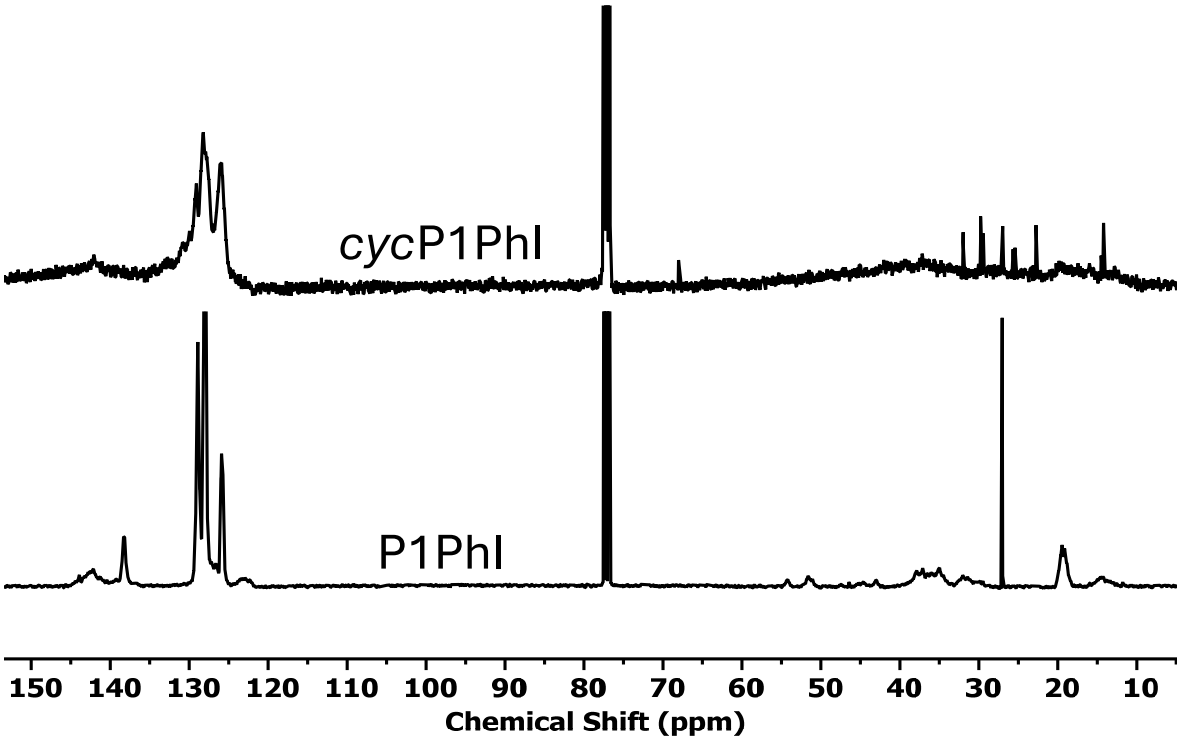


**Figure S31**: Stacked $^{13}$C NMR spectra (103 MHz, $CDCl_3$) of *cyc*P1PhI and P1PhI to identify the disappearing carbon species.

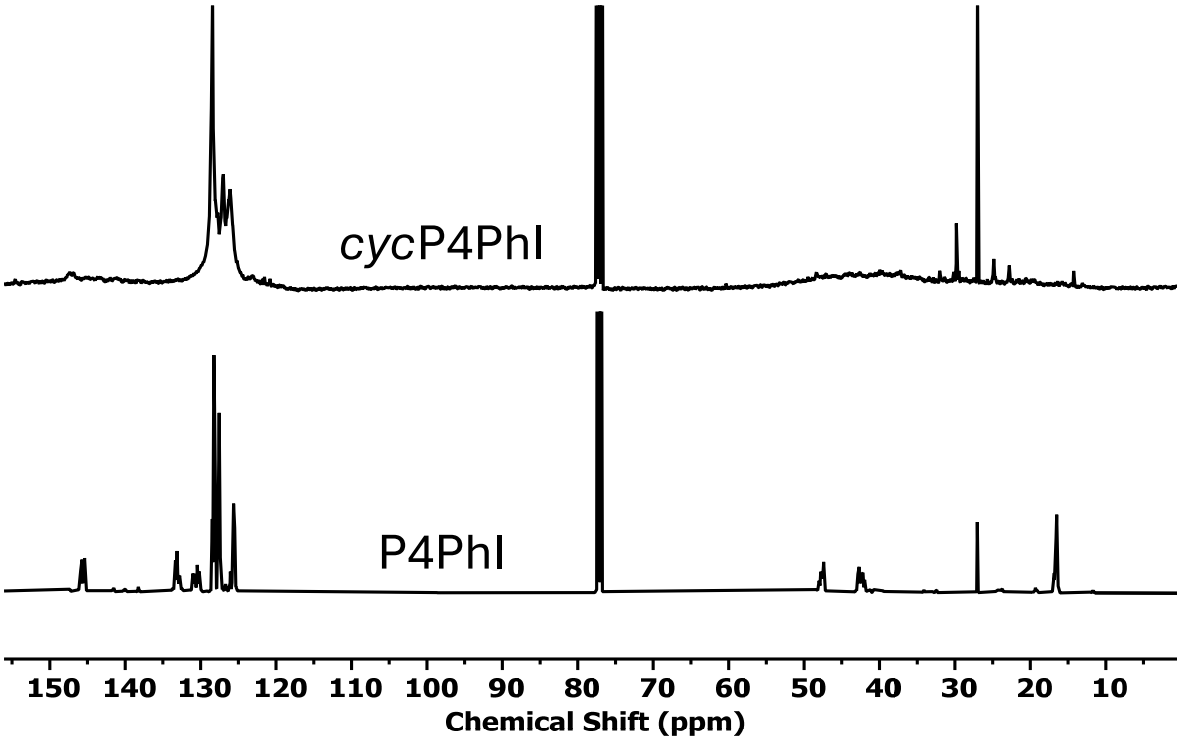


**Figure S32**: Stacked $^{13}C$ NMR spectra (103 MHz, $CDCl_3$) of *cyc*P4PhI and P4PhI to identify the disappearing carbon species.

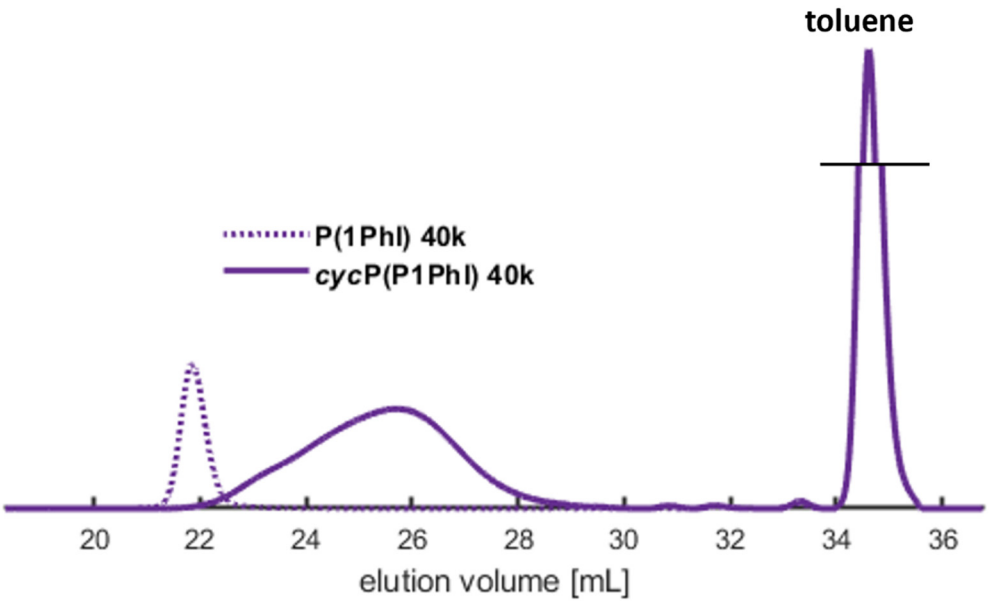


**Figure S33**: SEC traces of the P(1PhI) precursor and the cyclized sample *cyc*P(1PhI). Retention of the internal toluene standard also shown at 34.59 mL.

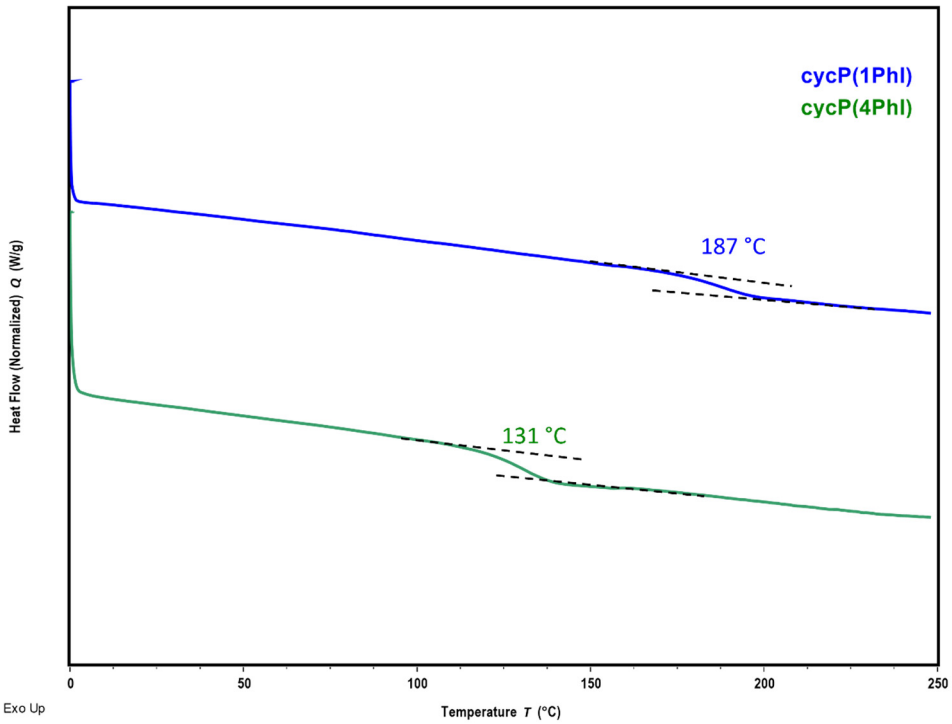


**Figure S34**: DSC curves of the cyclized *cyc*P(1PhI) (blue) and *cyc*P(4PhI) (green).

## Photophysical Analysis of cyclized samples

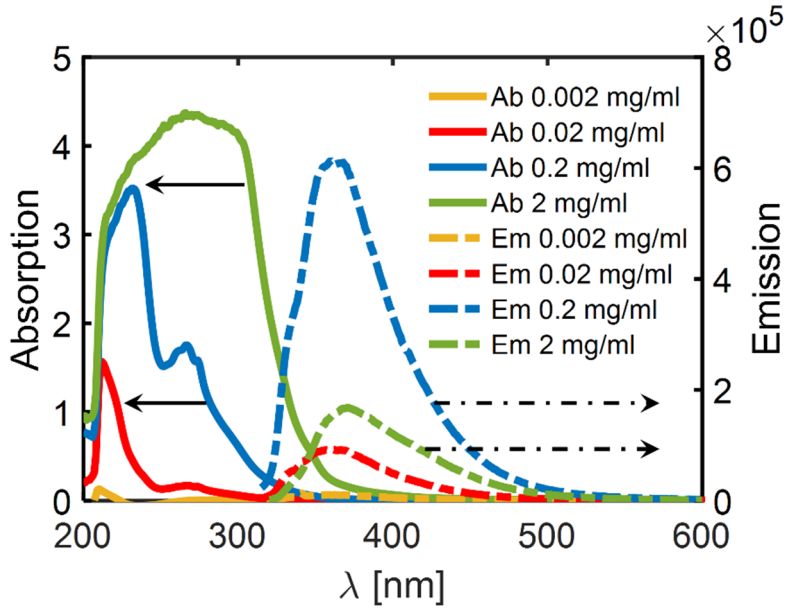


**Figure S35**: Absorption (solid) and emission (dashed) spectra of *cyc*P(1PhI) at different concentrations (0.002 – 2 mg/mL) in toluene ($\lambda_{exc}$ = 310 nm).

**Table S4**: Summary over obtained emission maxima for *cyc*P1PhI and *cyc*P4PhI with increasing concentrations.

| **Sample** | ***c*(*cyc*PPhI)** mg mL$^{-1}$ | $\lambda_{em,max}$ nm |
|---|---|---|
| *cyc*P1PhI | 0.02 | 362 |
| | 0.2 | 360 |
| | 2 | 371 |
| *cyc*P1PhI | 0.02 | 375 |
| | 0.2 | 377 |
| | 2 | 395 |

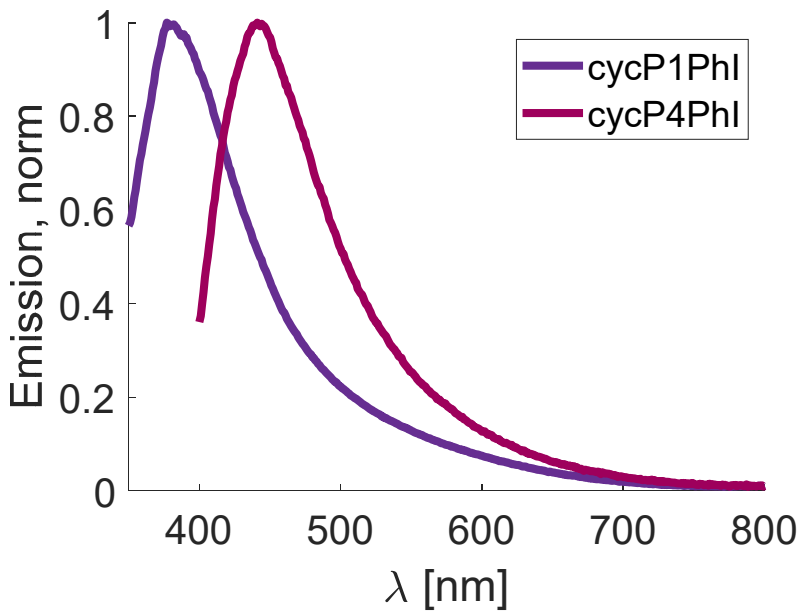


**Figure S36**: Obtained, normed emission spectra of the solid-state quantum yield determination. Worth mention, the conditions of both samples (excitement wavelength [$\lambda_{exc,cycP1PhI}$ = 330 nm; $\lambda_{exc,cycP4PhI}$ = 380 nm], bandwidth etc.) were different in both cases.

## References

1 K. Colizza, K. E. Mahoney, A. V. Yevdokimov, J. L. Smith and J. C. Oxley, *J Am Soc Mass Spectrom*, 2016, **27**, 1796–1804.

# CHAPTER 4

## Polydiene-Derived High Glass Transition Temperature Polymer in Thermoplastic Elastomers with a Non-Crystallin Polycaprolactone Middle Block

# CHAPTER 4

*To be published*

## Polydiene-Derived High Glass Temperature Polymer in Thermoplastic Elastomers with a Non-Crystallin Polycaprolactone Middle Block

Moritz Rauschenbach,[a] Luisa Krancan,[a] Philip Dreier,[a] and Holger Frey [a]

[a] Department of Chemistry, Johannes Gutenberg University, Duesbergweg 10 – 14, D-55128 Mainz (Germany)

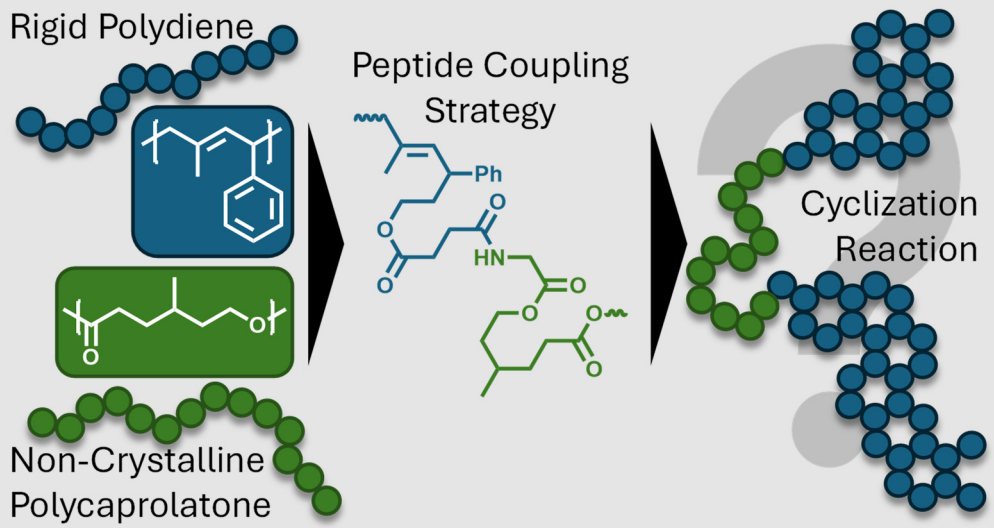


**Abstract:** Thermoplastic elastomers are ABA-type triblock copolymers made from styrene and butadiene. They are usually synthesized sequentially to yield rigid outer blocks and an elastic midblock. Nevertheless, triblock copolymers can also be produced by coupling of constituent homopolymer species after their respective synthesis. This work describes the anionic polymerization of the phenyl substituted isoprene derivatives, i.e. 1-phenyl isoprene (1PhI) and 4-phenyl isoprene (4PhI), obtaining molar masses up to 38 kg mol$^{-1}$. Controlled end-functionalization with ethylene oxide enabled the synthesis of *ω*-carboxy-functionalized polyphenyl isoprenes (PPhI). This allows a solid-phase peptide synthesis inspired coupling reaction when paired with *α,ω*-$NH_2$-poly-*γ*-methyl-*ε*-caprolactone (PMCL). This non-crystalline polyester exhibits a low glass temperature ($T_g$) and was synthesized in a traditional $Sn(Oct)_2$-catalyzed ring-opening transesterification polymerization with a subsequent two-step post-polymerization modification. The analytical methods employed did not yield consistent results regarding the successful formation of triblock polymers. PMCL demonstrated resilience to the highly acidic conditions present in the final cyclization reaction. Nevertheless, the targeted, exceptionally high $T_g$ through cyclized PPhI-blocks could not be verified in the final step.

## Introduction

The composition of ABA-type triblock copolymers typically comprises a rubbery mid-block and two rigid outer blocks. Their distinctive properties are induced by combing thermoplastic with elastomeric properties, resulting in the class of thermoplastic elastomers (TPEs). Commercial available TPEs such as Styrolux® are styrenic block copolymers (SBCs) composed of hard, high glass temperature ($T_g$) A blocks and an elastic B block, e.g. polybutadiene (PB) or polyisoprene (PI), bearing a low $T_g$.[1–3] The glassy A blocks create a network of physical crosslinks within the elastic matrix and therefore enable plastic processing, i.e. melt extrusion and injection molding.[1,3] However, the service temperature is limited by the $T_g$ of the glassy domains. Therefore, alternative thermoplastics with $T_g$s higher than PS have already been tested as substitutes to exploit elevated temperature applications.[2,4,5]

Thermoplastic structures are commonly linear and, thus, still feature some degree of freedom along the polymer backbone. Phenyl-substituted 1,3-dienes are known to be polymerized *via* anionic or catalytic techniques.[6–10] Takegami *et al*. fundamentally investigated the polymerization of 1-phenyl-1,3-butadiene (1PhB) and 2-phenyl-1,3-butadiene (2PhB). Both monomers showed almost exclusive 1,4-incorporation regardless of the polarity of the solvent, i.e. toluene or tetrahydrofuran (THF).[6,10–12] In 2017, Han and coworkers used P1PhB with varying microstructures in a triflic acid-induced cyclization reaction.[7] This was repeated by the group of Cui *et al*. utilizing a syndiotactic P(1PhB), which was characterized by a substantial increase in $T_g$ exceeding 300 °C.[8] Recently, we have reported on the anionic polymerization of two phenyl-substituted isoprene derivatives, i.e. poly(1-phenyl isoprene) (P1PhI) and poly(4-phenyl isoprene) (P4PhI). The resulting polymers were subsequently subjected to cyclization in accordance with previous reports, with the cyclized materials retaining solubility in common solvents, i.e., dichloromethane, THF, and toluene.[13] This enabled the analysis by size exclusion chromatography (SEC), which revealed notable elevations in dispersity and apparently decreasing molar masses as a result of a changed hydrodynamic radius, which are generally side-effects of cyclization reactions of poly(aryl-substituted polydienes).[14]

To the best of our knowledge these specific sterical demanding structures have not been applied in TPE-like structures. PI, also obtained by anionic polymerization techniques, cannot be utilized as the elastic polymer component. In fact, the cationic cyclization of polyisoprene was reported prior to the first polymerization of 1PhB.[15,16] Driven by an uncertain styrene availability, *Goodyear Tire and Rubber Company* synthesized ABA triblock copolymers based on the fully polydienes-based triblock copolymer polyisoprene-*block*-polybutadiene-*block*-polyisoprene (PI-*b*-PB-*b*-PI). After cyclization of the polyisoprene-blocks, the obtained materials showed promising performance as TPEs.[17]

The objective of this study is to utilize alternative polymer classes, such as polyether or polyester, that exhibit the requisite stability of the elastic middle block in the presence of strong acidic conditions during the cyclization reaction. Nevertheless, the most prominent candidates, poly(ethylene glycol) (PEG) and poly(ε-caprolactone) (PCL), both possess the disadvantage of emerging crystallinity with increasing molar mass.[18,19] Hillmyer and colleagues employed the introduction of methyl groups in polycaprolactone to effectively suppress the crystallization process.[20–24] Following comprehensive investigations, γ-methyl-ε-caprolactone (MCL) has emerged as the most promising candidate. The feasibility of synthesizing MCL from bio-derived *p*-cresol was techno-economically analyzed.[25] The low entanglement molar mass ($M_{ent}$) of 2.9 kg mol$^{-1}$ combined with its low $T_g$ of − 60 °C) was reported to be suitable as elastomeric block in TPEs.[22,26]

In the past, different strategies have been developed for the coupling of two polymers.[27] In accordance with low molar mass organic synthesis, compatible functional moieties are mandatory for the synthesis of symmetrical triblock copolymers which are not accessible *via* sequential monomer addition. PS-*b*-PEG-*b*-PS triblock copolymers were synthesized starting from a PEG-based, bifunctional macroinitiator. The respective end groups were transferred into reactive species suitable for the anionic or radical polymerization of styrene. However, the resulting polymers featured poorly defined structures.[28–30] The solid-phase peptide synthesis (SPPS) is a highly evolved pathway to achieve desired peptide sequences by utilizing efficient coupling and protection group chemistry. It is noteworthy that the development of coupling reagents enabled near-quantitative amide formation from the respective carboxylic acid and amine.[31] Besenius

*et al*. successfully transferred the analogous non-solid synthesis procedure on the synthesis of peptide-polymer conjugates.[32]

In the case of a bifunctional poly-*γ*-methyl-*ε*-caprolactone (PMCL) functional end groups are produced intrinsically. In contrast, P1PhI and P4PhI polymerized by anionic polymerization requires a highly sensitive termination reaction towards *ω*-functionalities. Here, ethylene oxide (EO) can be utilized to quantitatively insert a hydroxyl group at the chain-end.[33,34]

In this work, we report on the synthesis of PMCL targeting high molar masses and subsequently converting them to the respective *α,ω*-diamine-functionalized elastomer. Additionally, 1PhI and 4PhI were polymerized according to procedures of anionic polymerization and termination using EO. Then, *ω*-hydroxyl-polyphenylisoprenes were converted to obtain the *ω*-carboxy species allowing the PyAOP-directed coupling reaction. Finally, the cyclization of the PPhI blocks was performed to yield triblock copolymers with markedly rigid outer blocks.

## Experimental Section:

**Reagents**. All solvents and chemicals were purchased from commercial suppliers (*Carbolution*, *Fisher Scientific, Sigma-Aldrich, and TCI*). If not stated otherwise, all chemicals were used without further purification. Chloroform-$d_1$ was purchased from *Deutero GmbH*. Cyclohexane was dried over sodium and benzophenone.

**Instrumentation**. Nuclear magnetic resonance (NMR) measurements were performed on a *Bruker Avance II 400* spectrometer. Every spectrum was referenced internally to the residual proton of chloroform-$d^1$ and measured at respective maximum frequency, i.e. $^1$H at 400 MHz and $^{13}$C at 101 MHz. Diffusion-Ordered Spectroscopy (DOSY) was recorded on a *Bruker Avance III HD 400* spectrometer at 400 MHz. Analysis was performed utilizing *MestReNova* 15.0.1 software. Size exclusion chromatography (SEC) measurements were performed on an *Agilent 1260 Infinity II SEC* setup equipped with a column set from *MZ-Analysetechnik* (*MZ-GEL-DS plus* 105/103/100 Å) utilizing THF as the eluent with a flowrate of 1 mL min$^{-1}$. All measurements were conducted at 30 °C and analyzed *via* RI-detection. For calibration polyisoprene (PI) and polystyrene (PS) standards, purchased from *PSS*, were utilized. The software *PSS WinGPC UniChrom* was used for data recording and processing. Differential scanning calorimetry (DSC) measurements were performed

on a *DSC 250* from *TA Instruments*. The instrument was calibrated with *n*-octane and indium. In preparation for the measurement, the polymer samples were dried under high vacuum. To eliminate any thermal history, each sample was subjected to a heating cycle, reaching 120 °C, prior to being cooled to − 90 °C and reheated to 120 °C. The heating and cooling rates were set to a of 20 °C $min^{-1}$. The glass temperatures were determined from the second heating cycle using the software *TRIOS* 5.5.1.5 by *TA Instruments*. Matrix-assisted laser desorption ionization time-of-flight mass spectrometry (MALDI ToF MS) was carried out on a *MALDI ToF MS Autoflex Max* by *Bruker*. Prior to analysis the samples were dissolved in dichloromethane at a concentration of 1 mg $mL^{-1}$. All measurements were conducted in linear mode. PMCL-based polymers utilized *trans*-2-[3-(4-*tert*-butylphenyl)-2-methyl-2-propenyliden] malononitrile (DCTB) as matrix with addition of KTFA. The analysis of sample $4P^{4PhI}$ was achieved with dithranol as the matrix with AgTFA.

**Monomer synthesis**. *γ*-Methyl caprolactone (MCL) was prepared by a Baeyer-Villiger oxidation. The synthetic strategy is described in detail in the Supporting Information. The synthesis of 1PhI and 4PhI can be found in a recent publication. [13]

The polymer synthesis, the coupling reaction and the subsequent cyclization are described in the Supporting Information.

## Results & Discussion:

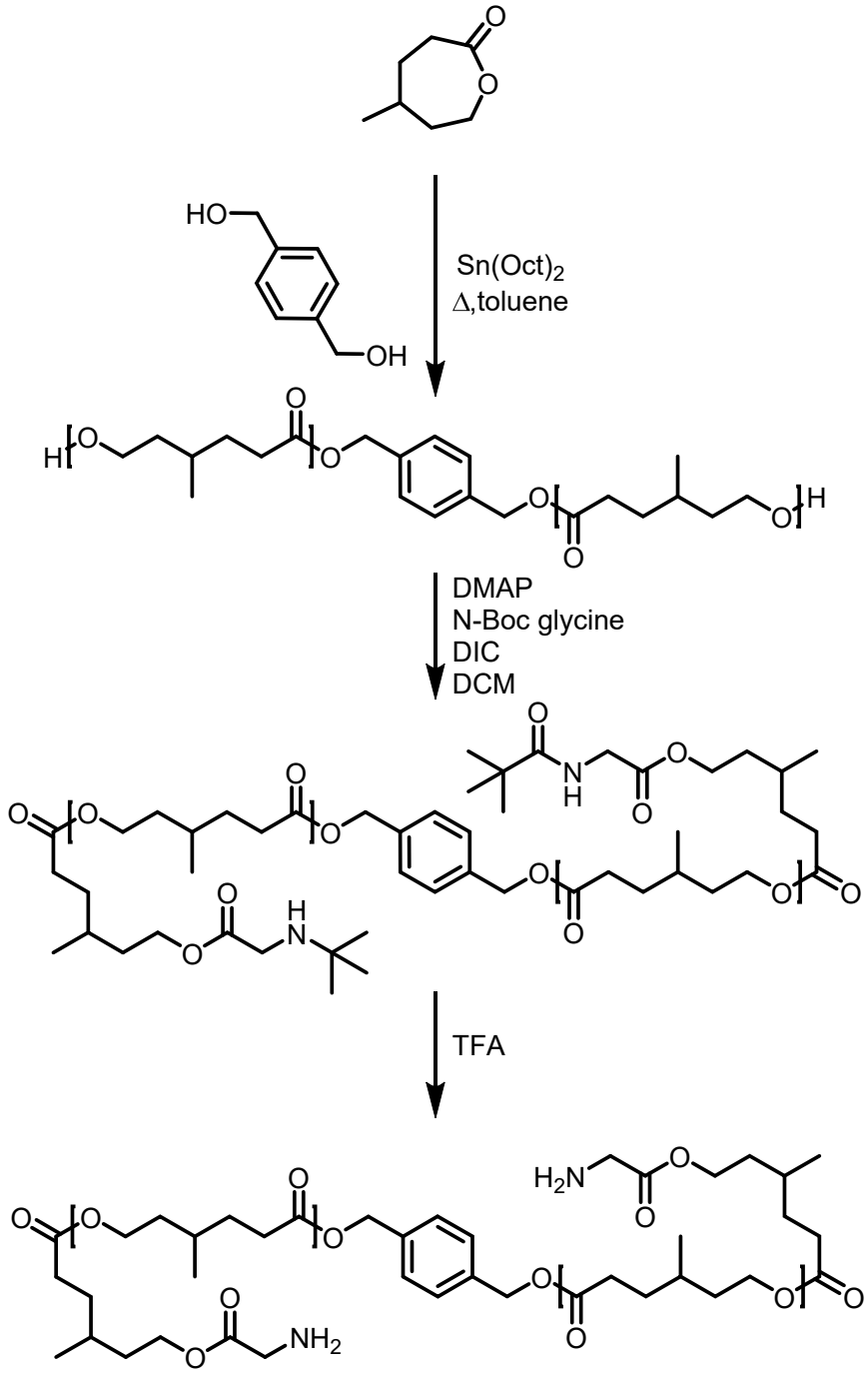


**Scheme 1:** Reaction pathway for the synthesis of *α,ω*-$NH_2$-PMCL.

### Synthesis and Polymerization of MCL

The synthesis of *γ*-methyl-ε-caprolactone (MCL) from *γ*-methyl cyclohexanone was conducted according to the established procedure of a traditional Baeyer-Villiger oxidation, utilizing *meta*-chloroperoxybenzoic acid. After purification, the cyclic MCL was obtained in good yield in its pure form *via* distillation (**Figure S1**).[35] Subsequently, the bifunctional initiator benzene dimethanol (BDM) was utilized for the traditional $Sn(Oct)_2$-

catalyzed ring-opening transesterification polymerization (ROTEP). The ROTEP was conducted in toluene at 100 °C yielding well-defined *α,ω*-hydroxyl telechelic poly(*γ*-methyl-*ε*-caprolactone) (PMCL) with molar masses of up to 33.4 kg mol$^{-1}$ within 2 d (**Table 1**). SEC analysis revealed low dispersities of $Đ < 1.16$ underlining the good control over the polymerization (**Figure 1**a)).

MALDI ToF MS was utilized to further confirm the purity of the polymers exemplary analizing 1P$^{MCL}$. As illustrated in **Figure 2**, the analysis demonstrates the presence of a single repetition unit with a molar mass that was consistent with that of MCL, thereby providing evidence of an indeed successful polymerization. However, the maximum molar mass observed by MALDI ToF MS of 8251 g mol$^{-1}$, suggests that the molar mass by SEC using a polyisoprene standard may be overestimated. Thermal analysis determined $T_g$s below – 49 °C, indicating the material's suitability for the use as the elastomeric component in TPEs. This finding is consistent with previous studies that have demonstrated the compatibility in materials with polylactide (PLA) (**Figure S9**).[35]

**Table 1**: Overview over PMCL obtained *via* ring-opening polymerization of MCL in toluene.

| Entry | $M_{n,targ}$ [kg mol$^{-1}$] | M:BDM:Sn | $M_{n,SEC}$[a] [kg mol$^{-1}$] | $Đ$[a] | $T_g$[b] [°C] |
|---|---|---|---|---|---|
| 1P$^{MCL}$ | 10 | 77:1:0.25 | 12.2 | 1.06 | − 62 |
| 2P$^{MCL}$ | 15 | 116:1:0.25 | 18.5 | 1.16 | − 61 |
| 3P$^{MCL}$ | 40 | 311:1:0.25 | 33.4 | 1.10 | − 49 |

[a] Determination *via* a SEC (Eluent: THF; 30°C) utilizing a PI-standard, [b] Determination through DSC measurements analyzing the second heating curve with a heating rate of 20 °C min$^{-1}$.

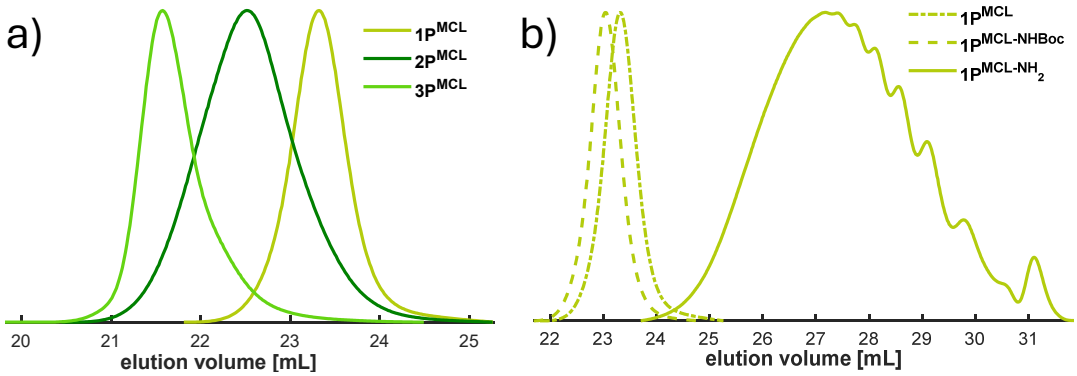


**Figure 1**: SEC curves of a) PMCL with increasing molar masses and b) 1P$^{MCL}$ functionalized to the *α,ω-N*-Boc-glycine-PMCL and after the cleavage of the protecting group towards the *α,ω*-$NH_2$-PMCL.

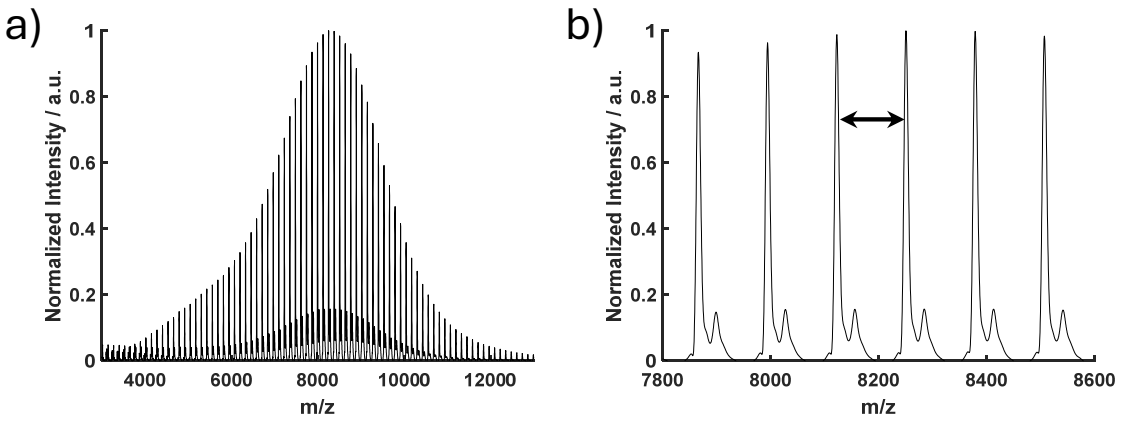


**Figure 2**: MALDI-TOF MS spectrum of $1P^{MCL}$.

$^1$H NMR spectroscopy revealed a significant influence of the degree of polymerization on the chemical shifts of the respective polymers. **Figure 3** highlights the chemical shifts of selected protons, demonstrating this effect. Notably, the signal of the methylene protons adjacent to the hydroxyl group in the polyester backbone shifts from 4.08 ppm in $2P^{MCL}$ to 4.84 ppm in the high molar mass sample $3P^{MCL}$. This shift is partially attributed to changes in the electronic environment as the polymer's molar mass increases. Since DSC measurements (**Figure S9**) confirm that PMCL is non-crystalline, these chemical shift changes cannot be linked to occurring crystallization as in polycaprolactone.

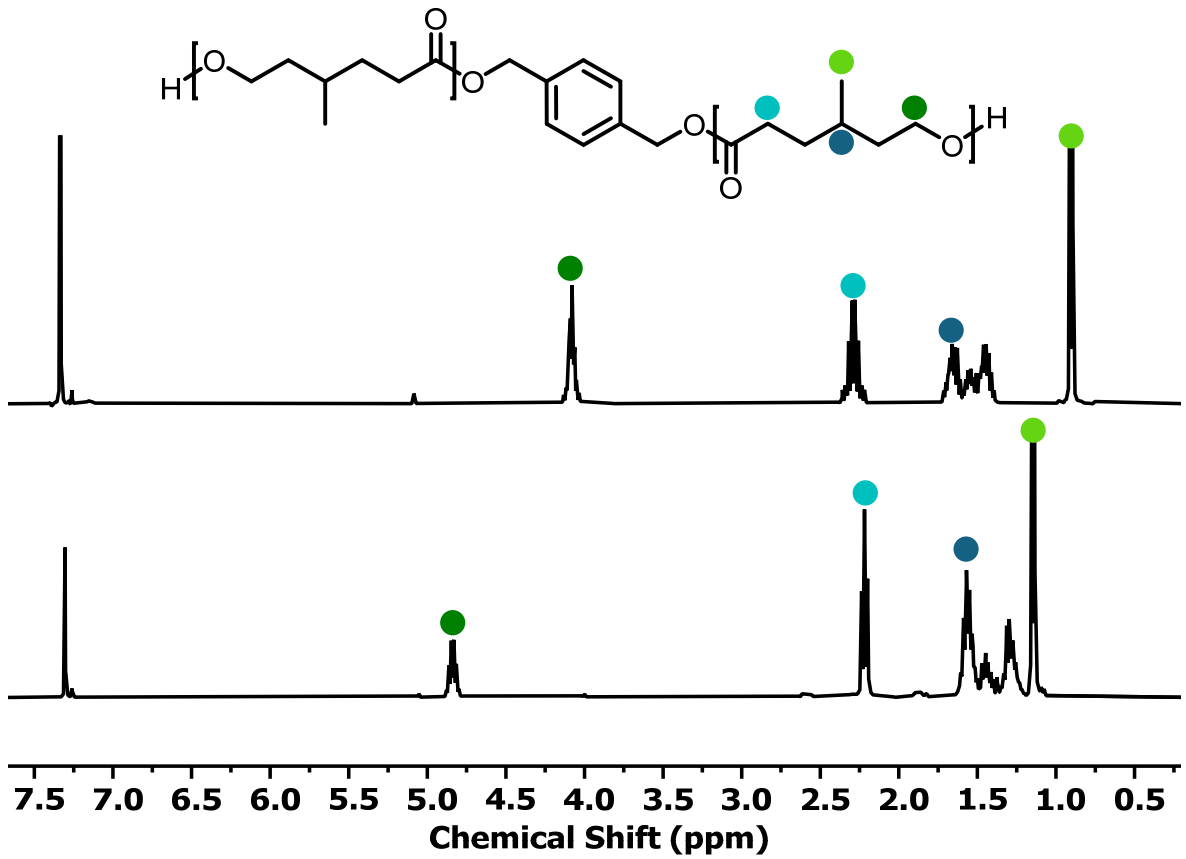


**Figure 3**: Stacked $^{1}$H NMR spectra ($CDCl_3$, 400 MHz) of $2P^{MCL}$ (top) and $3P^{MCL}$ (bottom).

Following the reaction pathway illustrated in **Scheme 1**, the polymer was reacted with *N*-Boc-glycine to produce *α,ω-N*-Boc-glycine-PMCL. The strategy of converting a hydroxyl group into a primary amine was previously demonstrated by Gallei and coworkers for the preparation of functional porous membranes.[36] The successful reaction was indicated by a slight shift to the higher molar mass region in the SEC traces (**Figure 1b)** and **Figure S8**) and by the appearance of a signal corresponding to the three methyl groups introduced by the Boc-protecting group in the respective $^{1}$H NMR spectrum. Furthermore, the appearing signal at 3.72 ppm, assigned to the methylene protons of glycine verifies the successful modification (**Figure S4**). Full proof was provided by MALDI ToF MS analysis (**Figure 4**). Only one distribution can be found tracing back to the glycine end groups in which the protective group was already cleaved by the conditions of the MALDI ToF MS measurements. DSC measurements revealed the noteworthy impact of the inserted *N*-Boc-glycine on the thermal properties (**Figure S9**). A comparison of the respective values in **Table 1** and **Table 2** reveals an increase of $\Delta T_g \leq +5$ °C for all three polymer samples. This demonstrates the stiffening effect of *N*-Boc glycine, which is caused by increased steric hindrance and increased interactions.

**Table 2**: Overview over the analysis of the modified PMCL-samples from **Table 1**.

| Sample | $M_{n,Precursor}$[a] [kg mol$^{-1}$] | $M_{n,SEC}$[a] [kg mol$^{-1}$] | $Đ$[a] | $T_g$[b] [°C] |
|---|---|---|---|---|
| 1P$^{MCL\text{-}N\text{-}Boc}$ | 12.2 | 14.7 | 1.06 | – 57 |
| 2P$^{MCL\text{-}N\text{-}Boc}$ | 18.5 | 19.2 | 1.19 | – 58 |
| 3P$^{MCL\text{-}N\text{-}Boc}$ | 33.4 | 35.0 | 1.10 | – 44 |
| 1P$^{MCL\text{-}NH2}$ | 14.7 | 1.2 | 1.53 | n.d. |
| 2P$^{MCL\text{-}NH2}$ | 19.2 | 19.3 | 1.22 | – 64 |
| 3P$^{MCL\text{-}NH2}$ | 35.0 | 35.4 | 1.11 | – 48 |

[a] Determination *via* a SEC (Eluent: THF; 30°C) utilizing a PI-standard, [b] Determination through DSC measurements analyzing the second heating curve with a heating rate of 20 °C min$^{-1}$.

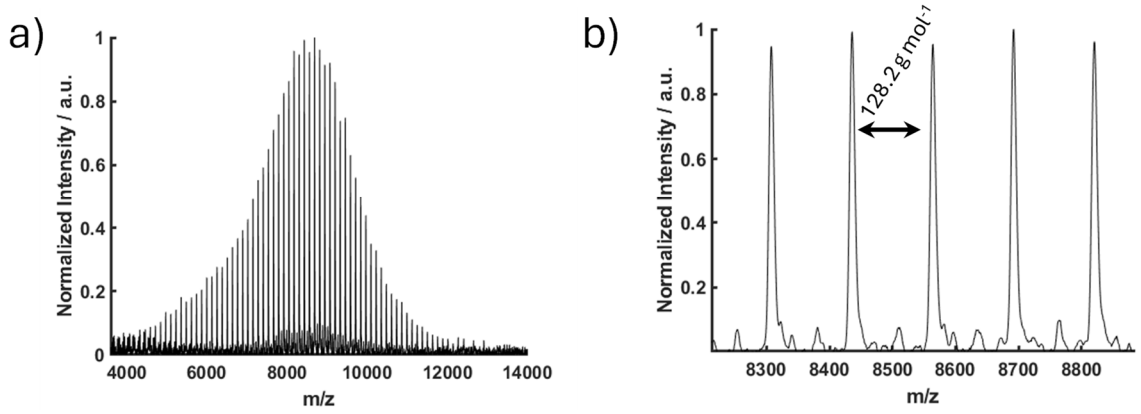


**Figure 4**: MALDI-ToF MS of 1P$^{MCL}$ after modification with *N*-Boc glycine.

## Removal of protecting group

The Boc-protecting group was cleaved according to established procedures using trifluoroacetic acid (TFA).[36] Although the reaction was cooled in an ice bath to ensure mild conditions, the corresponding SEC trace in **Figure 1b)** shows degradation of the polymer into oligomeric structures. This degradation is consistent with observation made by Li *et al.*, who attributed similar issues to the presence of basic amine functionalities.[37] Based on previous findings by Li group, maintaining low temperatures around – 20 °C can significantly enhance the stability of amine functional polyesters.[38] In this case, performing the aforementioned reaction at a temperature of – 15°C, accompanied by the storage of the resulting products at temperatures below 0 °C, proved an sufficient method

for the suppression of the initial polymer degradation. This conclusion is supported by the SEC traces presented in **Figure S8** and the minimal changes in $M_n$ and $Đ$, as summarized in **Table 2**. Furthermore, $^{19}F$ NMR spectroscopy verified the presence of the triflate, which reduces the basicity of the amine groups. Therefore, $\alpha,\omega$-$NH_2$-PMCL is stabilized in its ammonium salt form (**Figure S7**). In the $^{1}H$ NMR spectrum, the successful cleavage of the Boc group is indicated by the disappearance of the methyl group signal and the appearance of a broad signal at 9.24 ppm, corresponding to the protonated amino group (**Figure S5**). $T_g$ values of the $\alpha,\omega$-$NH_2$-PMCL polymers match the initial determined values in **Table 1**.

## Synthesis of $\omega$-hydroxyl-functionalized polydienes

The synthesis of $\omega$-hydroxyl-polyphenylisoprenes (PPhI-OH) was carried out following the synthesis pathway outlined in **Scheme 2**. The objective was to obtain materials with functional end groups suitable for the coupling reaction *via* living anionic polymerization. Therefore, ethylene oxide was utilized for quantitatively inserting hydroxyl groups to the living chain ends, following literature-known procedures.[33,39] SEC analysis revealed monomodal distributions with low dispersities ($Đ$ < 1.13), confirming the uniformity of the synthesized polymers (**Figure 5**). The only exception was the low molar mass polymer $4P^{4PhI\text{-}OH}$, which was synthesized for MALDI ToF MS analysis and exhibited an increased dispersity of $Đ$ = 1.31. Nevertheless, the MALDI ToF mass spectrum showed a single, distinct distribution (**Figure S14**), verifying quantitative end-functionalization.

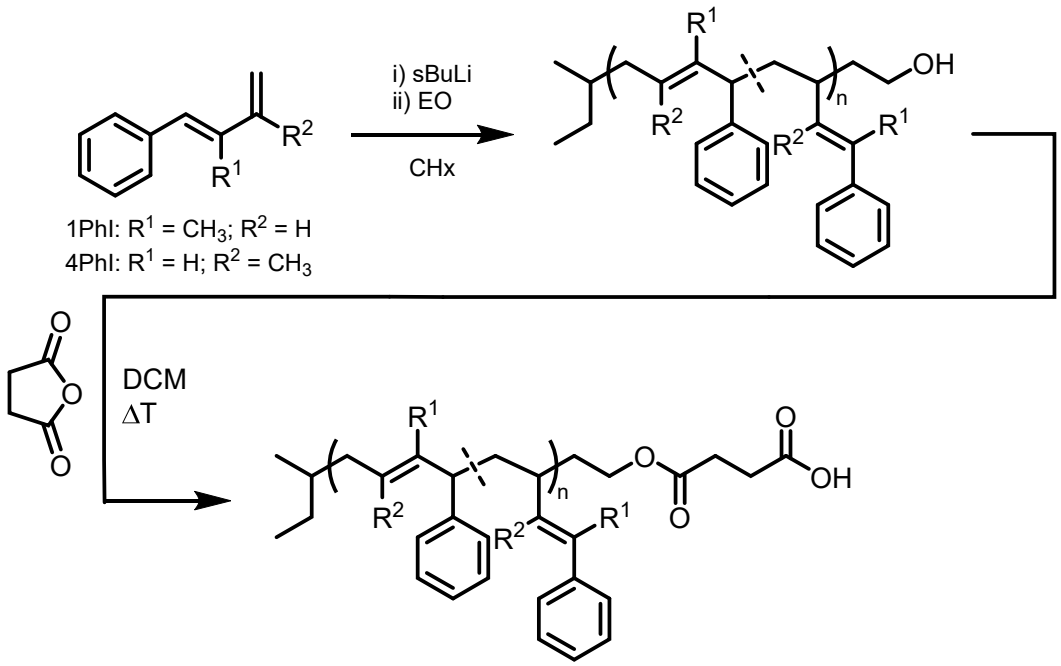


**Scheme 2**: Reaction route to *ω*-carboxy-functionalized PPhI.

Due to the sensitivity of the anionic polymerization, the conversion could not be monitored. Consequently, irreversible quenching of the reaction *via* end group functionalization prevented full conversion of the monomer. Therefore, discrepancies between the experimental and targeted molar masses were obtained, as indicated by SEC. To ensure accuracy, a PI calibration was employed for P4PhI, and a PS calibration was utilized for P1PhI, as this yielded results that were deemed plausible.[13] The determined $T_g$s in the region of 36 – 56 °C are in line with recently reported values (**Table 3**, **Figure S16**).[13] For each monomer, we proceeded the synthesis pathway with two polymers characterized by a molar mass of 20 and 35 kg mol$^{-1}$, respectively.

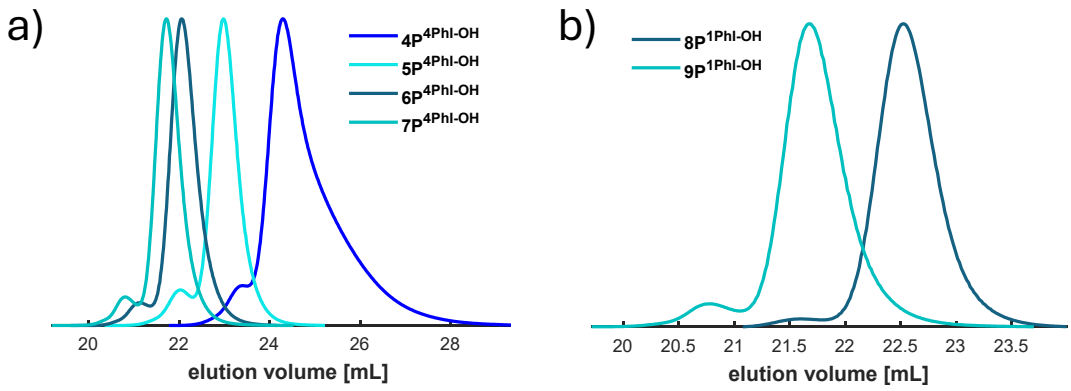


**Figure 5**: SEC traces of the synthesized poly phenyl isoprenes a) 4PhI and b) 1PhI terminated with ethylene oxide.

## Conversion to *ω*-carboxy-functionalized polydienes

In a polymer analogous reaction, the selected polymers were converted into the respective *ω*-carboxy-polyphenylisoprenes (PPhI-COOH) *via* esterification with succinic anhydride (**Scheme 2**). The dispersities of the resulting polymers remained consistent with no signs of undesired degradation or crosslinking, which would have impacted the resulting molar mass (**Table 3**). However, the use of high molar mass polymers does not enable quantitative end group analysis by $^{1}$H NMR spectroscopy due to poor signal to noise ratio. Nevertheless, the appearance of a small, partially overlapped signal at 4.12 ppm indicates the successful incorporation of succinic acid at the *ω*-position of the polymer (**Figure S11**).

**Table 3**: Summary of the polymers based on the phenyl isoprenes 1PhI and 4PhI.

| Sample | $M_{n,targ}$ [kg mol$^{-1}$] | $M_{n,SEC}$[a] [kg mol$^{-1}$] | $Đ$[a] | 1,4-[b] [%] | 3,4-[b] [%] | $T_g$[c] [°C] |
|---|---|---|---|---|---|---|
| 4P$^{4PhI-OH}$ | 5 | 4.5[d] | 1.31 | 99 | 1 | n.d. |
| 5P$^{4PhI-OH}$ | 20 | 13.9[d] | 1.09 | n.d. | n.d. | n.d. |
| 6P$^{4PhI-OH}$ | 40 | 24.7[d] | 1.10 | 99 | 1 | 46 |
| 7P$^{4PhI-OH}$ | 40 | 31.8[d] | 1.10 | 99 | 1 | 46 |
| 6P$^{4PhI-COOH}$ | - | 27.8[d] | 1.13 | 99 | 1 | 44 |
| 7P$^{4PhI-COOH}$ | - | 29.2[d] | 1.11 | 99 | 1 | 36 |
| 8P$^{1PhI-OH}$ | 30 | 21.3[e] | 1.05 | 37 | 63 | 56 |
| 9P$^{1PhI-OH}$ | 60 | 38.3[e] | 1.08 | 39 | 61 | 54 |
| 8P$^{1PhI-COOH}$ | - | 21.3[e] | 1.06 | 37 | 63 | 42 |
| 9P$^{1PhI-COOH}$ | - | 39.7[e] | 1.09 | 39 | 61 | 45 |

[a] Determination *via* a SEC (Eluent: THF; 30°C), [b] Determination trough integration of the respective signals in the $^{1}$H NMR spectra, [c] Determination through DSC measurements analyzing the second heating curve with a heating rate of 20 °C min$^{-1}$, [d] Determination utilizing a PI-calibration, [e] Determination utilizing a PS-calibration

## Synthesis of ABA triblock copolymers

In a coupling reaction, ABA triblock copolymers consisting of *ω*-carboxylated P(PhI) and freshly prepared *α,ω*-$NH_2$-P(MCL) were targeted. The amidation reaction was adapted

from solid phase peptide synthesis by using the coupling reagent PyAOP, (7-Azabenzotriazol-1-yloxy) tripyrrolidinophosphonium hexafluorophosphate, in the presence of $NEt_3$.[40] Based on the selected precursor polymers four different combination of ABA triblock copolymers were synthesized. For every PMCL a PPhI sample with a molar mass in a similar range was selected (**Table 4**). Hence, polymers with molar masses in the range of 60 (3 × ~ 20 kg mol$^{-1}$) and 120 kg mol$^{-1}$ (3 × ~ 40 kg mol$^{-1}$) were targeted.

To our surprise, the SEC traces did not shift to lower elution volume as anticipated. Consequently, no increase in molar mass was visible for all samples following the coupling reaction in (**Figure 6** and **Figure S18**). In fact, SEC analysis emphasizes only the existence of the utilized PPhI samples. In contrast, the $^1$H NMR spectra show the respective signals of both PMCL and PPhI as highlighted in **Figure 7** and **Figure S20**.

**Table 4**: Overview of the synthesized triblock copolymer PPhI-*b*-PMCL-*b*-PPhI.

| Sample | $M_{n,PPhI}$[a] [kg mol$^{-1}$] | $M_{n,PMCL}$[a] [kg mol$^{-1}$] | $M_{n,total}$[a] [kg mol$^{-1}$] | $Đ$[a] | $T_{g,1}$[b] [°C] | $T_{g,2}$[b] [°C] |
|---|---|---|---|---|---|---|
| 6P$^{4PhI}$-*b*-2P$^{MCL}$-*b*-6P$^{4PhI}$ | 24.7 | 19.3 | 24.8[c] | 1.14 | − 64 | 42 |
| 7P$^{4PhI}$-*b*-3P$^{MCL}$-*b*-7P$^{4PhI}$ | 31.8 | 35.4 | 32.2[c] | 1.10 | - | 33 |
| 8P$^{1PhI}$-*b*-2P$^{MCL}$-*b*-8P$^{1PhI}$ | 21.3 | 19.3 | 22.8[d] | 1.07 | − 67 | 68 |
| 9P$^{1PhI}$-*b*-3P$^{MCL}$-*b*-9P$^{1PhI}$ | 38.3 | 35.4 | 40.4[d] | 1.09 | − 56 | 51 |

[a] Determination *via* a SEC (Eluent: THF; 30°C), [b] Determination through DSC measurements analyzing the second heating curve with a heating rate of 20 °C min$^{-1}$, [c] Determination utilizing a PI-calibration, [d] Determination utilizing a PS-calibration

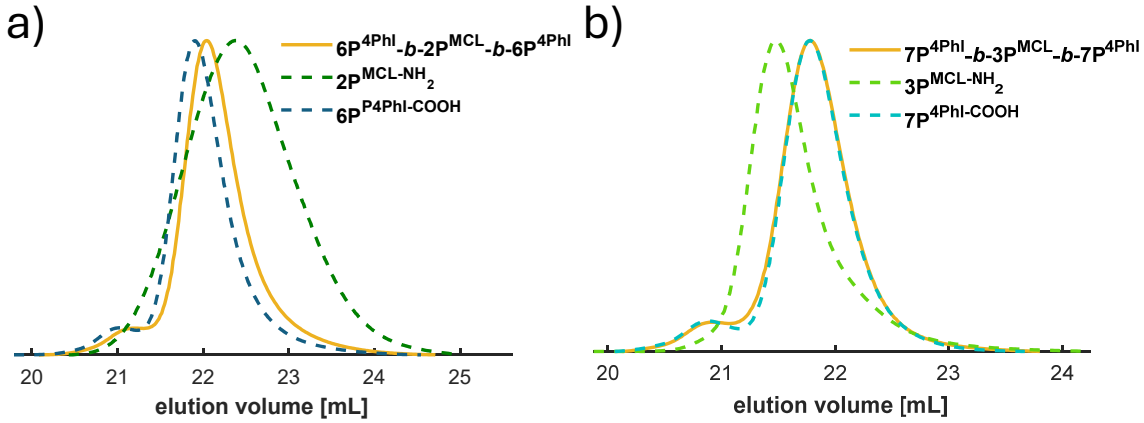


**Figure 6**: SEC traces of the triblock copolymers a) 6P$^{4PhI}$-*b*-2P$^{MCL}$-*b*-6P$^{4PhI}$ and b) 7P$^{4PhI}$-*b*-3P$^{MCL}$-*b*-7P$^{4PhI}$ with the respective polymers used for the coupling reaction.

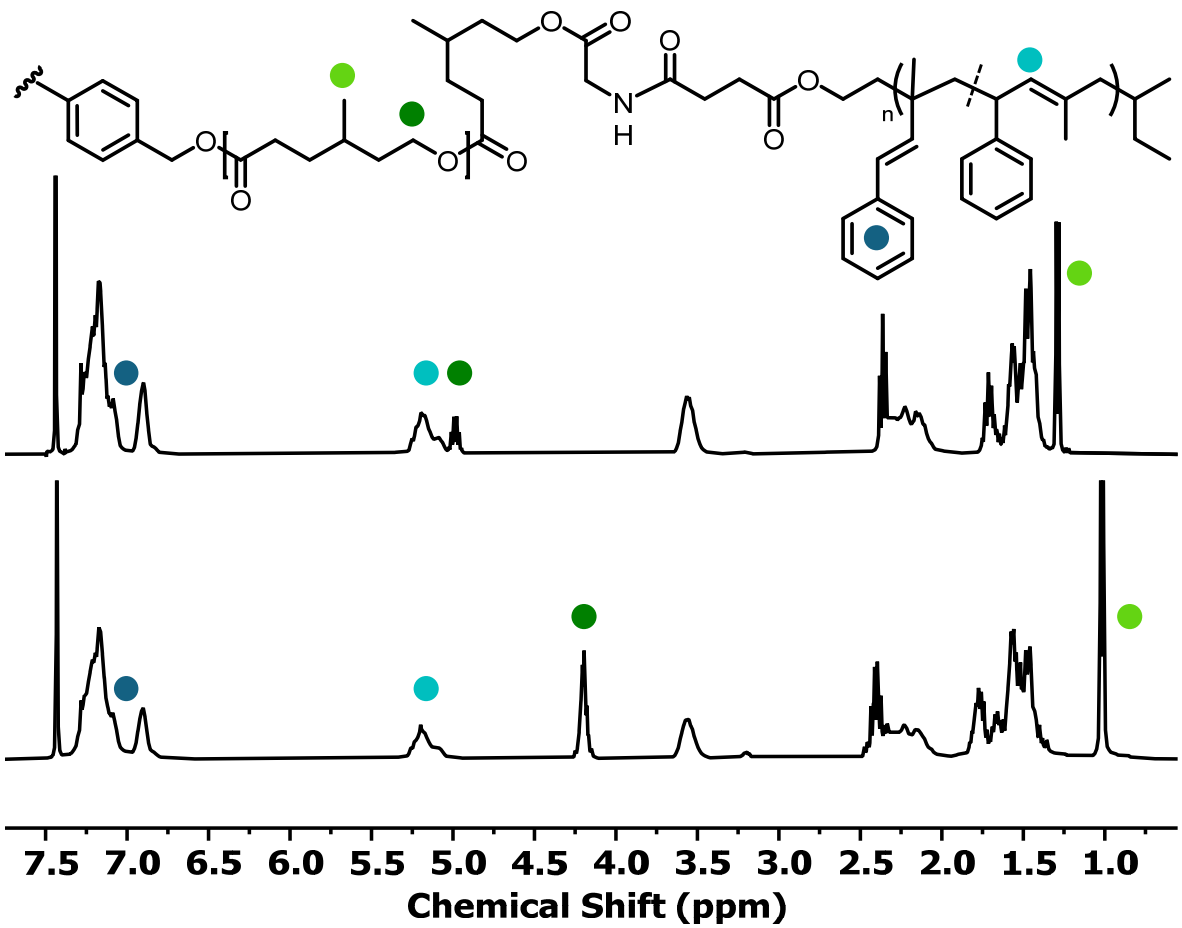


**Figure 7**: Stacked $^{1}$H NMR spectra ($CDCl_3$, 400 MHz) of the coupled polymers $6P^{4PhI}$-*b*-$2P^{MCL}$-*b*-$6P^{4PhI}$ (bottom) and $7P^{4PhI}$-*b*-$3P^{MCL}$-*b*-$7P^{4PhI}$ (top).

For the triblock copolymers containing $6P^{4PhI}$ and $7P^{4PhI}$ as the hard segments, DOSY NMR spectroscopy suggests the presence of a distinct polymer species (**Figure S21** and **Figure S22**). The respective spectra utilizing $8P^{1PhI}$ and $9P^{1PhI}$ indicate the presence of two species or tails within the aromatic region of the spectrum (**Figure S23** and **Figure S24**). The data suggest that there was no quantitative conversion into the carboxy species of the respective P1PhI polymers and that sufficient coupling did not occur. Thermal analysis of the four samples reveals two glass temperatures except for sample $7P^{4PhI}$-*b*-$3P^{MCL}$-*b*-$7P^{4PhI}$. Here, just one glass temperature could be observed (**Figure S25**). The appearance of both polymer species in two distinctive methods puts the results of SEC measurements in question. We attribute this phenomenon to a unique aggregation in solution resulting in an almost unchanged hydrodynamic radius as it has been reviewed as one potential reason by Michels *et al.*[41]

Cyclization reactions were conducted with all four samples listed in **Table 4**. In contrast to previous methods, the reactions were carried out under more dilute and milder conditions to minimize potential side reactions.[42] In accordance with earlier studies, all samples displayed elevated dispersities and decreased molar masses (**Table 5**).[9,13,42] Interestingly, SEC measurements revealed that the molar masses of the polymers with an initially higher molar mass were comparable to those with lower degree of polymerization (**Figure 8** and **Figure S26**). The $^{1}$H NMR spectra exhibited the anticipated broadening of the polyphenyl isoprene related signals while the signals of the inner PMCL block remained unaltered (**Figure S27** and **Figure S28**). Despite the absence of degradation, no $T_g$s were determined in the corresponding DSC measurements (**Figure S29**). This observation can be attributed to the low mobility of the cyclized blocks which impedes the necessary phase segregation required for the determination of $T_g$s through thermal analysis. Although the ultimate objective comprising two cyclized rigid blocks was not attained, this project successfully revealed a novel synthetic strategy with potential for future developments.

**Table 5**: Overview over obtained data after cyclization.

| Sample | $M_{n,ABA}$[a] [kg mol$^{-1}$] | $M_{n,cyc}$[a] [kg mol$^{-1}$] | $Đ$[a] |
|---|---|---|---|
| *cyc*6P$^{4Phl}$-*b*-2P$^{MCL}$-*b*-*cyc*6P$^{4Phl}$ | 24.8[b] | 1.3[b] | 1.25 |
| *cyc*7P$^{4Phl}$-*b*-3P$^{MCL}$-*b*-*cyc*7P$^{4Phl}$ | 32.2[b] | 1.1[b] | 1.25 |
| *cyc*8P$^{1Phl}$-*b*-2P$^{MCL}$-*b*-*cyc*8P$^{1Phl}$ | 22.8[c] | 6.7[c] | 1.65 |
| *cyc*9P$^{1Phl}$-*b*-3P$^{MCL}$-*b*-*cyc*9P$^{1Phl}$ | 40.4[c] | 3.0[c] | 1.91 |

[a] Determination *via* a SEC (Eluent: THF; 30°C), [b] Determination utilizing a PI-calibration, [c] Determination utilizing a PS-calibration

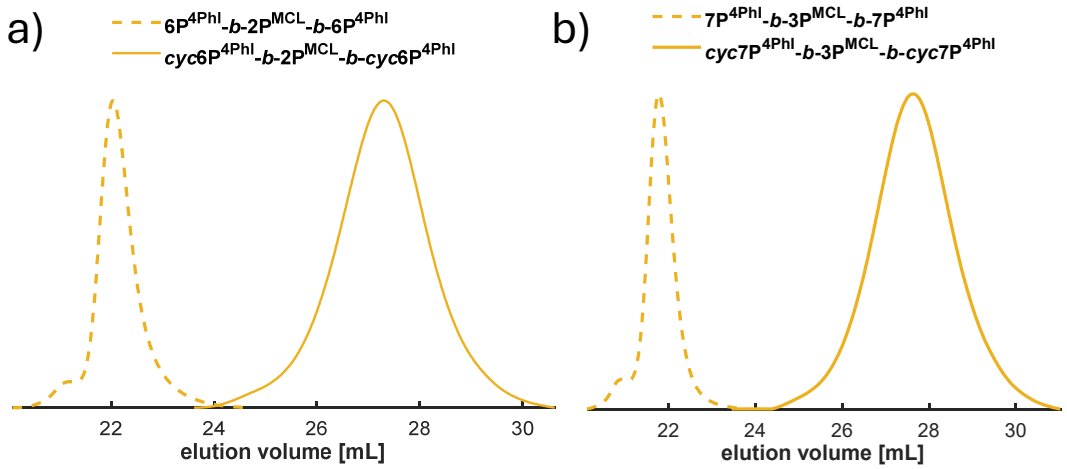


**Figure 8**: SEC traces of a) *cyc*6P$^{4PhI}$-*b*-2P$^{MCL}$-*b*-*cyc*6P$^{4PhI}$ and b) *cyc*7P$^{4PhI}$-*b*-3P$^{MCL}$-*b*-*cyc*7P$^{4PhI}$ with their respective precursors.

## Conclusion

This works describes the synthesis of a triblock copolymer *via* a coupling approach, which is inspired from polymer peptide conjugate synthesis. Prior to the coupling, low $T_g$ and non-crystalline PMCL was synthesized with molar masses up to 33.4 kg mol$^{-1}$. The end groups were converted to amines through esterification with *N*-Boc glycine and subsequent cleavage of the Boc group. Here, the synthetic pathway was modified accordingly preventing initially observed degradation. The successful end group modifications were tracked *via* SEC, NMR, and MALDI ToF MS. Additionally, termination of the anionic polymerization of 1PhI and 4PhI with ethylene oxide gave well-defined *ω*-functionalized phenyl substituted polydienes with molar masses between 4.5 – 38.3 kg mol $^{-1}$. An esterification gave *ω*-carboxy PPhI enabling the SPPS-analogous coupling *via* PyAOP. The successful coupling towards triblock copolymers was indicated by NMR and DSC experiments. The SEC measurements displayed indications of unanticipated behavior in solution, which yielded in misleading interpretation of the data. In contrast, NMR spectroscopy and DSC measurements evidence the existence of the respective utilized polymers. Therefore, a unique composition of a triblock copolymer which cannot be synthesized by combination of polymerization methods was obtained. Subsequently, the PPhI blocks were subjected to a cyclization process with the objective of inducing a significant increase in rigidity. NMR analysis revealed that the polyester signals remained unaltered. Nevertheless, thermal analysis did not present $T_g$s, indicating

that phase segregation was insufficient. In conclusion, the synthesis of unconventional triblock copolymers was achieved through considerable synthetic effort, which needs to be subjected to further analytical characterization.

## References


1 W. Wang, W. Lu, A. Goodwin, H. Wang, P. Yin, N. G. Kang, K. Hong and J. W. Mays, *Prog Polym Sci*, 2019, **95**, 1–31.

2 J. M. Bolton, M. A. Hillmyer and T. R. Hoye, *ACS Macro Lett*, 2014, **3**, 717–720.

3 K. Knoll and N. Nießner, *Macromol Symp*, 1998, **132**, 231–243.

4 M. K. Mahanthappa, L. S. Lim, M. A. Hillmyer and F. S. Bates, *Macromolecules*, 2007, **40**, 1585–1593.

5 R. E. Cunningham, *J Appl Polym Sci*, 1978, **22**, 2907–2913.

6 T. Suzuki, Y. Tsuji, Y. Takegami and H. J. Harwood, *Macromolecules*, 1979, **12**, 234–239.

7 Y. Cai, J. Lu, G. Jing, W. Yang and B. Han, *Macromolecules*, 2017, **50**, 7498–7508.

8 Y. Jiang, X. Kang, Z. Zhang, S. Li and D. Cui, *ACS Catal*, 2020, **10**, 5223–5229.

9 H. Bai, L. Han, W. Li, C. Li, S. Zhang, X. Wang, Y. Yin, H. Yan and H. Ma, *Macromolecules*, 2021, **54**, 1183–1191.

10 T. Suzuki, Y. Tsuji and Y. Takegami, *Macromolecules*, 1978, **11**, 639–644.

11 T. Suzuki, Y. Tsuji, Y. Watanabe and Y. Takegami, *Polym J*, 1979, **11**, 937–945.

12 T. Suzuki, Y. Tsuji, Y. Watanabe and Y. Takegami, *Polym J*, 1979, **11**, 651–660.

13 M. Rauschenbach, L. Stein, G. M. Linden, R. Barent, K. Heinze and H. Frey, *Polym Chem*, 2024, **15**, 3204–3213.

14 A. Nakahara, K. Satoh and M. Kamigaito, *Macromolecules*, 2009, **42**, 620–625.

15 R. K. Agnihotri, D. Falcon and E. C. Fredericks, *J Polym Sci A1*, 1972, **10**, 1839–1850.

16 R. Y. Asami, K.-I. Hasegawa and T. Onoe, *Polym J*, 1976, **8**, 43–52.

17 J. Lal, *Polymer (Guildf)*, 1998, **39**, 6183–6186.

18 J. N. Hay, M. Sabir and R. L. T. Steven, *Polymer (Guildf)*, 1969, **10**, 187–202.

19 M. J. Jenkins and K. L. Harrison, *Polym Adv Technol*, 2006, **17**, 474–478.

20 M. T. Martello and M. A. Hillmyer, *Macromolecules*, 2011, **44**, 8537–8545.

21 D. C. Batiste, M. S. Meyersohn, A. Watts and M. A. Hillmyer, *Macromolecules*, 2020, **53**, 1795–1808.

22 A. Watts, N. Kurokawa and M. A. Hillmyer, *Biomacromolecules*, 2017, **18**, 1845–1854.

23 S. Liffland, M. Kumler and M. A. Hillmyer, *ACS Macro Lett*, 2023, 1331–1338.

24 M. S. Meyersohn, F. M. Haque and M. A. Hillmyer, *ACS Polymers Au*.

25 D. J. Lundberg, D. J. Lundberg, M. A. Hillmyer and P. J. Dauenhauer, *ACS Sustain Chem Eng*, 2018, **6**, 15316–15324.

26 G. X. De Hoe, M. T. Zumstein, B. J. Tiegs, J. P. Brutman, K. McNeill, M. Sander, G. W. Coates and M. A. Hillmyer, *J Am Chem Soc*, 2018, **140**, 963–973.

27 C. Pascouau, M. Schweitzer and P. Besenius, *Biomacromolecules*, 2024, 25, 2659–2678.

28 N. Uyanik and B. M. Baysal, *J Appl Polym Sci*, 1990, **41**, 1981–1993.

29 P. J. Das, A. Barak, Y. Kawakami and T. Kannan, *J Polym Sci A Polym Chem*, 2011, **49**, 1376–1386.

30 E. H. Orhan, I. Yilgör and B. M. Baysal, *Polymer (Guildf)*, 1977, **18**, 286–290.

31 F. Albericio and A. El-Faham, *Org Process Res Dev*, 2018, **22**, 760–772.

32 R. Otter, C. M. Berac, S. Seiffert and P. Besenius, *Eur Polym J*, 2019, **110**, 90–96.

33 P. Dreier, J. Ahn, T. Chang and H. Frey, *Macromol Rapid Commun*, 2022, **43**, 2200560.

34 C. Tonhauser and H. Frey, *Macromol Rapid Commun*, 2010, **31**, 1938–1947.

35 A. Watts, N. Kurokawa and M. A. Hillmyer, *Biomacromolecules*, 2017, **18**, 1845–1854.

36 S. Schöttner, M. Brodrecht, E. Uhlein, C. Dietz, H. Breitzke, A. A. Tietze, G. Buntkowsky and M. Gallei, *Macromolecules*, 2019, **52**, 2631–2641.

37 A. Lv, Y. Cui, F. S. Du and Z. C. Li, *Macromolecules*, 2016, **49**, 8449–8458.

38 A. Lv, Z. L. Li, F. S. Du and Z. C. Li, *Macromolecules*, 2014, **47**, 7707–7716.

39 P. Dreier, A. Pipertzis, M. Spyridakou, R. Mathes, G. Floudas and H. Frey, *Macromolecules*, 2022, **55**, 1342–1353.

40 E. Frérot, J. Coste, A. Pantaloni, M. N. Dufour and P. Jouin, *Tetrahedron*, 1991, **47**, 259–270.

41 K. Philipps, T. Junkers and J. J. Michels, *Polym Chem*, 2021, **12**, 2522–2531.

42 Y. Cai, J. Lu, D. Zuo, S. Li, D. Cui, B. Han and W. Yang, *Macromol Rapid Commun*, 2018, **39**, 1800298.

# Supporting Information

## Synthesis Protocols

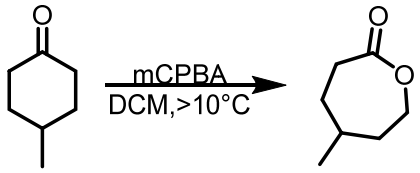


***γ*-Methyl-*ε*-Caprolactone**: Following literature known procedures[1], 125 g (0.56 mol) 77% *meta*-chloroperbenzoic acid (mCPBA) was dissolved in dichloro methane (1.5 L, DCM). The water phase was removed *via* a pipet, before the solution was further dried by magnesium sulfate. Subsequently, the solution was filtered into a round-bottom flask and then cooled in an ice-bath. 50 g (55 mL, 0.45 mol) 4-methylcyclohexanone (MCH) was added dropwise to the solution. The ice-bath was removed, and the reaction was slowly warmed up to room temperature. In the meantime, *meta*-chlorobenzoic acid (mCBA) started to precipitate, which was removed by filtration. The filtration was repeated after the filtrate was concentrated to half the volume. The solution was washed with 10% aqueous sodium bisulfite and subsequently saturated sodium bicarbonate. The solution was dried brine and by stirring over magnesium sulfate. The solvent was removed under reduced pressure. The pure product was obtained *via* fractionated distillation (36.5 g, 0.28 mol, yield = 64%).

**$^{1}$H NMR** ($CDCl_3$, 400 MHz): δ(ppm) = 4.23 (t, 2H, H−**1**), 2.62 (t, 2H, H-**5**), 1.91 (q, 2H, H-**2**), 1.76 (q, 1H, H-**3**), 1.60 – 1.24 (m, 2H, H-**4**), 0.98 (d, 3H, H-**7**).

**$^{13}$C NMR** ($CDCl_3$, 101 MHz): δ(ppm) = *176.04 (C-**6**), 68.02 (C−**1**), 37.15 (C-**3**), 35.11 (C-**2**), 33.11 (C-**5**), 30.69 (C-**4**), 22.05 (C-**7**).*

**Phenyl isoprenes (1PhI and 4PhI)**:

The synthesis of 1PhI and 4PhI was achieved according to previously reported Wittig reaction subsequent extraction.[2]

**Ring-Opening Transesterification Polymerization**:

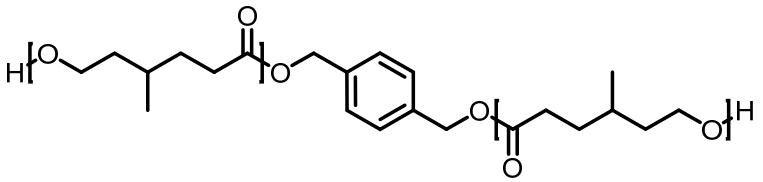

Prior to the polymerization, MCL was dried over calcium hydride overnight and then distilled. After repetition of the drying procedure, the required amounts of MCL, BDM and Sn(Oct)2 were transferred into a Schlenk tube under argon atmosphere in a glovebox. In addition, dry toluene (*c*(MCL) = 5 M) was added, and the reaction vessel was transferred outside of the glovebox in a 105°C heated oil bath. The polymer was precipitated in cold *n*-pentane and dried under vacuum.

**$^{1}$H NMR** ($CDCl_3$, 400 MHz) δ = 7.34 (m, H-**9**), 5.09 (s, H-**8**), 4.16 – 4.02 (t, H-**1**), 2.39 – 2.20 (t, H-**5**), 1.73 – 1.61 (q, H-**3**), 1.60 – 1.39 (m, H-**2,4**), 0.91 (d, H-**7**).

**$^{13}$C NMR** ($CDCl_3$, 101 MHz): δ(ppm) = 173.89 (C-**6**), 128.53 (C-**9**), 62.74 (C−**1,8**), 35.35 (C-**2**), 31.96 (C-**4,5**), 29.69 (C-**3**), 19.15 (C-**7**).

**Synthesis of *α,ω-N*-Boc-glycine-PMCL**:

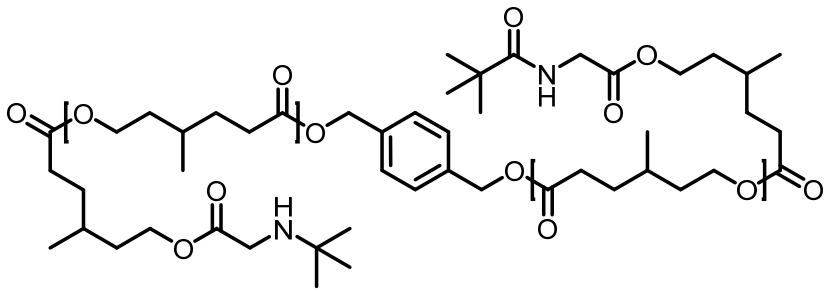

22 g (1.1 mmol) of PMCL was dried overnight with benzene in a flame dried Schlenk flask equipped with a septum. The polymer was dissolved in dry DCM (55 mL), then DMAP (54 mg, 440 µmol) and N-Boc glycine (1.54 g, 8.8 mmol) were added, and the solution was cooled to 0°C. Subsequently, DIC (1.11 g, 8.8 mmol) was added under stirring. The solution was allowed to slowly warm up to room temperature and stirred for 4 hours. The polymer was precipitated twice in cold *n*-pentane and dried under high vacuum yielding 19 g of *α,ω-N*-Boc-glycine-PMCL (1 mmol, 84%).

**$^{1}$H NMR** ($CDCl_3$, 400 MHz) δ = 7.34 (m, H-**9**), 5.09 (s, H-**8**), 4.16 – 4.02 (t, H−**1**), 2.39 – 2.20 (t, H-**5**), 1.73 – 1.61 (q, H-**3**), 1.60 – 1.39 (m, H-**2,4,10**), 0.91 (d, H-**7**).

**Synthesis of *α,ω*-$NH_2$-PMCL**:

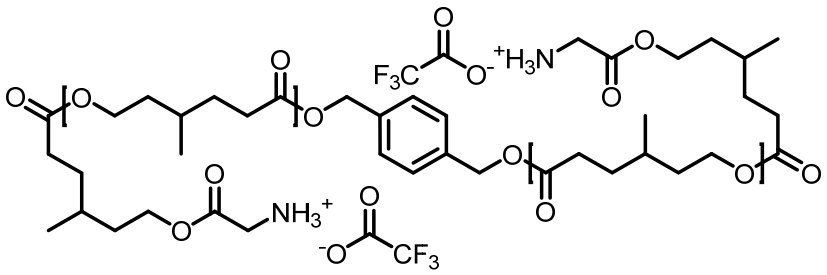

*α,ω-N*-Boc-glycine-PMCL (18 g, 975 µmol) was dissolved in 70 mL DCM. In an ice-bath, the reaction solution was cooled to − 20°C. TFA (15 mL, 195 mmol) was added under stirring. The cooled polymer solution was stirred for 2 hours before precipitation in a ten-fold cold *n*-pentane. The polymer was redissolved in DCM and again precipitated in cold *n*-pentane. Residual TFA was removed azeotropically with benzene under high vacuum.

**$^1$H NMR** ($CDCl_3$, 400 MHz) δ = 8.81 (broad, H-**10**), 7.34 (m, H-**9**), 5.09 (s, H-**8**), 4.16 – 4.02 (t, H-**1**), 2.39 – 2.20 (t, H-**5**), 1.73 – 1.61 (q, H-**3**), 1.60 – 1.39 (m, H-**2,4**), 0.91 (d, H-**7**).

**Synthesis of *ω*-Hydoxyl Poly(Phenylisoprene)**:

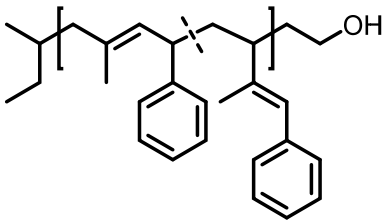

The preliminary determined amount of the respective phenyl isoprene derivative was degassed and dried in flame-dried flasks equipped with a teflon stopper. Under high vacuum ($10^{-3}$ mbar) it was transferred into the flame-dried reaction flask. Dry cyclohexane (90%$_{vol}$) was added, and the flask was flushed with argon. *Sec*-butyl lithium (1.3 M stock solution in cyclohexane/*n*-hexane) was introduced to the reaction solution utilizing a syringe. The solution was left stirring at room temperature for 1 – 2 days. The flask was evacuated to $10^{-3}$ mbar through repeated opening of the Teflon stopper to the vacuum line. Ethylene oxide (10 eq regarding the chain-end concentration), dried with *sec*-butyl lithium, was transferred to the reaction flask *via* cryo-distillation. The polymer solution was stirred overnight and precipitated in a ten-fold of methanol/2-propanol (1:1). The polymers were dried under vacuum.

4PhI: **$^1$H NMR** ($CDCl_3$, 400 MHz) δ = 7.37 – 7.05 (H-**7**), 6.99 – 6.79 (H-**7**), 5.43 – 4.95 (H-**4**), 3.57 (H-**5,9**), 2.41 – 1.99 (H-**2**), 1.69 – 1.36 (H-**6**).

1PhI: **$^1$H NMR** ($CDCl_3$, 400 MHz) δ = 7.49 – 6.76 (H-**7,7'**), 6.30 (H-**5'**), 5.59 – 4.71 (H-**3**), 3.80 (H-**5,9**), 2.84 (H-**3'**), 1.50 (H-**1,2,6,2',6',8**).

**Synthesis of *ω*-Carboxyl Poly(Phenylisoprene)**:

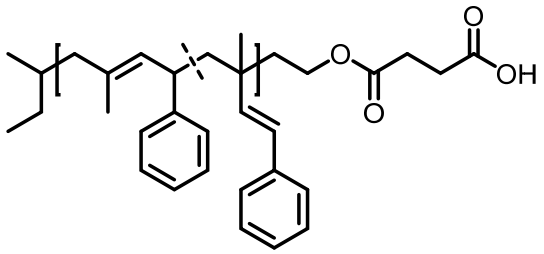


25.5 g (69 mmol) PPhI-OH was dissolved in benzene and freeze dried overnight. To the Schlenk flask further equipped with a stir bar and a condenser, dry DCM (35 mL) and 690 mg (690 mmol) succinic anhydride were added under argon. After dry pyridine (536 µL, 690 mmol) was added, the solution was heated under reflux and argon for 4 days. The reaction was cooled to room temperature and an excess of DCM (300 mL) was added. After extraction with saturated $Na_2CO_3$ (80 mL, twice), 0.1 M HCl (80 mL, twice) and brine (100 mL) the organic phase was dried over $MgSO_4$. After filtration, the solvent was removed under reduced pressure.

**Synthesis of P(PhI)-*b*-P(MCL)-*b*-P(PhI)**

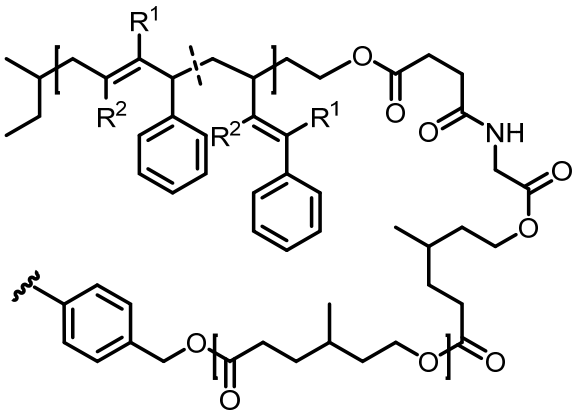


*α,ω*-$NH_2$-PMCL (3.5 g,100 µmol) and P1PhI-COOH (8.3 g, 208 µmol) were dissolved in benzene and freeze-dried overnight. The polymer mixture was dissolved in 85 mL DCM before PyAOP (115 mg, 220 µmol) was added under stirring. After adding $NEt_3$ (142 mg, 1.4 mmol) the solution was stirred for 5 h and subsequently poured in cold *n*-pentane. The polymer was redissolved in DCM and precipitated in cold *n*-pentane. The polymer

P1PhI-*b*-PMCL-*b*-P1PhI (8.7 g, 74%) was dried under vacuum and was obtained as a colorless solid.

**$^1$H NMR** ($CDCl_3$, 400 MHz) δ = 7.34 – 6.84 (H-**7',7''**), 5.36 – 4.98 (H-**4'**), 4.20 (H-**1**), 3.56 (H-**5'**), 2.52 – 2.06 (H-**5,2'**), 1.87 – 1.36 (H-**2,3,4,6',6''**), 1.02 (H-**7**)

**Synthesis of *cyc*P(PhI)-*b*-P(MCL)-*b*-*cyc*P(PhI)**

1 g of $6P^{4PhI}$-*b*-$2P^{MCL}$-*b*-$6P^{4PhI}$ was dissolved in 20 mL cyclohexane. To the heavy stirring solution 0.48 mL (5.4 mmol, 0.95 eq regarding the $P_{n,4PhI}$) of trifluoromethanesulfonic acid in 10 mL of dichloromethane was added. The reaction was left stirring for 1 h at room temperature. Subsequently, the reaction solution was poured into 15 mL of a 1% aqueous solution of $Na_2CO_3$. The organic phase was washed twice with 10 mL water and once with brine. After precipitation in a methanol/2-propanol mixture, the polymer was dried under vacuum. Yield 0.28 g (28%).

## Monomer analysis

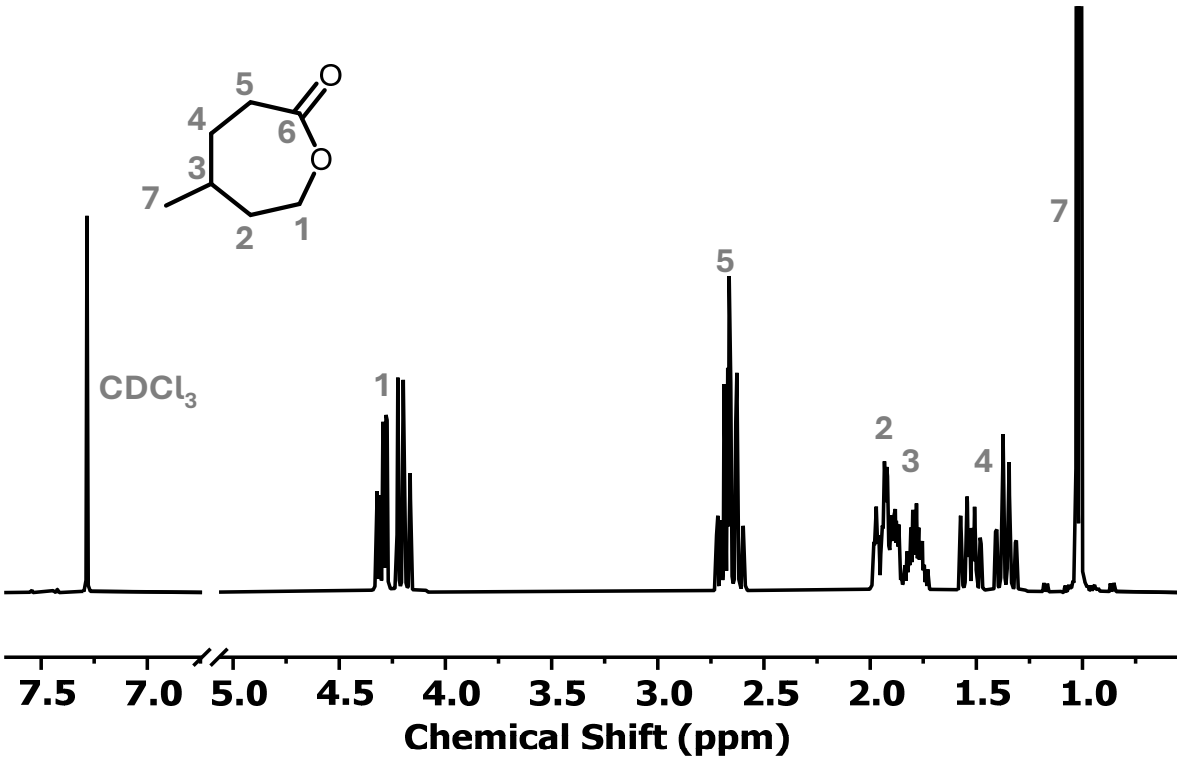


**Figure S1**:$^1$H NMR spectrum ($CDCl_3$, 400 MHz) of MCL.

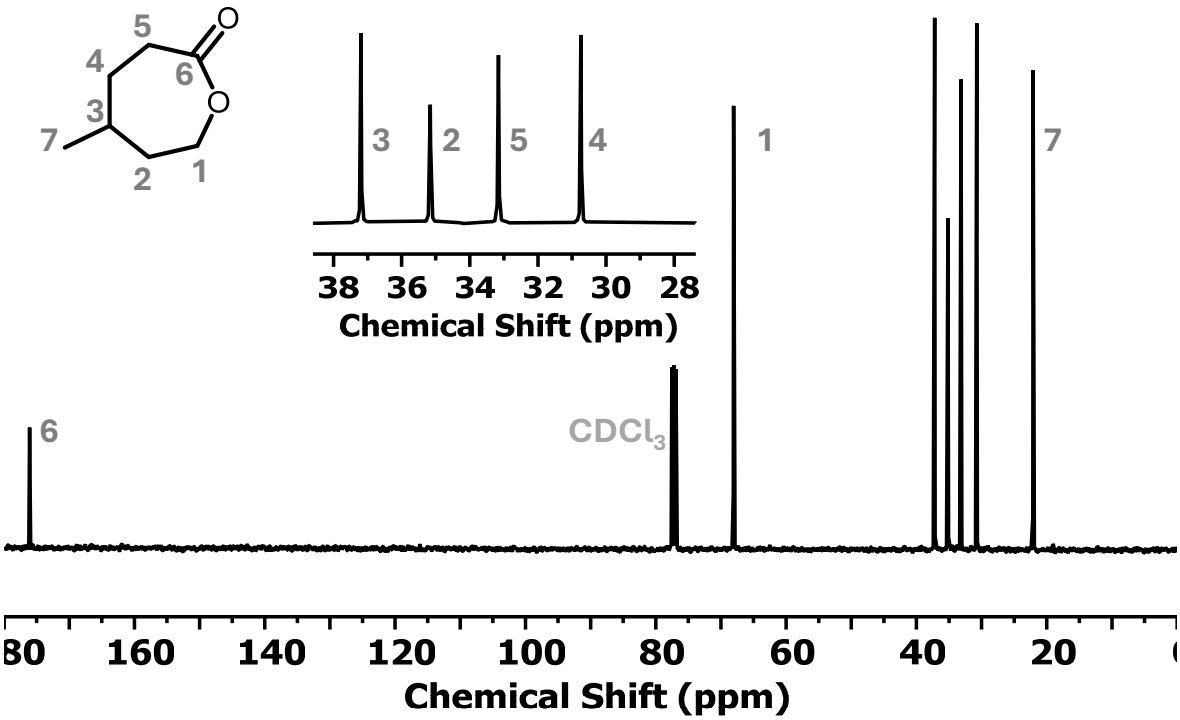


**Figure S2**: $^{13}C$ NMR spectrum ($CDCl_3$, 101 MHz) of MCL.

## Analysis of Polyester Samples

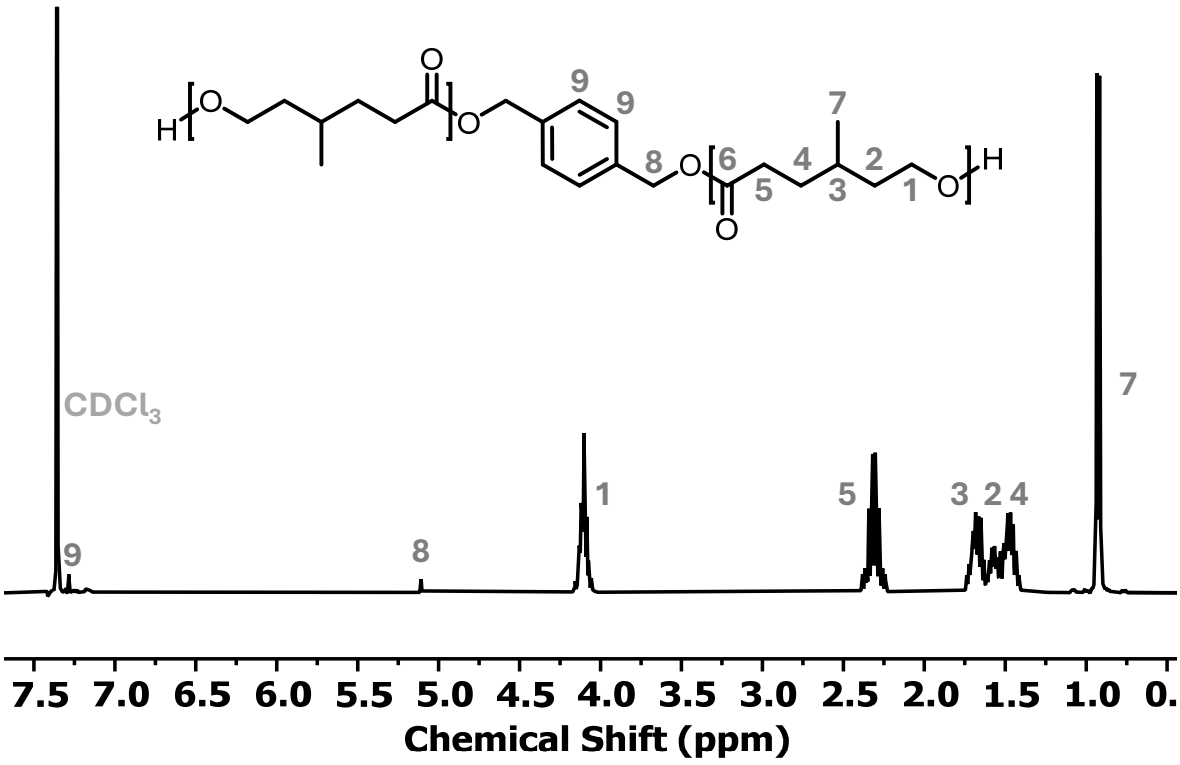


**Figure S3**: $^{1}H$ NMR spectrum ($CDCl_3$, 400 MHz) of $2P^{MCL}$.

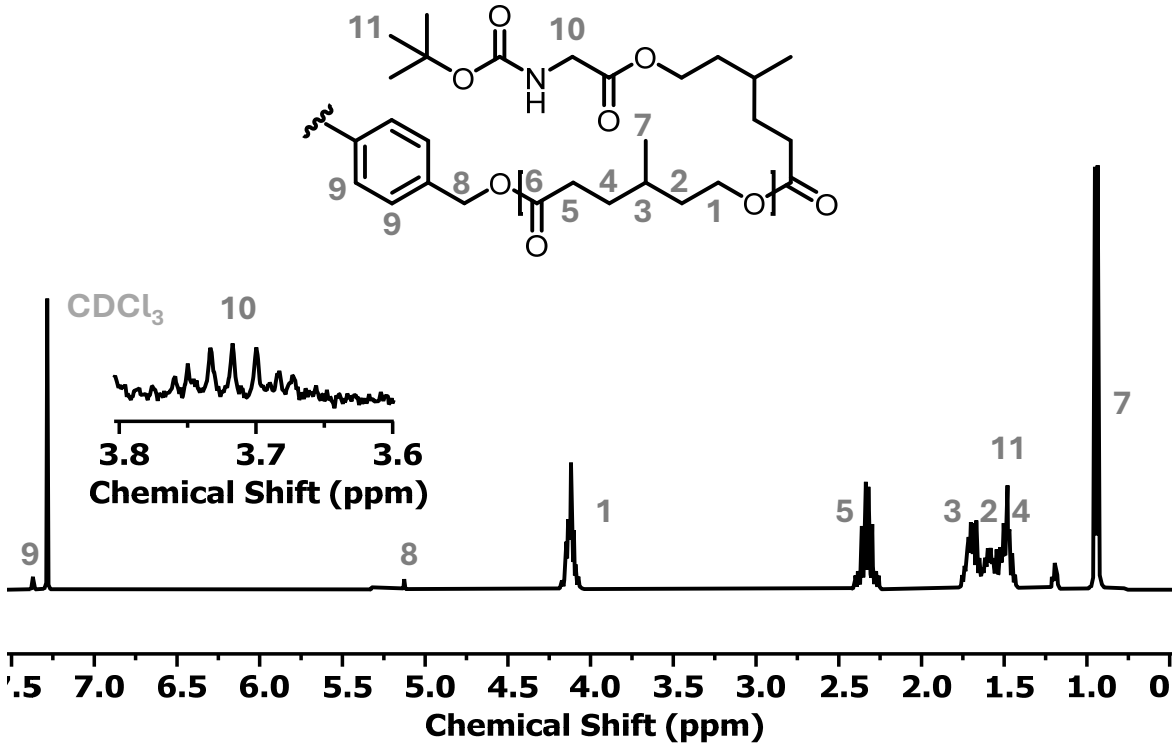


**Figure S4**: $^{1}$H NMR spectrum ($CDCl_3$, 400 MHz) of $2P^{MCL\text{-}N\text{-}Boc}$

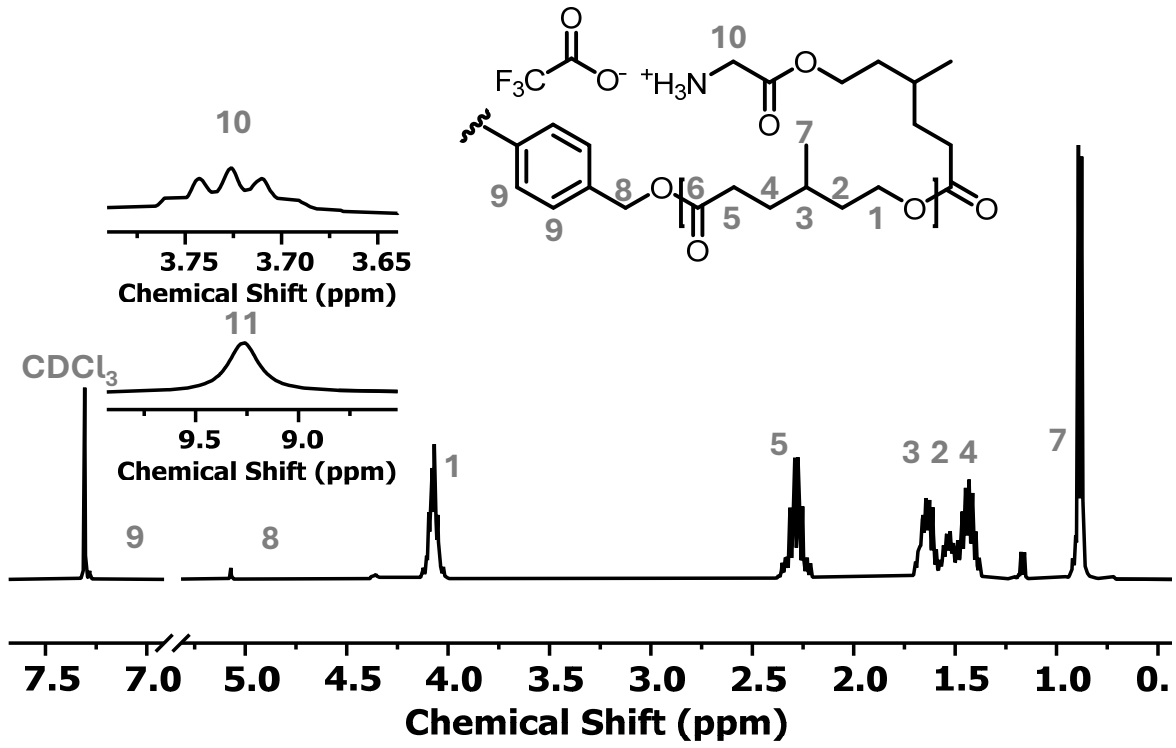


**Figure S5**: $^{1}$H NMR spectrum ($CDCl_3$, 400 MHz) of $2P^{MCL\text{-}NH2}$

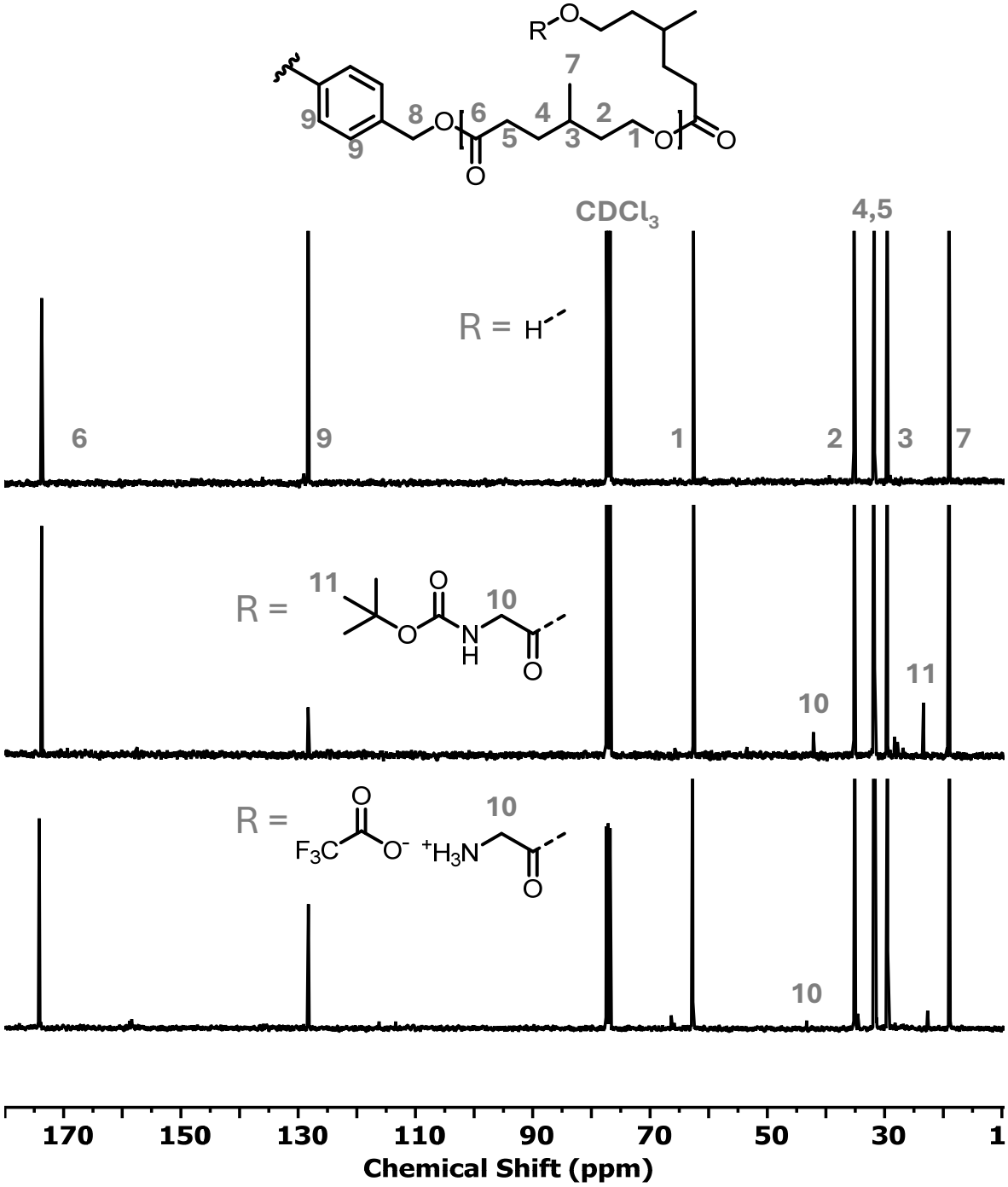


**Figure S6**: Stacked $^{13}C$ NMR (101 MHz, $CDCl_3$) spectra of the $2P^{MCL}$ (top) $2P^{MCL\text{-}N\text{-}Boc}$ (middle) and $2P^{MCL\text{-}NH2}$ (bottom).

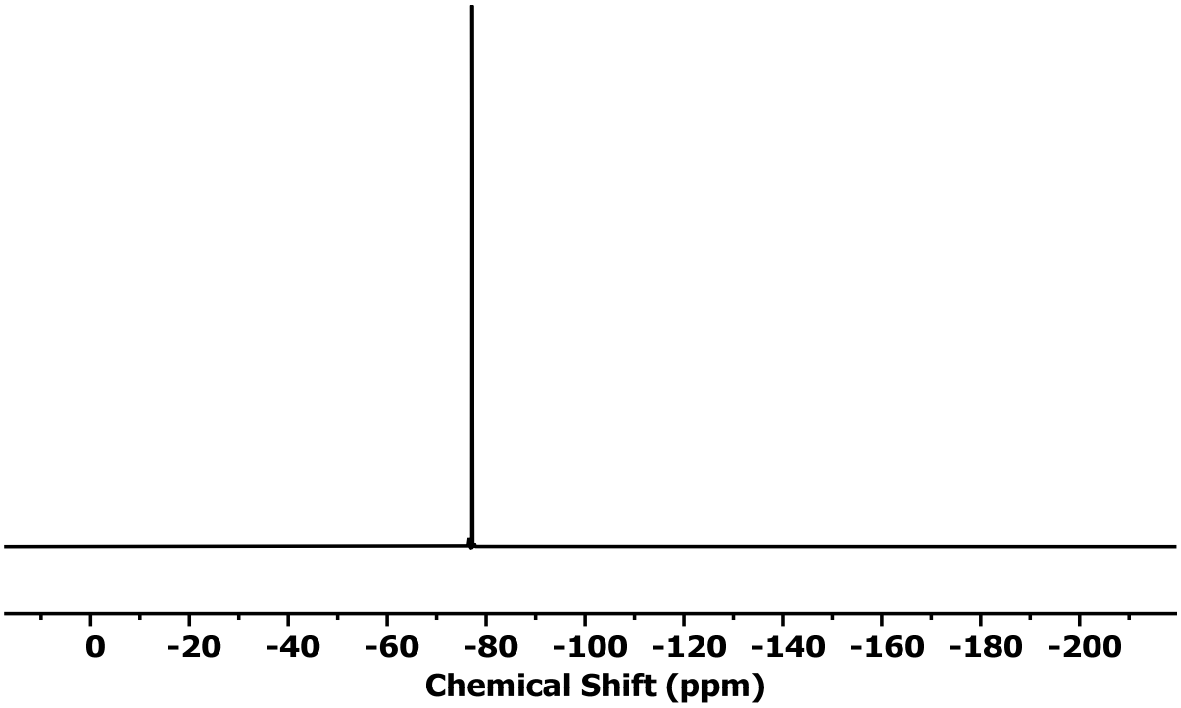


**Figure S7**: $^{19}F$ NMR spectrum ($CDCl_3$, 376 MHz) of $3P^{MCL\text{-}NH2}$

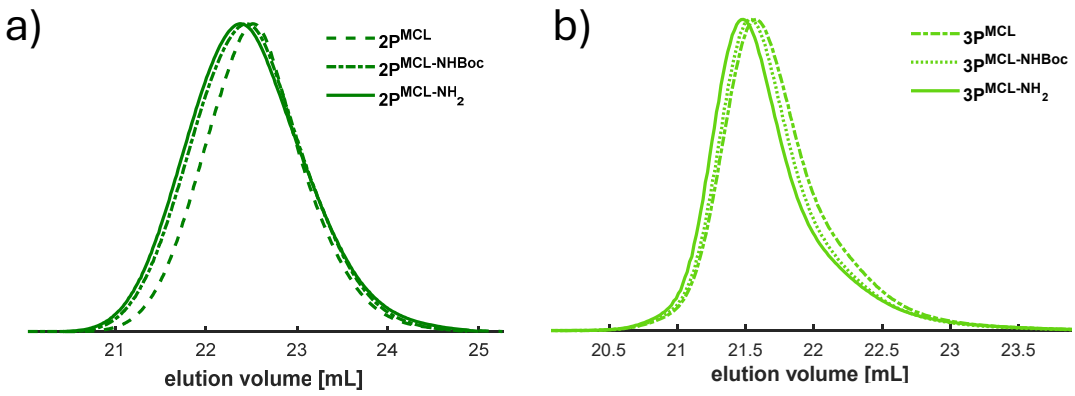


**Figure S8**: SEC traces of a) 2PMCL and b) 3PMCL after the functionalization to *α,ω-N*-Boc-glycine-PMCL and after the cleavage of the protection group to yield *α,ω*-$NH_2$-PMCL with the precursor (dashed) in comparison.

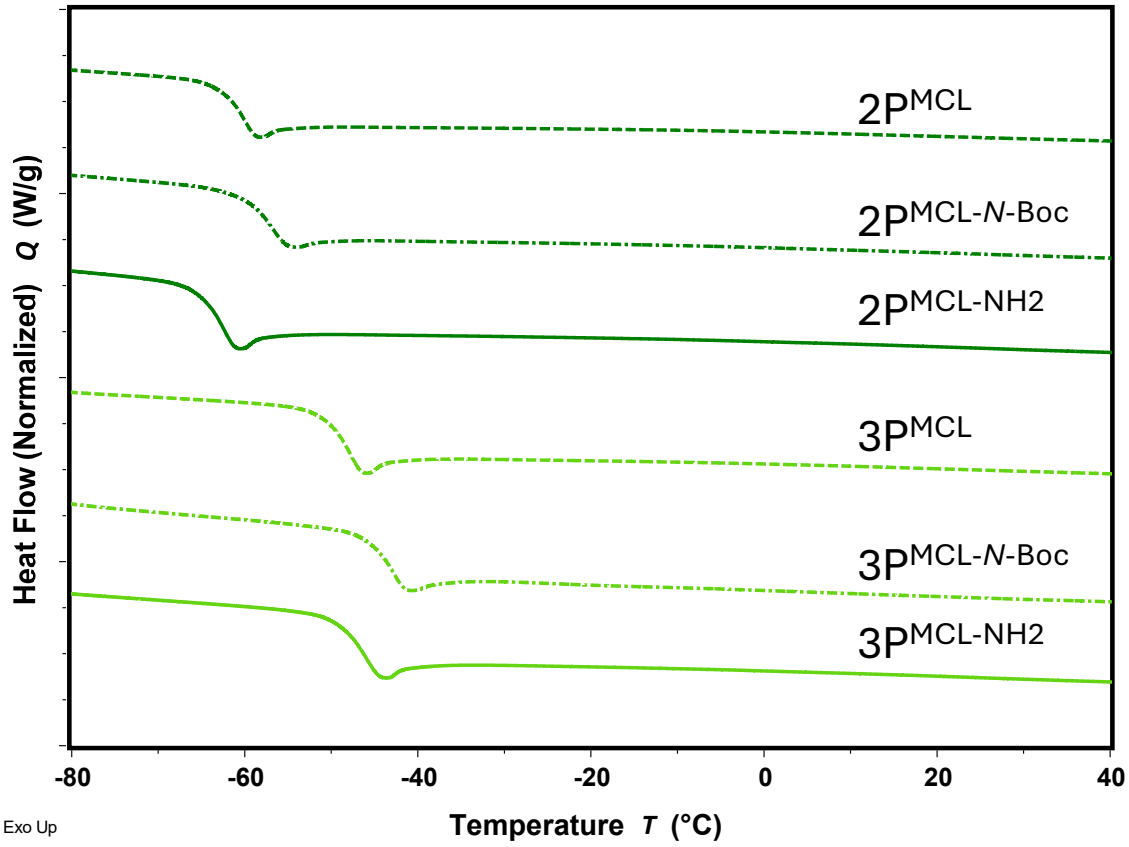


**Figure S9**: DSC curves of the polymers $2P^{MCL}$ and $3P^{MCL}$ with different end groups as listed in **Table 2**

## Analysis of Polydiene Samples

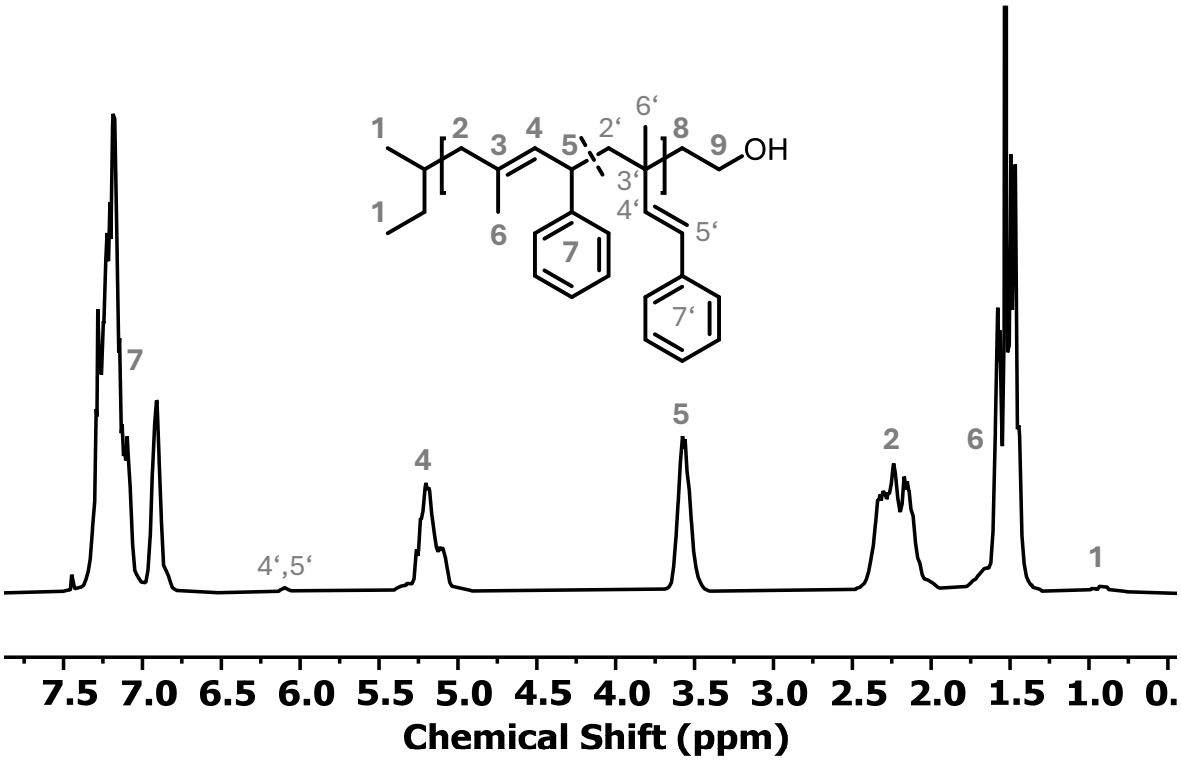


**Figure S10**: $^{1}H$ NMR spectrum ($CDCl_3$, 400 MHz) of $6P^{4PhI\text{-}OH}$.

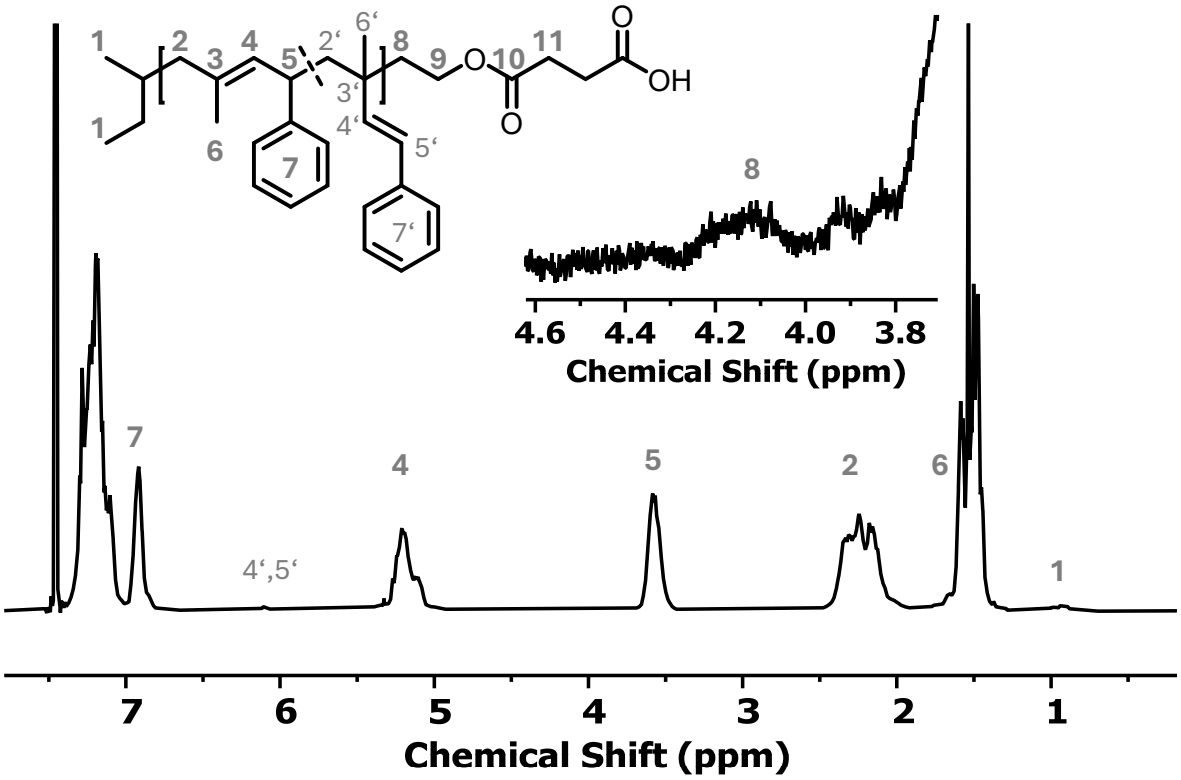


**Figure S11**: $^{1}$H NMR spectrum ($CDCl_3$, 400 MHz) of $6P^{4PhI\text{-}COOH}$.

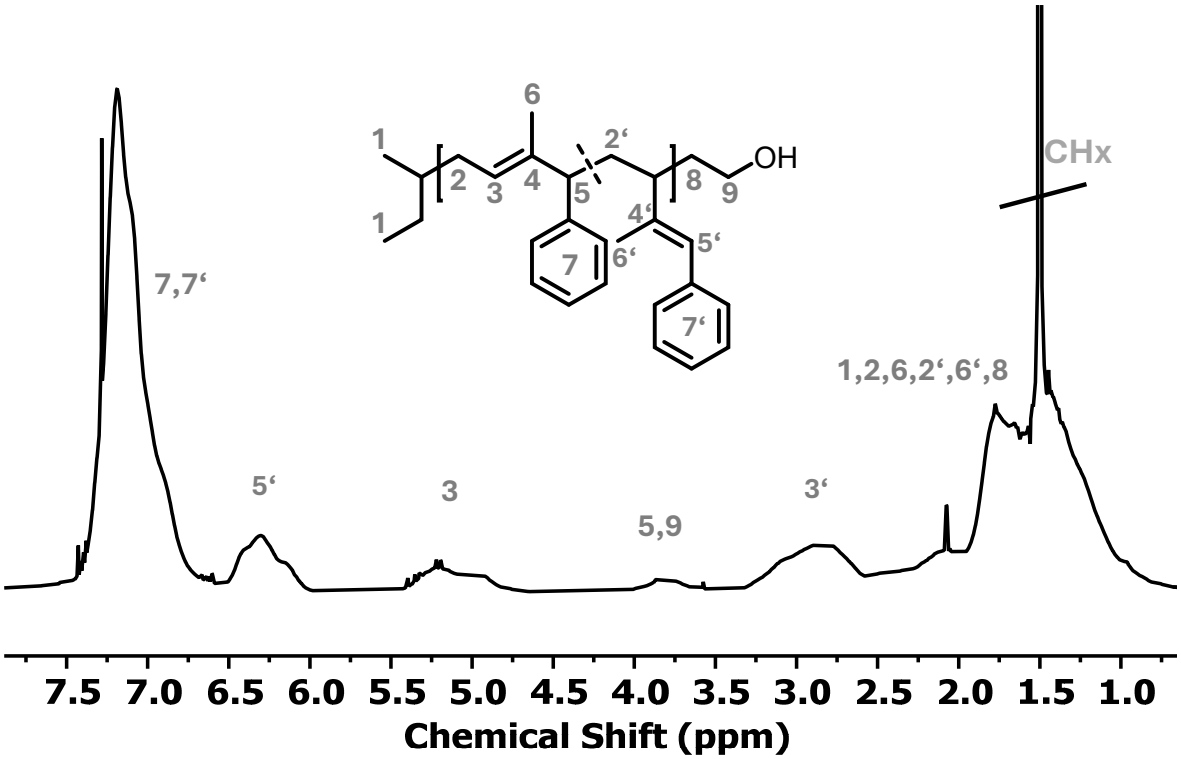


**Figure S12**: $^{1}$H NMR spectrum ($CDCl_3$, 400 MHz) of $7P^{1PhI\text{-}OH}$.

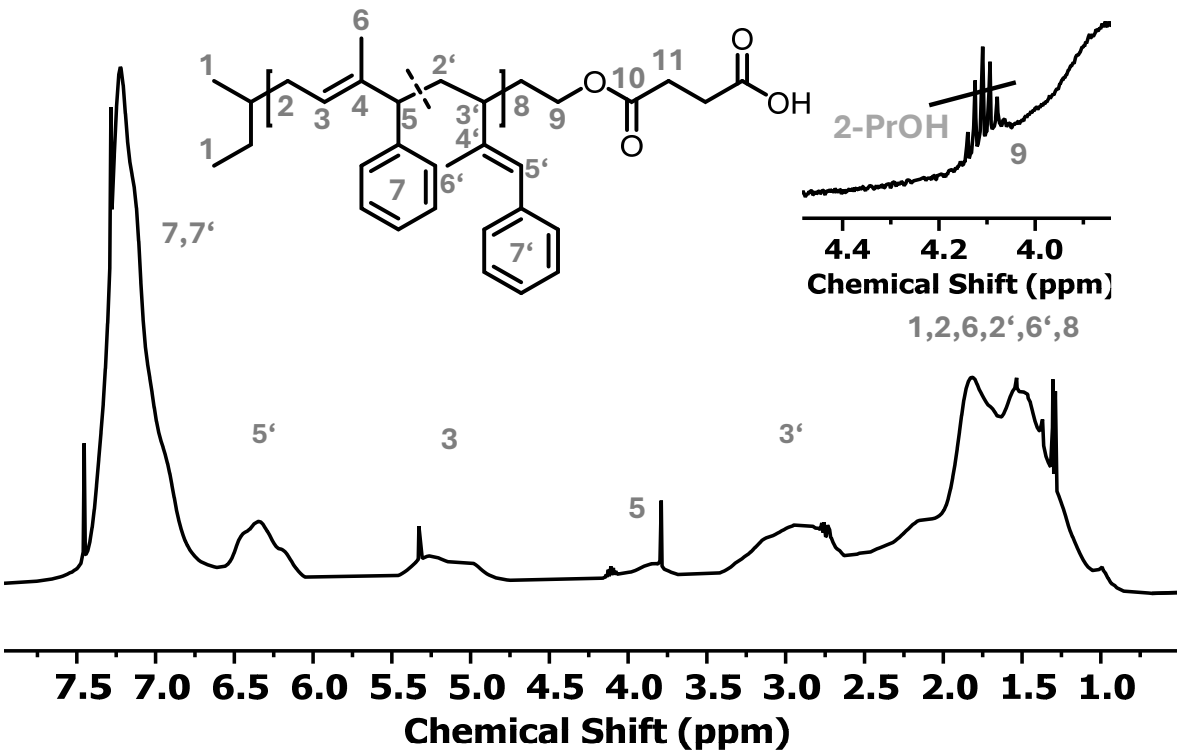


**Figure S13**: $^{1}$H NMR spectrum ($CDCl_3$, 400 MHz) of 7P$^{1PhI\text{-}COOH}$.

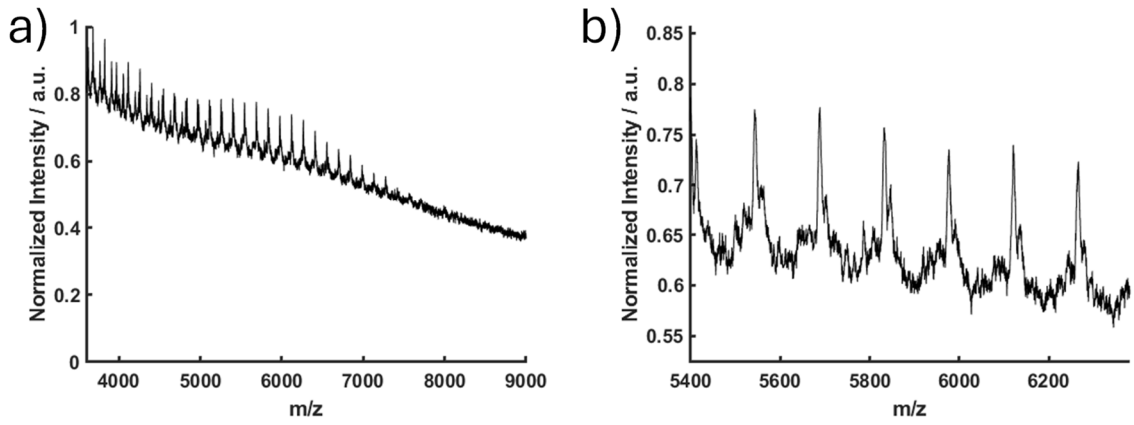


**Figure S14**: MALDI ToF mass spectrum of 4P$^{4PhI\text{-}OH}$ (**Table 3**).

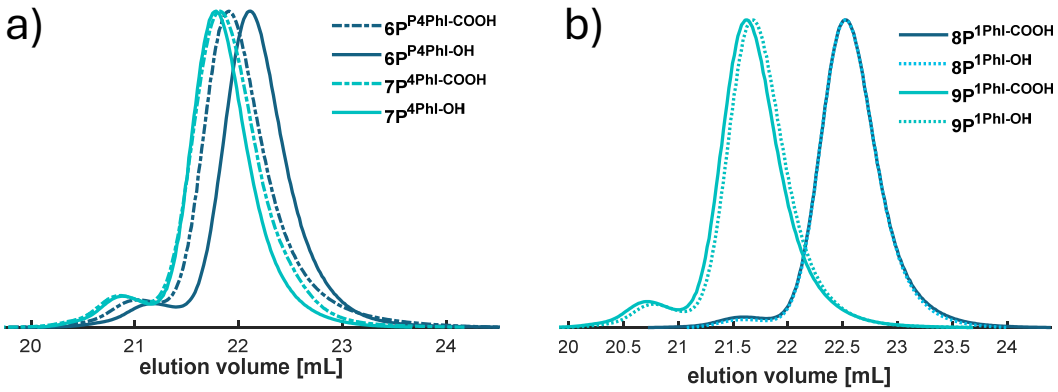


**Figure S15**: SEC traces of the carboxylated polymers based on a) 4PhI and b) 1PhI.

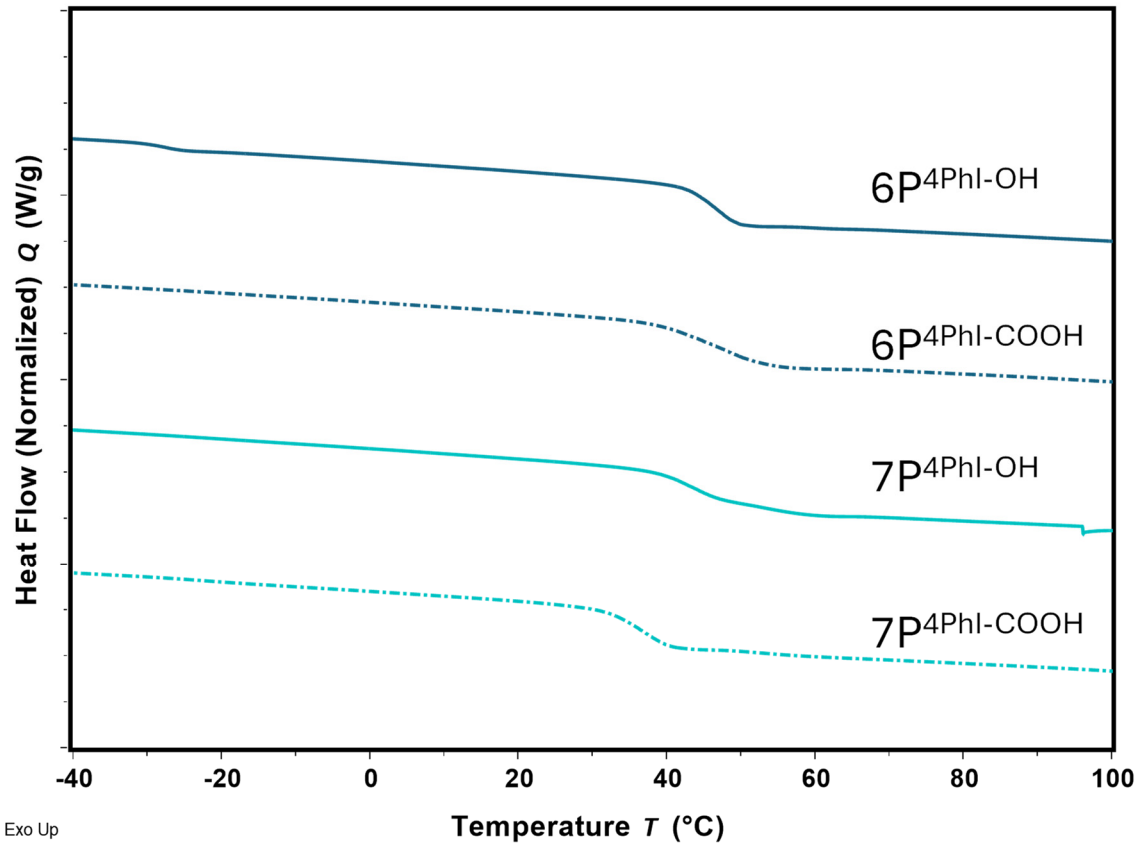


**Figure S16**: DSC curves of $6P^{4PhI\text{-}OH}$, $6P^{4PhI\text{-}COOH}$, $7P^{4PhI\text{-}OH}$and $7P^{4PhI\text{-}COOH}$.

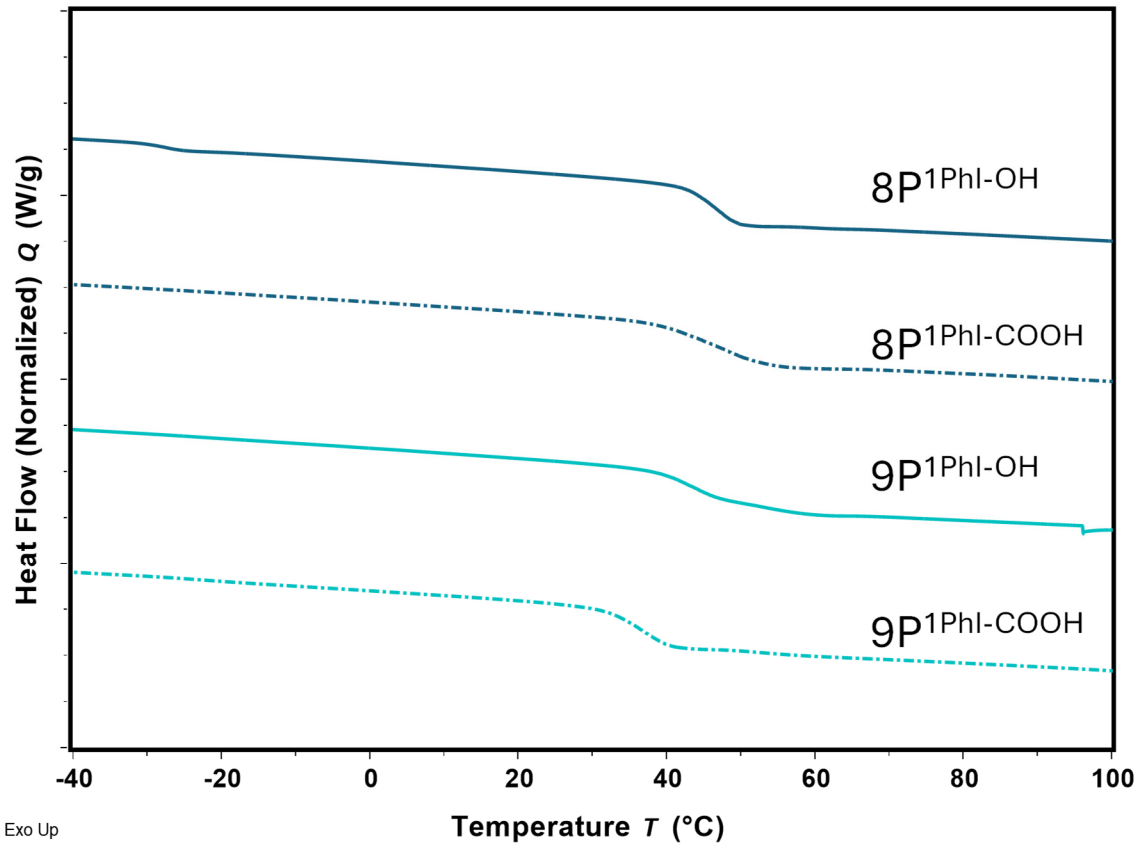


**Figure S17**: DSC curves of $8P^{1PhI\text{-}OH}$, $8P^{1PhI\text{-}COOH}$, $9P^{1PhI\text{-}OH}$and $9P^{1PhI\text{-}COOH}$.

## Analytics of Triblock Copolymers

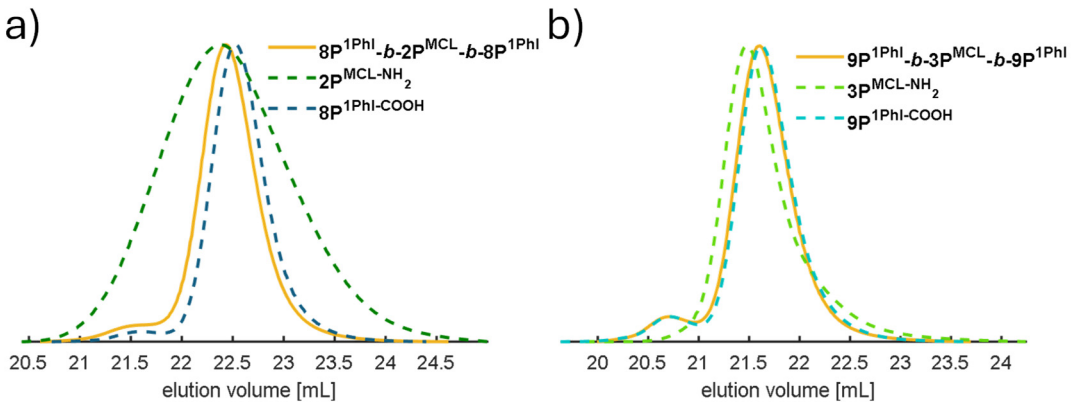


**Figure S18**: SEC traces of the triblock copolymers a) $8P^{1PhI}$-*b*-$2P^{MCL}$-*b*-$8P^{1PhI}$ and b) $9P1^{PhI}$-*b*-$3P^{MCL}$-*b*-$1P1^{PhI}$ with the respective polymers used for the coupling reaction.

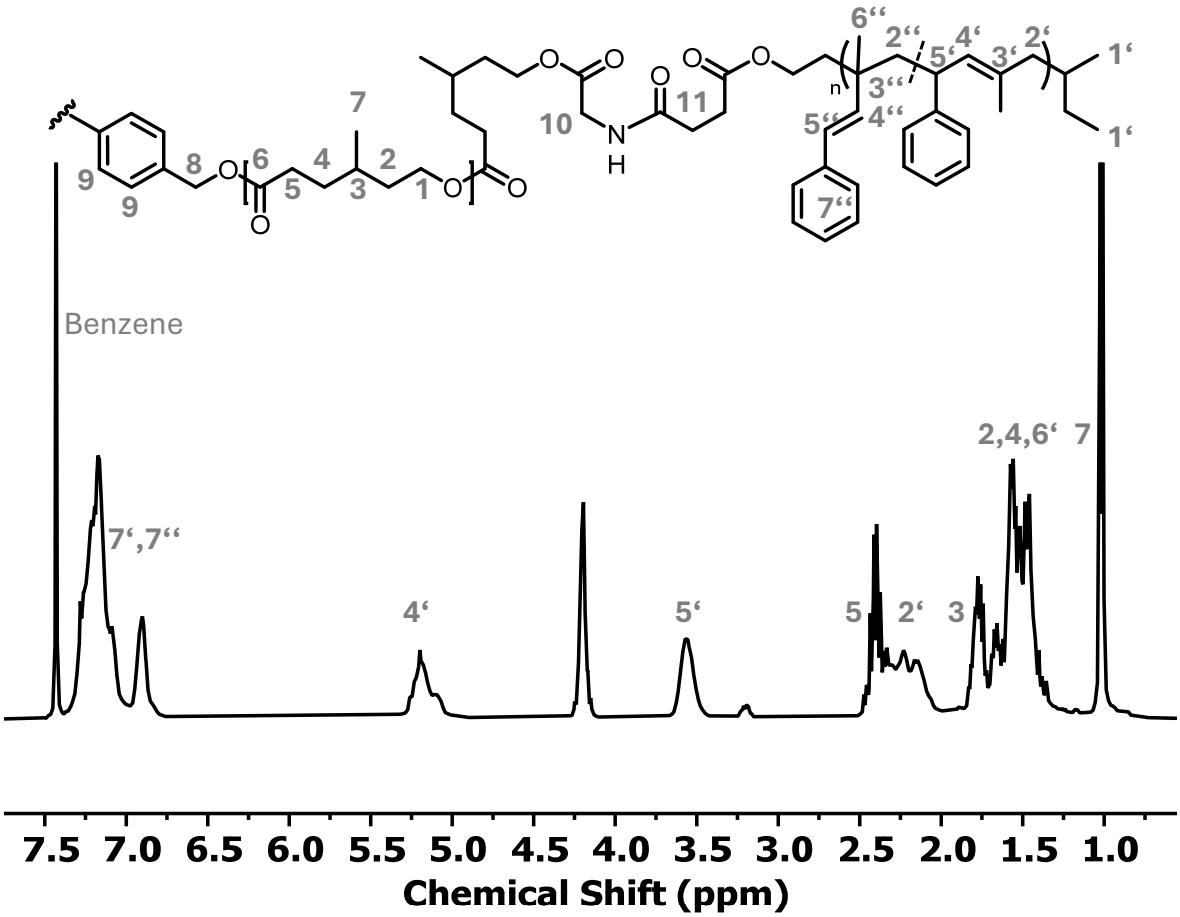


**Figure S19**: 1H NMR spectrum of the triblock copolymer $6P^{4PhI}$-*b*-$2P^{MCL}$-*b*-$6P^{4PhI}$ with the respective assignment of the signals.

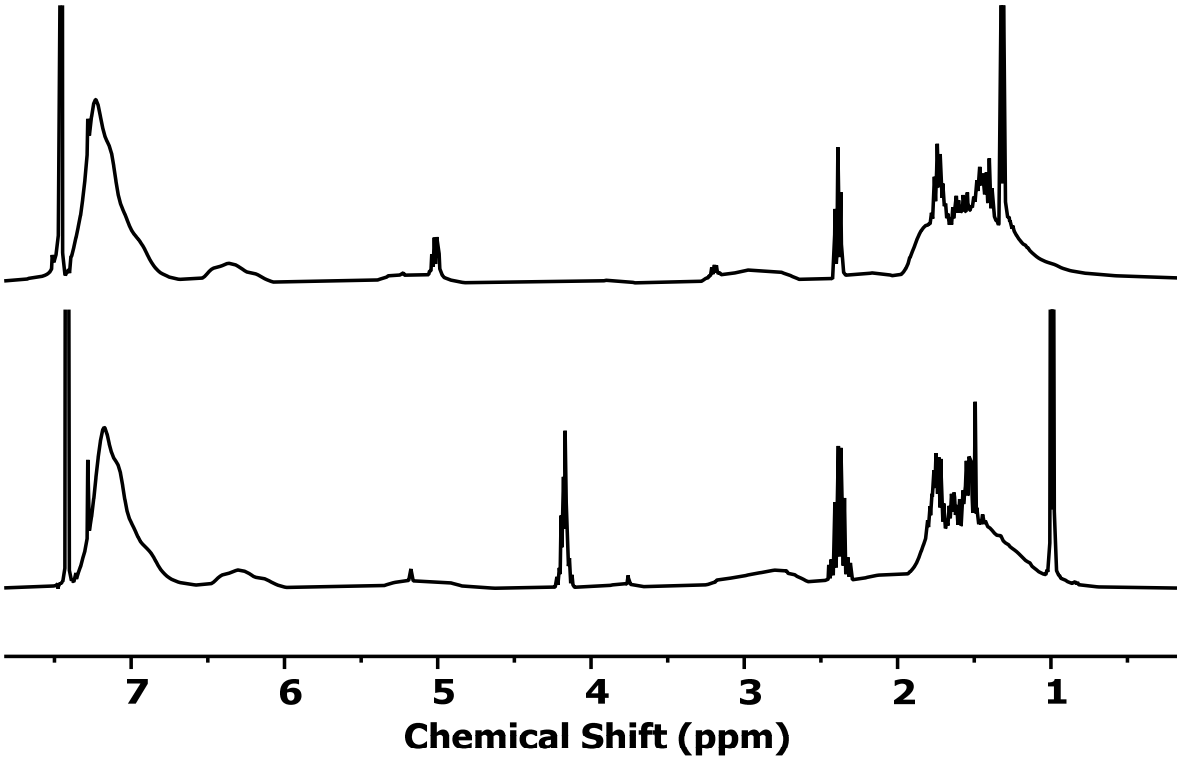


**Figure S20**: Stacked $^{1}$H NMR spectra ($CDCl_3$, 400 MHz) of the coupled polymers 8P$^{1PhI}$-*b*-2P$^{MCL}$-*b*-8P$^{1PhI}$ (bottom) and 9P1$^{PhI}$-*b*-3P$^{MCL}$-*b*-1P1$^{PhI}$ (top).

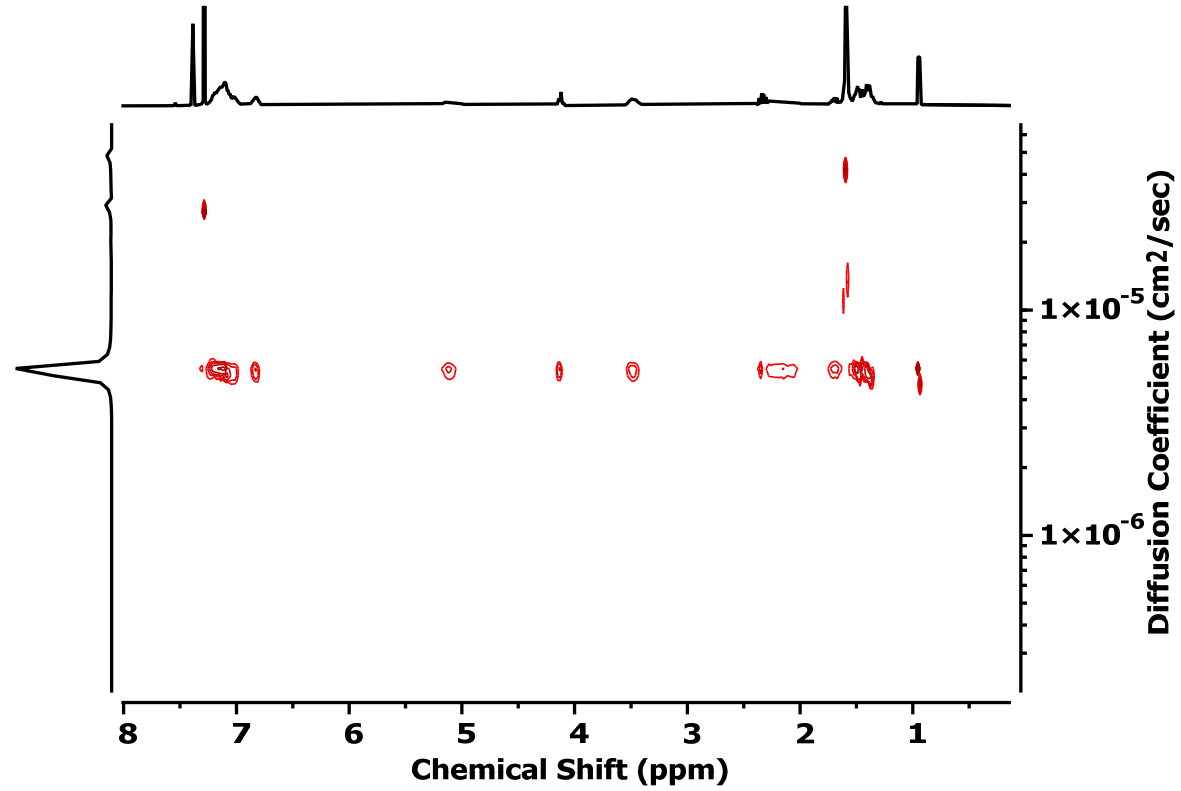


**Figure S21**: DOSY spectrum of 6P$^{4PhI}$-*b*-2P$^{MCL}$-*b*-6P$^{4PhI}$

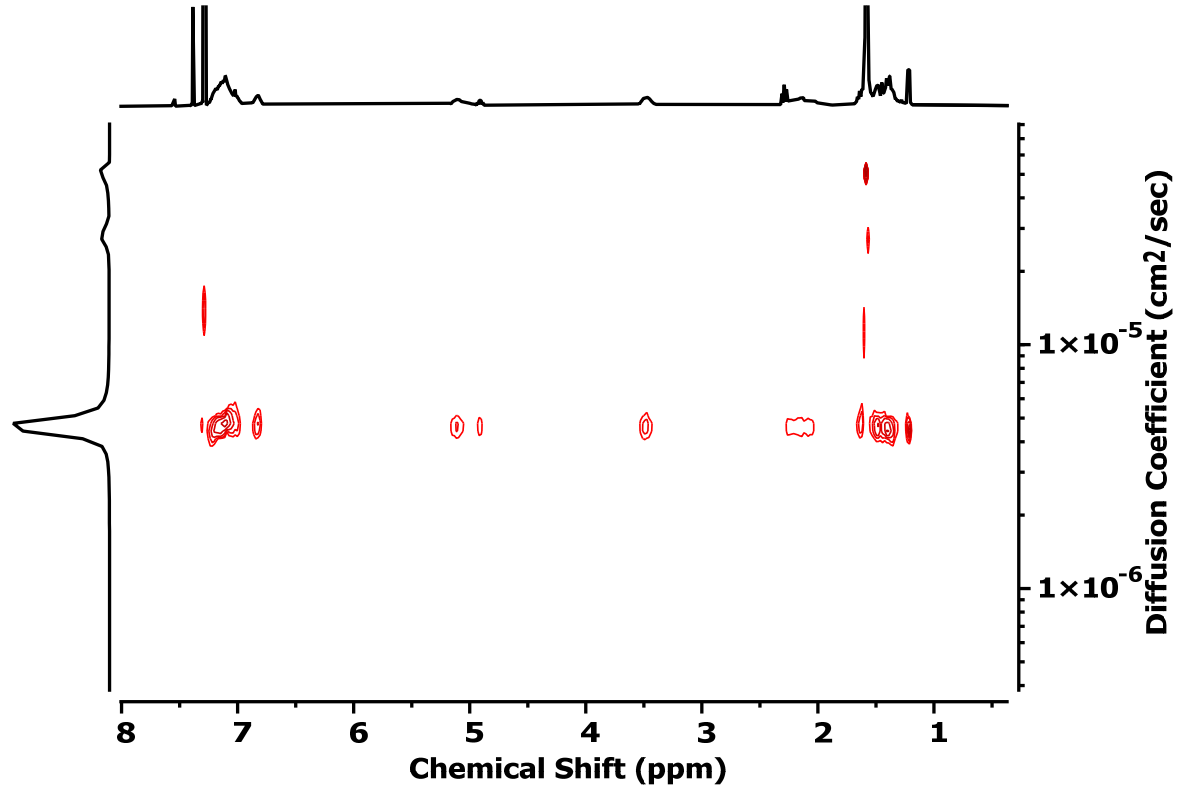


**Figure S22**: DOSY spectrum of 7P$^{4Phl}$-*b*-3P$^{MCL}$-*b*-7P$^{4Phl}$.

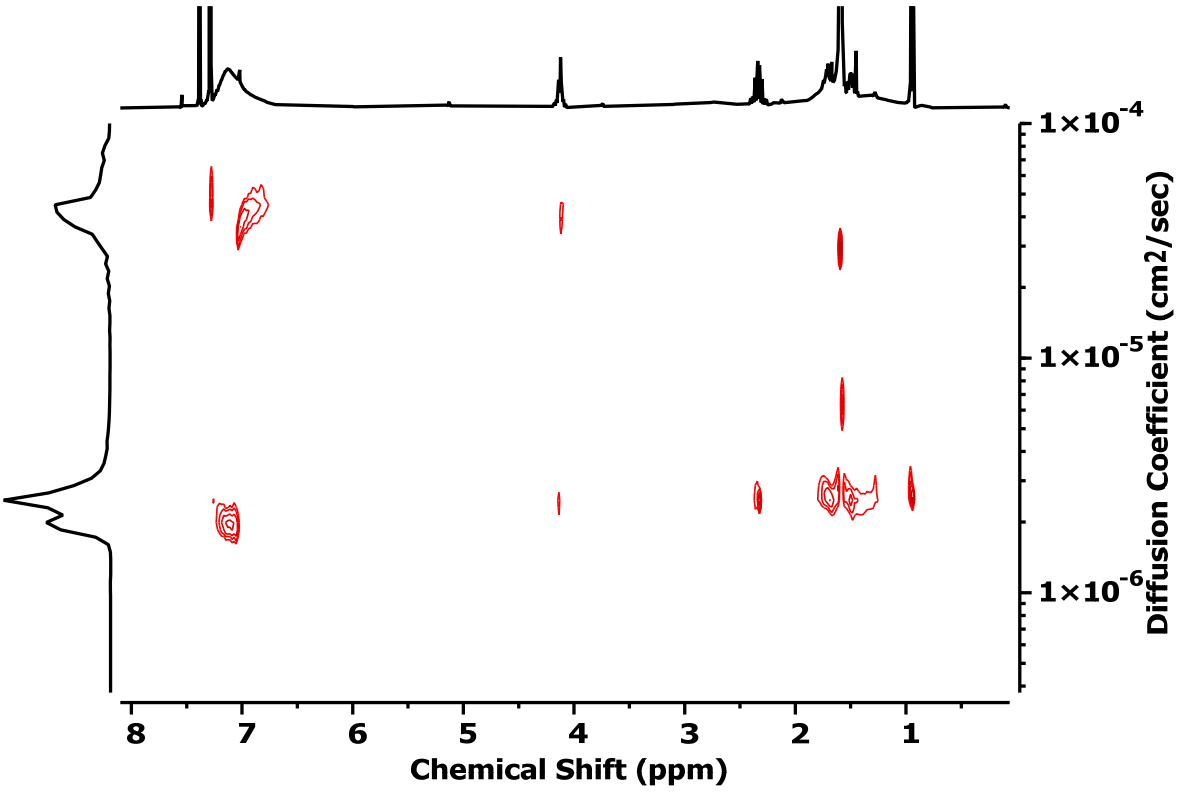


**Figure S23**: DOSY spectrum of 8P$^{1Phl}$-*b*-2P$^{MCL}$-*b*-8P$^{1Phl}$

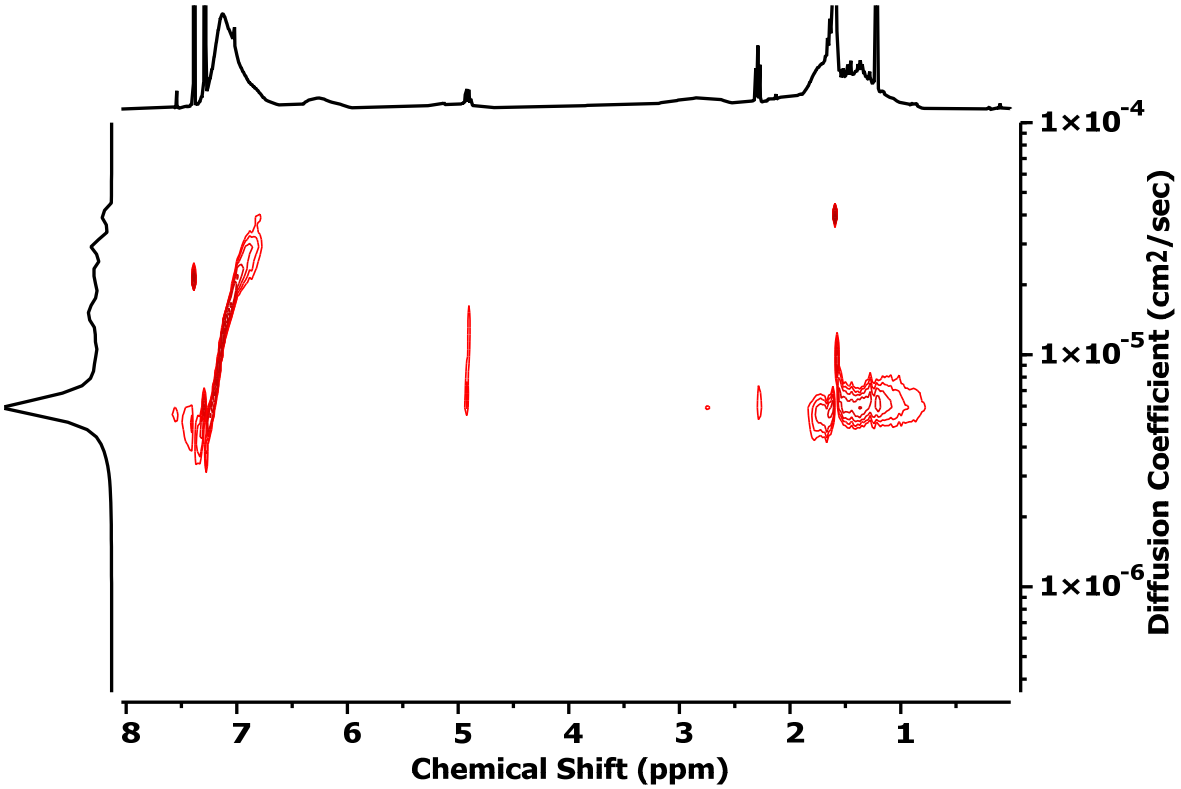


**Figure S24**: DOSY spectrum of 9P$^{1PhI}$-*b*-3P$^{MCL}$-*b*-9P$^{1PhI}$.

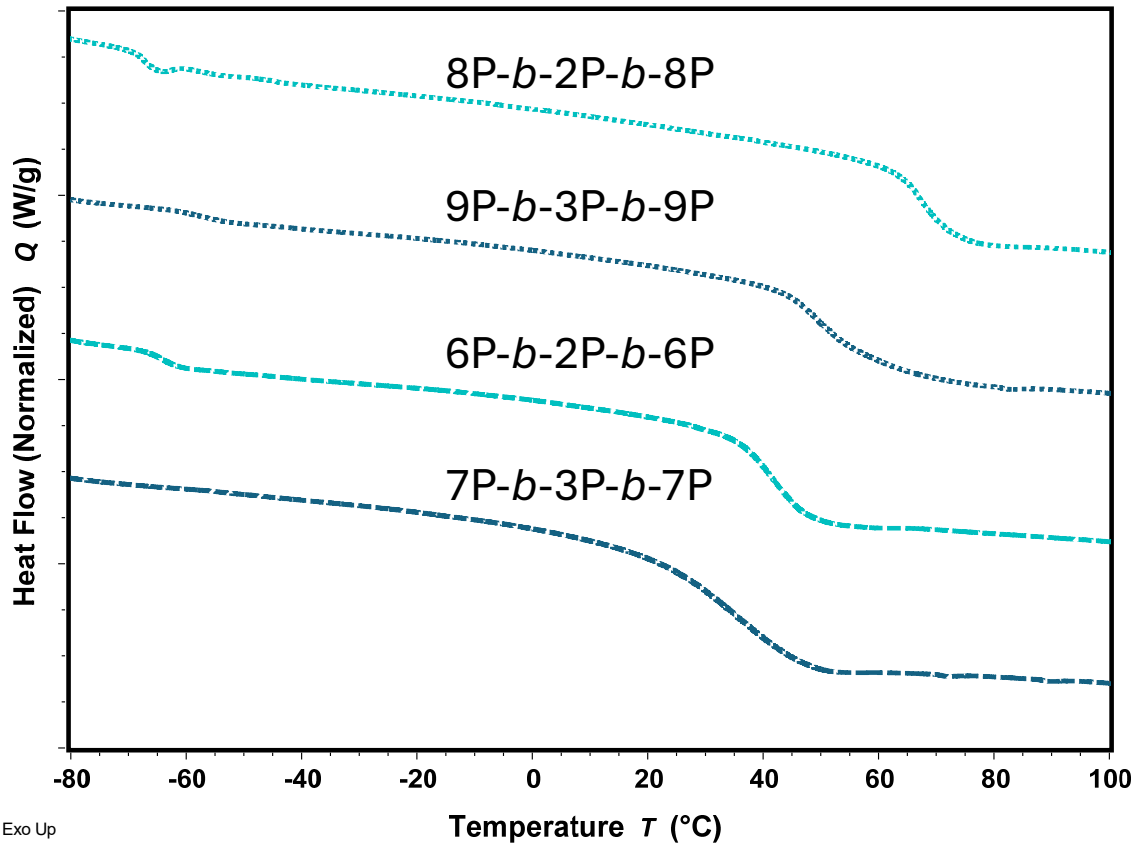


**Figure S25**: DSC curves of the four triblock copolymers 6P$^{4PhI}$-*b*-2P$^{MCL}$-*b*-6P$^{4PhI}$, 7P$^{4PhI}$-*b*-3P$^{MCL}$-*b*-7P$^{4PhI}$, 8P$^{1PhI}$-*b*-2P$^{MCL}$-*b*-8P$^{1PhI}$ and 9P$^{1PhI}$-*b*-3P$^{MCL}$-*b*-9P$^{1PhI}$

## Analytics of cyclized samples

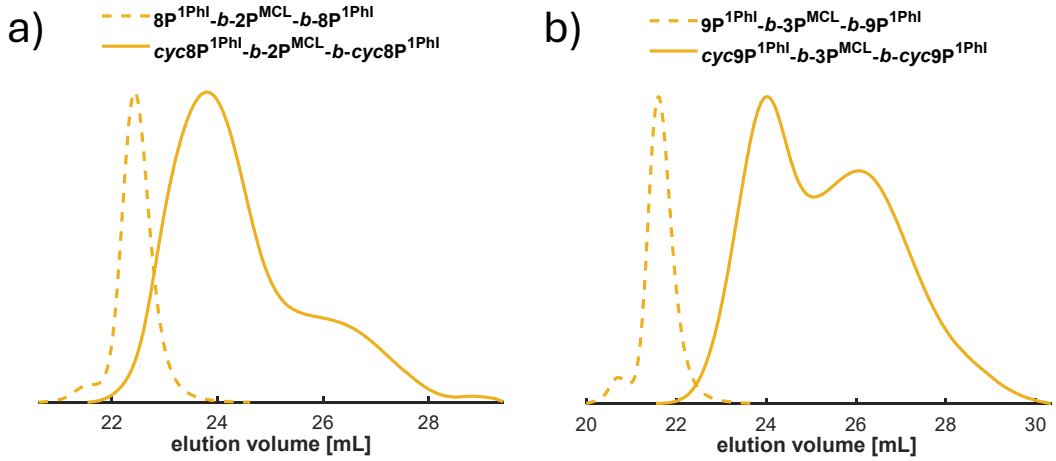


**Figure S26**: SEC traces of a) *cyc*8P$^{1PhI}$-*b*-2P$^{MCL}$-*b*-*cyc*8P$^{1PhI}$ and b) *cyc*9P$^{1PhI}$-*b*-3P$^{MCL}$-*b*-*cyc*9P$^{1PhI}$ with their respective precursors.

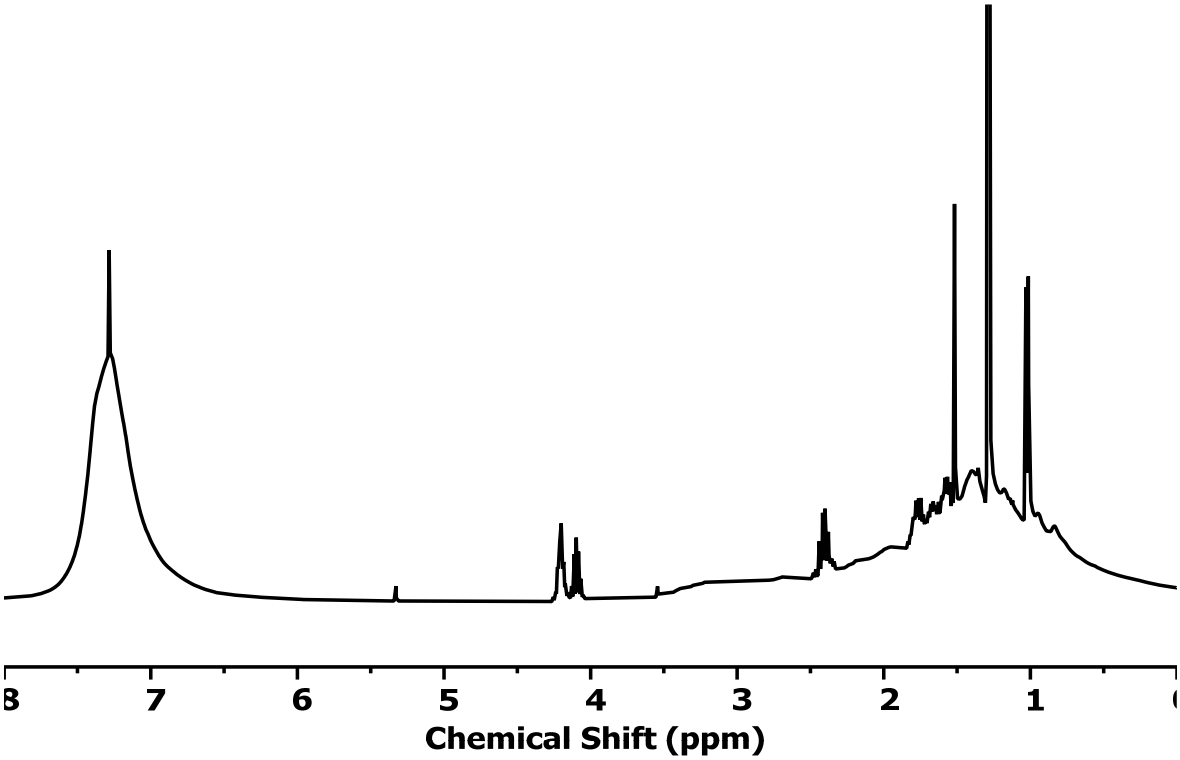


**Figure S27**: $^{1}$H NMR spectrum ($CDCl_3$, 400 MHz) of cyclized triblock copolymer *cyc*6P$^{4PhI}$-*b*-2P$^{MCL}$-*b*-*cyc*6P$^{4PhI}$

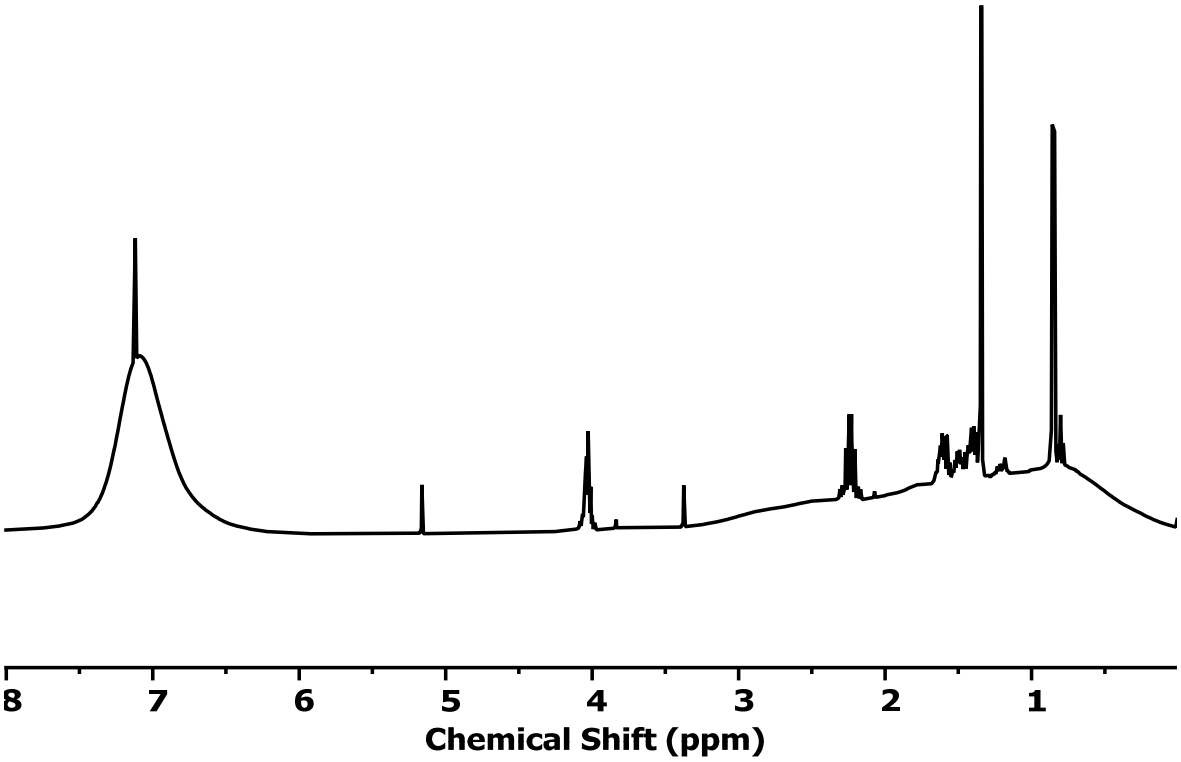


**Figure S28**: $^{1}$H NMR spectrum ($CDCl_3$, 400 MHz) of cyclized triblock copolymer *cyc*8P$^{1PhI}$-*b*-2P$^{MCL}$-*b*-*cyc*8P$^{1PhI}$.

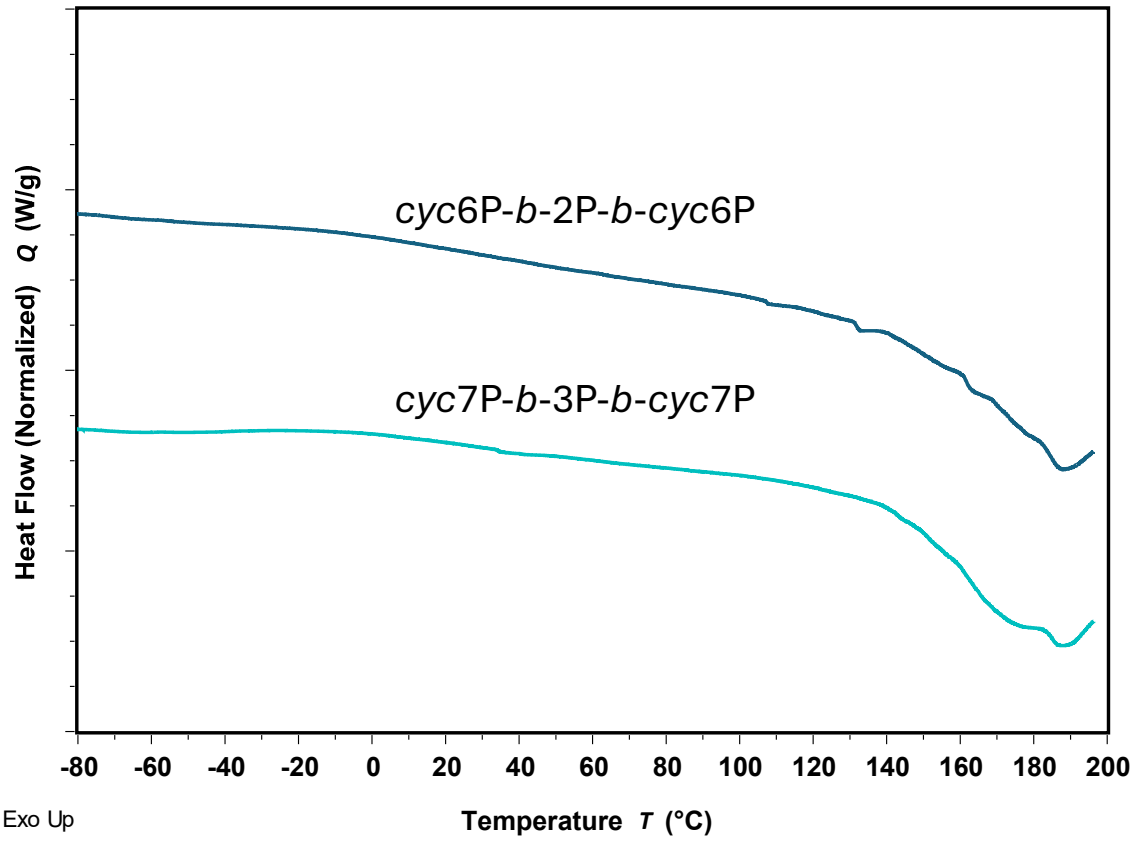


**Figure S29**: DSC curves of the samples *cyc*6P$^{4PhI}$-*b*-2P$^{MCL}$-*b*-*cyc*6P$^{4PhI}$ (top) and *cyc*7P$^{4PhI}$-*b*-3P$^{MCL}$-*b*-*cyc*7P$^{4PhI}$ (bottom).

## References

1 A. Watts, N. Kurokawa, M. A. Hillmyer, *Biomacromolecules* **2017**, *18*, 1845–1854.

2 M. Rauschenbach, L. Stein, G. M. Linden, R. Barent, K. Heinze, H. Frey, *Polym Chem* **2024**, *15*, 3204–3213.

# CHAPTER 5

## The Impact of Thioether Groups in Anionic Polymerization of Diene Monomers for Post-Polymerization Modification.

# CHAPTER 5

*To be published in Advanced Functional Materials*

## The Impact of Thioether Groups in the Anionic Polymerization of Diene Monomers for Post-Polymerization Modification.

Moritz Rauschenbach,[a] Annika Schmidt,[b] Matthias Bros,[c] Carsten Strohmann,[c] Holger Frey [a,*]

[a] Department of Chemistry, Johannes Gutenberg University Mainz, Duesbergweg 10 – 14, D-55128 Mainz, Germany
[b] Inorganic Chemistry, TU Dortmund University, D-44227 Dortmund, Germany
[c] University Medical Centre, Johannes Gutenberg University, Langenbeckstraße 1, D-55101 Mainz, Germany

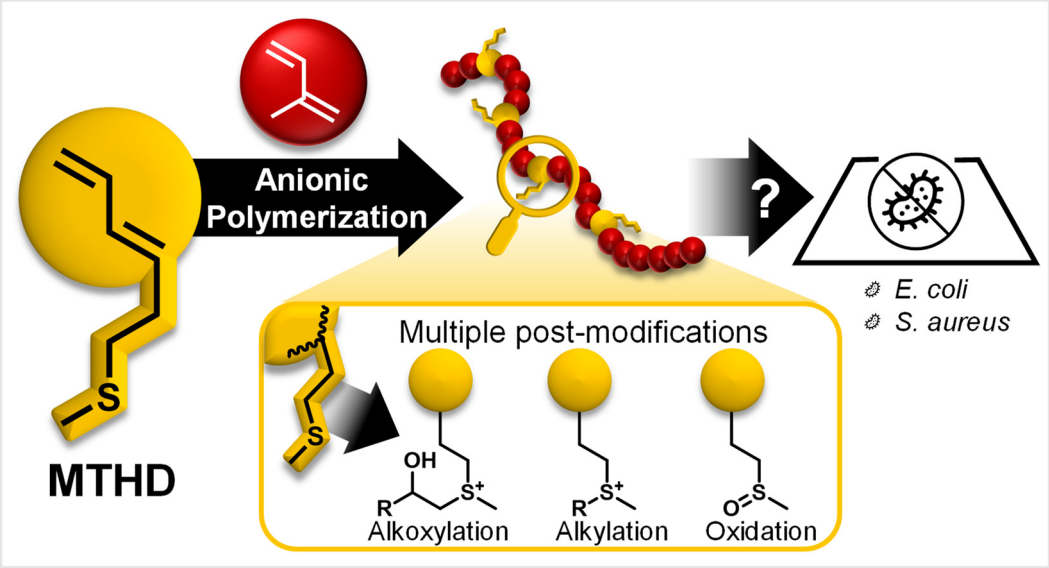


**Abstract:** The anionic polymerization of 1,3-dienes is one of the most-established approaches for the synthesis of synthetic rubber. Motivated by tailoring the properties of synthetic rubbers in post-polymerization reactions, we introduce the thioether-containing 6-methylthio hexa-1,3-diene (MTHD) as a building block. The obtained isomeric *cis*-/*trans*-mixture was successfully polymerized under anionic conditions. Consistent with earlier reports, *in situ* 1H nuclear magnetic resonance (NMR) kinetics revealed differing reactivities of the *trans* and *cis* isomer and increased dispersities of $Đ > 1.24$. The copolymerization with isoprene yielded notable improved distributions ($Đ < 1.19$). This demonstrated for a series of well-defined statistical copolymers with increasing molar masses up to 50 kg mol$^{-1}$ and precise adjustment of MTHD content from 2 to 10%. Targeting the thioether groups *via* post-polymerization modifications (i.e. alkoxylation and alkylation) permitted tailoring of the properties of the copolymer. Moreover, the respective sulfoxide was obtained selectively and may be seen as an internal antioxidant. Introduction and testing of sulfonium species regarding their inhibition of the growth of Gram-negative and Gram-positive bacteria strains showed significant antimicrobial performance against *E. coli* and *S. aureus*.

## Introduction

In recent years, thioethers have emerged as a subject of growing interest within the field of polymer science and have been introduced to various polymer classes. Although the thioether moiety is a non-protic group, modifications of thioethers enable applications ranging from drug delivery models[1–3] over polyelectrolytes[2,4] to antimicrobial polymers[5–8]. Furthermore, Du Prez and coworkers explored the transalkylation of sulfonium salts to synthesize vitrimers based on polythioethers.[9,10] The oxidation to polar sulfoxides is utilized to directly tailor the properties of the material.[3,11–13] Water-soluble polymersomes comprising a polymer block with thioethers in the core can be oxidized to the corresponding sulfoxide, thereby inducing oxidation-responsive behavior.[3,11,12,14] Deming and coworkers presented an additional click-type reaction with different electrophiles introducing "quaternization" of thioether moieties in poly(L-methionine).[15,16] This modification was systematically investigated with multiple alkyl halides and epoxides, affording highly functional polypeptide sulfonium derivatives. Among others, our group designed monomers inspired from L-methionine to take advantage of the broad toolbox of suitable reagents.[2–4,12,14,17] In the field of antimicrobial materials, sulfonium groups have emerged as a promising alternative to traditional nitrogen-based groups.[18] By passively targeting the anionic bacterial membrane, these cationic groups effectively disrupt the membrane and ultimately lead to bacterial cell death. Despite the broad utilization of thioether-bearing monomers and broad application range of the resulting polymeric materials in different research areas, to the best of our knowledge, the anionic polymerization of 1,3-dienes including a thioether group has not been reported to date. Additionally, the beforementioned potential modifications have not been applied to a polydiene-system.

The anionic polymerization of 1,3-dienes is a long-established process. Initially, the industrialization of vulcanization led to the development of butadiene rubber synthesis to reproduce the properties of *cis*-1,4 polyisoprene, as found in natural rubber.[19,20] Anionic polymerization has been identified as a method that is well-suited to achieve tunability, offering precise control over molar mass and distribution, while simultaneously yielding a low vinyl content in nonpolar media.[21,22] Consequently, this low vinyl content directly contributes to a low glass temperature ($T_g$) which is utilized in thermoplastic elastomers.

These can be found in medical applications that would benefit from antimicrobial properties.[23]

Although polydienes have been widely investigated as materials for an extraordinary variety of commercialized products, there are still limitations with respect to functional polymers. Incorporating functional moieties into a polydiene framework through suitable diene monomers could permit to tailor their properties. In fact, this would also be beneficial for the main application of polydienes: the tire industry. Polar fillers, such as silica particles, are incompatible with the nonpolar polydiene rubber network.[24] With regard to this matter, the degree of functionalization of polydienes can be controlled to a limited extent *via* post-polymerization reactions.[25] Moreover, only a confined selection of functional diene monomers have been identified to date. This is due to the incompatibility of functional groups, such as hydroxyl or amine groups that contain acidic protons or electrophilic moieties, with the carbanionic polymerization technique.[26–28] Therefore, suitable protective groups must be utilized. Besides challenges in the monomer synthesis, it is necessary to implement an alkyl spacer between the 1,3-diene moiety and the functional group to prevent the so-called "*back side collapse*". As described by Takenaka *et al.*, the reactive center can induce a $S_N2$-type reaction leading to the formation of a *ω*-isoprenyl group.[27,28]

Recently, based on the monoterpene myrcene functional diene-monomers were developed that exhibited an alkyl spacer in natural manner.[29,30] Hence, repeating units with a single or two hydroxyl groups, protected by silyl and ketal protection groups, respectively, were incorporated into the backbone of polydienes *via* living anionic polymerization. For instance, a silyl protecting group for myrcenol (MyrOSi) was utilized. Furthermore, polymerization of a dioxolane functionalized myrcene structure was reported. In both cases, evidence for interactions of the monomer with the counterion was postulated, explaining the observed increase of 3,4-units in the final polydiene backbone. The obtained polymers with free hydroxyl groups showed a significant increase in polarity compared to non-modified polydienes.

Both radical polymerization and catalytic polymerization techniques have been used to synthesize functional polydienes. In case of the *reversible addition-fragmentation chain-transfer* (RAFT) polymerization the high compatibility of functional groups with the polymerization method was utilized to obtain functional polydienes.[31–33] In comparison,

catalytic polymerizations are sensible to functional moieties. Recently, a broad variety of functional dienes were successfully polymerized stereoselectively. [34–39] Mecking *et al.* reported on the catalytic insertion polymerization of thioether functionalized dienes focusing on the mechanism of the polymerization.[34]

This work reports on the synthesis and anionic (co)polymerization of 6-methylthio-1,3-hexadiene (MTHD) prepared from L-methionine-derived methional. The thioether group enables the functional polydienes with high control over the degree of functionality by copolymerization with isoprene. Lastly, the impact of modifying MTHD in a variety of post-polymerization modifications on the polydienes properties were tested. Candidates from alkylation and alkoxylation reaction were subsequently investigated with respect to their antimicrobial properties.

## Results and Discussion

### Monomer Synthesis MTHD

MTHD was synthesized in a three-step route, based on a Grignard reaction of allyl magnesium bromide and methional in accordance with literature procedures.[40] Proceeding directly after work-up, we performed the tosylation of the hydroxyl group with tosyl chloride and subsequently accomplished the elimination of the tosylate towards the 1,3-diene in a DBU-catalyzed reaction.[41] Finally, the product was purified *via* fractionated distillation under reduced pressure. It is important to mention that this is the only purification step of this synthesis route, required to increase the total yield of the monomer. The product is obtained as an isomeric mixture, and the *trans*/*cis*-isomer ratio was determined *via* the $^{1}$H NMR spectrum (**Figure S2**) to be 78:22.

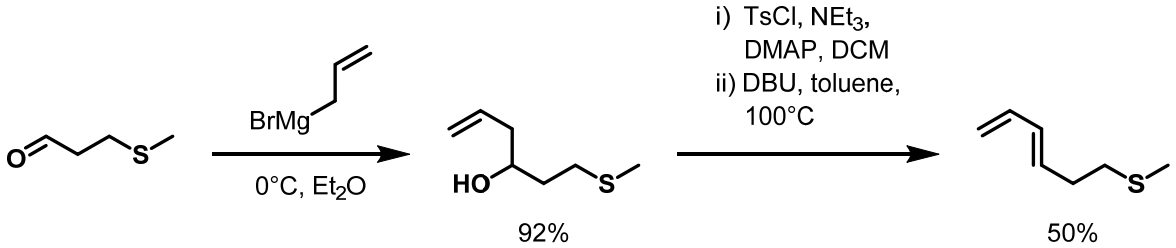


**Scheme 1**: Synthetic route for the synthesis of MTHD.

## Homopolymerization of MTHD

Homopolymerizations were conducted using established conditions.[42] The initial experiments were performed using the non-polar solvent cyclohexane at room temperature. A series of PMTHD polymers with molar masses ranging from 5 – 50 kg mol$^{-1}$ were targeted. Upon initiation, the polymer solutions turned pale yellow. The color persisted until termination, indicative of the living carbanionic chain end. Noteworthy, samples with targeted molar masses >10 kg mol$^{-1}$ turned turbid shortly after initiation, suggesting poor solubility. The results in **Table 1** indicate good control over molar mass, but dispersities are higher than typically expected for living polymerizations with values reaching 1.35. As reported for ocimene the occurrence of an isomeric mixture can be correlated with an increase in dispersity.[43] Similarly, we observe peculiar tailing to higher elution volume hinting towards complex polymerization kinetics.

In another series with molar masses up to 20 kg mol$^{-1}$, we elevated the polymerizations polarity by the utilization of MTBE. As shown before, MTBE is suitable for the anionic polymerization and is less prone to proton abstraction compared to the established polar solvent THF.[44] MTBE resulted in enhanced solubility of the polymethylthiohexadienyl chain ends. However, the resulting homopolymers exhibited slighty elevated dispersities, with *Đ* values exceeding 1.21. The successful synthesis of PMTHD was further proven by determination of the absolute molar mass *via* MALDI-ToF MS. Using PMTHD with a targeted molar mass of 5 kg mol$^{-1}$ (**Table 1**, entry 1), the incorporation of MTHD (128 g mol$^{-1}$) was confirmed. The MALDI ToF mass spectrum in **Figure S12** shows a reduced molar mass of $M_n^{MALDI}$ = 1.7 kg mol$^{-1}$ and therefore strongly deviates from the molar mass of determined by $M_n^{GPC}$ = 4.3 kg mol$^{-1}$.

We determined the glass temperatures of PMTHD *via* DSC measurements (**Figure S13**). Extrapolation of the inverse molar masses and the obtained glass temperature gave the respective value for $T_{g,\infty}$ = − 26°C (**Figure S14**). This revealed the synthesis of an elastomer and is a first indication for the regiostructure. The structurally related polybutadiene exhibits this increased $T_g$ for higher vinyl side chain content. The mcirostructure was investigated by NMR measurements, as discussed below.

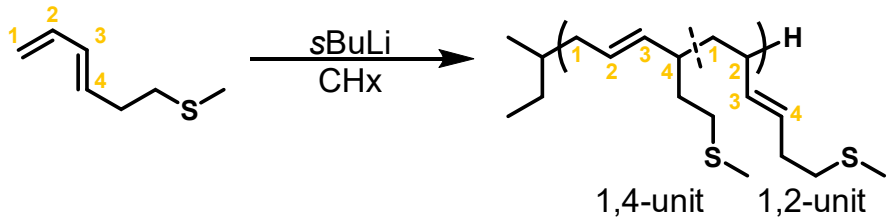


**Scheme 2**: Anionic Polymerization of MTHD.

**Table 1**: Data of the synthesized homopolymers PMTHD.

| Entry | Solvent | $M_{n,theo}$ [kg mol$^{-1}$] | $M_{n,GPC}$[a] [kg mol$^{-1}$] | $Đ$[a] | $t$ [h] | $T_g$[b] [°C] |
|---|---|---|---|---|---|---|
| 1 | CHx | 5 | 4.3 | 1.34 | 5 | − 34 |
| 2 | CHx | 10 | 8.4 | 1.35 | 6 | − 32 |
| 3 | CHx | 20 | 17.0 | 1.24 | 6 | − 30 |
| 4 | CHx | 50 | 38.3 | 1.28 | 6 | − 25 |
| 5 | MTBE | 5 | 4.0 | 1.29 | 7 | − 36 |
| 6 | MTBE | 10 | 8.7 | 1.21 | 7 | − 32 |
| 7 | MTBE | 20 | 11.5 | 1.39 | 7 | − 30 |

[a] Determination *via* a SEC (Eluent: THF; 30°C) utilizing a PI-standard, [b] Determination through DSC measurements analyzing the second heating curve

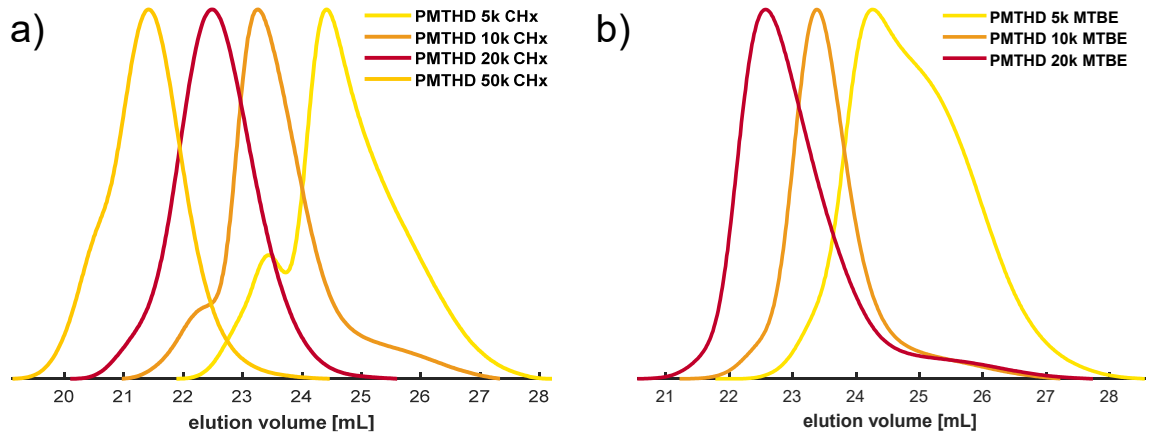


**Figure 1**: GPC traces (RI Signals, eluent: THF) of PMTHD polymerized a) in CHx or b) in MTBE.

*Microstructure of PMTHD:* The regiostructure of PMTHD was determined using combined NMR spectroscopy methods and referring to reports on comparable polydienes.[43,45] **Figure S7**-**Figure S11** illustrate the $^{1}$H NMR, $^{1}$H-$^{1}$H COSY, $^{13}$C DEPT, $^{1}$H-$^{13}$C HSQC and

$^{1}$H-$^{13}$C HMBC spectra. The $^{1}$H NMR spectrum (**Figure S7**) provides only evidence of 1,4- and 1,2-PMTHD, with no indications of vinyl protons, which are in principle present in a 3,4-regiostructure. Nonetheless, broad signals indicate no uniform microstructure resulting in strong signal overlap. Additionally, increased line width could be attributed to a short T2 time, which prevents the visualization of existing couplings in 2D NMR experiments. However, $^{1}$H-$^{13}$C HSQC and $^{1}$H-$^{13}$C HMBC gave valuable information for the assignment of the respective protons and carbon species in both 1,2- and 1,4-PMTHD. Prior to the HSQC and HMBC measurements (shown below), $^{13}$C DEPT measurements were utilized to differentiate between the methyl, methylene and methine groups. Relying on the HSQC and HMBC spectra, the signals of the side chains could be identified. Both the methylene (5, 5′) as well as the methyl carbons (7, 7′) show two separate signals, indicating the presence of both 1,4- and 1,2-microstructures. The relative intensities of the respective signals in the $^{13}$C NMR spectrum suggest that the ratio is almost equal. It can be concluded that no separated signals of both microstructures are present in the $^{1}$H NMR spectrum. As a result, the ratio could not be determined with exact values.

These findings indicated a significant amount of 1,2-microstructure that would associate a deviating mechanism over butadiene or isoprene. Recently, we postulated the self-modification where the oxygen atoms in the side chain of functional myrcene-derivatives coordinate the lithium-counterion leading to an increased amount of 3,4-units. Compared to oxygen, the electrons of sulfur in MTHD are less localized. Therefore, a weaker coordination of the soft sulfur to the hard lithium is expected. $^{1}$H-$^{7}$Li-HOESY experiments identify the protons in spatial proximity to lithium. In **Figure 2** is shown that the methyl group of the thioether is in spatial proximity to the lithium counterion. Besides this indirect indication of an interaction between the sulfur and the lithium the exact nature of the adduct, as illustrated in **Scheme S1**, is not revealed.

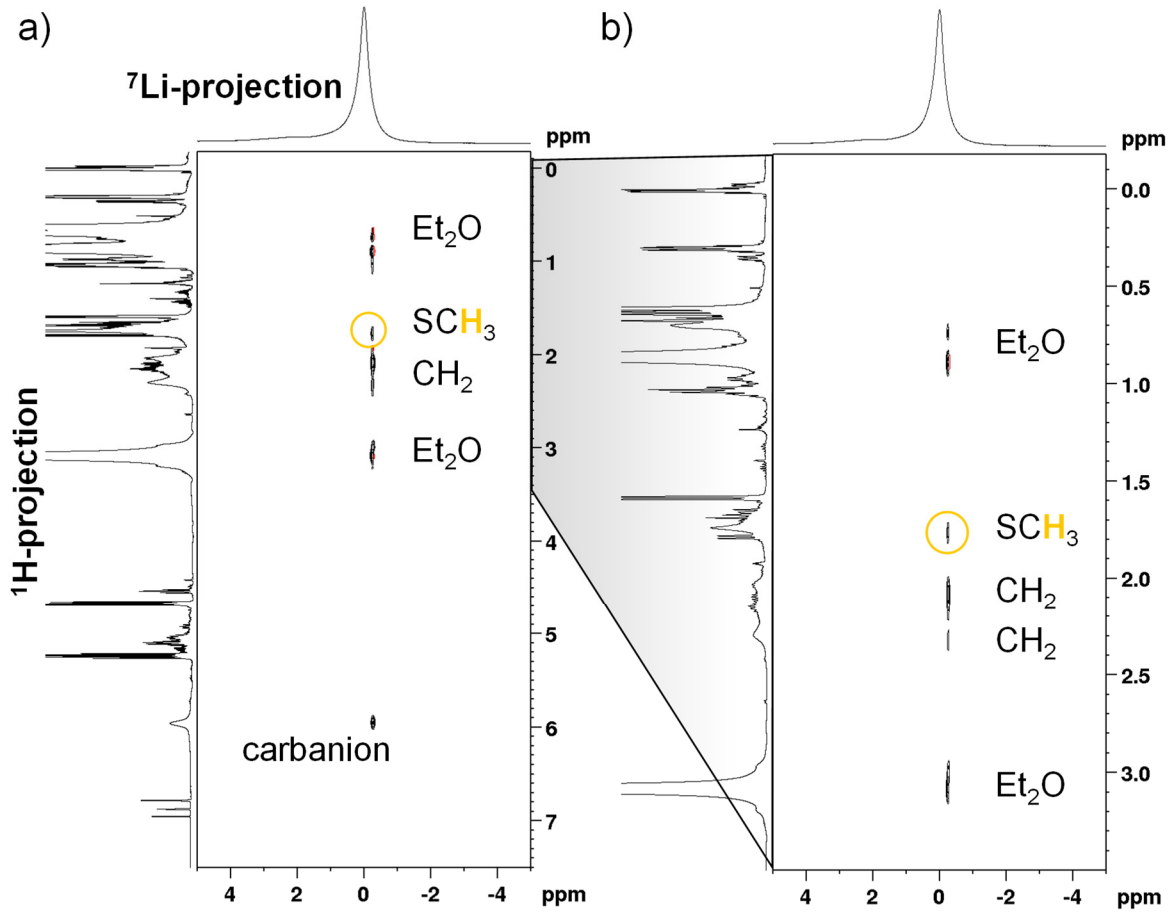


**Figure 2**: $^1$H-$^7$Li-HOESY spectrum of a *t*BuLi-MTHD-adduct identifying protons in spatial proximity to the lithium counterion showing a) the full spectrum and b) the region with the specific methyl group of the thioether.

## *In situ* NMR kinetics of MTHD

The broad distributions obtained from the anionic polymerization of the isomeric mixture of MTHD points towards unequal reactivity of both isomers, already reported for the anionic polymerization of *cis*- and *trans*-ocimene. *Cis*- and *trans*-MTHD show a significant separation of their respective olefinic signals in the $^1$H NMR spectrum (**Figure S2**). Therefore, *in situ* $^1$H NMR kinetic experiment was conducted under the conditions of the corresponding PMTHD synthesis in $C_6D_{12}$ tracking the integrals of the C2 vinyl protons of the *cis* (δ = 6.70 – 6.56 ppm) and *trans* (δ = 6.37 – 6.20 ppm) isomers over time, highlighted in **Figure 3**. As indicated in **Figure S16a** a rapid polymerization with almost full consumption of the *cis*-MTHD after 4 min while traces of *trans*-MTHD were still present after 12 min. However, *trans*-MTHD was present in excess over the *cis*-isomer. The reactivity ratios were evaluated with a non-terminal model ($r_1r_2$=1; Jaacks[46]) and yielding the values $r_{cis}$ = 2.75 and $r_{trans}$ = 0.364. Therefore, the higher reactivity of the *cis*-isomer is

illustrated, which consequently leading to the favorable incorporation over the *trans*-MTHD. This provides an additional example of the so-called "stereo-copolymerization". In contrast, the reactivity order in the reported isomeric mixture of ocimene was reversed with a favorable incorporation of the *trans*-ocimene. The following experiments deliberately neglect the presence of *cis*-MTHD in order to simplify the discussion. Nevertheless, despite the small fraction of the isomeric mixture and quantitative reaction within a relatively short time, its presence should not be overlooked.

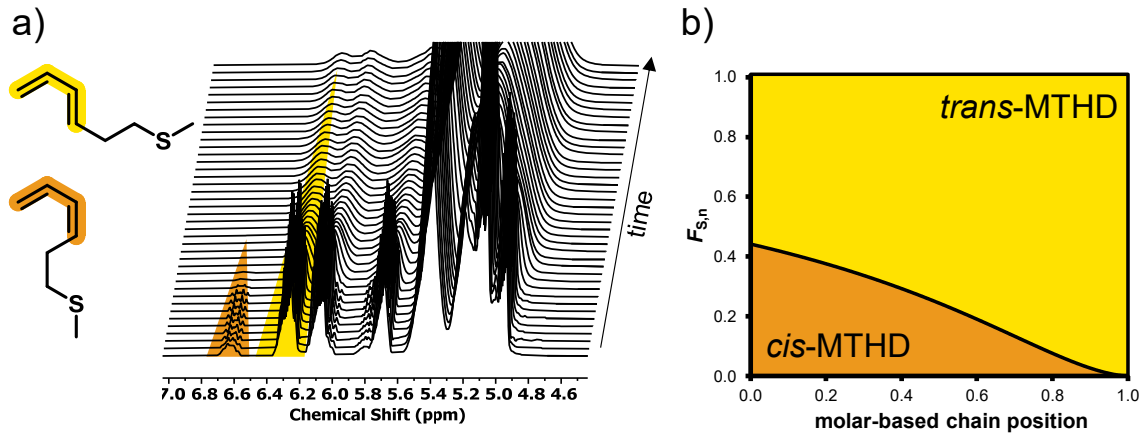


**Figure 3**: a) Zoomed-in region of stacked spectra as a function of time. The highlighted proton signals were used to study of the transformation of *trans*- and *cis*-MTHD in $C_6D_{12}$ at 20 °C and b) simulated molar composition profile based on the reactivity ratios with the obtained ratio of both isomers after the synthesis.

## Copolymerization reactions of MTHD with isoprene

In contrast to the vulcanization process, in which polydienes are crosslinked with sulfur-containing curatives as originally invented by Charles Goodyear[47], our objective was to achieve a distinct incorporation of sulfur to tailor the properties of polydienes. Therefore, copolymerizations of MTHD with isoprene were carried out. The MTHD composition, $x^{MTHD}$, was varied from 2 – 10% for polydienes with targeted molar masses between 10 – 50 kg mol$^{-1}$. The obtained polymers were analyzed regarding their molar mass, dispersity, and glass temperatures as shown in **Table 2** (entries 9 – 14).

The GPC traces (**Figure 4a**) of lower molar mass PMTHD-*co*-PI are monomodal with low dispersities $Đ$ < 1.07 indicating high control over the copolymerization regardless of $x^{MTHD}$. The copolymer with a targeted molar mass of 50 kg mol$^{-1}$ exhibited bimodality, which can be attributed to oxygen coupling introduced due to insufficient degassing of methanol utilized for termination. This resulted in an increase in dispersity of $Đ$ = 1.19. Within 8 h

the copolymers reached the targeted molar mass. As shown in **Figure S18**, $^{1}$H NMR spectroscopy can be used to confirm the increasing $x^{MTHD}$ and proofs the incorporation of both monomers. DSC of all copolymers revealed low glass temperatures of < – 59 °C (**Figure S19**). Therefore, the thermal properties are not affected by the presence of up to 10 mol% of MTHD making it suitable for rubber applications.

**Table 2**: Summary of statistical copolymerization of MTHD with isoprene and additional styrene (entry 15).

| Entry | Polymer composition | $x^{MTHD}$ | $x^{Isoprene}$ | $w^{MTHD}$ | $M_{n,theo}$ [kg mol$^{-1}$] | $M_{n,GPC}$ [a] [kg mol$^{-1}$] | $Đ$ [a] | $t$ [h] | $T_g$ [b] [°C] |
|---|---|---|---|---|---|---|---|---|---|
| 8 | PMTHD$_{0.05}$-*co*-PI$_{0.95}$ | 0.05 | 0.95 | 0.09 | 10 | 14.5 | 1.04 | 8 | – 62 |
| 9 | PMTHD$_{0.10}$-*co*-PI$_{0.90}$ | 0.10 | 0.90 | 0.17 | 10 | 13.7 | 1.05 | 8 | – 62 |
| 10 | PMTHD$_{0.02}$-*co*-PI$_{0.98}$ | 0.02 | 0.98 | 0.04 | 20 | 21.4 | 1.04 | 7 | – 63 |
| 11 | PMTHD$_{0.05}$-*co*-PI$_{0.95}$ | 0.05 | 0.95 | 0.09 | 20 | 19.7 | 1.06 | 7 | – 62 |
| 12 | PMTHD$_{0.10}$-*co*-PI$_{0.90}$ | 0.10 | 0.90 | 0.17 | 20 | 22.8 | 1.07 | 7 | – 59 |
| 13 | PMTHD$_{0.10}$-*co*-PI$_{0.90}$ | 0.10 | 0.90 | 0.17 | 50 | 59.2 | 1.19 | 8 | – 61 |

[a] Determination *via* a SEC (Eluent: THF; 30°C) utilizing a PI-standard, [b] Determination *via* DSC measurements, analyzing the second heating curve

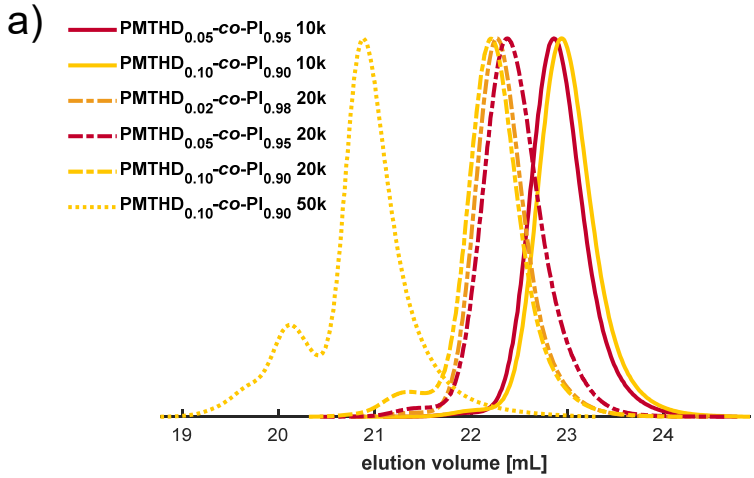


**Figure 4**: GPC traces (RI Signals, eluent: THF) of the copolymers with a) isoprene and varying $x^{MTHD}$ and increasing $M_{n,theo}$ as well as b) with additional 30mol% of styrene.

## *In situ* NMR kinetics of copolymerization of MTHD and isoprene

For any application, the distribution of MTHD within the copolymer chains is relevant. Therefore, *in situ* NMR kinetic studies were carried out in $C_6D_{12}$ recreating the conditions of the previous polymerizations. Detailed description of the preparation is given in

Supporting Information. As emphasized in **Figure 5**a) the signals of isoprene (red, δ = 6.48 – 6.38 ppm) and *cis*-MTHD (orange, δ = 6.34 – 6.21 ppm) were baseline-separated to track the individual consumption over time. The *in situ* NMR data revealed a preferential consumption of *trans*-MTHD over isoprene (**Figure 5b)**). This suggests a fast crossover reaction from polyisoprenyl chain ends to MTHD resulting in a gradient structure (**Figure 5d)**) The reactivity ratios of MTHD and isoprene were defined as $r_{MTHD} = 3.2$ and $r_I = 0.0027$. In this case, the logarithmic Meyer-Lowry fit was utilized to determine the reactivity ratios as this method gave theoretical values in good agreement with the obtained data (**Figure S20**). The formerly reported reactivity ratios of isoprene and butadiene $r_I = 0.42$ and $r_B = 2.82$[48] indicate an increasing statistical incorporation of a copolymerization of MTHD and the industrial-established butadiene.

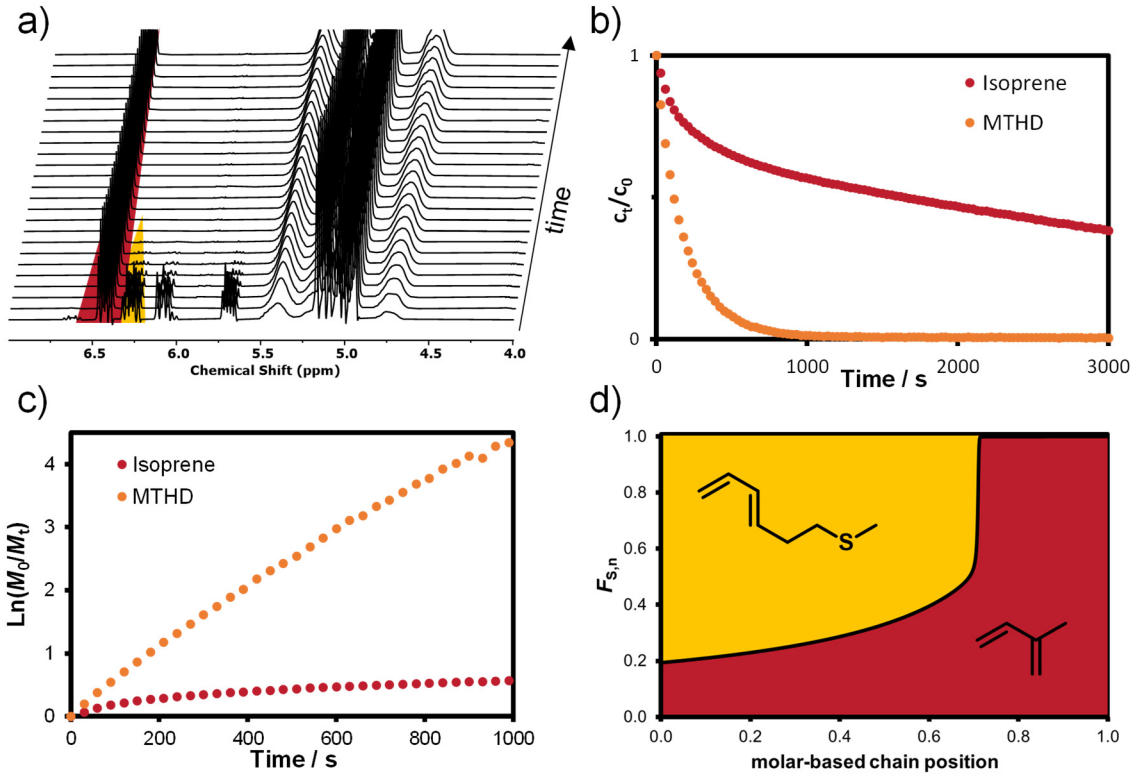


**Figure 5**: a) Stacked $^1$H NMR spectra of the copolymerization of MTHD and isoprene, b) individual conversion plot of MTHD and isoprene over time, c) pseudo-first-order plot for the polymerization of PMTHD-*co*-PI and d) the molar composition profile of an equimolar monomer mixture derived from the calculated reactivity ratios.

## Post-polymerization modification

Functional diene monomers have already been explored in the context of specific applications. Nevertheless, their somewhat constrained range of accessible chemistry and complexity resulted in limited potential for industrial applications. In contrast,

multiple studies reported on post-polymerization modifications, such as oxidation, alkylation, and alkoxylation of thioethers in the side chain.[2–5,11–17] Nevertheless, the specific effect of these modifications on polydienes remain unknown. For instance, it would be of great interest to ascertain whether the positive charges generated by alkylation and alkoxylation confer antimicrobial properties or if the oxidation reaction competes with the double bonds in the polymer backbone.

*Oxidation:* Various works take advantage of the selective oxidation to sulfoxide or sulfone moieties. Consequently, the formation of the sulfoxide strongly increases the dipole moment. The change in the polarity was utilized in aqueous systems to disrupt the formed micelles. Hence, oxidation-responsive materials were obtained.[3,11,12] So far, oxidation of polydienes have been reported to convert the double bonds of the polymer backbone to epoxides.[49,50] Thus, selective oxidation solely of the thioether was targeted without affecting the polydiene backbone. Inspired by small molecule synthesis,[51] we accomplished the selective oxidation of the sulfide to sulfoxide using *meta* chlorobenzoic peroxide in DCM while keeping the reaction time short. The obtained polymer with 6-methylsulfinyl hexadiene (MSHD) as the new repeating units were analyzed. The formed sulfoxide was identified using FT-IR-spectroscopy (**Figure 6**a), evidenced by the respective band at 1040 $cm^{-1}$ assigned to the S=O double bond. Concurrently, the C=C double bond remains unaltered, thereby demonstrating its stability under the chosen conditions. In analogy to the earlier described modifications, DSC measurements revealed the remaining low $T_g$ = − 58 °C (**Figure S31**).

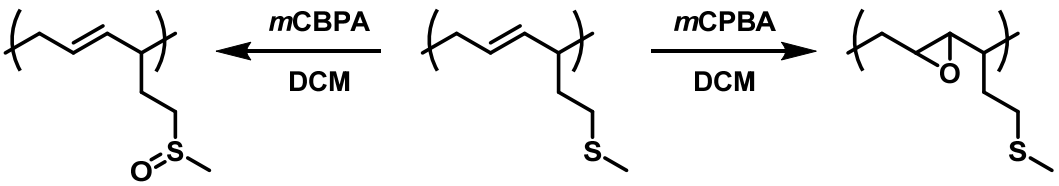


**Scheme 3**: Simplified scheme of the two possible oxidations of a MTHD repeating unit.

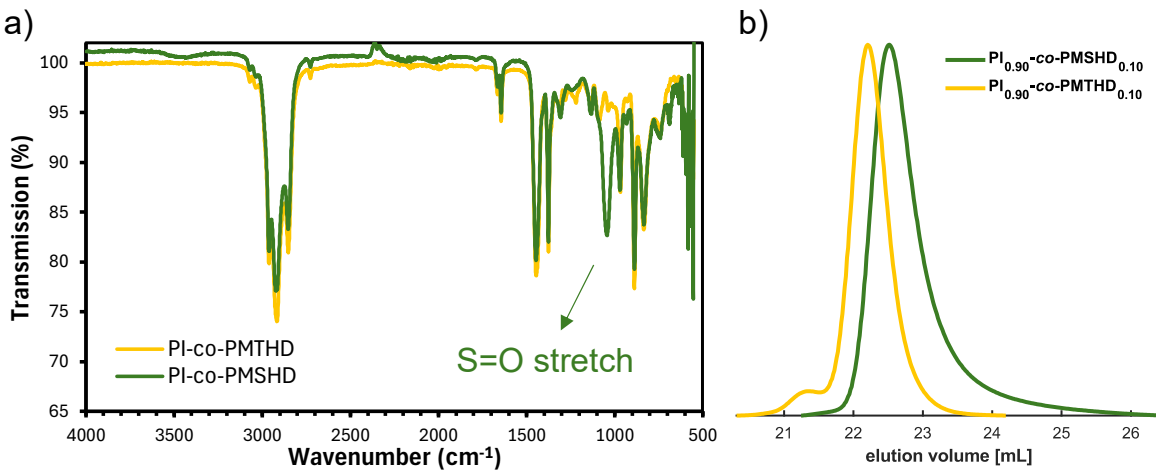


**Figure 6**: Comparison of the oxidized copolymer (green) and the respective precursor (yellow) in a) IR spectra permitting to identify the stretching vibration of the formed sulfoxide at 1040 $cm^{-1}$ and b) GPC measurements to identify the expected shift in molar mass.

*Alkoxylation:* Deming and coworkers reported the successful addition of epoxides onto thioether groups in polypeptides based on L-methionine.[16] A variety of functional epoxides was utilized to address the thioether groups in poly(L-methionine). Soon after, thioether groups were also introduced in polyethers and polycarbonates, respectively.[3,17] In all cases, the reactivity of the sulfur (II) species was successfully manipulated by the pH value. At low pH, the sulfide attacks the activated epoxide ring. Similarly, this functionalization was studied with the copolymer PI-*co*-PMTHD (entry 10). Three exemplary epoxides were chosen for polymer modification in this work (**Scheme 4**). Apart from the industrially highly-established propylene oxide (PO), we selected 4-[(2,3-epoxypropoxy) methyl]-2,2-dimethyl-1,3-dioxolane (IGG) and glycidyl propargyl ether (GPE) due to their functionalities. We expected that the acidic conditions of the alkoxylation would cleave the acetal group of IGG to form two additional hydroxyl groups. The obtained $^{1}$H NMR spectra (**Figure 7**) illustrate full conversion of the thioether group. The signal of the methyl group (marked yellow) broadens and shifts from 2.1 to around 3.2 ppm. Additional signals arise with respect to the epoxide employed. FT-IR measurements further prove the formation of hydroxyl groups with the characteristic broad band (**Figure S21**-**Figure S23**). DSC measurements were conducted as well to investigate the influence of the functionalities attached on the glass temperature. As illustrated in **Figure S24** the incorporation of 10 mol% of the building block does not affect the thermal properties. All three samples retain low glass temperatures below – 60°C.

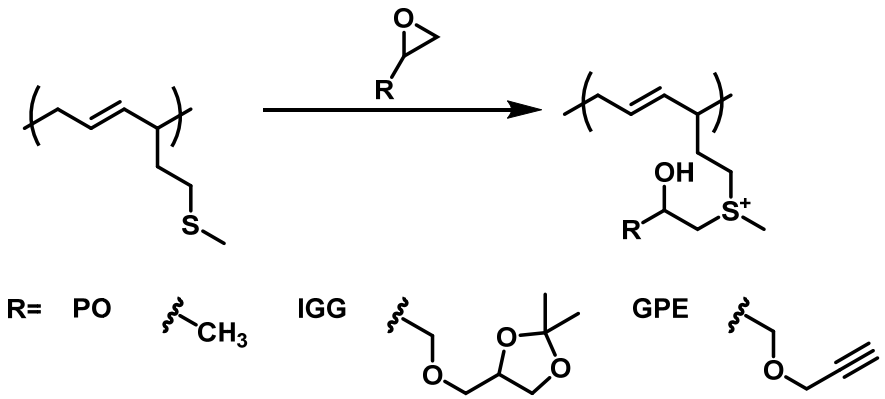


**Scheme 4**: Reaction scheme of the alkoxylation reaction with the three epoxides exemplary used (PO, IGG and GPE).

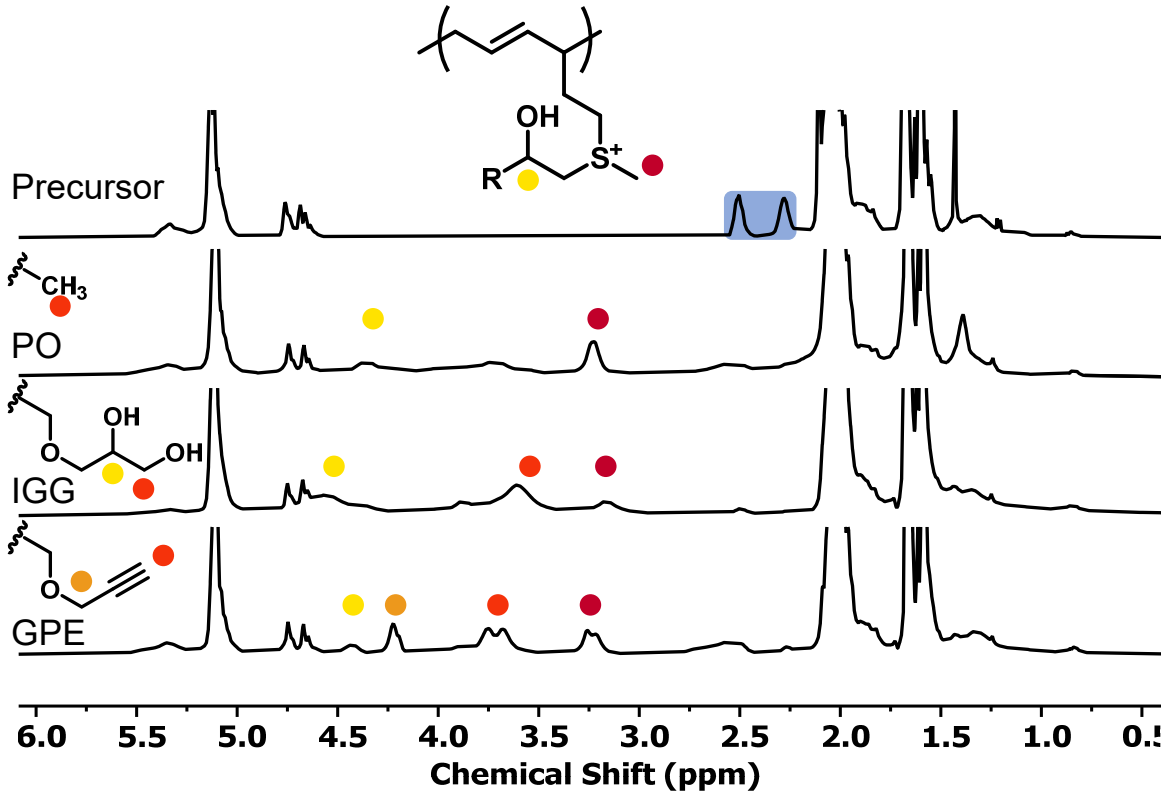


**Figure 7**: Stacked $^{1}$H NMR spectra (400 MHz, $CDCl_3$) of alkoxylation reaction with either PO, IGG or GPE in comparison to the precursor $PI_{0.9}$-*co*-$PMTHD_{0.1}$ (methyl group of the thioether highlighted in blue).

*Alkylation:* In analogy to the alkoxylation, Deming and coworkers also fundamentally investigated the click-type reaction of thioethers, with alkyl halides based on poly(L-methionine). Due to the high nucleophilicity of thioethers compared to common ethers, the variation of alkyl halides enables access to highly functional sulfonium derivatives.[15] The groups of Long and Matyjaszewski utilized this tertiarization for the bio-inspired 2-(methylthio)-ethyl methacrylate in the reaction with methyl iodide. Thus, polymer electrolytes for siRNA and DNA delivery were generated.[2,4] As demonstrated in

**Scheme 5**, methyl iodide and 2-bromoacetic acid were selected in the current work. The $^1$H NMR spectra (**Figure S25**) confirm high conversion of the sulfur species, indicated by decreasing signals of the neighboring methylene groups (δ = 2.6 – 2.2 ppm). New signals arise in both cases which can be assigned to the methyl group attached to the sulfur (I) atom. The FT-IR spectrum in **Figure S27** of the carboxylated copolymer shows new bands that are assigned to the carboxyl group (1628 cm$^{-1}$). DSC measurements showed no impact of the glass temperature for the methylated copolymer with a $T_g$ = − 59 °C. A slight increase with a $T_g$ = − 57 °C was found for the carboxylated PI-*co*-PMTHD (**Figure S28**).

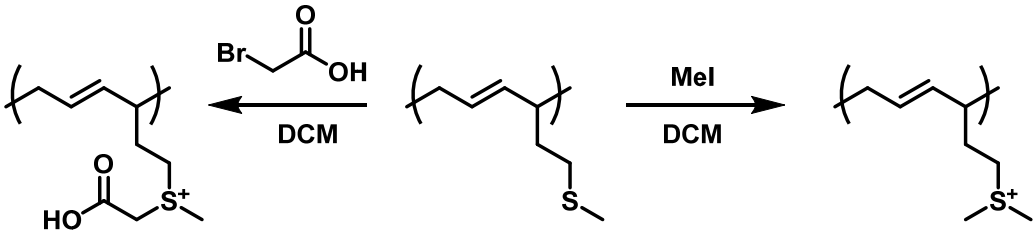


**Scheme 5**: Reaction schemes of the two performed alkylation reactions.

## Evaluation of Inhibition of Bacterial Growth

It is well-known that positively charged polyelectrolytes represent an effective class of antimicrobial agents, with demonstrated efficacy against various bacterial strains, e.g. *Escherichia coli* (*E. coli*). This effect is attributed to the anionic microbial membrane, particularly in Gram-negative bacteria, which can be effectively targeted passively. This ultimately leads to a disruption of the membrane, which results in the death of the cell. Hitherto, the induction of electrostatic interaction has typically been achieved through the use of nitrogen-containing moieties.[18,52] In the past, sulfonium groups have also been identified as highly active against Gram-positive and Gram-negative strains.[7,8,18] To obtain preliminary insights, we sought to examine the performance of the copolymer PMTHD$_{0.1}$-*co*-PI$_{0.9}$ (**Table 2**, entry 13) with tertiary sulfonium species as an antimicrobial coating. We selected the PO-functionalized and the methylated samples as typical representatives of both alkoxylation and alkylation. MTS assays were carried out to quantify the inhibitory effect of the modified polymers on the growth of *E. coli* strains (**Figure 8**). Following the coating of the polymer containing stock solution to technical replicas, *E. coli* was introduced and incubated overnight. The sample modified with propylene oxide demonstrated a comparable inhibitory effect on bacterial growth as that observed with

the antibiotic ampicillin. In comparison, modification with methyl iodide did not show signs of inhibition under the chosen conditions. Also, the precursor copolymer does not affect bacterial growth, proving the high impact of modification with propylene oxide. Furthermore, we were able to identify a concentration dependency of the PO-transformed copolymer (**Figure 8**b)).

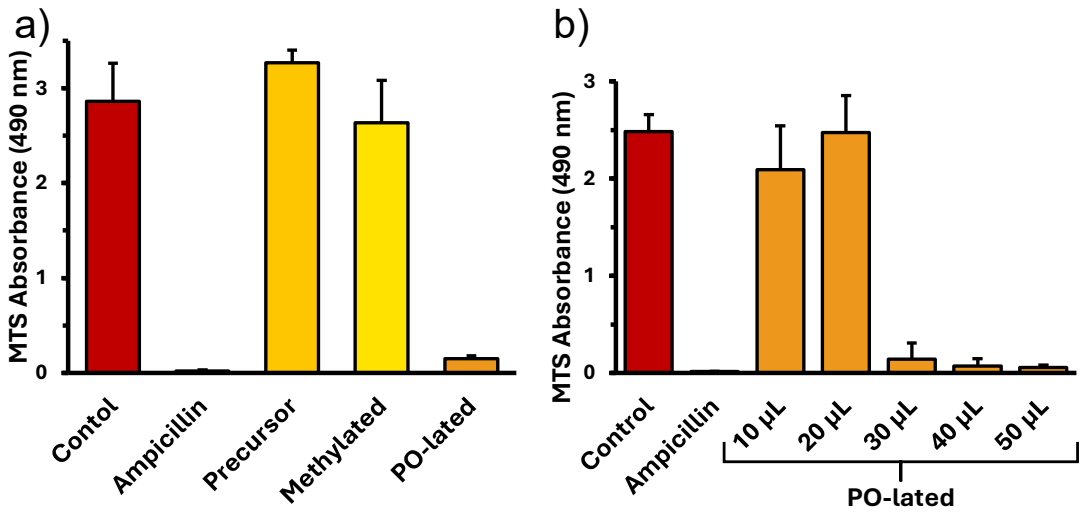


**Figure 8**: MTS assays analyzing the bacterial growth of *E. coli* a) on different variations PMTHD0.1-co-PI0.9 of 50 µL/1 mL aliquots and b) on increasing volume fraction of the PO-lated $PMTHD_{0.1}$-*co*-$PI_{0.9}$ in the total 1 mL sample volume.

Moreover, the growth of Gram-positive *Staphylococcus aureus* (*S. aureus*) on diverse surfaces was examined. As with the observations made for *E. coli*, the copolymer modified with propylene oxide demonstrated comparable inhibitory effects on bacterial growth to those observed with the utilized antibiotic, kanamycin (**Figure 9**). Subsequent experiments conducted, decreasing concentrations of the PO-lated copolymer, demonstrated the enhanced performance against *S. aureus*. As illustrated in **Figure S32** a notable effect can be achieved with a mere sixth of the volume of the copolymer-containing solution. This advanced potency against Gram-positive over Gram-negative strains has already been described by Hirayama *et al*.[53] The elevated bacterial density observed for the setup with the highest copolymer concentration (**Figure 9**c)) is presumably attributed to aggregation. This is supported by the fact that the microbial activity in **Figure 9**d) exhibits comparable low values to those observed for the lower concentrations.

We hypothesize that modification of the thioether with glycidyl ethers with functional groups known for their antimicrobial impact, could further improve the performance. Nevertheless, this system possesses further potential for the preparation of blends with industrially established thermoplastic elastomers.

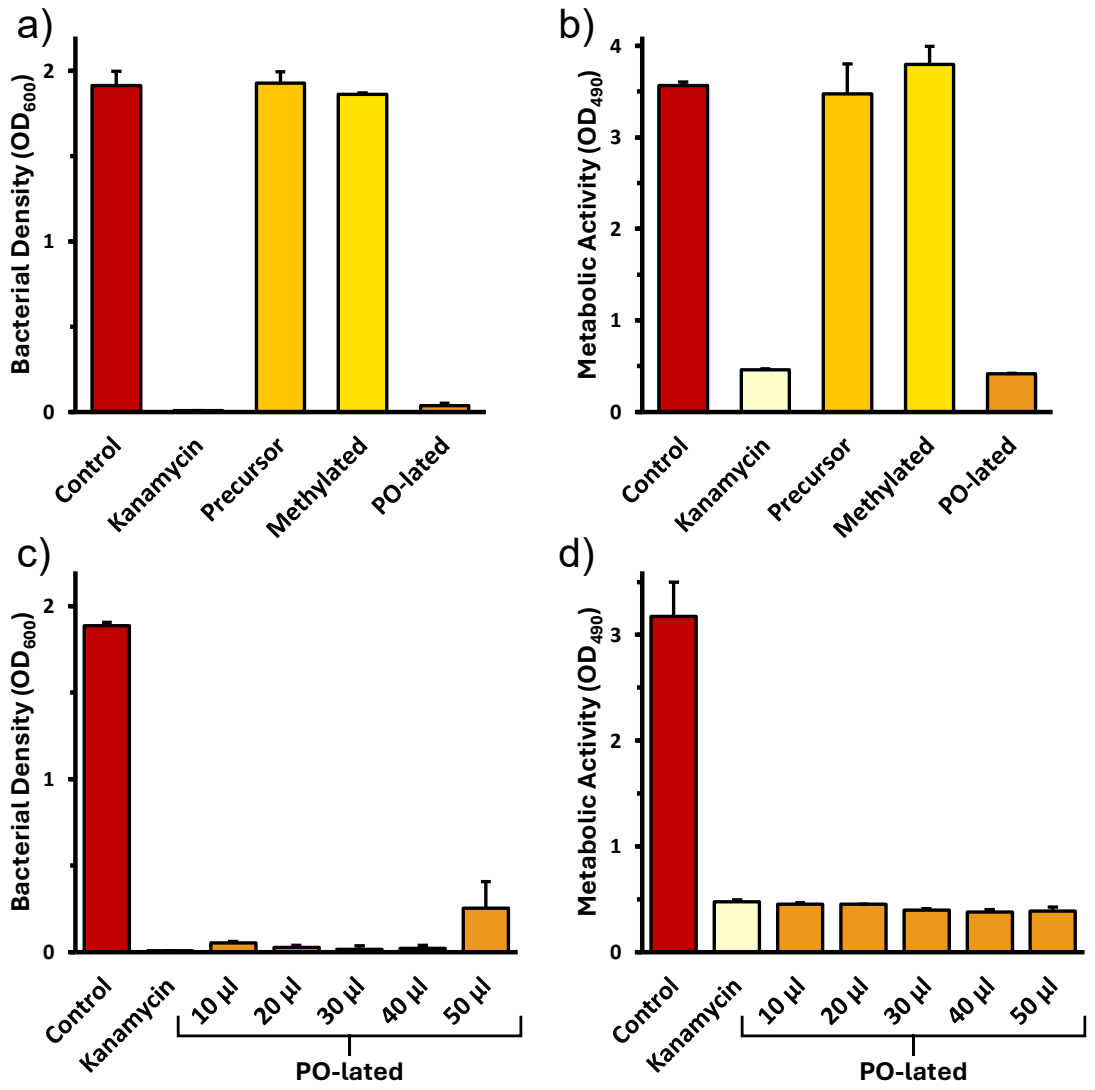


**Figure 9**: Illustration of a), c) the bacterial density and b), d) metabolic activity of Gram-positive S aureus strains on surfaces coated with a), b) modified and unmodified $PI_{0.9}$-*co*-$PMTHD_{0.1}$, respectively, and c), d) decreasing concentrations of the PO-lated copolymer $PI_{0.9}$-*co*-$PMTHD_{0.1}$ and the antibiotic Kanamycin as a reference.

## Conclusion

We have presented the synthesis of a thioether functional diene monomer, 6-methylthio hexa-1,3-diene (MTHD). A straightforward synthesis with only one purification step was accomplished with a preferred formation of the *trans*-isomer. The anionic homopolymerization with targeted molar masses of $M_n^{targ} = 5 – 50$ kg mol$^{-1}$ resulted in

increased dispersities of $Đ$ >1.24 which are most likely explained by the presence of an isomeric monomer mixture. *In situ* $^1$H NMR kinetics revealed disparate reactivities between the *cis*- and the *trans*-MTHD isomer. Copolymerization with isoprene resulted in well-defined structures with dispersities of $Đ$ < 1.19. The molar composition of the copolymers with molar MTHD fractions of $x^{MTHD}$ = 2 – 10% were further examined *via* $^1$H NMR kinetics revealing weak gradients ($r_{MTHD}$ = 3.2 and $r_I$ = 0.0027). We further established various post-polymerization functionalization based on PI-*co*-PMTHD copolymer. Alkoxylation was performed utilizing epoxides with methyl-, propargyl- and glyceryl groups. Additionally, alkylation reactions with methyl iodide and bromoacetic acid were conducted. Finally, the thioether group was selectively oxidized to the corresponding sulfoxide. All post-polymerization modifications change the solubility of the copolymers while not affecting the $T_g$. Moreover, the modification with propylene oxide induced antimicrobial properties with high performance against *S. aureus* strains. It is our contention that this represents a feasible platform for the future preparation of antimicrobial surfaces and that it may prove suitable for the development of next-generation tires.

## References


1 J. Seiwert, J. Herzberger, D. Leibig and H. Frey, *Macromol Rapid Commun*, 2017, **38**, 1600457.

2 M. C. Mackenzie, A. R. Shrivats, D. Konkolewicz, S. E. Averick, M. C. McDermott, J. O. Hollinger and K. Matyjaszewski, *Biomacromolecules*, 2015, **16**, 236–245.

3 J. Herzberger, K. Fischer, D. Leibig, M. Bros, R. Thiermann and H. Frey, *J Am Chem Soc*, 2016, **138**, 9212–9223.

4 S. T. Hemp, M. H. Allen, A. E. Smith and T. E. Long, *ACS Macro Lett*, 2013, **2**, 731–735.

5 P. Pham, S. Oliver, D. T. Nguyen and C. Boyer, *Macromol Rapid Commun*, 2022, **43**, 2200377.

6 Y. Gong, X. Xu, M. Aquib, Y. Zhang, W. Yang, Y. Chang, H. Peng, C. Boyer, A. K. Whittaker and C. Fu, *ACS Appl Polym Mater*, 2024, **6**, 6975.

7 J. Oh and A. Khan, *Biomacromolecules*, 2021, **22**, 3534–3542.

8 B. Zhang, M. Li, M. Lin, X. Yang and J. Sun, *Cite this: Biomater. Sci*, 2020, **8**, 6969.

9 V. Scholiers, B. Hendriks, S. Maes, T. Debsharma, J. M. Winne and F. E. Du Prez, *Macromolecules*, 2023, **56**, 9559–9569.

10 B. Hendriks, J. Waelkens, J. M. Winne and F. E. Du Prez, *ACS Macro Lett*, 2017, **6**, 930–934.

11 H. Phan, R. Cavanagh, D. Destouches, F. Vacherot, B. Brissault, V. Taresco, J. Penelle and B. Couturaud, *ACS Appl Polym Mater*, 2022, **4**, 7778–7789.

12 S. Xu, G. Ng, J. Xu, R. P. Kuchel, J. Yeow and C. Boyer, *ACS Macro Lett*, 2017, **6**, 1237–1244.

13 T. J. Deming, *Bioconjug Chem*, 2017, **28**, 691–700.

14 S. Dong, Y. Jiang, G. Qin, L. Liu and H. Zhao, *Biomacromolecules*, 2020, **21**, 4063–4075.

15 J. R. Kramer and T. J. Deming, *Biomacromolecules*, 2012, **13**, 1719–1723.

16 E. G. Gharakhanian and T. J. Deming, *Biomacromolecules*, 2015, **16**, 1802–1806.

17 N. H. Park, M. Fevre, Z. X. Voo, R. J. Ono, Y. Y. Yang and J. L. Hedrick, *ACS Macro Lett*, 2016, **5**, 1247–1252.

18 P. Pham, S. Oliver and C. Boyer, *Macromol Chem Phys*, 2023, **224**, 2200226.

19 A. Holt, *Angew. Chem.*, 1914, **27**, 153.

20 M. Steube, T. Johann, R. D. Barent, A. H. E. Müller and H. Frey, *Prog Polym Sci*, 2022, **124**, 101488.

21 R. Quirk, *Handbook of Polymer Synthesis, Characterization, and Processing*, 2013, 127–162.

22 H. Hsieh and R. Quirk, *Anionic polymerization: principles and practical applications*, Dekker, New York, 1996.

23 W. Wang, W. Lu, A. Goodwin, H. Wang, P. Yin, N. G. Kang, K. Hong and J. W. Mays, *Prog Polym Sci*, 2019, **95**, 1–31.

24 C. Hayichelaeh, L. A. E. M. Reuvekamp, W. K. Dierkes, A. Blume, J. W. M. Noordermeer and K. Sahakaro, *Rubber Chemistry and Technology*, 2018, **91**, 433–452.

25 D. Leibig, A. H. E. Müller and H. Frey, *Macromolecules*, 2016, **49**, 4792–4801.

26 K. Takenaka, T. Hattori, A. Hirao and S. Nakahama, *Macromolecules*, 1989, **22**, 1563–1567.

27 K. Takenaka, D. Nakashima, M. Miya, H. Takeshita and T. Shiomi, *Journal of Soft Materials*, 2013, **9**, 14–19.

28 K. Takenaka, Y. Akagawa, H. Takeshita, M. Miya and T. Shiomi, *Polym J*, 2009, **41**, 106–107.

29 C. Wahlen, M. Rauschenbach, J. Blankenburg, E. Kersten, C. P. Ender and H. Frey, *Macromolecules*, 2020, **53**, 9008–9017.

30 C. Hahn, M. Wagner, A. H. E. Müller and H. Frey, *Macromolecules*, 2022, **55**, 4046–4055.

31 W. Luo, P. Yang, Q. Gan, Z. Zhao, F. Tang, Y. Xu, X. Jia and D. Gong, *Polym Chem*, 2021, **12**, 3677–3687.

32 X. Xu, Z. Chen, Y. Zhou, X. Jia and D. Gong, *Polym Int*, 2022, **71**, 1127–1133.

33 Y. Xu, J. Zhao, Q. Gan, W. Ying, Z. Hu, F. Tang, W. Luo, Y. Luo, Z. Jian and D. Gong, *Polym Chem*, 2020, **11**, 2034–2043.

34 H. Leicht, I. Göttker-Schnetmann and S. Mecking, *J Am Chem Soc*, 2017, **139**, 6823–6826.

35 H. Leicht, I. Göttker-Schnetmann and S. Mecking, *Macromolecules*, 2017, **50**, 8464–8468.

36 H. Leicht, I. Göttker-Schnetmann and S. Mecking, *ACS Macro Lett*, 2016, **5**, 777–780.

37 C. Yao, N. Liu, S. Long, C. Wu and D. Cui, *Polym Chem*, 2016, **7**, 1264–1270.

38 D. Gong, F. Tang, Y. Xu, Z. Hu and W. Luo, *Polym Chem*, 2021, **12**, 1653–1660.

39 L. Cai, S. Long, C. Wu, S. Li, C. Yao, X. Hua, H. Na, D. Liu, T. Tang and D. Cui, *Polym Chem*, 2020, **11**, 1646–1652.

40 S. Uchida, K. Togii, S. Miyai, R. Goseki and T. Ishizone, *Macromolecules*, 2020, **53**, 10107–10116.

41 P. R. Blakemore, S. K. Kim, V. K. Schulze, J. D. White and A. F. T. Yokochi, *J Chem Soc Perkin 1*, 2001, **0**, 1831–1847.

42 S. P. Wadgaonkar, S. Schüttner, E. Berger-Nicoletti, A. H. E. Müller and H. Frey, *Macromolecules*, 2022, **55**, 4721–4732.

43 S. P. Wadgaonkar, M. Wagner, L. A. Baptista, R. Cortes-Huerto, H. Frey and A. H. E. Müller, *Macromolecules*, 2023, **56**, 664–677.

44 M. Meier-Merziger, D. A. H. Fuchs, H. Frey and A. H. E. Müller, *Macromolecules*, 2024, **57**, 8154–8161.

45 K. Liu, Q. He, L. Ren, L. J. Gong, J. L. Hu, E. C. Ou and W. J. Xu, *Polymer (Guildf)*, 2016, **89**, 28–40.

46 V. Jaacks, *Makromol. Chem.*, 1972, **161**, 161–172.

47 C. Goodyear, US 3633, 1844.

48 D. J. T. Hill, J. H. O□Donnell, P. W. O□Sullivan, J. E. McGrath, I. C. Wang and T. C. Ward, *Polymer Bulletin*, 1983, **9**, 292–298.

49 A. Matic, A. Hess, D. Schanzenbach and H. Schlaad, *Polym Chem*, 2020, **11**, 1364–1368.

50 V. Hirschberg, M. G. Schußmann, M. C. Röpert, N. Dingenouts, S. Buchheiser, H. Nirschl, J. Berson and M. Wilhelm, *Macromolecules*, 2024, **57**, 3387–3396.

51 T. Sato, T. Ito, H. Ishibashi and M. Ikeda, *Chem Pharm Bull (Tokyo)*, 1990, **38**, 3331–3334.

52 M. Hartlieb, E. G. L. Williams, A. Kuroki, S. Perrier and K. E. S. Locock, *Curr Med Chem*, 2017, **24**, 2115–2140.

53 M. Hirayama, *Biocontrol Sci*, 2011, **16**, 23–31.

# Supporting Information

## Instrumentation

### Gel Permeation Chromatography (GPC)

GPC analysis was conducted utilizing an *Agilent 1260 Infinity II* instrument. It is equipped with a MZ-GEL-DS plus $10^5/10^3/100$ Å column set from *MZ-Analysetechnik* (Mainz, Germany) and a RI detector (*Agilent G1362A*) was used for every detection. The eluent used was THF, with an injection volume of 100 µL. The columns were heated to 30°C and a flow rate of 1 mL/min was used for all measurements. Calibrated was performed using a toluene standard, and polyisoprene standards were sourced from *PSS Polymer Standard Service GmbH* (Mainz, Germany).

### Nuclear Magnetic Resonance (NMR) spectroscopy

$^1$H, $^{13}$C, $^1$H-$^1$H COSY, $^1$H-$^{13}$C HSQC, $^1$H-$^{13}$C HMBC NMR spectra were recorded on a *Bruker Avance III HD 300*, *Bruker Avance II HD 400* and *Bruker Avance III 600* spectrometer. *In situ* NMR kinetics were investigated on a *Bruker Avance III HD 400* spectrometer. All spectrometers are equipped with a 5 mm BBFO-SmartProbe with z-gradient and ATM as well as a SampleXPress 60 sample changer. The signals were referenced internally to the assigned proton signal of the used deuterated solvent ($CDCl_3$, DMSO-$d_6$ and $C_6D_{12}$). All spectra were evaluated using *MestReNova* 14.2.0 developed by *Mestrelab Research S.L.* (Santiago de Compostela, Spain).

$^1$H-$^7$Li HOESY spectrum was measured on a 600 MHz *Bruker Avance III HD*. The signals were referenced internally to the assigned proton signal of the used deuterated solvent (toluene-$d^8$); temperature 25 °C. The spectra were evaluated using *TopSpin* 4.2.0 developed by *Bruker Cooperation* (Billerica, MA, USA).

### Differential Scanning Chromatography (DSC)

The thermal properties were investigated with a DSC 250 from *TA Instruments* with an RCS 90 compressor. Calibration was achieved with an indium and *n*-octane standard. Prior to the measurements the polymers were dried under high vacuum. At least 5 mg polymer was placed into a subsequently sealed pan. Any thermal history of the samples was removed through heating to 120°C. The glass temperature values were extracted from the second heating ramp starting from − 90 °C to 120°C using a rate of 10 K min$^{-1}$. All measurements were performed under a nitrogen atmosphere.

**Fourier-Transformed Infrared-Spectroscopy**

FT-IR spectroscopy was conducted on a diamond ATR unit-equipped *Nicolet* iS10 FT-IR spectrometer (*Thermo Scientific*, Waltham, MA, USA).

**Matrix-assisted Laser Desorption Ionization Time-of-Flight (MALDI-ToF) Mass Spectrometry**

MALDI-ToF analysis was performed with a MALDI-ToF MS Autoflex Max by *Bruker*. The sample was dissolved in dichloromethane at a concentration of 1 mg $mL^{-1}$. The measurement was conducted in linear mode, while *trans*-2-[3-(4-*tert*-butylphenyl)-2-methyl-2-propenyliden] malononitrile (DCTB) was used as a matrix with AgTFA.

**Gaschromatography/ electron impact-mass spectroscopy (GC/EI-MS)**

Gas chromatograph: Model 8890 from *Agilent*; HP-5 MS capillary column from *Agilent* (length 30 m, ID 0.25 mm); carrier gas helium. The sample is separated with a splitter between the EI-MS and the flame ionization detector (FID), the hydrogen for the FID is for the FID is generated using the Precision SL hydrogen generator from *PEAK SCIENTIFIC* with a purity of 99.9995 %. EI-MS: Mass Selective Detector 5977B from *Agilent* (electron impact ionization, 70 eV). The measurement was based on the following temperature program: [50 °C (0.5 min) – 290 °C (2 min with 20 °C $min^{-1}$).

## Experimental Section

**Reagents**

All reagents were purchased from commercial suppliers. Methional was received from *Sigma Aldrich*. We further purchased from *Fisher Scientific*, *TCI* and *Acros Organics*. Chloroform-*d*, dimethyl sulfoxide-$d_6$ and cyclohexane-$d_{12}$ were purchased from *Deutero GmbH*. All reagents were used as received if not stated otherwise. Methional was distilled prior to use. Cyclohexane was dried before use with sodium and benzophenone as an indicator while MTBE was purified with *s*BuLi and DPE as an indicator.

**Monomer Synthesis**

6-Methylthiohexa-1,3-diene was synthesized in a three-step synthesis.

1-Methylthiohexa-5-en-3-ol was prepared in a Grignard reaction starting from methional. In three-necked round-bottom flask Mg-turnings (6.3 g; 0.26 mol) were suspended in 40 mL anhydrous diethyl ether. A solution of 24.3 mL (0.28 mol) in

180 mL was added dropwise so that the suspension was mildly boiling. Once all the allyl bromide was added the solution was stirred for an additional hour. In another three-necked round-bottom methional (20 mL; 0.2 mol) was dissolved in 50 mL anhydrous diethyl ether and cooled in an ice-bath. To the cooled solution the freshly prepared Grignard-solution was added dropwise. Upon complete addition, the solution was stirred for an additional 30 minutes before warmed up to room temperature. The reaction was quenched by the addition of 200 mL of a saturated $NH_4Cl$-solution. The aqueous phase was extracted with 80 mL of diethyl ether. The combined organic extracts were washed twice with 100 mL of water and one time with 100 mL brine before dried over $Na_2SO_4$. The solvent was removed under reduced pressure to yield 22.7 g (77%) of the crude alcohol which was used without further purification.

The crude 1-methylthiohexa-5-en-3-ol was converted into the respective tosylate was adapted from Yokochi *et al*.[1] 21.5 g (0.15 mol) of 1-methylthiohexa-5-en-3-ol, 41.0 mL (0.29 mol) triethyl amine and 19.8 g (0.16 mol) DMAP were dissolved in dichloromethane (130 mL) and cooled to 0 °C. 46.5 g (0.24 mol) of *p*-toluenesulfonyl chloride was dissolved in 50 mL DCM and was added dropwise to the solution. The mixture was allowed to heat to room temperature before stirred for 2 hours. The solution got poured in 200 mL saturated ammonium chloride solution. The mixture was extracted three times with 70 mL of diethyl ether. The etheric solutions were washed with 100 mL of 1 M HCL, twice 100 mL $H_2O$ and with 100 mL of brine. After drying over $Na_2SO_4$ the solvent was removed under reduced pressure. Without further purification the compound was used.

The synthesis of the 6-methylthiohexa-1,3-diene started by dissolving the tosylate in 180 mL toluene. 36.8 mL (0.59 mol) DBU was added, and the solution was heated to 100°C overnight. After cooling to room temperature 60 mL of saturated ammonium chloride solution, 60 mL deionized water and 80 mL diethyl ether were added. The product was extracted three times with diethyl ether. The combined organic extracts were washed with 1 M HCl-solution (2 x 50 mL), water (60 mL) and brine (60 mL). The solvent was removed under reduced pressure. The product was purified by fractionated distillation at 30 mbar to yield 9.23 g of MTHD as a colorless liquid (50%).

**$^1$H NMR** ($CDCl_3$; 300 MHz): δ[ppm]= 6.65 (dddd, H-**2**$^{cis}$), 6.34 (dt, H-**2**$^{trans}$, 1H), 6.20 – 6.03 (m, H-**3**, 1H), 5.80 – 5.69 (m, H-**4**, 1H), 5.20 – 4.99 (m, H-**1**, 2H), 2.59 (ddd, H-**6**, 3H), 2.41 (q, H-**5**, 2H), 2.14 (s, H-**7**, 3H).

**$^{13}$C NMR** ($CDCl_3$; 101 MHz): δ[ppm] = 136.89 (C-**2**$^{trans}$), 132.70 (C-**4**$^{trans}$), 132.24 (C-**3**$^{trans}$), 131.88 (C-**2**$^{cis}$), 130.49 (C-**4**$^{cis}$), 130.09 (C-**3**$^{cis}$), 117.83 (C-**1**$^{cis}$), 115.76 (C-**1**$^{trans}$), 34.11 (C-**6**), 32.34 (C-**5**), 15.55 (C-**7**).

**Table S1**: Tested conditions for the elimination of the tosylate to yield the highest ratio of *cis*/*trans* on a small scale. Values might change when upscaled.

| Entry | Solvent | Base | *T* °C | *trans*[a] % | *cis*[a] % | Conversion. after 1h[a] |
|---|---|---|---|---|---|---|
| 1 | DMSO | KOtBu | 75 | 67 | 37 | >99% |
| 2 | DMSO | KOtBu | 35 | 77 | 23 | >99% |
| 3 | DMF | KOtBu | 35 | 85 | 15 | >99% |
| 4 | THF | KOtBu | 35 | 80 | 20 | >99% |
| 5 | THF | KOH[b] | 35 | 71 | 29 | <50% |

a) determined *via* $^1$H NMR spectroscopy b) addition as a 4M solution in MeOH

**Alternative monomer synthesis was achieved using the Wittig reaction**

In a Schlenk-flask 34.5 g (0.09 mol, 1.2 eq) allyl triphenyl phosphonium bromide was suspended in 140 mL anhydrous THF. 10.10 g (0.09 mol, 1.2 eq) potassium *tert*-butoxide was added and the suspension was stirred for 30 min at room temperature. Subsequently, 7.5 mL (0.075 mol) methional were added dropwise and the solution was stirred overnight. The reaction was quenched by the addition of 15 mL n-pentane. The solution was concentrated by removing THF at reduced pressure before the TPPO salts were removed *via* centrifugation. The residual solvent was removed at reduced pressure and 1.71 g (18%) MTHD was obtained through fractionated distillation (1.0 $10^{-3}$ mbar) yielding a *trans*/*cis* ratio of 54:46.

**General Polymerization Procedure**

The homopolymerizations and copolymerizations were conducted in an Argon-filled glovebox (*MBraun*, < 0.1 ppm $O_2$, < 0.1 ppm $H_2O$). Prior, the monomers were suspended in dried calcium hydride and degassed using the *freeze-pump* technique. After stirring overnight, the monomers were distilled in another flask equipped with a

Teflon stop cock filled with trioctyl aluminium to remove residual traces of impurities. The next day, the monomers were distilled into an empty Teflon stop cock-equipped flask.

**Procedure for *in situ* NMR kinetics**

In analogy to general polymerization procedures, the monomers were dried before use. Deuterated cyclohexane was freeze-dried over $CaH_2$ and stirred overnight. This was repeated twice before $C_6D_{12}$ was transferred to a flame-dried flask. Monomers and solvent were transferred into the glovebox. Subsequently, the volumetrically prepared solution was filled into a conventional NMR tube and sealed with a septum. After initiation, we recorded spectra with a preset frequencency. The decreasing integrals of the monomers were then evaluated with *NIREVAL* to obtain the reactivity ratios.[2] For the stereo copolymerization, we selected one scan every 5 seconds and a temperature of 20 °C to obtain enough data points for the evaluation of this fast polymerization reaction. In case of the copolymerization with isoprene, one scan every 30 seconds and a temperature of 25 °C was selected.

**Preparation of $^{1}$H-$^{7}$Li-HOESY measurement**

Prior to the analysis, the adduct of *t*BuLi and MTHD was formed at − 80 °C in diethyl ether (**Scheme S1**). Diethyl ether was partially removed and deuterated toluene was added to obtain stable conditions with similar apolar conditions found in the anionic polymerization. The formation of the adduct was proven by gas chromatography (GC/EI-MS) (**Figure S15**).

**General Procedure for Alkoxylation**

The alkoxylation method of Deming *et al*.[3] was adjusted to the polydiene system. 700 mg of the copolymer $PMTHD_{0.1}$-*co*-$PI_{0.9}$ were dissolved in a mixture of 5 mL DCM and 2.7 mL acetic acid (8 eq per MTHD units). Subsequently, the epoxide (3 eq per MTHD unit) was added, and the solution was stirred for 48 hours at room temperature. The solution was quenched by the addition of 7 mL of deionized water. The organic phase was washed with 7 mL of a 0.5 M HCl solution and 2 –3 times with 7 mL brine. The solvent was removed under reduced pressure and the crude polymer was dispersed in water. The alkylated polymer was purified *via* dialysis. Finally, the freeze drying gave the alkylated polymer (yield: 68 − 88 %).

**General Procedure for Alkylation**

The alkylation procedure was performed in accordance with the procedure reported by Boyer *et al*.[4] 700 mg of the copolymer $PMTHD_{0.1}$-*co*-$PI_{0.9}$ were dissolved in 7 mL DCM, prior to the addition of the alkyl halogenide (10 eq per MTHD unit). After 24 – 48 h of stirring at room temperature, the reaction was quenched by the addition 7 mL water. The organic phase was washed with 2 – 3 times with 7 mL brine. The solvent was removed under reduced pressure and the crude polymer was dispersed in water. The alkylated polymer was purified *via* dialysis. Finally, the freeze drying gave the alkylated polymer (yield: 83 – 94 %).

**Procedure of Post-polymerization Oxidation**

500 mg of the copolymer $PMTHD_{0.1}$-*co*-$PI_{0.9}$ were dissolved in 6 mL DCM. To the ice-cooled solution 0.23 g (1.5 eq per MTHD unit) *m*CPBA was added. The mixture was stirred for 1 h at 0 °C. The mixture was poured into 6 mL saturated $NaHCO_3$ and then washed with water and brine. The solvent was removed under reduced pressure and the polymer was finally freeze-dried with benzene.

**Procedure of the Determination of Antimicrobial Activity**

*E. coli* K12 strain NEB-5a (PMID: 27834703) was cultured overnight in Luria-Bertani (LB) medium (10 g $L^{-1}$ tryptone, 5 g $L^{-1}$ yeast extract and 10 g $L^{-1}$ sodium chloride; all from *Carl Roth*, Karlsruhe, Germany). *S. aureus* strain USA300 (PMID: 16517273) was grown overnight in tryptic soy broth (17 g $L^{-1}$ pancreatic digest of casein, 5 g sodium chloride, 3 g peptic digest of soybean, 2.5 g glucose, 2.5 g dipotassium phosphate). Bacterial liquid cultures were grown in a bacterial shaker at 37 °C and 140 rpm (MaxQ 4000; *Thermo Fisher*, Waltham, MA). On the next day, bacterial liquid cultures were diluted 1:1,000 into fresh media, and 1 ml aliquots were set up. Antibotic (NEB-5α: 50 µg $mL^{-1}$Ampicillin, USA300: 25 µg/ml Kanamycin) and polymers at various doses were added to triplicate cultures per condition. After overnight incubation, optical density (OD600) was measured using a spectrophotometer (V-1200; *VWR*, Radnor, PA). Metabolic activity was assayed by detecting NAP(D)H oxidase activity. To this end, each 100 µl of cell suspension was transferred per well of a 96 well plate, and 20 µl of detection reagent comprised of a tetrazolium compound (MTS; 3-(4,5-dimethylthiazol-2-yl)-5-(3-carboxymethoxyphenyl)-2-(4-sulfophenyl)-2H-tetrazolium, inner salt) and phenazine ethosulfate as an electron coupling reagent. Plates were incubated for

1 – 3 h at 37 °C to allow for formation of formazane product, Then, absorbance at OD490 was recorded (*Spark Multimode Microplate Reader*, Männedorf, Switzerland).

## Characterization for Monomer Synthesis of 6-Methylthiohexa-1,3-diene (MTHD)

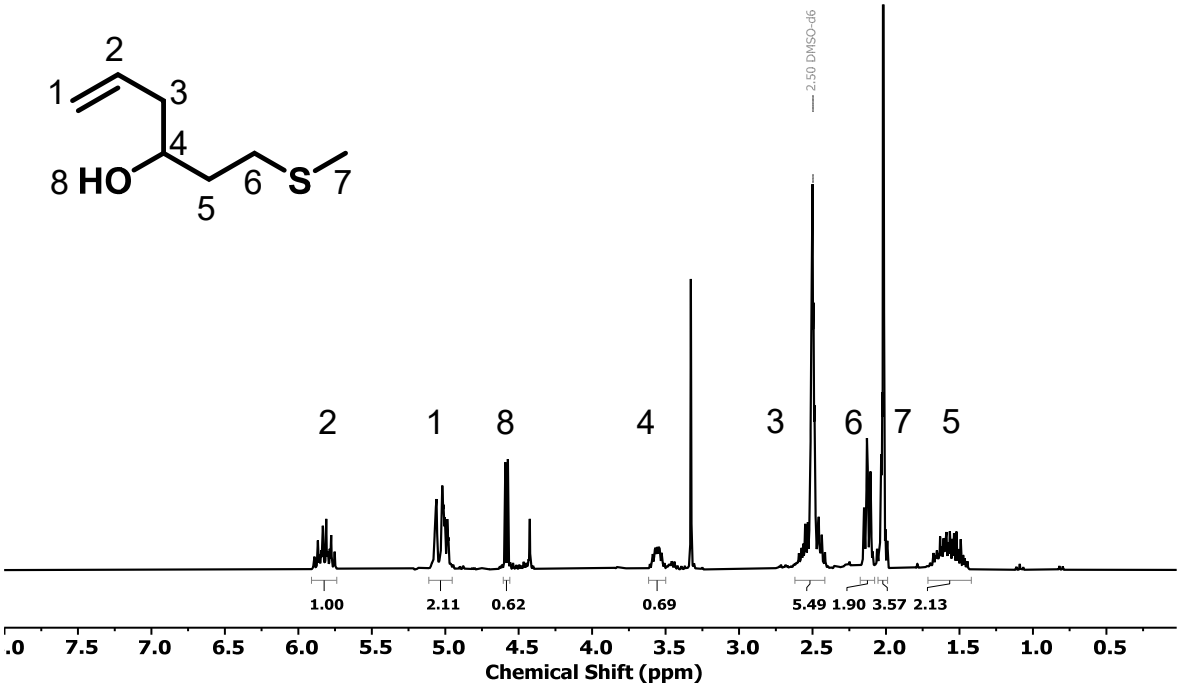


**Figure S1**: Crude $^{1}$H NMR spectra (DMSO-$d^{6}$, 300 MHz) of 1-methylthiohexa-5-en-3-ol.

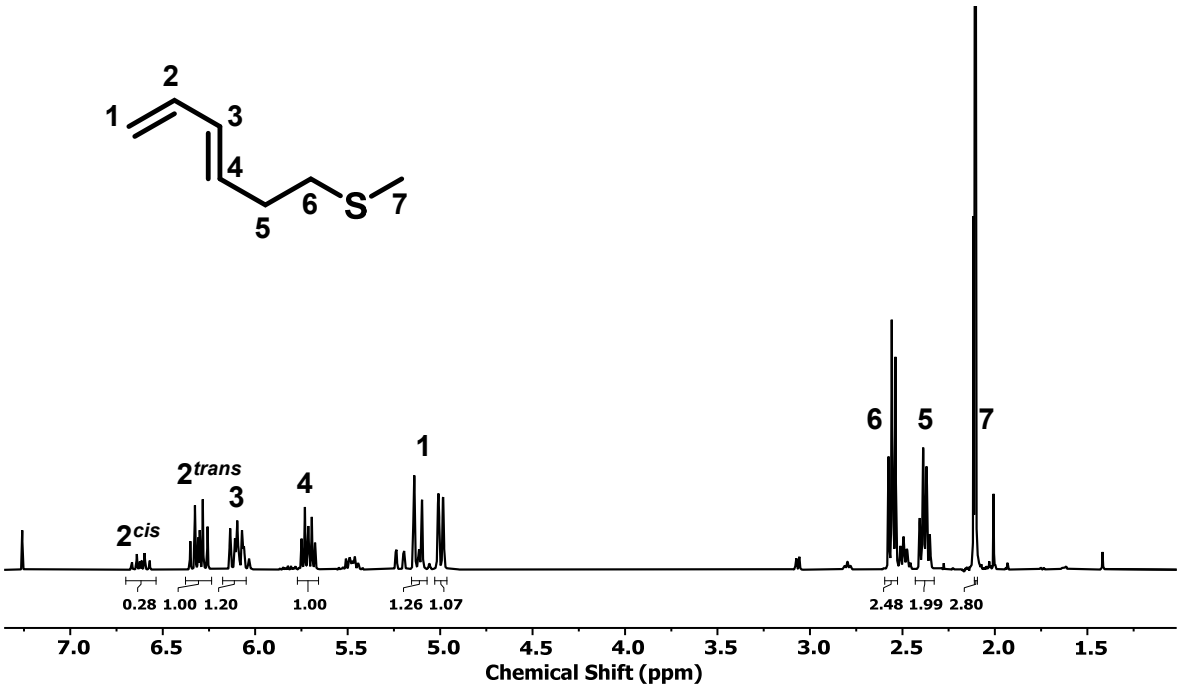


**Figure S2**: $^{1}$H NMR spectrum ($CDCl_3$, 400 MHz) of 6-methylthio hexa-1,3-diene.

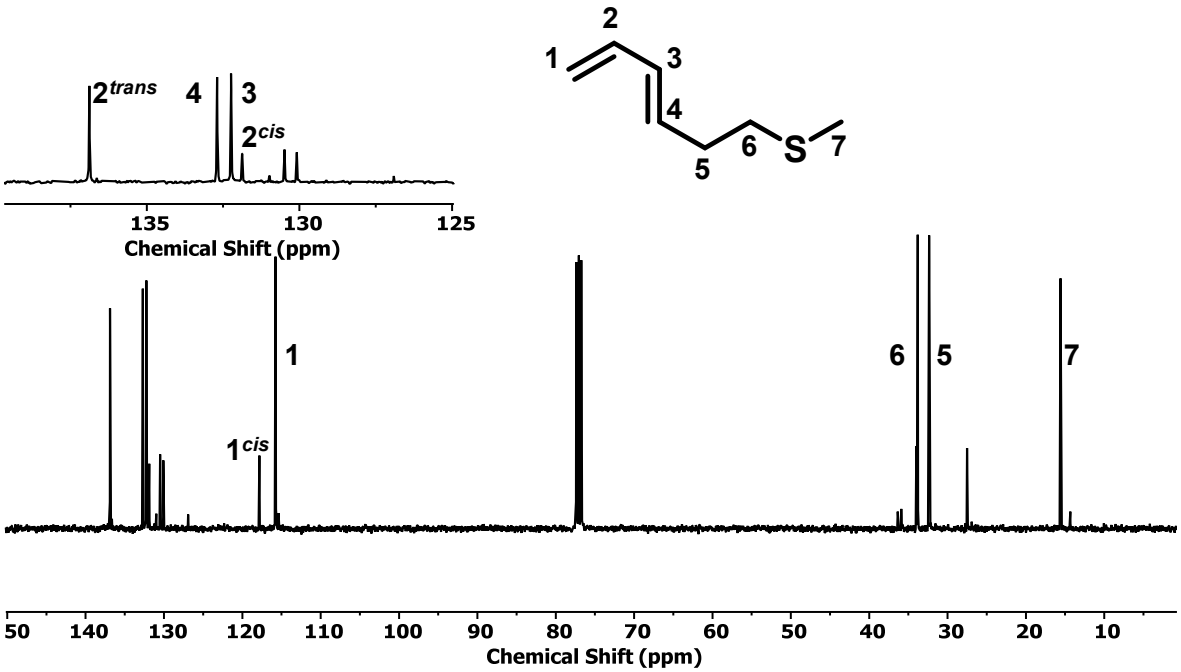


**Figure S3**: $^{13}C$ NMR spectrum ($CDCl_3$, 101 MHz) of 6-methylthio hexa-1,3-diene.

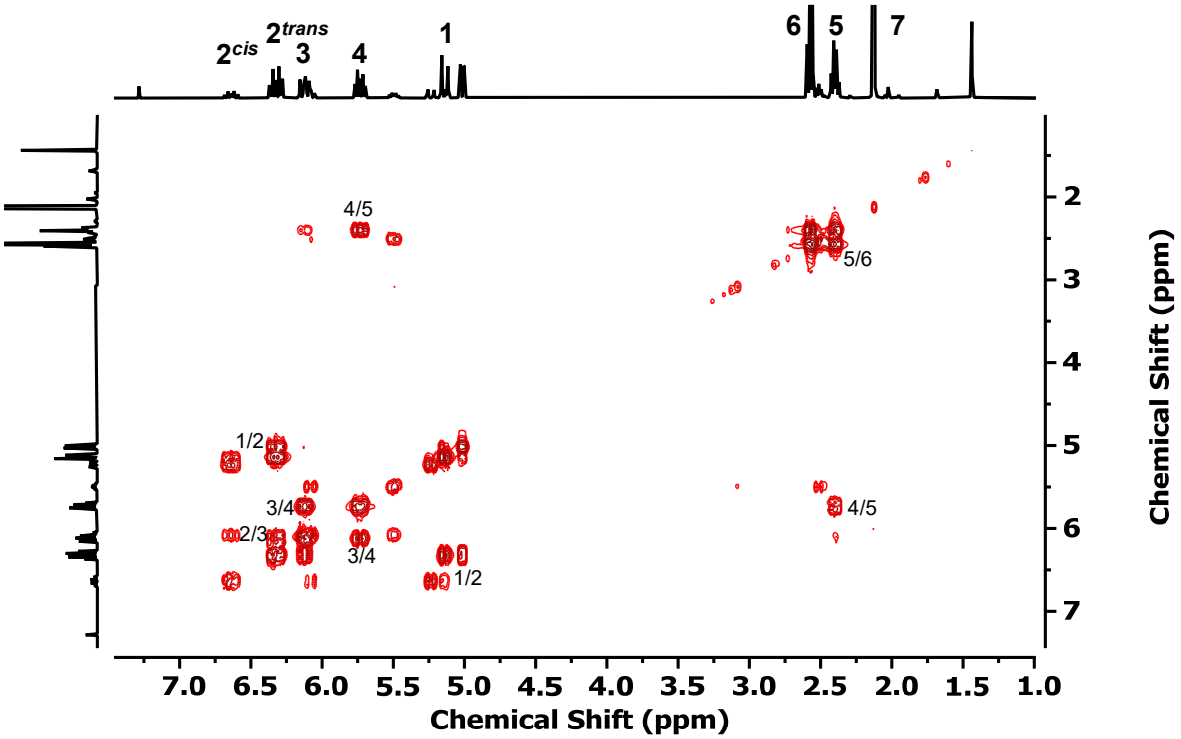


**Figure S4**: $^{1}H$-$^{1}H$ COSY NMR spectrum ($CDCl_3$, 400 MHz) of 6-methylthio hexa-1,3-diene.

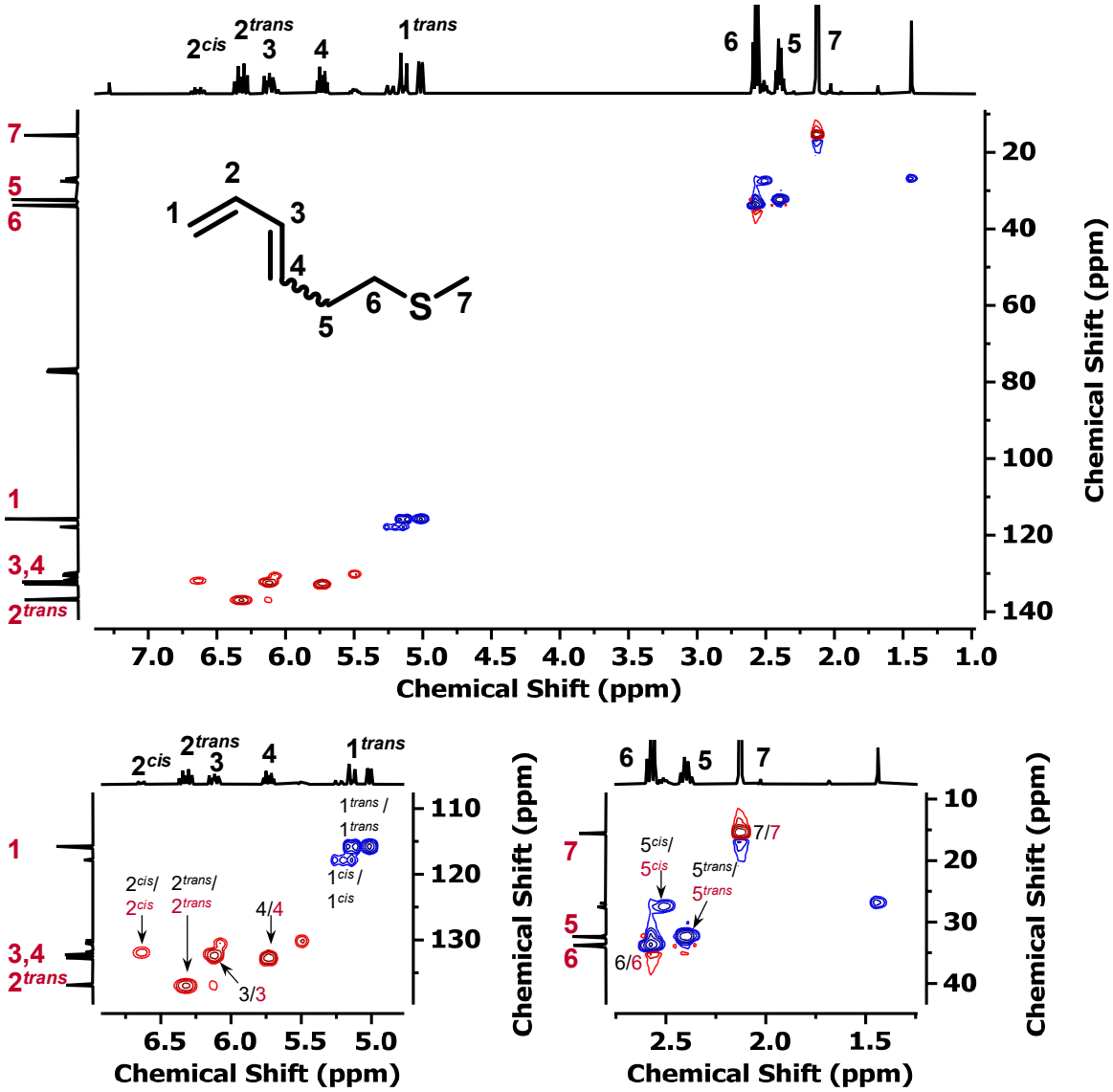


**Figure S5**: $^{1}H$-$^{13}C$ HSQC NMR spectrum ($CDCl_3$, 400MHz, 101 MHz) of 6-methylthio hexa-1,3-diene with the expansion of relevant parts of the spectrum.

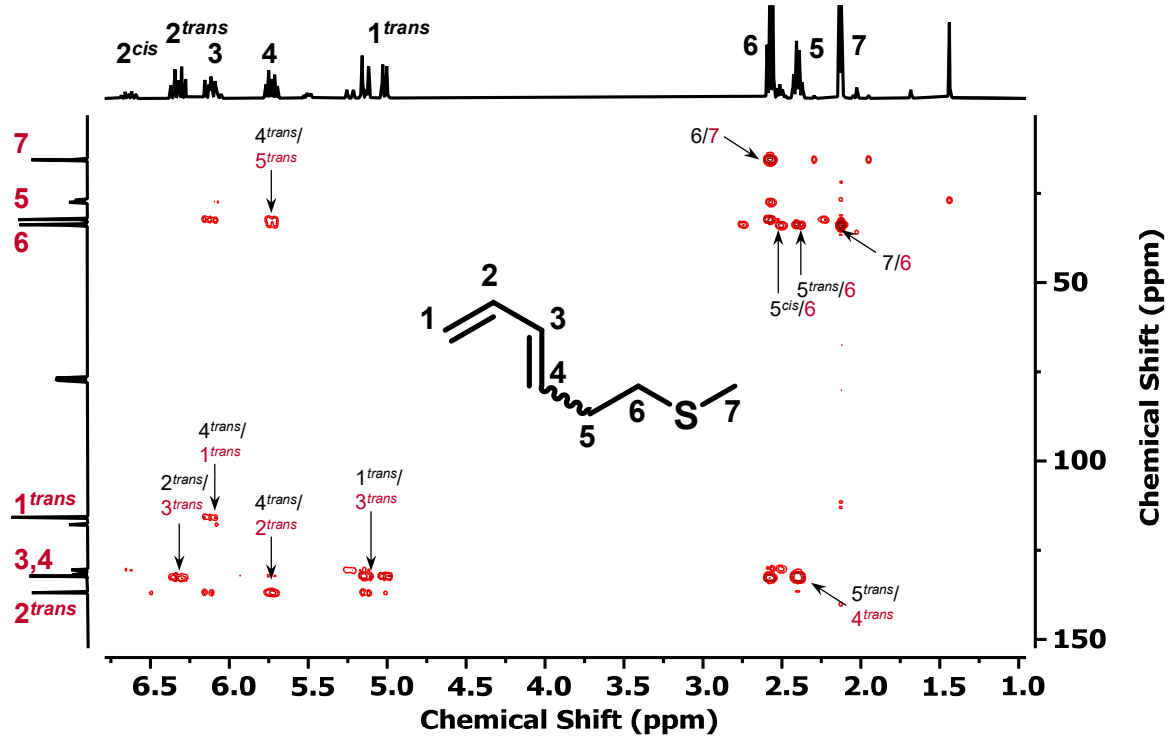


Figure S 6: $^{1}H$-$^{13}C$ HMBC NMR spectrum ($CDCl_3$, 400MHz, 101 MHz) of 6-methylthio hexa-1,3-diene.

## Characterization for Homopolymers PMTHD

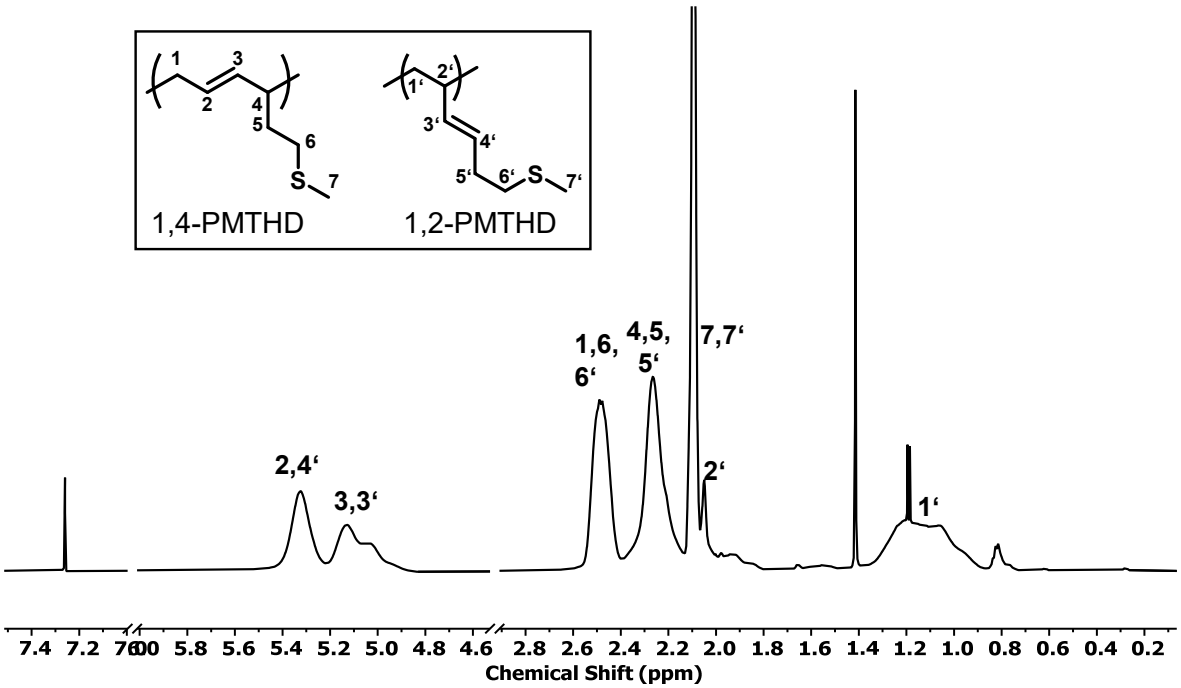


**Figure S7**: $^{1}H$ NMR spectrum ($CDCl_3$, 600 MHz) of the homopolymer PMTHD (**Table 1**, entry 1).

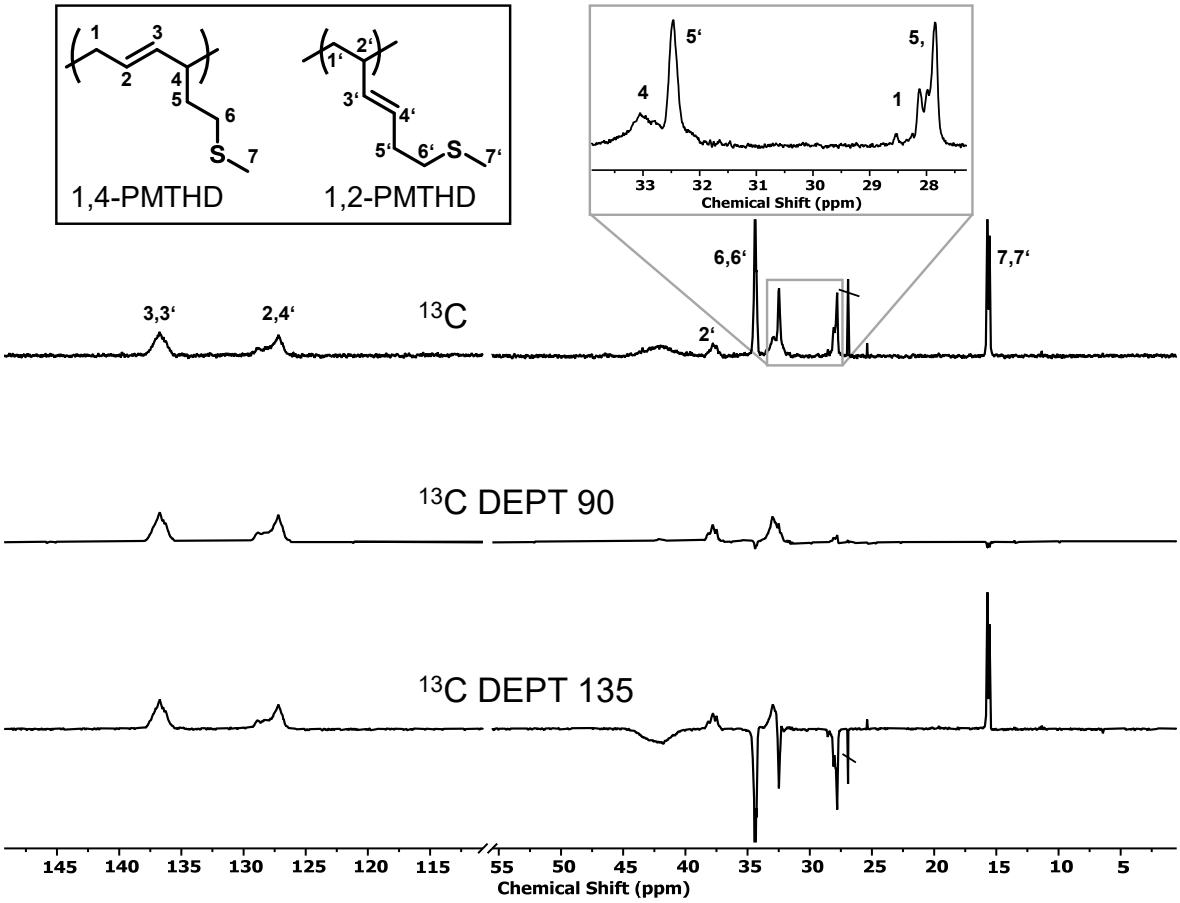


**Figure S8**: $^{13}C$, $^{13}C$ DEPT 90 and $^{13}C$ DEPT 135 spectra ($CDCl_3$, 101 MHz) of the homopolymer PMTHD (**Table 1**, entry 1).

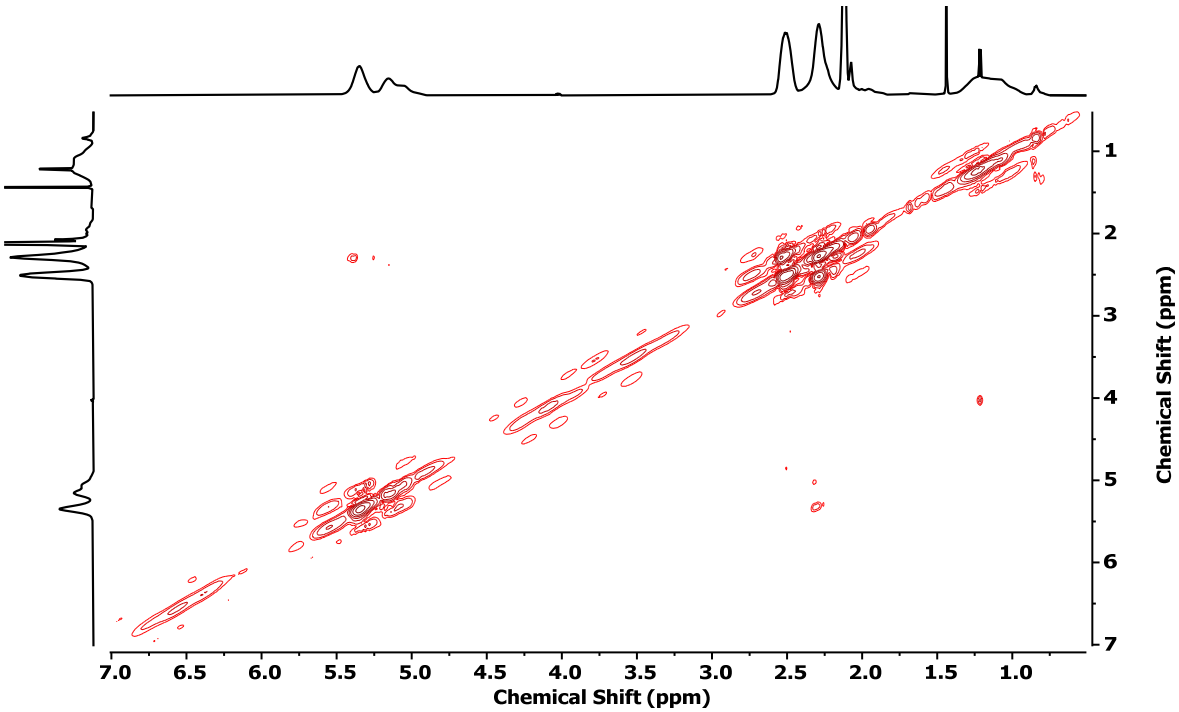


**Figure S9**: $^{1}H$-$^{1}H$ COSY spectrum ($CDCl_3$, 600 MHz) of the homopolymer PMTHD of the homopolymer PMTHD (**Table 1**, entry 1).

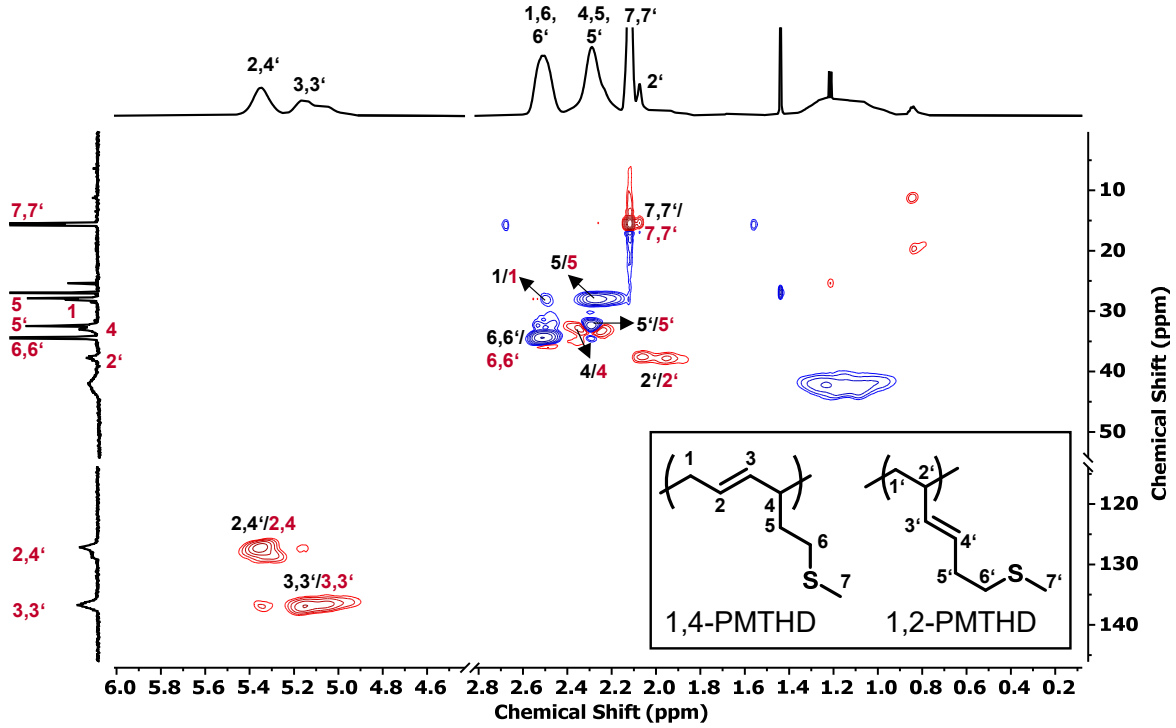


**Figure S10**: $^{1}H$-$^{13}C$ HSQC spectrum ($CDCl_3$, 600 MHz) of the homopolymer PMTHD of the homopolymer PMTHD (**Table 1**, entry 1).

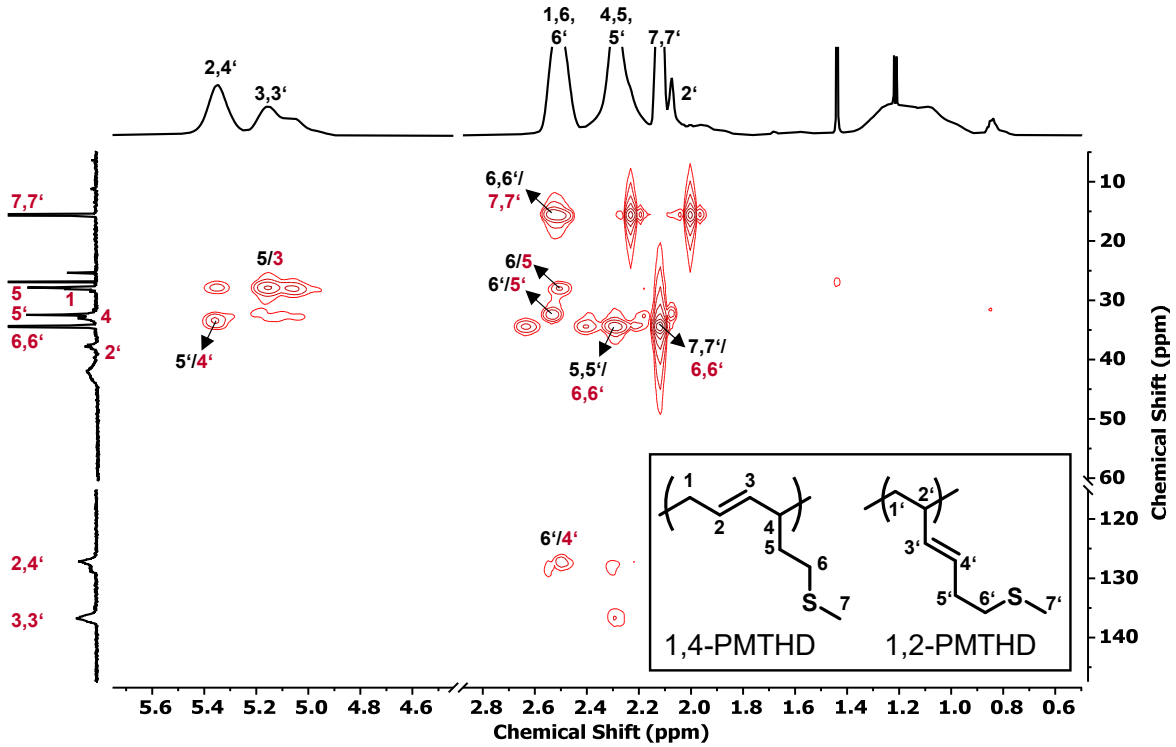


**Figure S11**: $^{1}H$-$^{13}C$ HMBC spectrum ($CDCl_3$, 600 MHz) of the homopolymer PMTHD of the homopolymer PMTHD (**Table 1**, entry 1).

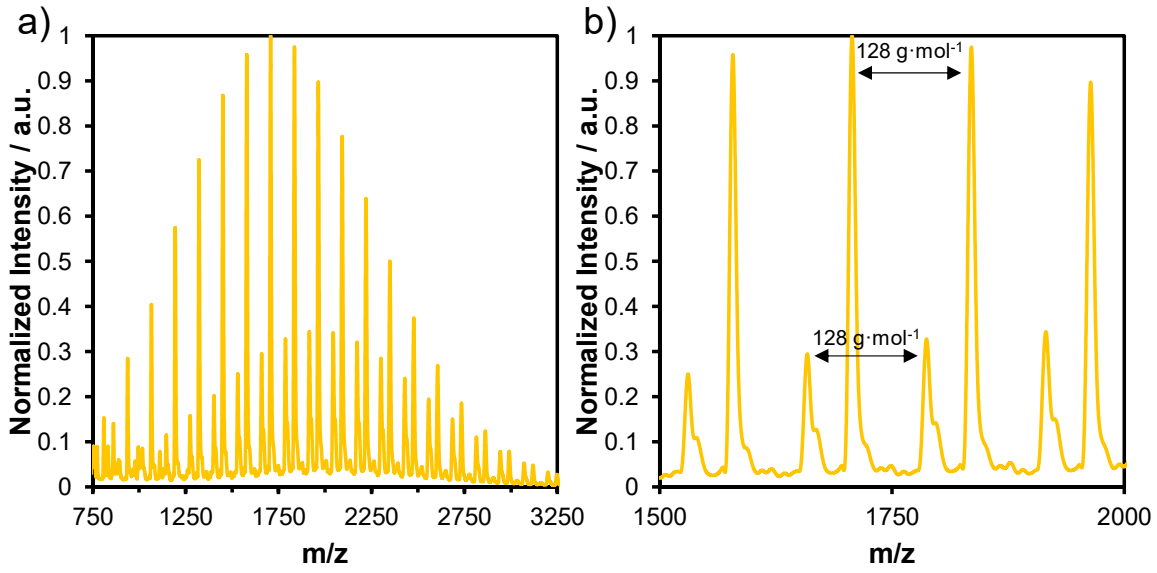


**Figure S12**: Maldi TOF mass spectrum of PMTHD (**Table 1**; entry 1) as a) the whole distribution and b) the cutout of the maximum.

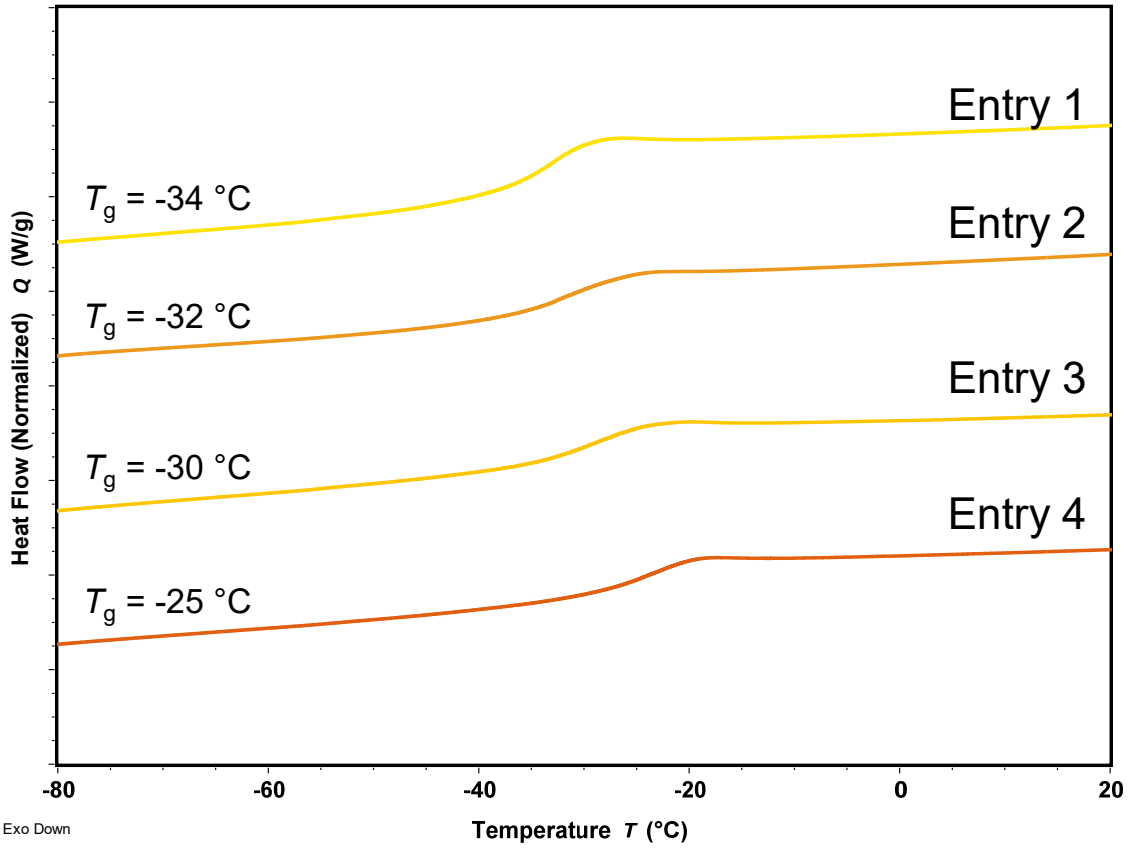


**Figure S13**: DSC curves of PMTHD polymerized in CHx (**Table 1**; entries 1-4).

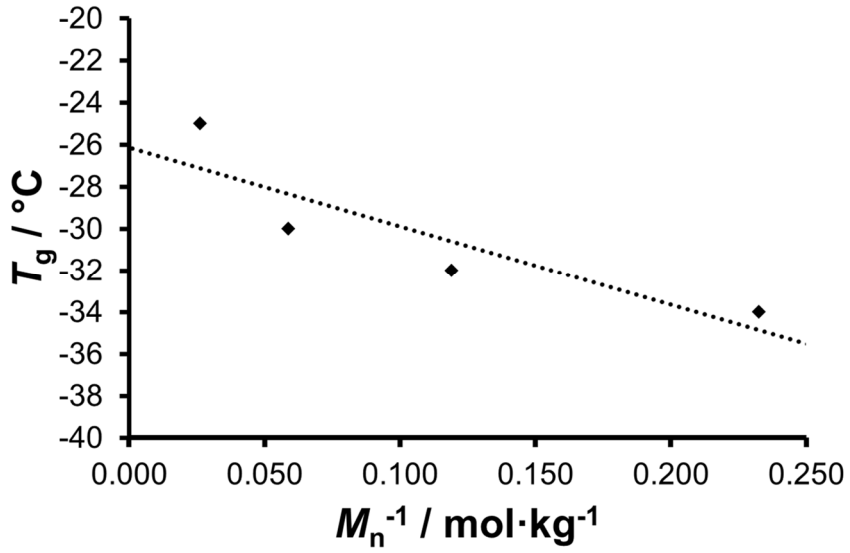


**Figure S14**: Plot of glass temperature vs. the inverse molar mass for PMTHD (**Table 1**, Entries 1-4)

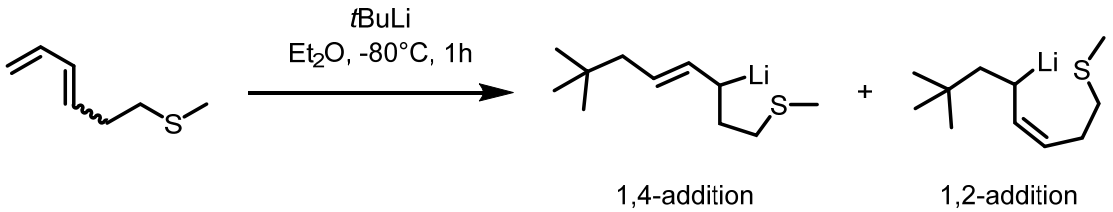


**Scheme S1**: Preparation prior to the HOESY measurement in **Figure 2** starting from *t*BuLi and MTHD towards the two potential adducts.

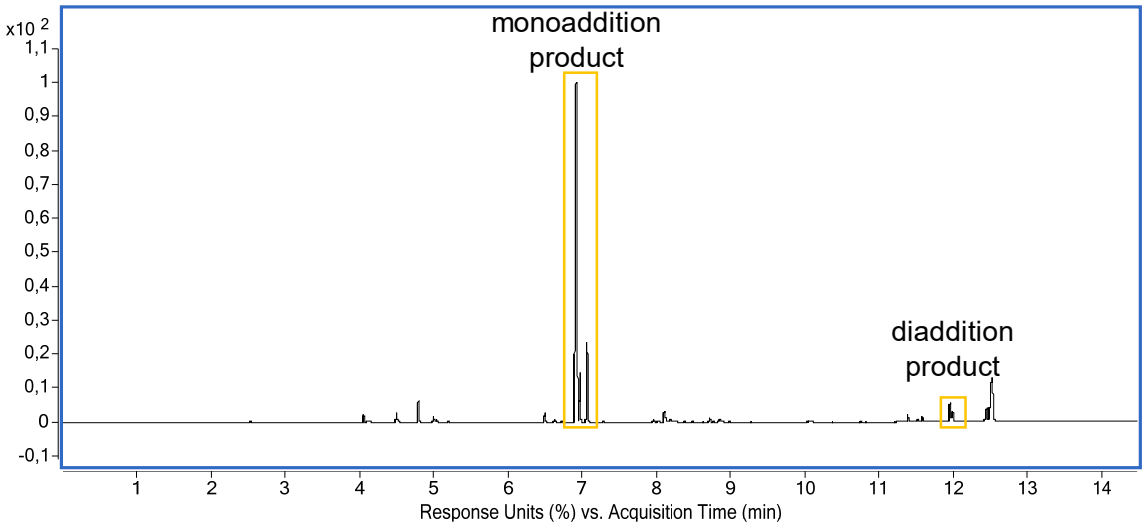


**Figure S15**: Gas chromatography spectrum after the preparation and protonation of the *t*BuLi-MTHD-adduct.

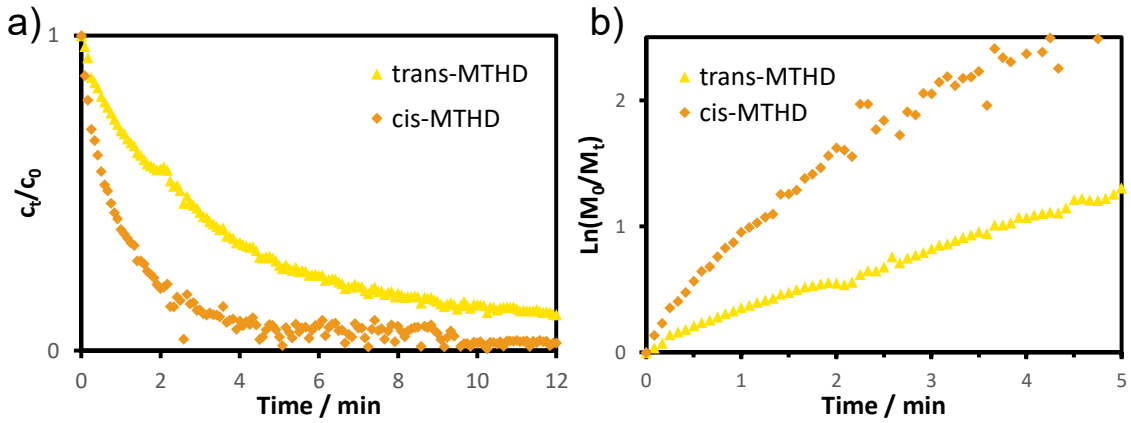


**Figure S16**: a) Monomer consumption over time of the two isomers of MTHD in the homopolymerization and b) the first-order-plot of the *cis*- and *trans*-isomers of MTHD.

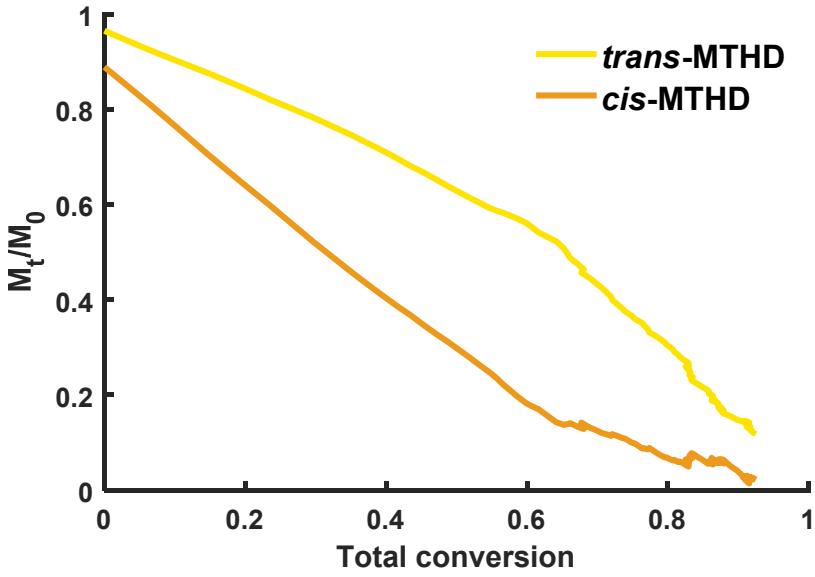


**Figure S17**: Plot of the individual monomer conversion versus the total monomer conversion of the stereo-copolymerization of cis- and trans-MTHD.

## Characterization for Copolymers PI-*co*-PMTHD

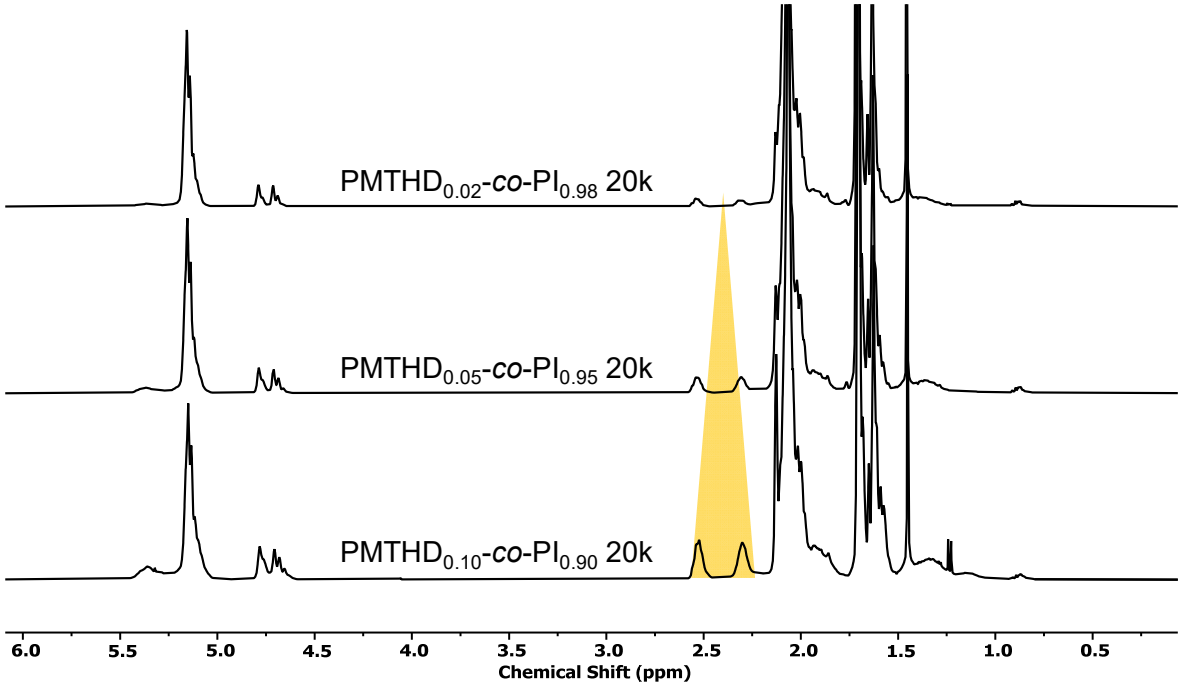


**Figure S18**: Stacked NMR spectra of the copolymers PMTHD-*co*-PI (entries 10 – 12, **Table 2**) with a targeted molar mass of 20 kg mol$^{-1}$. Increasing MTHD content is observable through the highlighted signals corresponding to MTHD.

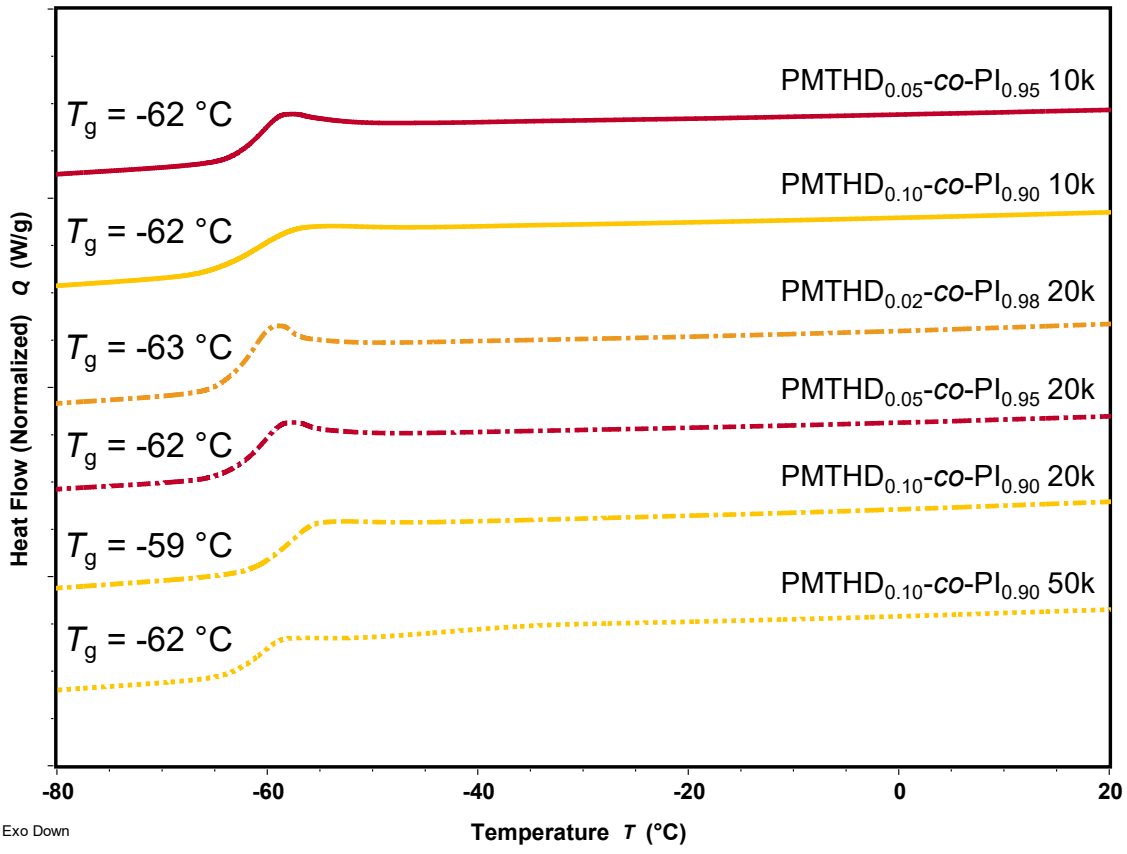


**Figure S19**: DSC curves of the synthesized copolymers PMTHD-co-PI (Table 2; entries 8 – 13) with increasing molar mass.

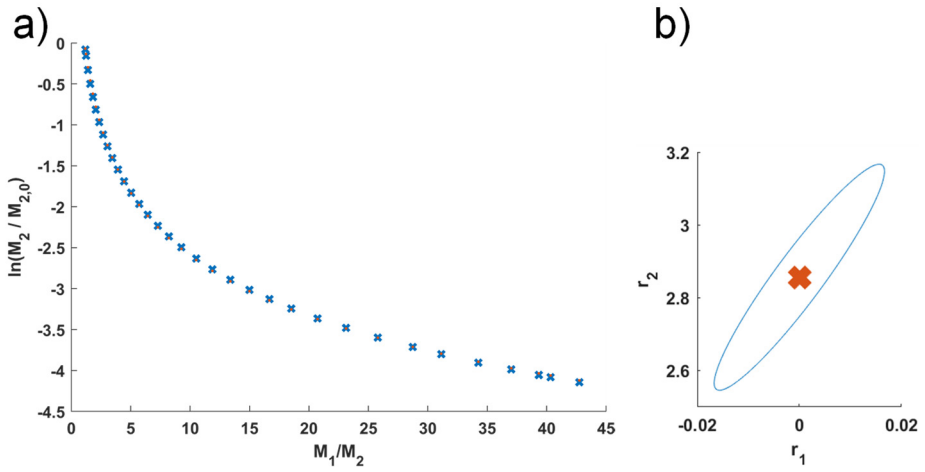


**Figure S20**: a) Log Meyer-Lowry fit of the NMR kinetic experiment of the copolymerization of MTHD and isoprene and b) the graphical illustration of the errors of the reactivity ratios.

## Characterization for Alkoxylation Reactions

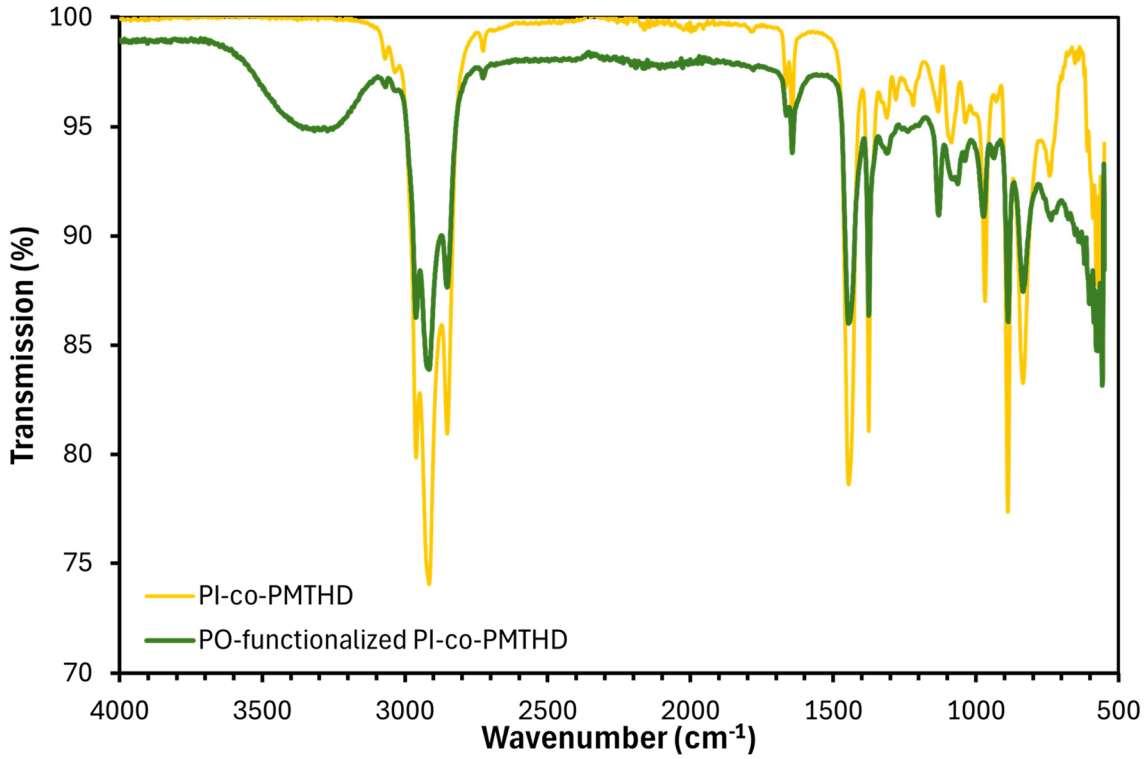


**Figure S21**: IR spectra of the precursor PI-*co*-PMTHD (yellow) and the PO-functionalized copolymer (green).

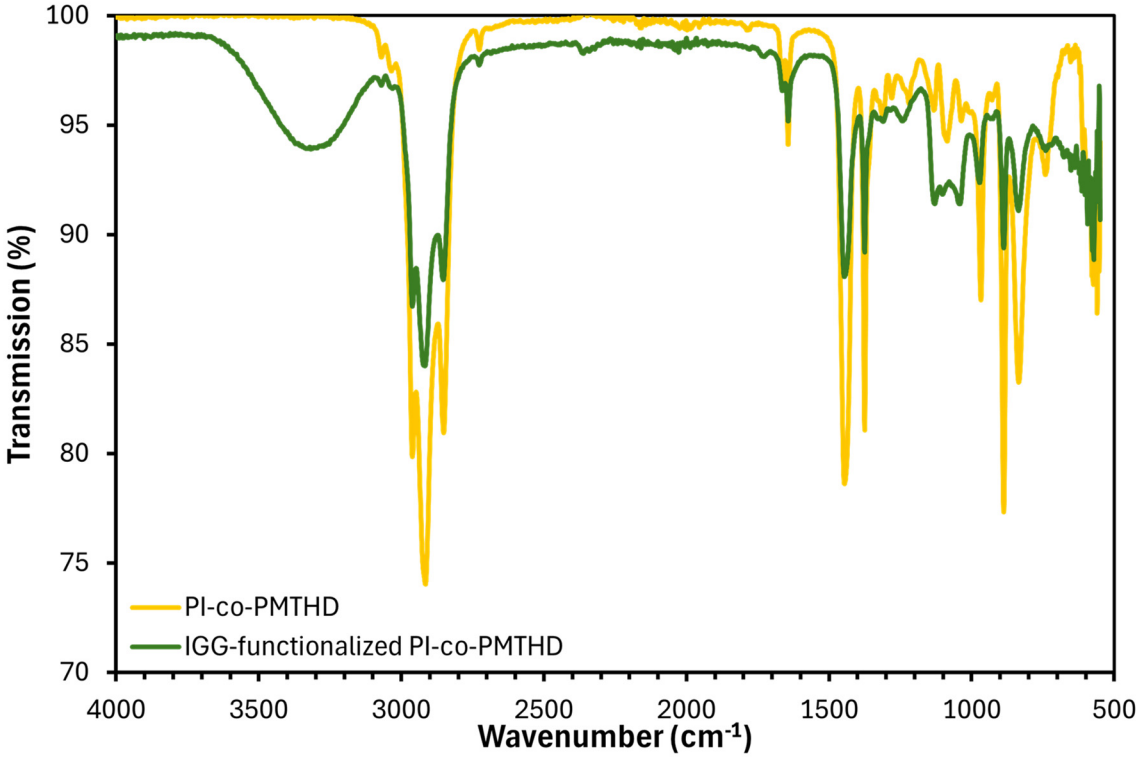


**Figure S22**: IR spectra of the precursor PI-*co*-PMTHD (yellow) and the IGG-functionalized copolymer (green).

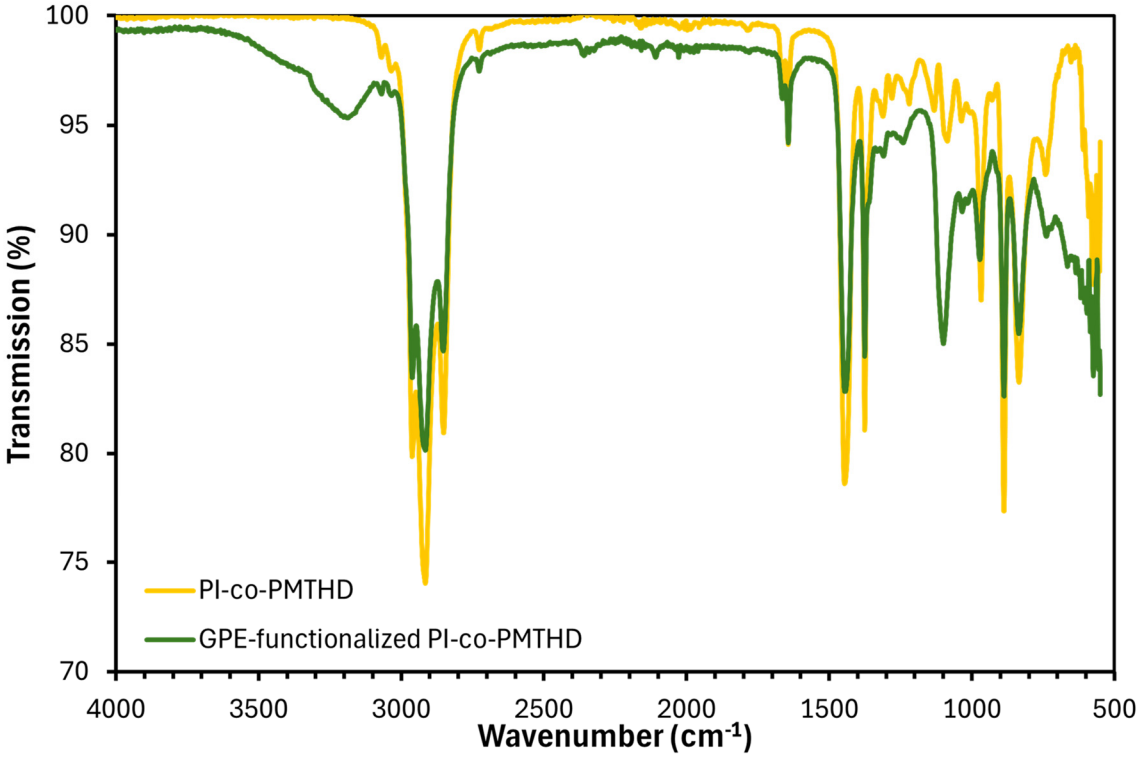


**Figure S23**: IR spectra of the precursor PI-*co*-PMTHD (yellow) and the GPE-functionalized copolymer (green).

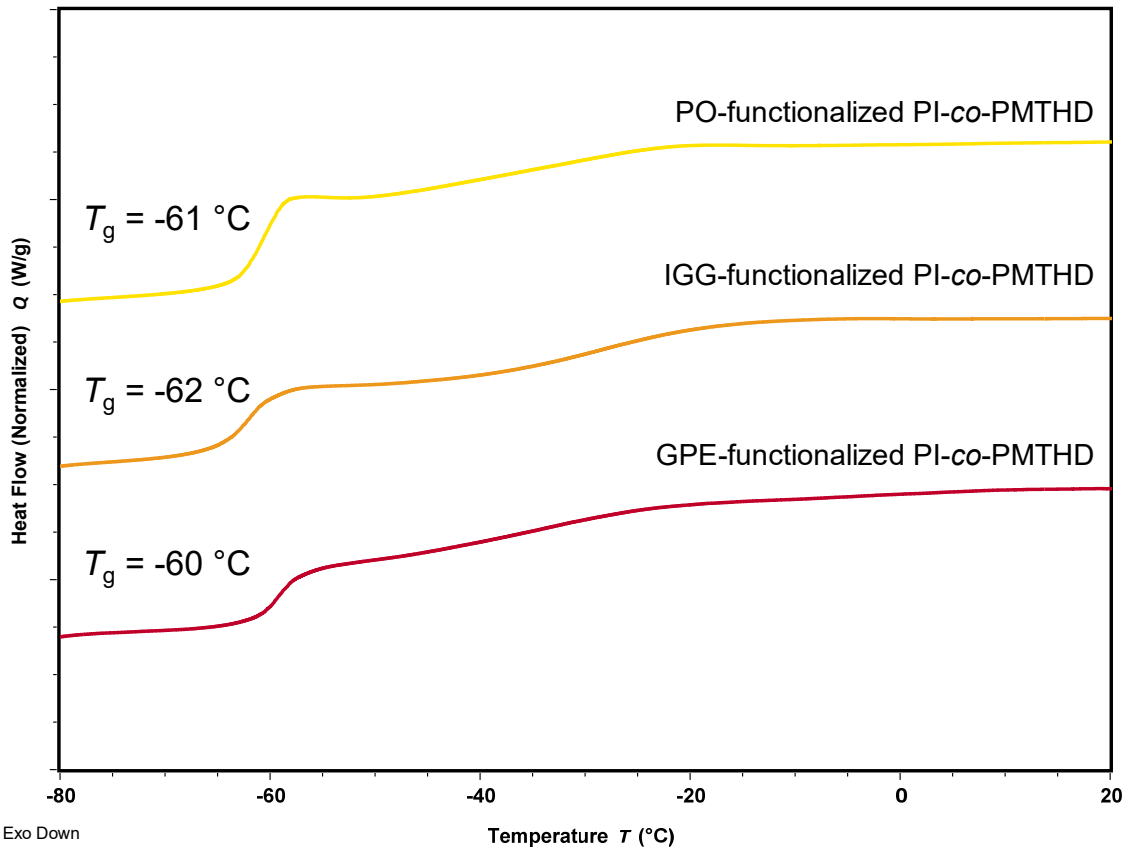


**Figure S24**: DSC curves of the modified copolymer PI-*co*-PMTHD through alkoxylation with either PO, IGG or GPE.

## Characterization for Alkylation Reactions

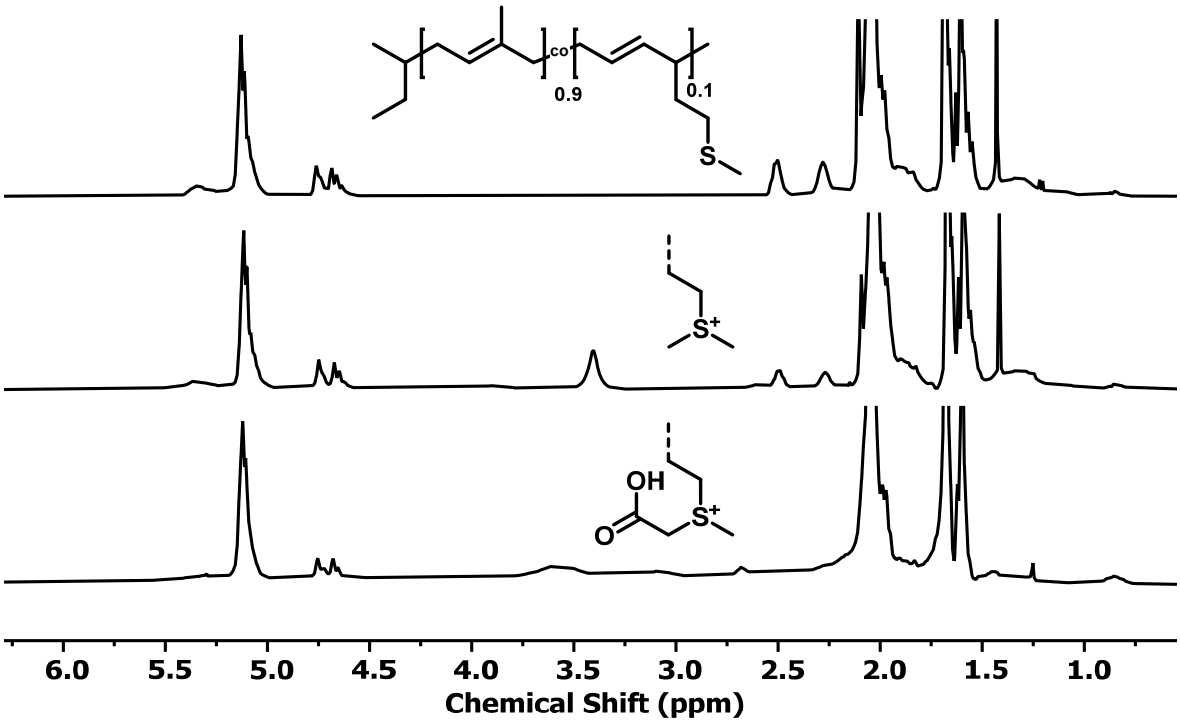


**Figure S25**: $^1$H NMR spectra (400 MHz, $CDCl_3$) of the alkylated PI-*co*-PMTHD.

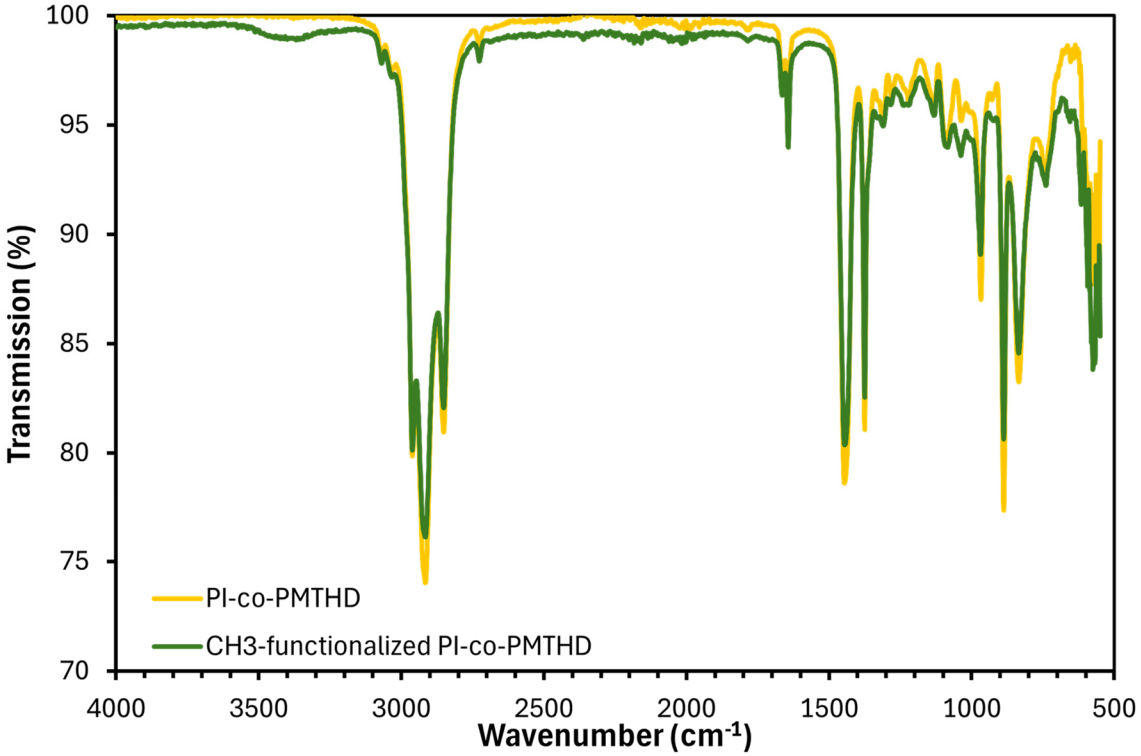


**Figure S26**: IR spectra of the precursor PI-*co*-PMTHD (yellow) and the methylated copolymer (green).

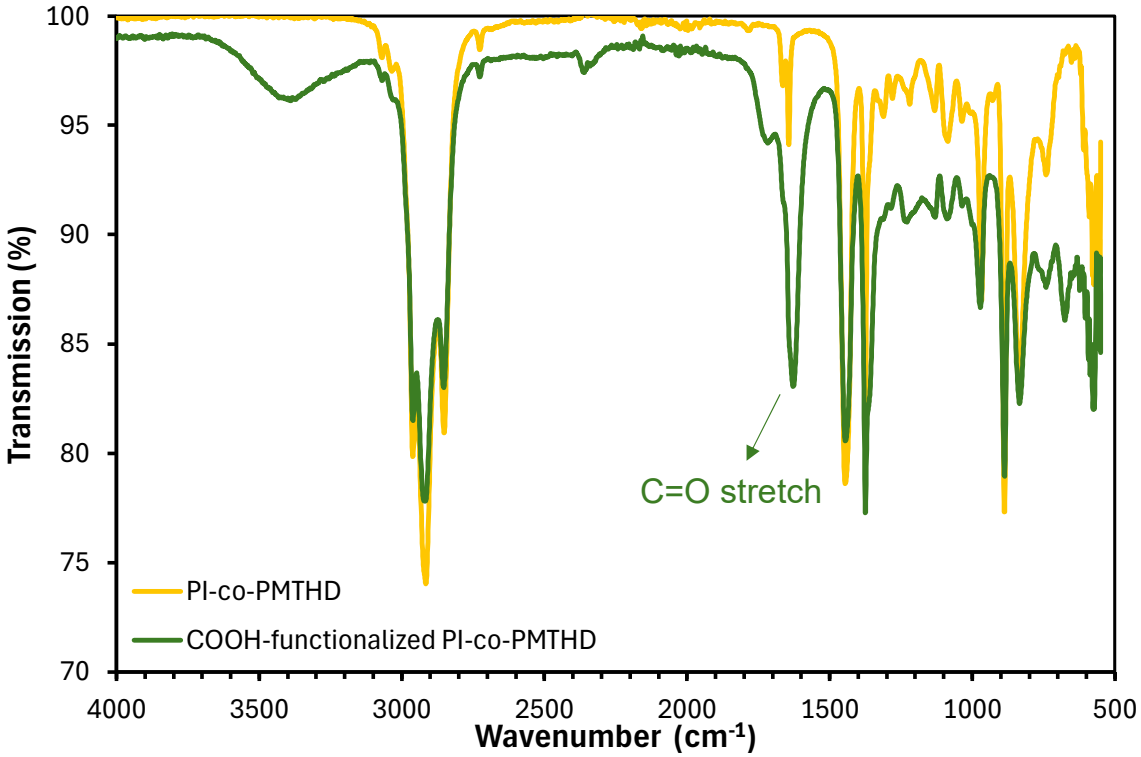


**Figure S27**: IR spectra of the precursor PI-*co*-PMTHD (yellow) and the carboxyl-functionalized copolymer (green).

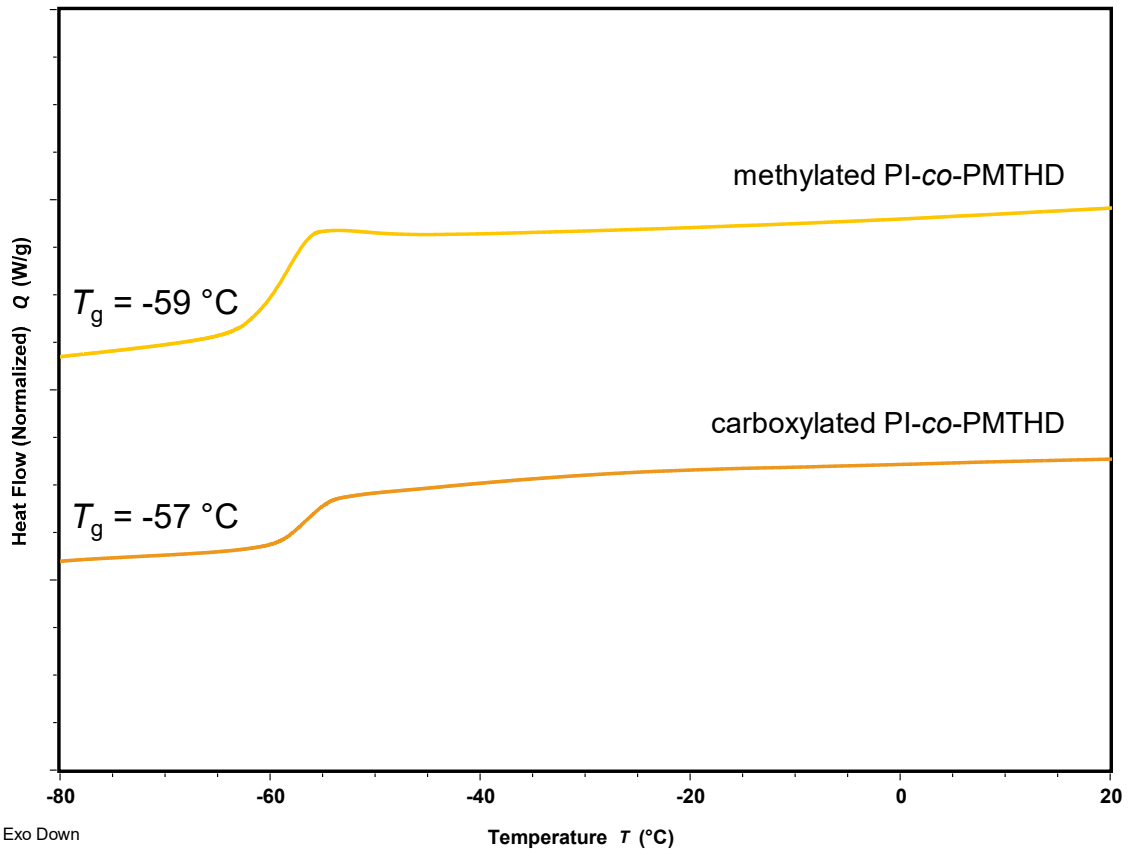


**Figure S28**: DSC curves of the modified copolymer PI-*co*-PMTHD through alkylation with methyl iodide or bromoacetic acid.


**Figure S29**: Visualization of the changed properties of the copolymer (middle) after the functionalization through alkylation with methyl iodide (left) and alkoxylation with propylene oxide (right).

## Characterization for Oxidation Reaction

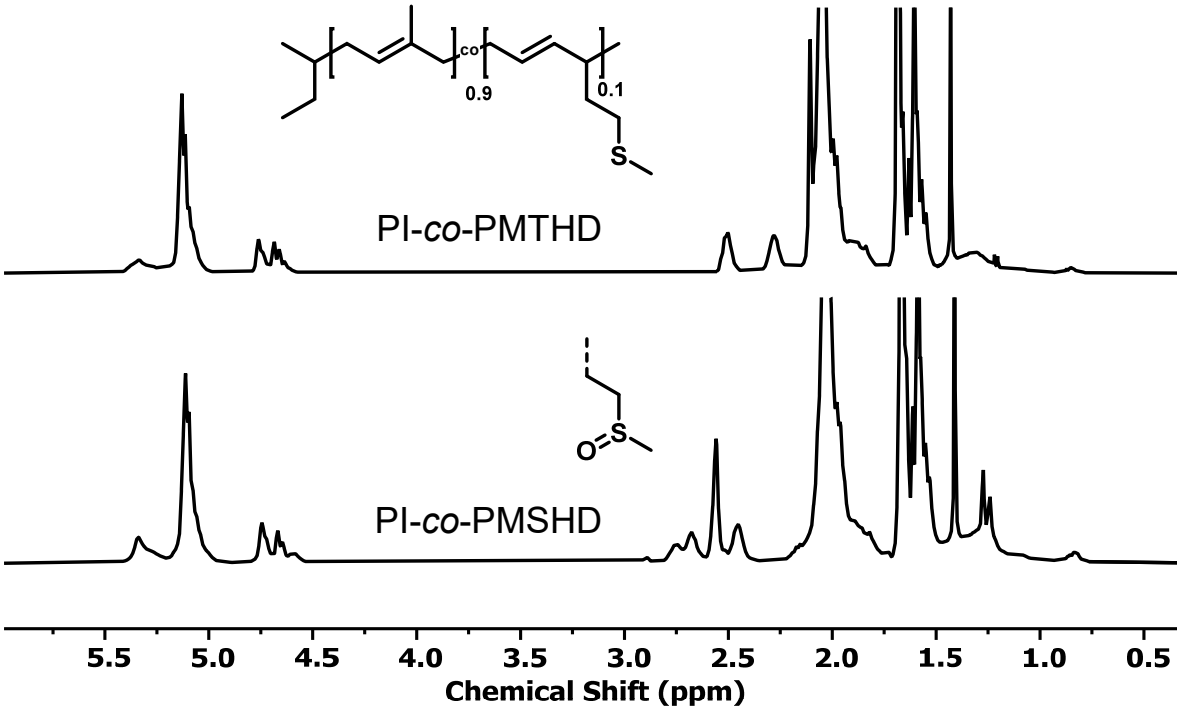


**Figure S30**: $^{1}$H NMR spectra (400 MHz, $CDCl_3$) of the oxidized copolymer PI-*co*-PMSHD in comparison to the precursor PI-*co*-PMTHD.

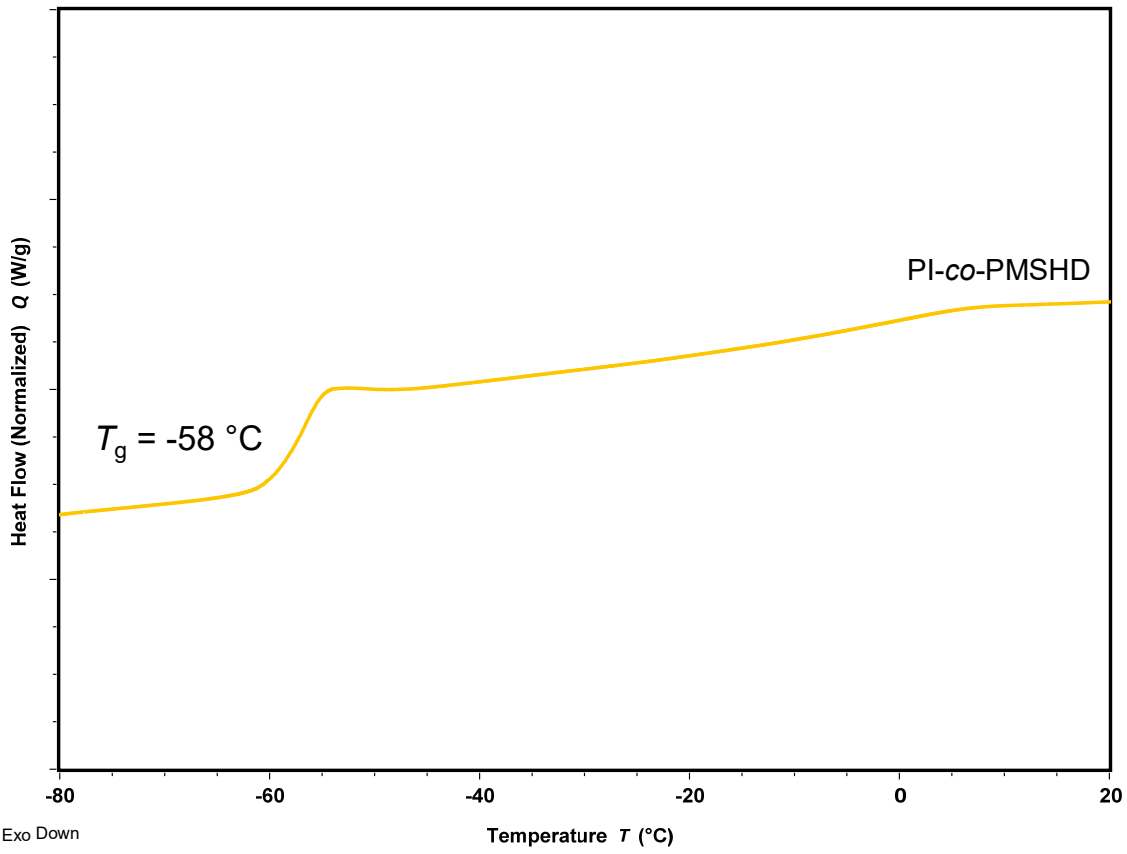


**Figure S31**: DSC curve of the oxidized copolymer PI-*co*-PMSHD.

### Characterization for Antimicrobial Behavior

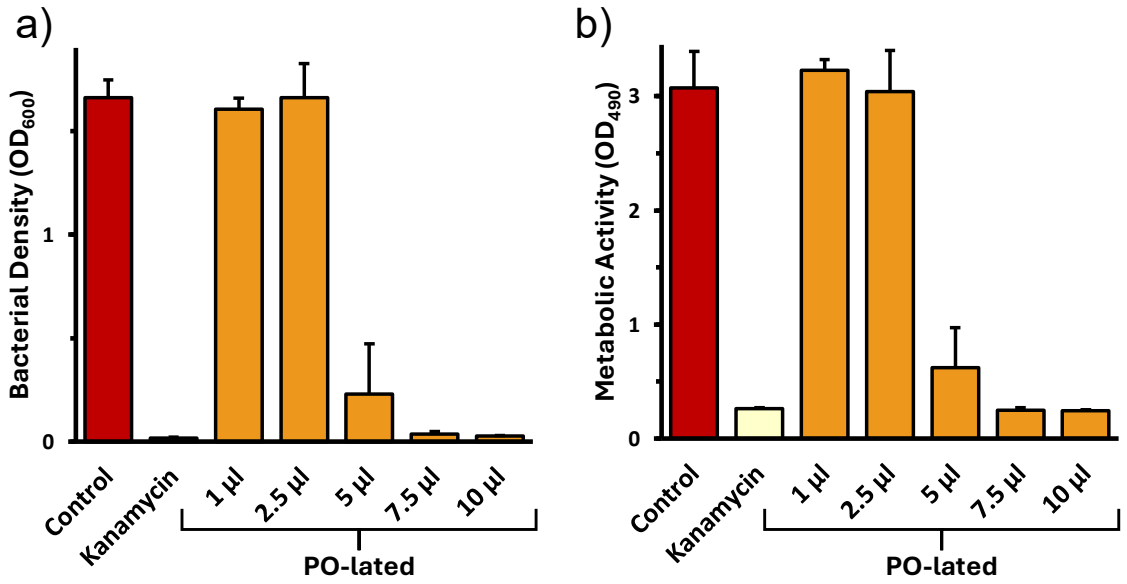


**Figure S32**: Illustration over a) the bacterial density and b) metabolic activity of *S. aureus* bacterial strains on surfaces with decreasing concentrations of the PO-lated copolymer $PI_{0.9}$-*co*-$PMTHD_{0.1}$ and the antibiotic Kanamycin as a reference.

## References

1 P. R. Blakemore, S. K. Kim, V. K. Schulze, J. D. White and A. F. T. Yokochi, J Chem Soc Perkin 1, 2001, 0, 1831–1847.

2 M. Steube, T. Johann, M. Plank, S. Tjaberings, A. H. Gröschel, M. Gallei, H. Frey and A. H. E. Müller, Macromolecules, 2019, 52, 9299–9310.

3 E. G. Gharakhanian and T. J. Deming, Biomacromolecules, 2015, 16, 1802–1806.

4 P. Pham, S. Oliver, D. T. Nguyen and C. Boyer, Macromol Rapid Commun, 2022, 43, 2200377.

# CHAPTER A1

## German Translation: Kombination von Styrol- und Dien-Struktur zu einem zyklischen Dien: Anionische Polymerisation von 1-Vinylcylohexen (VCH)

# APPENDIX A1

Published in *Angewandte Chemie International Edition,* 2023, **62**, e202302907.
Supplementary material relating to this work is available online: *DOI: 10.1002/anie.202302907.*

# Kombination von Styrol- und Dien-Struktur zu einem zyklischen Dien: Anionische Polymerisation von 1-Vinyl-cyclohexen (VCH)

Christoph Hahn,[a,b,†] Moritz Rauschenbach,[a,†] and Holger Frey [a,†*]

[a] Department of Chemistry, Johannes Gutenberg University, Duesbergweg 10 – 14, D-55128 Mainz (Germany)
[b] Max-Planck Graduate Center, MPGC, Staudingerweg 9, D-55128, Mainz (Germany)

[†] All authors have contributed equally

The following chapter was written in equal parts by the first two authors and is adapted with permission from C. Hahn, M. Rauschenbach, and H. Frey; Kombination von Styrol- und Dien-Struktur zu einem zyklischen Dien: Anionische Polymerisation von 1-Vinylcyclohexen (VCH), *Angewandte Chemie International Edition*, 2023, **62**, e202302907. 

GDCh Zuschriften Angewandte Chemie www.angewandte.org
Check for updates
Zitierweise: *Angew. Chem. Int. Ed.* **2023**, *62*, e202302907
doi.org/10.1002/anie.202302907

**Polymerisation**

# Kombination von Styrol- und Dien-Struktur zu einem zyklischen Dien: Anionische Polymerisation von 1-Vinylcyclohexen (VCH)

*Christoph Hahn[+], Moritz Rauschenbach[+], und Holger Frey**

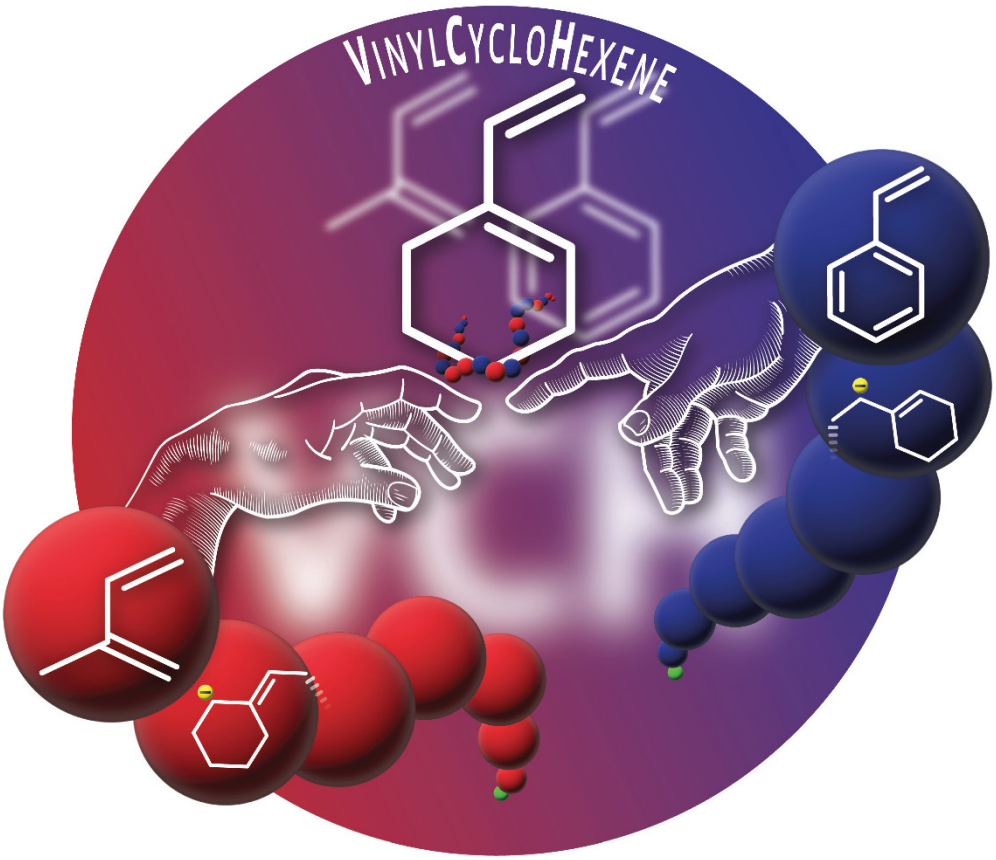


Angewandte Chemie

*Angew. Chem.* **2023**, *135*, e202302907 (1 of 5)

**Abstract:** Wir berichten über die erste anionische Polymerisation von 1-Vinylcyclohexen (VCH). Diese Struktur kann als eine Kombination von Dien und Styrol betrachtet werden. Die Polymerisation dieses zyklischen, 1,2-disubstituierten 1,3-Diens verlief quantitativ in Cyclohexan bei 25 °C mit sec-Butyllithium als Initiator. Die erhaltenen Polymere wiesen gut kontrollierte Molekulargewichte im Bereich von 5 bis 142 kg mol$^{-1}$ auf, die durch das molare Verhältnis von Monomer und Initiator einstellbar waren, mit engen Molekulargewichtsverteilungen ($Đ < 1.07$–$1.20$). Die kinetische *in situ* Untersuchung der Polymerisation mittels $^1$H NMR ergab eine schwach ausgeprägte Gradientenstruktur für die Copolymere von Styrol und VCH ($r_{Sty} = 2.55$, $r_{VCH} = 0.39$). PVCH, das in Cyclohexan mit sec-BuLi als Initiator erhalten wurde, zeigte sowohl 1,4- als auch 3,4-Einbau von VCH (Verhältnis: 64:36). Es wurde weiterhin gezeigt, dass die Mikrostruktur des resultierenden PVCH durch Zugabe eines polaren Additivs (THF) verändert werden kann, was zu einem erhöhten Anteil der 3,4-Mikrostruktur (bis zu 78 %) und einer erhöhten Glasübergangstemperatur von bis zu 89 °C führte. Somit polymerisiert das Monomer VCH carbanionisch lebend wie ein Dien, liefert dabei jedoch recht rigide Polymere mit hoher Glasübergangstemperatur, was interessante Möglichkeiten für die Kombination mit anderen Dienen zu hoch definierten Polymerarchitekturen und Materialien bietet.

Lineare 1,3-Diene können durch verschiedene Polymerisations-techniken wie Emulsionspolymerisation, kontrollierte und freie radikalische Polymerisation, lebende anionische Polymerisation und katalytische oder durch Insertionspolymerisation polymerisiert werden.[1] Lineare Diene spielen eine Schlüsselrolle als hochflexible Polymere für vielfältige Elastomer-Anwendungen. Allerdings wurden cyclische 1,3-Diene mit einer Vinyl-Doppelbindung nur begrenzt erforscht. Die erste Arbeit über die Polymerisation von 1-Vinylcyclohexen (VCH) von Hara et al. erschien 1971.[2] Die Autoren polymerisierten VCH unter Einsatz kationischer Initiatoren und berichteten sowohl über eine 3,4- als auch eine 1,4-Propagationsweise. Jedoch wurden keine GPC-Messungen durchgeführt. Bonnans-Plaisance untersuchte die Polymerisation von VCH mit kationischen oder radikalischen Initiatoren.[3] Im Jahr 1997 berichteten Longo et al., dass VCH in Gegenwart von Methylaluminoxan (MAO) und *rac*-[Ethylen-bis-(1-indenyl)]$ZrCl_2$ ausschließlich im 3,4-Anlagerungsmodus polymerisiert.[4] Allerdings führte die geringe katalytische Aktivität zu extrem niedrigen Monomerumsätzen (0.1 %). Im Gegensatz dazu lieferte das (Flu)-(Cp)$^i$Pr$ZrCl_2$-MAO-System Polymere mit einer 1,4-*trans*-Mikrostruktur.

Im Allgemeinen wurde für andere Strukturen gezeigt, dass cyclische 1,3-Diene mit unterschiedlichem Substitutionsmuster für eine lebende anionische Polymerisation geeignet sind. Gemäß der Definition von Szwarc treten während der lebenden Polymerisation keine Übertragungs- oder Terminierungsreaktionen auf.[5] Ishizone et al. berichteten über die anionische Polymerisation einer Reihe von sterisch extrem gehinderten Allyliden-Monomeren. 1,1-disubstituierte 1,3-Butadien-Derivate wurden in einer lebenden Polymerisation umgesetzt, unter Verwendung von *sec*-BuLi entweder in Cyclohexan bei 40 °C oder in THF bei 0–30 °C.[6] In 1,1-Position wurden Dimethyl-, Cyclohexyl-, Cycloheptyl-, 2,2,5,5-Tetramethylcyclopentyl- und Bornyl-Substituenten verwendet. Die Autoren zeigten, dass weniger sperrige Substituenten zu Polymeren führten, bei denen die 1,4-*trans*-Mikrostruktur vorherrschend war, während sperrigere Substituenten unter denselben Bedingungen eine ausschließliche 3,4-Mikrostruktur ergaben.[6] Die selektive Hydrierung von PI in PS-*b*-PI-*b*-PS Triblockcopolymeren wird eingesetzt, um die thermische Stabilität zu erhöhen und verbesserte mechanische Eigenschaften wie ausgeprägte Dehnungsverfestigung zu induzieren.[7,8] Darüber hinaus führt die Hydrierung von Polymeren zur Erhöhung des Flory-Huggins-Parameters ($\chi$) und der Ordnungs-Unordnungs-Übergangstemperatur ($T_{ODT}$). Die zentrale Herausforderung besteht darin, den PI-Block selektiv zu hydrieren, während die PS-Blöcke unter den harschen Bedingungen keine Kettenbrüche eingehen und ungesättigt bleiben.[9] Zur vollständigen Sättigung aller Doppelbindungen in PI-PS-Copolymeren (olefinisch und aromatisch) kann ein heterogener Palladiumkatalysator auf Calciumcarbonat verwendet werden. Die gesättigte 3,4-Mikrostruktur von PVCH ist identisch mit einem aus der vollständig Hydrierung von Polystyrol erhaltenem Polyvinylcyclohexan.[4,10]

Im Folgenden wird die in Schema 1 gezeigte anionische Polymerisation von VCH beschrieben, mit dem Ziel das Verhalten eines konjugierten zyklischen 1,3-Dien zu unter-

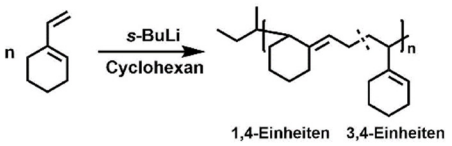


***Schema 1.*** Anionische Polymerisation von VCH in Cyclohexan. Aus Gründen der Übersichtlichkeit ist nur die *trans*-1,4 Mikrostruktur in diesem Schema gezeigt. (Details bezüglich der Charakterisierung der Mikrostrukturen siehe Hintergrundinformationen).

[*] C. Hahn,[+] M. Rauschenbach,[+] H. Frey
Department Chemie, Johannes Gutenberg-Universität Mainz
Duesbergweg 10–14, 55128 Mainz (Deutschland)
E-mail: h.frey@uni-mainz.de
C. Hahn[+]
Max-Planck Graduate Center, MPGC
Staudingerweg 9, 55128 Mainz (Deutschland)
[ ] Diese Autoren haben zu gleichen Teilen zu der Arbeit beigetragen.

suchen, das eine endozyklische und eine exozyklische, vinylische Doppelbindung aufweist. Hierbei stellt sich die Frage, ob das Polymerisationsverhalten mit einem konjugierten Dien (wie Isopren) oder mit Styrol aufgrund der verwandten molekularen Struktur vergleichbar ist. Hinsichtlich der resultierenden Polymereigenschaften sollte die zyklische 1,3-Dien-Struktur ausreichende Steifigkeit aufweisen, um ein Polymer zu erzeugen, das eine mit PS vergleichbare, hohe Glasübergangstemperatur ($T_g$) aufweist. Zudem kann das zyklische 1,3-Dien als ein weniger delokalisiertes Styrol-Analogon mit einem teilweise hydrierten aromatischen Ring betrachtet werden. Im Gegensatz zur oben genannten katalytischen Polymerisation von VCH wird ein quantitativer Monomerumsatz und eine lebende Polymerisation erwartet.

Das Monomer 1-Vinylcyclohexen (VCH) wurde nach einer Literaturvorschrift aus 1-Ethinylcyclohexen durch partielle Hydrierung des terminalen Alkins mit $Pb(OAc)_2$-vergiftetem $Pd/CaCO_3$ Katalysator synthetisiert.[11]

Unseres Wissens wurde die lebende anionische Polymerisation von VCH Organo-Lithium-Initiatoren bisher nicht beschrieben. Der Start der lebenden Polymerisation ist visuell mit einer intensiven gelben Färbung (Abbildung S21) nach der Initiierung mit *sec*-Butyllithium erkennbar, welche auf die Delokalisierung des lebenden Carbanions hinweist. Der lebende Charakter der Polymerisation wird durch die lineare Steigung von $\ln(M_0/M)$ in der Auftragung gegen die Reaktionszeit (Hintergrundinformationen Abbildung S20) nachgewiesen.

Es wurde eine Reihe von Homopolymeren mit angestrebten Molekulargewichten im Bereich von 5 bis 142 kg mol$^{-1}$ (GPC, THF, PS-Kalibrierung) synthetisiert (Tabelle 1). Die resultierenden Dispersitäten lagen im Bereich von $Đ = 1.07–1.20$. Zusätzlich wurde das absolute Molekulargewicht eines niedermolekularen Polymers mittels MALDI-ToF MS bestimmt, wodurch die enge Verteilung und der Einbau von 1-Vinylcyclohexen (108.18 g mol$^{-1}$) bestätigt wurden. Das MALDI-ToF-Spektrum (Abbildungen S6,S7) zeigt die verschiedenen Spezies, die den Verteilungen mit den jeweiligen Kationen zugeordnet sind. Das relative Molekulargewicht (GPC, 5.1 kg mol$^{-1}$) und das absolute Molekulargewicht gemäß MALDI-ToF MS (4.8 kg mol$^{-1}$) stimmen gut überein.

Die $T_g$s von PVCH, welche über DSC-Messungen ermittelt wurden, liegen in einem Bereich von 62–78 °C und somit niedriger als für PS. Ab einem Molgewicht von 18 kg mol$^{-1}$ wird ein konstanter Wert erhalten. Die Polymerisation von VCH wurde auch hinsichtlich der Zugabe von polaren Additiven untersucht, um ihren Einfluss auf die Mikrostruktur zu bestimmen. Die Mikrostruktur wurde durch Integration der allylischen Protonen (5.1 ppm und 5.3 ppm) in den $^1$H-NMR-Spektren des resultierenden Polymers bestimmt (Abbildung 1).

Das durch anionische Polymerisation mit dem Initiator *sec*-BuLi erhaltene Poly(vinylcyclohexen, PVCH) weist 64 % der 1,4-Mikrostruktur (bzw. 36 % 3,4-Mikrostruktur) auf. Die Bestimmung der 1,4- und 3,4-Einheiten durch NMR-Spektroskopie wurde gemäß der Literatur durchgeführt.[4] Abbildung 1 zeigt die durch $^1$H-NMR-Spektroskopie nachgewiesene Veränderung der Mikrostruktur von PVCH bei zunehmender THF-Konzentration, mit deutlich erhöhtem 3,4-Monomereinbau. Weitere Untersuchungen zur Polymerstruktur mittels NMR-Spektroskopie sind in der Hintergrundinformationen dargestellt (Abbildungen S9–S12).

Analog zu der bekannten katalytischen Polymerisation wurde keine 1,2-Mikrostruktur des VCH nachgewiesen (siehe Hintergrundinformationen, Abbildung S11)). Polare Additive wie THF sind bekannt dafür, die Mikrostruktur von 1,3-Dienen zu höheren Anteilen an 3,4-Einheiten (und 1,2-Mikrostruktur) zu verschieben.[12] Geringe Erhöhung der Polarität des Systems führt zur bevorzugten Bildung einer 3,4-Mikrostruktur. Diese Mikrostruktur ist vergleichbar mit einem (teil)-hydrierten Polystyrol. Nach Zugabe von mehr als 20 Äquivalenten THF pro Lithium-Ion wurde keine weitere Zunahme der 3,4-Einheiten beobachtet. Bei den

***Tabelle 1:*** Zusammenfassung der Charakterisierung der synthetisierten Homopolymere von VCH in Cyclohexan und unter Zugabe von THF, sowie der Mikrostruktur und Glasübergangstemperaturen.

| Nr. | $M_{theo}$ [kg mol$^{-1}$] | $M_n$[a] [kg mol$^{-1}$] | $Đ$ | [THF]/[Li] | 1,4/3,4 [%] | $T_g$ [°C] |
|---|---|---|---|---|---|---|
| P1 | 5 | 5.1 | 1.07 | 0 | 64/36 | 62 |
| P2 | 7.5 | 6.5 | 1.15 | 0 | 64/36 | 65 |
| P3 | 15 | 15.4 | 1.17 | 0 | 64/36 | 77 |
| P4 | 20 | 18.7 | 1.20 | 0 | 64/36 | 76 |
| P5 | 40 | 36.2 | 1.09 | 0 | 64/36 | 78 |
| P6 | 50 | 48.7 | 1.07 | 0 | 64/36 | 77 |
| P7 | 140 | 142.6 | 1.19 | 0 | 64/36 | n.d. |
| P8 | 15 | 15.3 | 1.05 | 0.5 | 56/44 | 74 |
| P9 | 15 | 15.2 | 1.07 | 1 | 39/61 | 75 |
| P10 | 15 | 16.2 | 1.11 | 2 | 25/75 | 83 |
| P11 | 15 | 18.1 | 1.08 | 4 | 25/75 | 83 |
| P12 | 15 | 19.8 | 1.09 | 20 | 22/78 | 89 |

[a] GPC, Eluent THF, PS-Eichung.

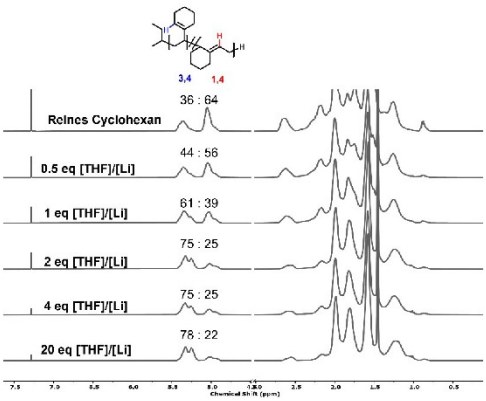


***Abbildung 1.*** Vergleich der $^1$H NMR-Spektren ($CDCl_3$, 25 °C, 400 MHz) von PVCH mit unterschiedlichen THF-Äquivalenten (von oben nach unten: reines Cyclohexan, 0.5 Äquiv., 1 Äquiv., 2 Äquiv., 4 Äquiv., 20 Äquiv.) als polares Additiv.

Polymeren, welche durch THF-Zugaben modifizierte Mikrostrukturen aufweisen, wurden signifikant höhere Glasübergangstemperaturen im Vergleich zu Polymeren, die in Cyclohexan erhalten wurden, festgestellt ($T_g$ − 74 bis 89 °C).

Aufgrund der strukturellen Verwandtschaft wurde die statistische Copolymerisation mit Styrol sowie Isopren untersucht. Von besonderem Interesse war hierbei die Untersuchung des VCH-Monomers im Hinblick auf die Vergleichbarkeit mit einem 1,3-Dien oder einem Vinylmonomer (z. B. Styrol).

Die detaillierten Ergebnisse der Echtzeit-Kinetik der Copolymerisation von VCH mit Styrol beziehungsweise Isopren sind ebenso wie die Beschreibung der Messung in der Hintergrundinformationen dargestellt. Die Copolymerisationsparameter von Styrol und VCH wurden zu $r_{Sty} = 2.55$ und $r_{VCH} = 0.39$ bestimmt. Der Übergang des PS-Li Kettenendes auf PVCH-Li bei VCH-Anlagerung wird durch einen signifikanten Farbumschlag bei der Blockcopolymerisation von P(S-*b*-VCH) angezeigt (siehe Hintergrundinformationen Abbildung S21).

Zu unserer Überraschung stellten wir eine Umkehrung der Copolymerisationsparameter von VCH und Styrol im Vergleich zu konventionellen Dien/Styrol-Copolymeren fest.[13] In der Regel führt die Copolymerisation von Styrol und 1,3-Dienen (z. B. Isopren und Butadien) zu ausgeprägten Gradientenstrukturen aufgrund des langsamen Kreuzwachstumsschritts von PI–Li zu Styrol. Im Gegensatz dazu zeigen die Echtzeit NMR-Daten für das Styrol/VCH System, dass Styrol bei der statistischen Copolymerisation stark bevorzugt eingebaut wird. Dieses Ergebnis legt nahe, dass der Übergang von PVCH–Li zu Styrol schnell erfolgt, im Gegensatz zu linearen Dienen wie Isopren oder Myrcen.[14] Im Allgemeinen bietet die β-Kohlenstoff-Verschiebung in der $^{13}$C NMR-Spektroskopie eine Möglichkeit zur Abschätzung der Reaktivität von Styrolderivaten. Die Reaktivität eines Monomers basiert hauptsächlich auf der Elektronendichte der reaktiven Vinylbindung, die mit der chemischen Verschiebung des β-Kohlenstoffs korreliert. VCH zeigt eine signifikant niedrigere β-Kohlenstoff-Verschiebung (109.72 ppm) im Vergleich zu Styrol (113.36 ppm).[15] Basierend auf diesen Beobachtungen schlussfolgern wir eine geringere Reaktivität von VCH im Vergleich zu Styrol. Dies wird vorläufig damit erklärt, dass die Vinylbindung im 1,3-Dien wesentlich weniger delokalisiert ist als die Vinylgruppe am aromatischen Ring im Fall von Styrol. Anders ausgedrückt wird eine geringere Stabilisierung im Vergleich zu Styrol angenommen.

Die sequentielle Blockcopolymerisation von VCH mit Isopren führte zu bimodalen Verteilungen mit erhöhten Dispersitäten von >1.35. Dies lässt sich auf einen hohen Reaktivitätsunterschied zwischen Isopren und VCH zurückführen, welcher zu einer sehr niedrigen Crossover-Geschwindigkeit zum weniger bevorzugten Monomer führt. Dieses sehr langsame Kreuzwachstum wurde durch Initiierung von VCH mit lebenden Poly(isoprenyl)-Lithium-Verbindungen und umgekehrt nachgewiesen. Die Ergebnisse zeigen, dass unabhängig vom ersten Monomer die GPC-Kurven bimodale Verteilungen aufweisen (Abbildung S23). Folglich ist die Bedingung einer schnellen Initiierung für eine kontrollierte Polymerisation nicht erfüllt, was zu der beobachteten bimodalen Molekulargewichtsverteilung führt. Überraschenderweise zeigten die lebenden Kettenenden von Isopren und VCH in beiden Fällen eine unvollständige Initiierung des jeweils anderen Monomers, was zu bimodalen Verteilungen in beiden Fällen führte. Darüber hinaus führte eine Erhöhung der Polymerisationstemperatur auf 40 °C nicht zu verbesserten Molekulargewichtsverteilungen (Abbildung S23). Die Echtzeit-Kinetikuntersuchung der statistischen Copolymerisation von Isopren und VCH zeigte einen vollständigen Verbrauch von Isopren. Die Integrale der dem VCH zugeordneten Signale blieben nahezu unverändert, und die Propagation von VCH begann erst, als kein Isopren mehr vorhanden war. Dies deutet auf extrem unterschiedliche Copolymerisationsparamter von $r_I \gg 1$ und $r_{VCH} \ll 1$ hin, was die ungünstige Crossover-Reaktion bestätigt (Abbildungen S24–S27), und zu einem sehr steilen Gradienten, wie vom System Isopren/4-Methylstyrol bekannt, führen sollte.[16]

PVCH-Proben, die durch Polymerisation in Cyclohexan (P3, 36 % 3,4-Addition) und PVCH-Proben, die unter Zusatz von 20 Äquivalenten THF erhalten wurden (P11, 78 % 3,4-Addition), wurden mit Palladium auf Kohlenstoff (10 Gew.-%) als Katalysator bei 30 bar Wasserstoffdruck bei 130 °C in einem Parr-Reaktor hydriert. Die Hydrierung führte zur vollständigen Umsetzung der Doppelbindungen, wie durch $^1$H NMR-Spektroskopie bestätigt wurde (Abbildungen S28, S29). Poly(vinylcyclohexan) (PCHE) wurde zuvor durch Koordinationspolymerisation von Vinylcyclohexan oder durch vollständige katalytische Hydrierung von PS hergestellt. Im Vergleich zur Literatur fanden wir identische Verschiebungen in den $^1$H- und $^{13}$C NMR-Spektren für hydriertes PVCH.[4]

Für die Probe P11 wird nach der Hydrierung eine Erhöhung der Glasübergangstemperatur von 89 °C auf 114 °C beobachtet. Das hydrierte Polymer besteht zu 78 % aus Poly(vinylcyclohexan)-Einheiten mit einer Glasübergangstemperatur von 140 °C.[7] Es wurden keine Hinweise auf Kettenbrüche oder Abbau des Polymer-Rückgrats nach der Hydrierung gefunden (siehe GPC-Diagramme, Abbildung S30). Eine verringerte $T_g$ von 70 °C wurde nach der Hydrierung von Probe P3 beobachtet (Abbildung S31), was unter Vorbehalt auf eine erhöhte Rotationsfreiheit des gesättigten Polymer-Rückgrats zurückgeführt wird.

Die lebende anionische Polymerisation von VCH, welche bisher nicht berichtet wurde, liefert Polymere mit guter Kontrolle über die Molekulargewichte und mäßig bis enge Molekulargewichtsverteilungen. Im Vergleich zum katalytischen Ansatz[4] wurde immer eine vollständige Umsetzung aufgrund des lebenden Charakters der anionischen Polymerisation erreicht. Die Ergebnisse zeigen, dass die Mikrostruktur von PVCH durch die Zugabe des polaren Additivs THF verändert werden kann, was zu einem höheren Ausmaß an 3,4-Einbau führt.[17] In Fall des VCH wird ein starres Polydien mit einem einstellbaren $T_g$ im Bereich von 77–89 °C erhalten.

Eingangs wurde die Frage aufgeworfen, ob das VCH-Monomer als 1,3-Dien oder eher als Styrol-Monomer reagiert. Basierend auf dieser Studie verhält sich VCH in der

anionischen Polymerisation vergleichbar wie etablierte Diene, jedoch sind die resultierenden Materialeigenschaften vergleichbar mit Polystyrol. Die Hydrierung von PVCH führte zu Polymeren, die Poly(vinylcyclohexan)-Segmente enthalten, was zu einer Erhöhung der Glasübergangstemperatur auf 114 °C führte, bei einer monomodalen Molekulargewichtsverteilung ohne Anzeichen von Kettenabbau.

Diese Arbeit zeigt die signifikanten Auswirkungen einer sterisch stark eingeschränkten Doppelbindung in einem 1,3-Dien auf das Verhalten in der anionischen Polymerisation. Es ist wichtig zu betonen, dass VCH ein Modellsystem für verschiedene biobasierte 1,3-Diene darstellt, die aus natürlichen Terpenen abgeleitet sind. VCH selbst zeigt faszinierendes Potenzial zur Herstellung von vollständig hydrierten Materialien mit hohem $T_g$, verbessertem Phasenseparationsverhalten und ermöglicht den Zugang zu komplexen Polymerarchitekturen mittels lebender anionischer Copolymerisation.

## Autorenbeiträge

*Christoph Hahn**: Erforschung, Synthese, Datenaufbereitung, Methodik, Konzeptualisierung, Schreiben. *Moritz Rauschenbach**: Erforschung, Datenaufbereitung, Methodik, Schreiben. *Holger Frey*: Betreuung, Konzeptualisierung, Schreiben – Überprüfung und Bearbeitung. * trugen beide im gleichen Umfang zu dieser Arbeit bei.

## Danksagung

Diese Arbeit wurde teilweise durch die Max-Planck-Graduiertenschule Mainz (MPGC) unterstützt. Die Autoren danken Philip von Tiedemann für sein ursprüngliche Konzeptualisierung dieses Projekts. Wir danken weiterhin Manfred Wagner für die Echtzeitkinetik-Messungen sowie Prof. A. H. E. Müller für wertvolle Diskussionen. Open Access Veröffentlichung ermöglicht und organisiert durch Projekt DEAL.

## Interessenkonflikt

Die Autoren erklären, dass keine Interessenkonflikte vorliegen.

## Erklärung zur Datenverfügbarkeit

Die Daten, die die Ergebnisse dieser Studie unterstützen, sind auf Anfrage beim Autor erhältlich.

**Stichwörter:** Copolymerization Kinetics · 1,3-Dienes · Living Anionic Polymerization · Polyisoprene · Polystyrene

[1] a) W. Cooper, G. Vaughan, *Prog. Polym. Sci.* **1967**, *1*, 91; b) S. Bywater, Y. Firat, P. E. Black, *J. Polym. Sci. Polym. Chem. Ed.* **1984**, *22*, 669.
[2] K. Hara, Y. Imanishi, T. Higashimura, M. Kamachi, *J. Polym. Sci. A* **1971**, *9*, 2933.
[3] C. Bonnans-Plaisance, *Eur. Polym. J.* **1979**, *15*, 581.
[4] P. Longo, A. Grassi, F. Grisi, S. Milione, *Macromol. Rapid Commun.* **1998**, *19*, 229.
[5] a) I. Natori, S. Inoue, *Macromolecules* **1998**, *31*, 4687; b) R. D. Barent, M. Wagner, H. Frey, *Polym. Chem.* **2022**, *13*, 5478; c) M. Szwarc, *Nature* **1956**, *178*, 1168.
[6] S. Uchida, K. Togii, S. Miyai, R. Goseki, T. Ishizone, *Macromolecules* **2020**, *53*, 10107.
[7] B. S. Beckingham, R. A. Register, *Macromolecules* **2013**, *46*, 3084.
[8] a) F. S. Bates, G. H. Fredrickson, D. Hucul, S. F. Hahn, *AIChE J.* **2001**, *47*, 762; b) A. Laramée, P. Goursot, J. Prud'homme, *Colloid Polym. Sci.* **1977**, *255*, 1141.
[9] P. von Tiedemann, J. Yan, R. D. Barent, R. J. Spontak, G. Floudas, H. Frey, R. A. Register, *Macromolecules* **2020**, *53*, 4422.
[10] D. A. Hucul, S. F. Hahn, *Adv. Mater.* **2000**, *12*, 1855.
[11] E. N. Marvell, J. Tashiro, *J. Org. Chem.* **1965**, *30*, 3991.
[12] D. A. H. Fuchs, H. Hübner, T. Kraus, B.-J. Niebuur, M. Gallei, H. Frey, A. H. E. Müller, *Polym. Chem.* **2021**, *12*, 4632.
[13] a) D. J. Worsfold, S. Bywater, *Can. J. Chem.* **1964**, *42*, 2884; b) S. Quinebèche, C. Navarro, Y. Gnanou, M. Fontanille, *Polymer* **2009**, *50*, 1351.
[14] E. Grune, J. Barcuther, J. Blankenburg, M. Appold, L. Shaw, A. H. E. Müller, G. Floudas, L. R. Hutchings, M. Gallei, H. Frey, *Polym. Chem.* **2019**, *10*, 1213.
[15] P. von Tiedemann, J. Blankenburg, K. Maciol, T. Johann, A. H. E. Müller, H. Frey, *Macromolecules* **2019**, *52*, 796.
[16] E. Grune, T. Johann, M. Appold, C. Wahlen, J. Blankenburg, D. Leibig, A. H. E. Müller, M. Gallei, H. Frey, *Macromolecules* **2018**, *51*, 3527.
[17] A. Forens, K. Roos, C. Dire, B. Gadenne, S. Carlotti, *Polymer* **2018**, *153*, 103.

Manuskript erhalten: 26. Februar 2023
Akzeptierte Fassung online: 25. April 2023
Endgültige Fassung online: 6. Juni 2023

# Curriculum Vitae

# CURRICULUM VITAE

## Moritz Rauschenbach